NATURAL PRODUCTS AS A TOOL TO DESIGN NEW ANTI-MDR LEAD MOLECULES

EDITED BY: Patrícia Mendonça Rijo, Francisco Estévez, Przemysław Sitarek and Maria José U. Ferreira

PUBLISHED IN: Frontiers in Pharmacology and Frontiers in Oncology

frontiers Research Topics

ISSN 1664-8714
ISBN 978-2-88971-191-8
DOI 10.3389/978-2-88971-191-8

About Frontiers

Frontiers is more than just an open-access publisher of scholarly articles: it is a pioneering approach to the world of academia, radically improving the way scholarly research is managed. The grand vision of Frontiers is a world where all people have an equal opportunity to seek, share and generate knowledge. Frontiers provides immediate and permanent online open access to all its publications, but this alone is not enough to realize our grand goals.

Frontiers Journal Series

The Frontiers Journal Series is a multi-tier and interdisciplinary set of open-access, online journals, promising a paradigm shift from the current review, selection and dissemination processes in academic publishing. All Frontiers journals are driven by researchers for researchers; therefore, they constitute a service to the scholarly community. At the same time, the Frontiers Journal Series operates on a revolutionary invention, the tiered publishing system, initially addressing specific communities of scholars, and gradually climbing up to broader public understanding, thus serving the interests of the lay society, too.

Dedication to Quality

Each Frontiers article is a landmark of the highest quality, thanks to genuinely collaborative interactions between authors and review editors, who include some of the world's best academicians. Research must be certified by peers before entering a stream of knowledge that may eventually reach the public - and shape society; therefore, Frontiers only applies the most rigorous and unbiased reviews.
Frontiers revolutionizes research publishing by freely delivering the most outstanding research, evaluated with no bias from both the academic and social point of view. By applying the most advanced information technologies, Frontiers is catapulting scholarly publishing into a new generation.

What are Frontiers Research Topics?

Frontiers Research Topics are very popular trademarks of the Frontiers Journals Series: they are collections of at least ten articles, all centered on a particular subject. With their unique mix of varied contributions from Original Research to Review Articles, Frontiers Research Topics unify the most influential researchers, the latest key findings and historical advances in a hot research area! Find out more on how to host your own Frontiers Research Topic or contribute to one as an author by contacting the Frontiers Editorial Office: frontiersin.org/about/contact

NATURAL PRODUCTS AS A TOOL TO DESIGN NEW ANTI-MDR LEAD MOLECULES

Topic Editors:
Patrícia Mendonça Rijo, Universidade Lusófona, Portugal
Francisco Estévez, University of Las Palmas de Gran Canaria, Spain
Przemysław Sitarek, Medical University of Lodz, Poland
Maria José U. Ferreira, University of Lisbon, Portugal

Citation: Rijo, P. M., Estévez, F., Sitarek, P., Ferreira, M. J. U., eds. (2022). Natural Products as a Tool to Design New anti-MDR Lead Molecules. Lausanne: Frontiers Media SA. doi: 10.3389/978-2-88971-191-8

Table of Contents

frontiers in Pharmacology

EDITORIAL
published: 21 June 2021
doi: 10.3389/fphar.2021.694674

Editorial: "Natural Products as a Tool to Design New anti-MDR Lead Molecules."

Patrícia Rijo[1,2]*, *Francisco Estévez*[3], *Przemysław Sitarek*[4] and *Maria-José U. Ferreira*[2]

[1]CBIOS—Universidade Lusófona's Research Center for Biosciences & Health Technologies, Lisboa, Portugal, [2]Research Institute for Medicines (iMed.ULisboa), Faculty of Pharmacy, Universidade de Lisboa, Lisboa, Portugal, [3]University of Las Palmas de Gran Canaria, Las Palmas de Gran Canaria, Spain, [4]Department of Biology and Pharmaceutical Botany, Medical University of Lodz, Lodz, Poland

Keywords: traditional medicines, herbal medicines, natural products, MDR, cancer

Editorial on the Research Topic

"Natural Products as a Tool to Design New anti-MDR Lead Molecules."

Natural products have been used in traditional medicine, since ancient times, for the treatment of several diseases. Characterized by a high structural diversity, they have long represented an important source of medicines or drug leads, playing a key role in drug discovery and development, namely in cancer. Currently, there is great interest in identifying small molecules from natural sources for overcoming multidrug resistance (MDR), a major obstacle in cancer treatment, by restoring the efficacy of chemotherapeutic agents, preventing MDR, or re-sensitizing tumour cells to anticancer drugs.

This special issue collects ten contributions, two reviews and eight original articles, highlighting the importance of natural products as source of new anti-MDR lead molecules in cancer.

A review article by Ferreira et al. focused on the disruption of nuclear and cell protein nuclear exports *via* CRM1, which has become a promising therapeutic strategy for the treatment of patients with viral infections and cancer. The clinical approval of the first-in-class CRM1 inhibitor, Selinexor, has demonstrated the therapeutic potential of inhibiting CRM1 in cancer treatment. Compounds derived from natural sources hold promise to support the discovery of new nuclear export inhibitors with a novel mode of action.

The review work by Tinoush et al. summarized reports of several secondary metabolites, with different scaffolds, capable of reversing MDR in cancer by inhibiting the transport activity or the expression of P-gp, MRP1, and BRCP, which are the three main ABC transporters implicated in MDR. Moreover, synergistic interactions of different natural product-derived compounds, in combination with anticancer drugs, were also addressed. Although the efficacy of phytochemicals requires clinical confirmation, there are many studies providing evidence for their promising anti-MDR role, being, currently, considered as 4th generation ABC transporter modulators.

Changes of cancer cells responsible for resistance to anticancer drugs might, at the same time, generate vulnerabilities that may rend drug-resistant cells more sensitive to other compounds, named collateral sensitivity agents (CS). Using this anti-MDR approach, Reis et al. evaluated the CS effect of a set of macrocyclic diterpene derivatives of the lathyrane-type against several human cancer cell lines and corresponding drug-resistant sub-lines. Some compounds were found to be promising CS agents, being many-fold more effective against MDR sublines, mainly in relation to gastric carcinoma cells. These compounds were able to induce apoptosis *via* caspase-3 activation. Structure-activity relationships of the compounds were also obtained through regression models.

Edited and reviewed by:
Javier Echeverria,
University of Santiago, Chile

***Correspondence:**
Patrícia Rijo
patricia.rijo@ulusofona.pt

Specialty section:
This article was submitted to Ethnopharmacology, a section of the journal Frontiers in Pharmacology

Received: *13 April 2021*
Accepted: *04 June 2021*
Published: *21 June 2021*

Citation:
Rijo P, Estévez F, Sitarek P and Ferreira M-JU (2021) Editorial: "Natural Products as a Tool to Design New anti-MDR Lead Molecules.". Front. Pharmacol. 12:694674. doi: 10.3389/fphar.2021.694674

In turn, Liao et al. attempted to elucidate whether the combination of tanshinone IIA and cisplatin could generate a synergistic antitumor effect on esophageal squamous cell carcinoma (ESCC) cells. The authors revealed that the combination suppressed cell migration and invasion abilities, arrested the cell cycle, and induced apoptosis in HK and K180 cells. Molecular docking studies indicated that tanshinone IIA and cisplatin could be docked into active sites with the tested proteins. Additionally, the expression levels of E-cadherin, β-catenin, Bax, cleaved caspase-9, P21, P27, and c-Fos were upregulated, and the expression levels of fibronectin, vimentin, Bcl-2, cyclin D1, p-Akt, p-ERK, p-JNK, P38, COX-2, VEGF, IL-6, NF-κB, and c-Jun proteins were downregulated.

He et al. work reported that dioscin promoted apoptosis of prostate cancer cells and inhibited cell invasion by increasing SHP1 phosphorylation and suppressing the downstream MAPK signalling pathway. The results of *in vitro* and *in vivo* studies have showed that dioscin reversed IL-6 and DHT-stimulated PCa cell proliferation and invasion and increased apoptosis in these cells. The anticancer activity of dioscin may be due to its effects of increasing SHP1 phosphorylation and inhibiting the subsequent MAPK signalling pathway. Therefore, the results suggested that dioscin may be a potential drug to treat both androgen-sensitive and androgen-independent PCa.

Liu et al. reported the phytochemical study of the traditional Chinese medicine Marsdeniae tenacissimae Caulis, whose constituents were submitted to cytotoxicity screening, pharmacology analysis, and cellular and molecular experiments. The study showed that four C21 steroidal saponins were able to induce apoptosis in lung adenocarcinoma (A549), by downregulating the anti-apoptotic protein Bcl2 and upregulating the pro-apoptotic protein Bax. In addition, these compounds also downregulated the expression of MMP-2 and MMP-9 proteins, thus providing evidence for the potential of Marsdeniae tenacissimae Caulis against lung cancer.

AlQathama et al. studied the influence of selected Nigerian medicinal plants on the viability, mobility, and resistance mechanisms in liver, colon and skin cancer cell lines. They demonstrated that some of herbal medicines were endowed with significant *in vitro* cytotoxicity and inhibited MDR mechanisms. The aqueous extracts of *Gongronema latifolium* and *Strophanthus hispidus* were the most cytotoxic against Caco2 cells. In turn, *Bridelia ferruginea*, and *Ximenia americana* extracts showed the strongest inhibition of P-gp efflux activity. Moreover, inhibitory effects on other MDR mechanisms, namely depletion of glutathione, were also observed for some extracts, whereas others exerted *in vitro* anti-migratory activity against the highly metastatic B16-F10 cell line.

Vágvölgyi et al. unveiled two new ecdysteroid squalenylated prodrugs that were characterized and formulated as self-assembling nanoparticles. The authors revealed that, in the checkerboard microplate assay, one of the starting ecdysteroids showed strong synergism with doxorubicin, in multidrug resistant mouse lymphoma cells, whereas the other compound showed strong antagonism when combined with paclitaxel, in the human breast cancer cell line MCF7, thus having a cytoprotective effect against this anticancer agent. However, in both cases, it was observed antagonism for the corresponding nanoassemblies, due to the acid-sensitive acetonide groups in the lysosomes. The authors concluded that acid-resistant substituents should be considered in future works.

In the work of Garcia et al., the authors presented royleanone derivatives from Plectranthus spp. as a novel class of P-glycoprotein inhibitors. They reported that regarding their stability and P-gp inhibition potential, the results suggested that the formation of benzoyl esters is a more convenient approach for future derivatives with enhanced cytotoxicity. Furthermore, the authors observed that the moieties in positions six and seven of royleanones are also important for interaction with the P-pg.

Chen et al. studied the *in vivo* and *in vitro* effects of magnolol, a biphenyl extracted from *Magnolia officinalis*, on the proliferation, migration, and invasion of pancreatic cancer. They noted that magnolol, by suppressing the TGF-β signal pathway and epithelial-mesenchymal-transition (EMT), could inhibit proliferation, migration, and invasion. The authors concluded that magnolol might represent an effective drug for the treatment of pancreatic cancer, however its mechanism of action needs further investigation.

Overall, the works presented in this special issue provide experimental evidence and assembled scientific data, which clearly emphasize the medicinal value of natural products to fight multidrug resistant cancer cells. Nature has many bioactive molecules to offer, some of which have yet to be discovered, thus giving hope that in the future we will be able to sustainably use natural resources and find stronger and safer anti-cancer agents.

AUTHOR CONTRIBUTIONS

PR-supervison and writing, FE-visualization, PS-writing, M-JF-validation and writing.

Conflict of Interest: The authors declare that the research was conducted in the absence of any commercial or financial relationships that could be construed as a potential conflict of interest.

frontiers in Pharmacology

MINI REVIEW
published: 07 May 2020
doi: 10.3389/fphar.2020.00625

Small Molecule Inhibitors of CRM1

Bibiana I. Ferreira[1,2,3], *Bastien Cautain*[4,5], *Inês Grenho*[1,2,3] *and Wolfgang Link*[6]*

[1] Centre for Biomedical Research (CBMR), University of Algarve, Faro, Portugal, [2] Regenerative Medicine Program, Department of Biomedical Sciences and Medicine, University of Algarve, Faro, Portugal, [3] Algarve Biomedical Center (ABC), University of Algarve, Faro, Portugal, [4] Fundacion MEDINA Parque tecnológico ciencias de la salud, Granada, Spain, [5] Evotec France, Toulouse, France, [6] Instituto de Investigaciones Biomédicas "Alberto Sols" (CSIC-UAM), Madrid, Spain

The transport through the nuclear pore complex is used by cancer cells to evade tumor-suppressive mechanisms. Several tumor-suppressors have been shown to be excluded from the cell nucleus in cancer cells by the nuclear export receptor CRM1 and abnormal expression of CRM1 is oncogenic. Inhibition of CRM1 has long been postulated as potential approach for the treatment of cancer and to overcome therapy resistance. Furthermore, the nuclear export of viral components mediated by the CRM1 is crucial in various stages of the viral lifecycle and assembly of many viruses from diverse families, including coronavirus. However, the first nuclear export inhibitors failed or never entered into clinical trials. More recently CRM1 reemerged as a cancer target and a successful proof of concept was achieved with the clinical approval of Selinexor. The chemical complexity of natural products is a promising perspective for the discovery of new nuclear export inhibitors with a favorable toxicity profile. Several screening campaigns have been performed and several natural product-based nuclear export inhibitors have been identified. With this review we give an overview over the role of CRM1-mediated nuclear export in cancer and the effort made to identify and develop nuclear export inhibitors in particular from natural sources.

Keywords: CRM1, nuclear export, natural products (NP), leptomycin B, Selinexor, high content screening (HCS)

OPEN ACCESS

Edited by:
Patrícia Mendonça Rijo, Universidade Lusófona Research Center for Biosciences & Health Technologies, Portugal

Reviewed by:
Hsu-Wen Chao, Taipei Medical University, Taiwan
Yuh Min Chook, University of Texas Southwestern Medical Center, United States
Célia Maria Cardona Faustino, University of Lisbon, Portugal

***Correspondence:**
Wolfgang Link
walink@iib.uam.es

Specialty section:
This article was submitted to Translational Pharmacology, a section of the journal Frontiers in Pharmacology

Received: *10 December 2019*
Accepted: *20 April 2020*
Published: *07 May 2020*

Citation:
Ferreira BI, Cautain B, Grenho I and Link W (2020) Small Molecule Inhibitors of CRM1. Front. Pharmacol. 11:625. doi: 10.3389/fphar.2020.00625

INTRODUCTION

Human diseases often involve alterations in the structure, localization, interactions, and as a consequence, the function of cellular proteins (Hung and Link, 2011). Normal cell physiology requires a tightly regulated, coordinated activity of thousands of proteins, that must be in the right place at the right time. Protein function depends on the subcellular localization as it determines access of the protein to binding partners and enzymes that catalyze post-translational modification and facilitates its contribution to functional networks. For example, transcription factors have to be in the cell nucleus in order to have access to the target gene promoters and to exert their transcriptional activity. With the exception of red blood cells, all eukaryotic cells contain a nucleus which is surrounded by a nuclear envelope made up of two lipid bilayer membranes. The nuclear envelope represents a greater physical barrier than the single lipid bilayer of the plasma membrane. The movement of molecules between the nucleoplasm and the cytoplasm is controlled by nuclear pore complexes (NPCs). The NPC is one of the largest cellular protein complexes and is responsible for the controlled passage of macromolecules into and out of the nucleus. The NPCs are permeable only to small molecules such as salts, nucleotides, small proteins. Proteins over 40 kDa are required

to be moved through the nuclear pore complex (NPCs) by soluble nuclear transport receptors (Cautain et al., 2015b). Proteins that enter and exit through the NPC usually contain specific transport signals namely a nuclear localization signal (NLS) or a nuclear export signal (NES). These sequences are recognized by soluble transport receptors of the karyopherin family.

THE CRM1 EXPORT RECEPTOR

The best studied export protein is chromosome region maintenance 1 (CRM1 also known as XPO1 or exportin 1) (Fornerod et al., 1997; Fukuda et al., 1997; Ossareh-Nazari et al., 1997; Kudo et al., 1998). CRM1 is expressed in all eukaryotic cells. CRM1 belongs to the karyopherin-β family of transport receptors and mediates the nuclear exports of proteins that contain leucine-rich NESs (Fukuda et al., 1997). Over 200 proteins have been verified as cargoes of CRM1. Ran-GTP binds to CRM1 in the nucleus causing an increased affinity to the NES containing cargo protein and a complex between Ran, CRM1 and the cargo forms. This complex is exported through the NPC into the cytoplasm where Ran-GTP is converted into Ran-GDP and the complex dissociates. Human CRM1 consists of 1071 amino-acid residues and contains several functional regions (**Figure 1**). CRM1 is made up of 21 tandemly repeated, 37–47 amino acid long modules called HEAT protein domains (Dong et al., 2009a; Dong et al., 2009b; Monecke et al., 2009). Each repeat forms a hairpin of two helices called A and B helices building a ring-shaped structure. While the outer surface of the ring comprise the A helices, the B helices form the inner surface (Güttler et al., 2010; Koyama and Matsuura, 2010; Dian et al., 2013; Monecke et al., 2013; Saito and Matsuura, 2013). The NES binding cleft is formed by HEAT repeats 11 and 12 at the outer surface of CRM1. The N-terminal CRIME domain shares sequence homology with importin-β and is involved in binding to RanGTP. The acidic loop within HEAT-repeat 9 also contributes to RanGTP binding and is thought to inhibit the interaction with NES in the absence of RanGTP. While the central part of CRM1 is involved the interaction with NES, the C-terminal end of CRM1 is thought to modulate its affinity to NES (Dong et al., 2009a; Dian et al., 2013).

The Role of CRM1 in Cancer

CRM1 is responsible for the nuclear export of a large number of tumor suppressor and oncogenic proteins including retinoblastoma, APC, FOXO proteins, INI1/hSNF5, galectin-3, Bok, NPM1, RASSF2, Merlin, p53, p21CIP, p27KIP1, N-WASP/FAK, estradiol receptor, Tob, BRAC1, BCR–ABL and eIF4E. Importantly, many of these proteins were found to be mislocalized in cancer cells (Hill et al., 2014). RNAi-mediated silencing of the CRM1 induced nuclear retention of p53 and cell death in cervical cancer cell lines (Santiago et al., 2013). Somatic mutations in CRM1 have been identified in chronic lymphocytic leukemia (Puente et al., 2011) and in other hematological malignancies (Sendino et al., 2018). The great majority of these mutations affect a single amino acid at position 571. The E571K mutation localizes near the NES-binding site and substitutes a glutamic acid with a lysine. This variation replaces a negatively charged residue with a positively charged amino acid and might lead to an increased affinity for NES (García-Santisteban et al., 2016).

The expression of CRM1 is increased in a broad variety of cancer types including cervical (van der Watt et al., 2009), ovarian (Noske et al., 2008), kidney (Inoue et al., 2013), lung (Gao et al., 2015) and gastric cancers (Zhou et al., 2013), as well as in glioma (Shen et al., 2009), osteosarcoma (Yao et al., 2009), esophageal carcinoma (Van Der Watt et al., 2014), hepatocellular carcinoma (Zheng et al., 2014), multiple myeloma (Schmidt et al., 2013), acute myeloid leukemia (Kojima et al., 2013), chronic myeloid/lymphoid leukemia (Lapalombella et al., 2012), mantle cell lymphoma (Yoshimura et al., 2014) and plasma cell leukemia (Tai et al., 2014). In line with these observations, high level of CRM1 expression is correlated with tumor size, the presence of distant metastasis and poor prognosis in many cancer types. Therefore, CRM1 expression might have the potential to predict clinical outcome for several human tumor types. Importantly, CRM1 also plays an important role in drug resistance (Turner and Sullivan, 2008; Turner et al., 2012). Several different nuclear export inhibitors (NEIs) have been shown to sensitize drug-resistant cancer cells to anti-cancer drugs. These data suggest that interfering with the nuclear export

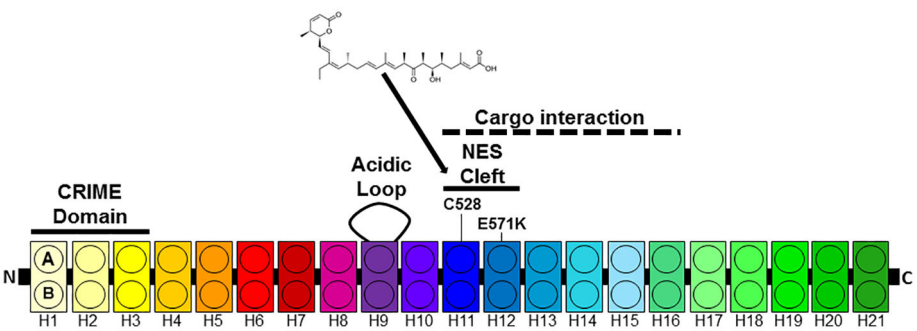

FIGURE 1 | Architecture of CRM1. CRM1 consists of 21 HEAT repeats each composed of two anti-parallel helices **(A, B)** connected by a linker loop. The N-terminal CRIME domain and the acidic loop contribute to RanGTP binding. The A helices of HEAT tandem 11 and 12 form the NES cleft. HEAT repeats 11–16 are involved in cargo e.g. Snurportin1 (Spn1) binding.

of tumor suppressor proteins or cell cycle inhibitors might contribute to overcome therapy resistance.

Binding of CRM1 to Leptomycin B

The progress made in understanding CRM1-mediated nuclear export is greatly based on the identification of Leptomycin B (LMB) as a CRM1 inhibitor (Kudo et al., 1998). LMB is natural product polyketide isolated from Streptomyces and has been originally discovered as a potent antifungal compound (Hamamoto et al., 1983). LMB contains two conjugated dienes, an α,β-unsaturated δ-lactone, a β-hydroxy-ketone moiety, and a terminal carboxylate (**Figure 2A**). Its molecular weight is 540-Da. LMB binds covalently to a cysteine residue in CRM1 in HEAT repeat 11 of CRM1 (Cys-528 in the human CRM1) which is located in the NES-binding groove by a Michael-type addition reaction *via* its α,β-unsaturated δ-lactone moiety (Kudo et al., 1999a). As LMB modifies a cysteine residue in CRM1 critical for NES-cargo binding, it inhibits the formation of the NES–CRM1–RanGTP complex and thereby the export of the cargo protein to the cytoplasm. Surprisingly, CRM1 acts as an enzyme hydrolyzing the lactone of LMB and thereby optimizing the LMB–CRM1 interaction. CRM1-induced modification of LMB leads to the irreversibility of the conjugation (Sun et al., 2013). LMB showed promising anti-cancer activity in preclinical experiments, but failed in clinical trial due to its systemic toxicity (Newlands et al., 1996). The dose limiting toxicity associated with LMB is thought to be due to a permanent block of nuclear export of essential macromolecules.

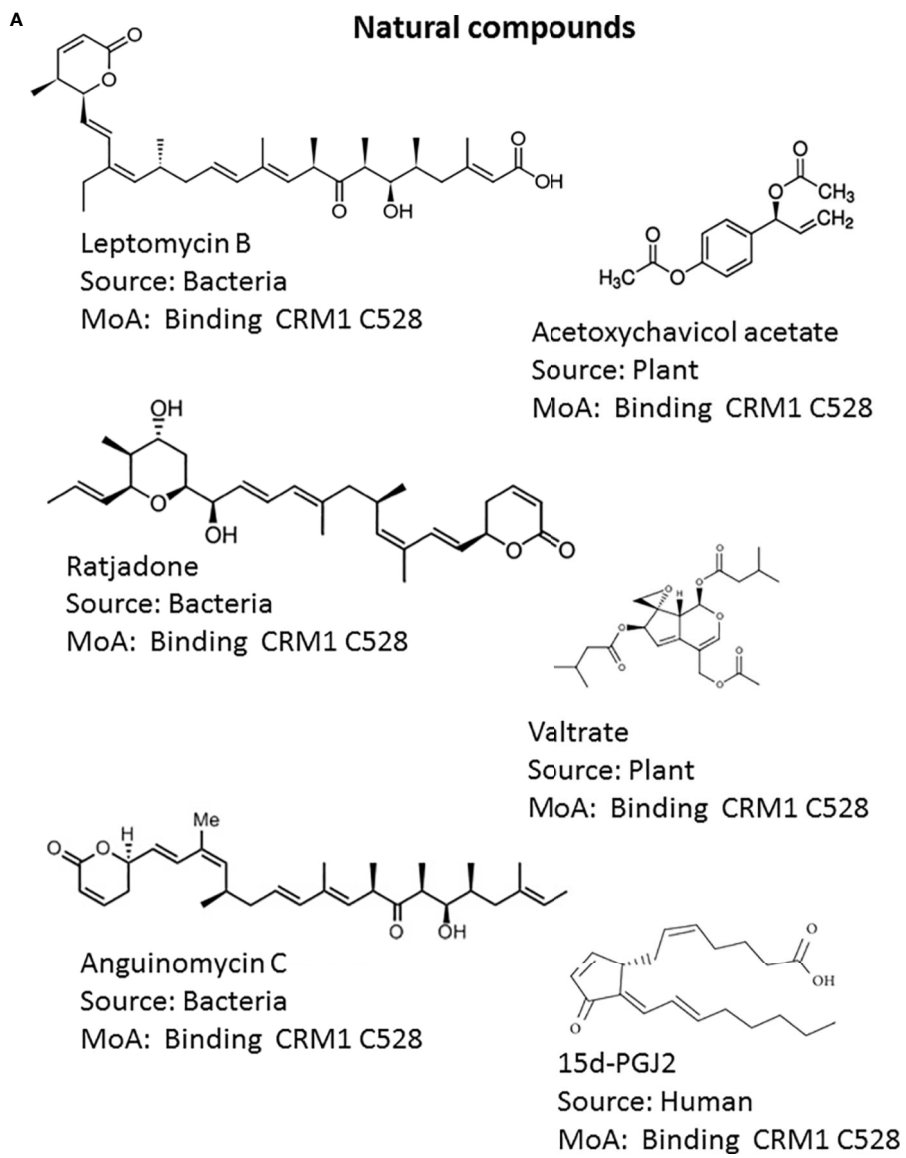

FIGURE 2 | Continued

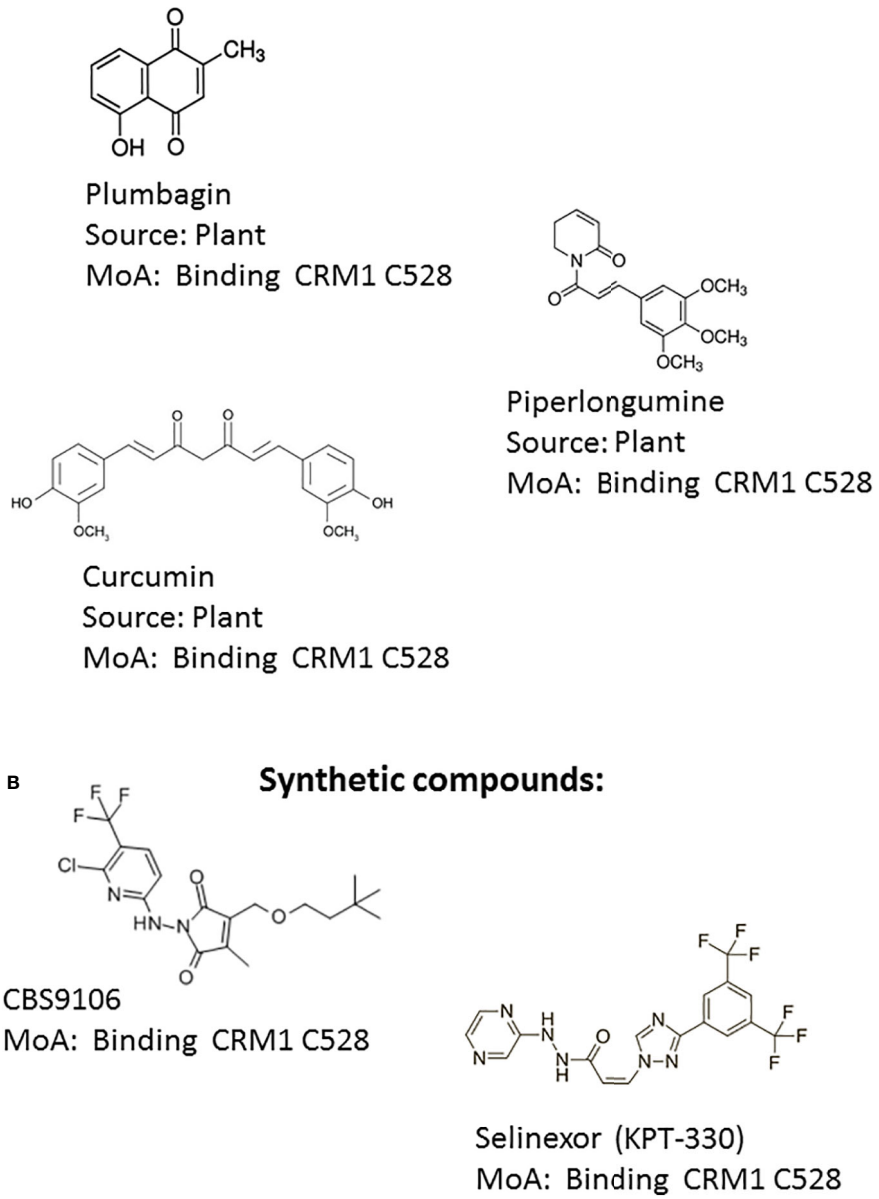

FIGURE 2 | Structures of CRM1 inhibitors. **(A)** Natural compounds: (1) Leptomycin B, (2) Acetoxychavicol acetate (3) Ratjadone, (4) Valtrate, (5) Anguinomycin C, (6) 15d-PGJ2, (7) Plumbagin, (8) Curcumin (9) Piperlongumine **(B)** Synthetic compounds: (10) CBS9106, (11) KPT-330 (Selinexor).

TARGETING THE CRM1-DRIVEN NUCLEAR EXPORT

Due to the crucial regulatory role and the alteration in human cancer, CRM1 has emerged as a therapeutic target for anticancer therapy. Although, altered CRM1 expression or activity is not always the driving force behind protein mislocalization, the inhibition of the nuclear export can prevent or correct aberrant subcellular protein localization (Hung and Link, 2011). For example, FOXO proteins are shuttled from the cell nucleus where they can act as tumor suppressors to the cytoplasm *via* CRM1-mediated nuclear export when they are phosphorylated by the AKT. AKT is a serine/threonine protein kinase and a key component of the PI3K/AKT signaling pathway, which is thought to be the most frequently activated signaling pathway in human cancer. While NEIs do not interfere with the signaling event that led to cytoplasmic mislocalization of FOXOs, they can trap FOXO factors in the cell nucleus and thereby promote their tumor suppressive function. Indeed, the clinically approved NEI Selinexor partially acts through trapping FOXO into the nucleus (Corno et al., 2018). Therefore, NEIs might not only be useful to treat tumors with altered CMR1 expression or function, but relocalize many tumor suppressor proteins or even mislocalize and thereby inactivate oncogenic proteins (Hung and Link,

2011). Although the groundwork to understand CRM1-mediated nuclear export has been developed over the last decades and the first generation of NEIs including LMB turned out to be to toxic to be used in the clinic, only more recently a significant therapeutic window for these inhibitors has been reported (Mutka et al., 2009). The therapeutic indications of these inhibitors are not limited to cancer but have also the potential to be used as antiviral agents.

Natural Product and Synthetic NEIs

The known NEIs can be classified into natural products and synthetic NEIs (**Figures 2A, B**). Natural product NEIs are derived from bacterial, plant, fungal or animal sources (**Table 1**) (Sun et al., 2016). The bacterial NEIs contain a polyketide chain with a lactone ring and include LMB, anguinomycin A/B/C/D and ratjadone A/C (Hamamoto et al., 1983; Köster et al., 2003; Bonazzi et al., 2010). Anguinomycins are analogs of LMB isolated from Streptomyces sp. Ratjadone is a cytotoxin isolated from myxobacteria from soil at Cala Ratjada on Mallorca island. These polyketide natural products covalently bind to Cys-528 in the human CRM1 and have IC50 values in the low nanomolar range (Sun et al., 2013). However, these NEIs are associated with severe dose limiting toxicities. While they are very powerful tools to study CRM1 function, they are not useful as therapeutic agents. NEIs derived from plants include acetoxychavicol acetate, valtrate, piperlongumine, curcumin, dibenzylideneacetone, gonionthalamin, and plumbagin. They are thought to bind to Cys528 of CRM1 with low affinity and inhibit CRM1 in the micromolar range. Acetoxychavicol acetate (ACA) is found in *Alpinia galangal* and was identified as an inhibitor of CRM1-dependent nuclear export by screening extracts from more than 600 medical plants (Ye and Li, 2006). Pharmacophore features of ACA have been defined. Similar to ACA, the chemically unrelated valtrate was found through screening 200 plant extracts. Valtrate is an iridoid ester with moderate lipophilicity extracted from *Valerianae radix* (Murakami et al., 2002). Both, ACA and valtrate have been shown to inhibit virus production (Watanabe et al., 2011). Furthermore, two food additives, namely piperlongumine and curcumin were found to inhibit CRM1-mediated nuclear export. The alkaloid piperlongumine is extracted from *Piper longum* Linn and exhibits multiple beneficial effects including selective cytotoxicity against several cancer cell lines. Accordingly, piperlongumine was shown to inhibit the CRM1 dependent transport of tumor suppressor proteins including FOXO1 and p21 (Niu et al., 2015b). Curcumin is a polyphenol compound present in *Curcuma longa* plant and is the main component of the Indian spice turmeric. It is known for its antioxidant, anti-cancer and anti-inflammatory effects. Curcumin and its structural analogue dibenzylideneacetone were shown to prevent the cytoplasmic accumulation of a reporter protein fused with NES in a CRM1-dependent manner (Niu et al., 2013). Similarly, a nuclear export assay and molecular modeling were used to characterize the styryl-lactone compound goniothalamin present in *Goniothalamus macrophyllus* as an inhibitor of nucleocytoplasmic transport *via* CRM1 (Wach et al., 2010). The natural bicyclic naphthoquinone plumbagin found in roots of plumbaginaceae which have been used in Indian traditional medicine was also identified as a CRM1 inhibitor and capable of blocking the nuclear export of RanBP1 and FOXO1 (Liu et al., 2014). Interestingly, the endogenous, anti-inflammatory prostaglandin 15d-PGJ2 has been shown to inhibit CRM1 by a LMB-like mechanism but with much less potency (Hilliard et al., 2010). Conversely, the mechanism of action for the diterpenoid oridonin present in *Rabdosia rubescens* remains to be determined. Oridonin inhibits inflammation and carcinogenesis and has been used in Chinese traditional medicine. It was shown to induce nuclear translocation of Crm1 and to increase the expression and nuclear accumulation of nucleoporin98, involved in Crm1-mediated nuclear export (Li et al., 2014).

The failure of the first generation of NEIs in clinical trials raised skepticism about the therapeutic potential of inhibiting nuclear export. Furthermore, preclinical evaluation of the semi-synthetic LMB derivative KOS-2462 (Mutka et al., 2009) and the synthetic small molecule CRM1 inhibitor CBS9106 (Sakakibara et al., 2011) did not lead to their clinical development (Parikh et al., 2014). The realization that there is the possibility of targeting nuclear export with an acceptable level of toxicity have spurred the development of second generation, synthetic CRM1 inhibitors, including CBS9106 (Sakakibara et al., 2011), PKF050-638 (Daelemans et al., 2002), 5219668 (Kau et al., 2003), compound3/4 (Monovich et al., 2009) and S109 (Niu et al., 2015a) and Selective Inhibitors of Nuclear Export (SINEs) (Kalid

TABLE 1 | Natural product nuclear export inhibitors.

Natural Product	Source	Mode of Action	Effect
Leptomycin B	Streptomyces	CRM1-Cys528	Potent nuclear export inhibition
Anguinomycin	Streptomyces	CRM1-Cys528	Potent nuclear export inhibition
Ratjadone	Myxobacteria	CRM1-Cys528	Potent nuclear export inhibition
Acetoxychavicol acetate	Alpinia galangal	CRM1-Cys528	Inhibit viral production
Valtrate	Valerianae Radix	CRM1-Cys528	Inhibit viral production
Piperlongumine	Piper longum	CRM1-Cys528	Nuclear tumor suppressor proteins
Curcumin	Curcuma longa	CRM1-Cys528	Nuclear reporter protein
Gonionthalamin	Goniothalamus macrophyllus	CRM1-Cys528	Nuclear reporter protein
Plumbagin	Plumbaginaceae	CRM1-Cys528	Nuclear RanBP1 and FOXO1
15d-PGJ2	Human prostaglandine	CRM1-Cys528	Nuclear TFIIAα
Oridonin	Rabdosia rubescens	n/d	Increased and nuclear Nup98
MDN-0105	Fungal metabolite	CRM1 n/d	Nuclear FOXO3, Rev, NF-κB

et al., 2012; Lapalombella et al., 2012; Ranganathan et al., 2012). The first molecule of this family of small molecule compounds was found by a screening effort aimed to identify new anti-HIV Rev inhibitors (Daelemans et al., 2002). The authors analyzed a collection of small molecules using a Rev-dependent luciferase reporter assay and identified PKF050-638 as an anti-viral agent. The SINE compounds include selinexor (KPT-330), verdinexor (KPT-335), KPT-185, KPT-276, and KPT-251. SINEs covalently bind to Cysteine 528 residue in a slowly reversible fashion. While a homozygous or heterozygous mutation of Cys528 conferred resistance to SINE treatment, the E571K mutation did not affect their inhibitory efficacy on the CRM1-mediated nuclear export (García-Santisteban et al., 2016; Jardin et al., 2016). Although, LMB and SINE share the same target amino acid residue of CRM1, SINEs are smaller and occupy less space of the NES groove (Lapalombella et al., 2012; Etchin et al., 2013; Haines et al., 2015; Hing et al., 2016). In addition, SINEs don´t undergo hydrolysis upon binding to CRM1 and don´t form a salt bridge with CRM1 (Etchin et al., 2013; Sun et al., 2013; Haines et al., 2015). Therefore, the binding of SINEs to CRM1 is slowly reversible (Sun et al., 2013). As a consequence inhibition of CRM1 mediated nuclear export is transient which might explain the reduced toxicity of SINEs compared to the one associated with LMB. SINE compounds have been analyzed in preclinical and clinical studies for numerous solid and hematologic cancers. These clinical trials include the treatment of lymphomas (non-Hodgkin's and diffuse large B-cell lymphoma), gliomas, sarcomas, breast cancer, lung cancer, pancreatic cancer, Myelodysplastic Syndromes (MDS), acute myeloid leukemia (AML), Acute lymphocytic leukemia (ALL) multiple myeloma, gastric cancer, esophageal cancer, colorectal cancer, prostate cancer, melanoma, thymic cancer, and gynecologic cancers (Wang and Liu, 2019). The spectrum of malignancies evaluated in these clinical trials underlines the broad applicability of CRM1 inhibitors (Wang and Liu, 2019). The recent clinical approval of Selinexor (Xpovio) also known as KPT-330 is the proof of concept for the therapeutic utility of manipulating the nuclear export. Selinexor has been approved for the treatment of patients with relapsed refractory multiple myeloma (Chari et al., 2019). Side effects associated with SINE treatment are less severe as expected from agents capable of inhibiting a core physiological process as the nuclear export of macromolecule.

NATURAL PRODUCTS AS A SOURCE OF NOVEL CRM1 INHIBITORS

Natural products are considered as an extremely valuable source for the discovery of new drugs against diverse pathologies. As yet only a fraction of the diversity of bioactive compounds has been explored and opportunities for discovering new natural products leading to new drugs are huge. Several approaches for identifying CRM1 Inhibitors have been reported (**Box 1**). Bacterial CRM1 inhibitors like LMB might provide Streptomyces with the capacity to kill fungi which restrict their growth. CRM1 is essential for the fungus. A change from Cys529 to Ser in a CRM1 mutant of *Saccharomyces pombe* render the fungus resistant to LMB, whereas Saccharomyces cerevisiae which does not carry a cysteine at that position is LMB insensitive (Kudo et al., 1999b; Yashiroda and Yoshida, 2003). Many organisms might have developed similar or slightly different capacities to fight and resist competitors. Therefore, is not fare-fetched to expect metabolites from natural origin to represent a rich source of potential nuclear export inhibitors with novel modes of action. Mutating Cys528 is an obvious yet not evaluated possibility of cancer cells to escape the selective pressure imposed by the treatment with covalent CRM1 inhibitors. It is also possible, that the therapeutic efficacy of CRM1 inhibition might also be limited in cancer cells that strongly overexpress CRM1, but increasing the dosing of covalent CRM1 inhibitors is impossible due to on-target and off-target toxicity. For the time being, all known CRM1

BOX 1 | Approaches for identifying CRM1 Inhibitors.

Approaches for identifying CRM1 Inhibitors

Several methods are useful in identifying CRM1 inhibitors including gene reporter assays and image-based high content screening.

Gene reporter assay

Daelemans et al. reported a screening campaign to identify inhibitors of the CRM1-mediated nuclear export of HIV-1 Rev protein using Rev-dependent luciferase reporter gene assay in Jurkat T cells (Daelemans et al., 2002). The reporter gene is flanked by splice sites under the control of the HIV-1 Rev response element (RRE). The cells are co-transfected firefly luciferase reporter gene fused to the p17 gag sequences and the RRE, flanked by the HIV-1 major splice sites, and driven by the CMV promoter and a vector that expresses HIV-1 Rev protein. Inhibitors of the Rev function cause a dose-dependent inhibition of Rev-dependent luciferase expression. The specificity of the compounds on Rev function can be tested on a Rev independent luciferase gene.

High Content Screening (HCS)

Image-based HCS (Zanella et al., 2010) has been widely used to screen for CRM1 inhibitors. The U2nesRELOC system uses human U2OS osteosarcoma cells that stably express a green fluorescent protein (GFP)-labeled Rev reporter protein that contains a heterologous nuclear export signal (NES). The fluorescent signal of U2nesRELOC cells is exclusively expressed in the cytoplasm. Treatment with NEIs such as LMB the fluorescent reporter rapidly accumulates in the nucleus (Cautain et al., 2015a). Acquisition and analysis of images is based on high content screening technology (Zanella et al., 2010). LMB is used as a positive control. As the cell nucleus is stained with 4,6-diamidino-2-phenylindole (DAPI), the cell nucleus can be visualized and the definition of its boundaries can support automated image analysis (Machado et al., 2019). In order to identify small molecule agents that inhibit the nuclear export of tumor suppressors from the nucleus *via* CRM1, we used the U2nesRELOC system to screen a library of natural product extracts from microbial origin. The collection of products was enriched in secondary metabolites (Cautain et al., 2014). 14,000 different extracts were evaluated for the capacity to accumulate the fluorescent signal in the nucleus of the reporter cells. From the 14,000 extracts, 6000 were obtained from fungi, another 6000 were derived from actinomycetes, and the remaining 2000 extracts were of marine actinomycete origin. 12 extracts with nuclear export inhibitory activities that were not associated with previously known active metabolites were identified. After purification of active compounds, several chemical structures of novel nuclear export inhibitors were identified including the fungal metabolite MDN-0105.

inhibitors act through covalent binding to Cys528 of CRM1. In addition, they all contain a Michael acceptor which makes them prone to target off effects by non-specific interaction with other targets. The perspective to identify and develop non-covalent inhibitors of CRM1 holds promise to increase efficacy by reducing drug resistance and on-target and off-target toxicity.

Natural product drug discovery is associated with specific limitations including the complexity of natural product chemistry, intellectual property landscape and sustainable supply. Bioavailability challenges associated with natural products could potentially be addressed by designing suitable drug delivery strategies.

CONCLUDING REMARKS

Interrupting the nuclear export of viral and cellular proteins mediated by CRM1 has emerged as an extremely promising therapeutic strategy to treat patients with viral infections and cancer. The clinical approval of the first-in-class CRM1 inhibitor Selinexor has proven the therapeutic potential of CRM1 inhibition for the treatment of cancer. Compounds derived from natural sources hold promise to support the discovery of new NEIs with a novel mode of action. Image-based high content screening of extract and compound collections is a very efficient way to identify natural products with inhibitory effect on the nuclear export.

AUTHOR CONTRIBUTIONS

All authors contributed to the critical discussion, text and figure preparation, and proofreading of the current manuscript.

FUNDING

This work was supported by Fundação para a Ciência e a Tecnologia (FCT) Research Center Grant UID/BIM/04773/2013 Centre for Biomedical Research 1334 and by the Spanish Ministry of Science, Innovation and Universities through Grant RTI2018-094629-B-I00 to WL. BF was supported by FCT-SFRH/BPD/100434/2014 and Marie Curie Individual Fellowship project TRIBBLES (#748585). This work was also supported by two LPCC-NRS/Terry Fox grants (2016/2017; 2017/2018).

ACKNOWLEDGMENTS

The authors would like to acknowledge the contribution of the COST Action CM1407 "Challenging organic syntheses inspired by nature—from natural products chemistry to drug discovery" and COST Action CA17104 "New diagnostic and therapeutic tools against multidrug resistant tumors".

REFERENCES

Bonazzi, S., Eidam, O., Güttinger, S., Wach, J. Y., Zemp, I., Kutay, U., et al. (2010). Anguinomycins and derivatives: Total syntheses, modeling, and biological evaluation of the inhibition of nucleocytoplasmic transport. *J. Am. Chem. Soc* 132, 1432–1442. doi: 10.1021/ja9097093

Cautain, B., de Pedro, N., Murillo Garzon, V., Munoz de Escalona, M., Gonzalez Menendez, V., Tormo, J. R., et al. (2014). High-content screening of natural products reveals novel nuclear export inhibitors. *J. Biomol. Screen* 19, 57–65. doi: 10.1177/1087057113501389

Cautain, B., de Pedro, N., Reyes, F., and Link, W. (2015a). Image-based identification of nuclear export inhibitors from natural products. *Methods Mol. Biol.* 1270, 307–319. doi: 10.1007/978-1-4939-2309-0_22

Cautain, B., Hill, R., de Pedro, N., and Link, W. (2015b). Components and regulation of nuclear transport processes. *FEBS J.* 282, 445–462. doi: 10.1111/febs.13163

Chari, A., Vogl, D. T., Gavriatopoulou, M., Nooka, A. K., Yee, A. J., Huff, C. A., et al. (2019). Oral Selinexor–Dexamethasone for Triple-Class Refractory Multiple Myeloma. *N. Engl. J. Med.* 381, 727–738. doi: 10.1056/nejmoa1903455

Corno, C., Stucchi, S., De Cesare, M., Carenini, N., Stamatakos, S., Ciusani, E., et al. (2018). FoxO-1 contributes to the efficacy of the combination of the XPO1 inhibitor selinexor and cisplatin in ovarian carcinoma preclinical models. *Biochem. Pharmacol.* 147, 93–103. doi: 10.1016/J.BCP.2017.11.009

Daelemans, D., Afonina, E., Nilsson, J., Werner, G., Kjems, J., De Clercq, E., et al. (2002). A synthetic HIV-1 Rev inhibitor interfering with the CRM1-mediated nuclear export. *Proc. Natl. Acad. Sci. U. S. A.* 99, 14440–14445. doi: 10.1073/pnas.212285299

Dian, C., Bernaudat, F., Langer, K., Oliva, M. F., Fornerod, M., Schoehn, G., et al. (2013). Structure of a truncation mutant of the nuclear export factor CRM1 provides insights into the auto-inhibitory role of its C-terminal helix. *Structure* 21, 1338–1349. doi: 10.1016/j.str.2013.06.003

Dong, X., Biswas, A., and Chook, Y. M. (2009a). Structural basis for assembly and disassembly of the CRM1 nuclear export complex. *Nat. Struct. Mol. Biol.* 16, 558–560. doi: 10.1038/nsmb.1586

Dong, X., Biswas, A., Süel, K. E., Jackson, L. K., Martinez, R., Gu, H., et al. (2009b). Structural basis for leucine-rich nuclear export signal recognition by CRM1. *Nature* 458, 1136–1141. doi: 10.1038/nature07975

Etchin, J., Sun, Q., Kentsis, A., Farmer, A., Zhang, Z. C., Sanda, T., et al. (2013). Antileukemic activity of nuclear export inhibitors that spare normal hematopoietic cells. *Leukemia* 27, 66–74. doi: 10.1038/leu.2012.219

Fornerod, M., Ohno, M., Yoshida, M., and Mattaj, I. W. (1997). CRM1 is an export receptor for leucine-rich nuclear export signals. *Cell* 90, 1051–1060. doi: 10.1016/S0092-8674(00)80371-2

Fukuda, M., Asano, S., Nakamura, T., Adachi, M., Yoshida, M., Yanagida, M., et al. (1997). CRM1 is responsible for intracellular transport mediated by the nuclear export signal. *Nature* 390, 308–311. doi: 10.1038/36894

Güttler, T., Madl, T., Neumann, P., Deichsel, D., Corsini, L., Monecke, T., et al. (2010). NES consensus redefined by structures of PKI-type and Rev-type nuclear export signals bound to CRM1. *Nat. Struct. Mol. Biol.* 17, 1367–1376. doi: 10.1038/nsmb.1931

Gao, W., Lu, C., Chen, L., and Keohavong, P. (2015). Overexpression of CRM1: A characteristic feature in a transformed phenotype of lung carcinogenesis and a molecular target for lung cancer adjuvant therapy. *J. Thorac. Oncol.* 10, 815–825. doi: 10.1097/JTO.0000000000000485

García-Santisteban, I., Arregi, I., Alonso-Mariño, M., Urbaneja, M. A., Garcia-Vallejo, J. J., Bañuelos, S., et al. (2016). A cellular reporter to evaluate CRM1 nuclear export activity: functional analysis of the cancer-related mutant E571K. *Cell. Mol. Life Sci.* 73, 4685–4699. doi: 10.1007/s00018-016-2292-0

Haines, J. D., Herbin, O., De La Hera, B., Vidaurre, O. G., Moy, G. A., Sun, Q., et al. (2015). Nuclear export inhibitors avert progression in preclinical models of inflammatory demyelination. *Nat. Neurosci.* 18, 511–520. doi: 10.1038/nn.3953

Hamamoto, T., GUNJI, S., TSUJI, H., and BEPPU, T. (1983). Leptomycins A and B, new antifungal antibiotics. I. Taxonomy of the producing strain and their fermentation, purification and characterization. *J. Antibiot. (Tokyo)* 36, 639–645. doi: 10.7164/antibiotics.36.639

Hill, R., Cautain, B., de Pedro, N., and Link, W. (2014). Targeting nucleocytoplasmic transport in cancer therapy. *Oncotarget* 5, 11–28. doi: 10.18632/oncotarget.1457

Hilliard, M., Frohnert, C., Spillner, C., Marcone, S., Nath, A., Lampe, T., et al. (2010). The anti-inflammatory prostaglandin 15-deoxy-Δ12,14- PGJ2 inhibits CRM1-dependent nuclear protein export. *J. Biol. Chem.* 285, 22202–22210. doi: 10.1074/jbc.M110.131821

Hing, Z. A., Fung, H. Y. J., Ranganathan, P., Mitchell, S., El-Gamal, D., Woyach, J. A., et al. (2016). Next-generation XPO1 inhibitor shows improved efficacy and in vivo tolerability in hematological malignancies. *Leukemia* 30, 2364–2372. doi: 10.1038/leu.2016.136

Hung, M. C., and Link, W. (2011). Protein localization in disease and therapy. *J. Cell Sci.* 124, 3381–3392. doi: 10.1242/jcs.089110

Inoue, H., Kauffman, M., Shacham, S., Landesman, Y., Yang, J., Evans, C. P., et al. (2013). CRM1 blockade by selective inhibitors of nuclear export attenuates kidney cancer growth. *J. Urol.* 189, 2317–2326. doi: 10.1016/j.juro.2012.10.018

Jardin, F., Pujals, A., Pelletier, L., Bohers, E., Camus, V., Mareschal, S., et al. (2016). Recurrent mutations of the exportin 1 gene (XPO1) and their impact on selective inhibitor of nuclear export compounds sensitivity in primary mediastinal B-cell lymphoma. *Am. J. Hematol.* 91, 923–930. doi: 10.1002/ajh.24451

Köster, M., Lykke-Andersen, S., Elnakady, Y. A., Gerth, K., Washausen, P., Höfle, G., et al. (2003). Ratjadones inhibit nuclear export by blocking CRM1/exportin 1. *Exp. Cell Res.* 286, 321–331. doi: 10.1016/S0014-4827(03)00100-9

Kalid, O., Toledo Warshaviak, D., Shechter, S., Sherman, W., and Shacham, S. (2012). Consensus Induced Fit Docking (cIFD): methodology, validation, and application to the discovery of novel Crm1 inhibitors. *J. Comput. Aided. Mol. Des.* 26, 1217–1228. doi: 10.1007/s10822-012-9611-9

Kau, T. R., Schroeder, F., Ramaswamy, S., Wojciechowski, C. L., Zhao, J. J., Roberts, T. M., et al. (2003). A chemical genetic screen identifies inhibitors of regulated nuclear export of a Forkhead transcription factor in PTEN-deficient tumor cells. *Cancer Cell* 4, 463–476. doi: 10.1016/S1535-6108(03)00303-9

Kojima, K., Kornblau, S. M., Ruvolo, V., Dilip, A., Duvvuri, S., Davis, R. E., et al. (2013). Prognostic impact and targeting of CRM1 in acute myeloid leukemia. *Blood* 121, 4166–4174. doi: 10.1182/blood-2012-08-447581

Koyama, M., and Matsuura, Y. (2010). An allosteric mechanism to displace nuclear export cargo from CRM1 and RanGTP by RanBP1. *EMBO J.* 29, 2002–2013. doi: 10.1038/emboj.2010.89

Kudo, N., Wolff, B., Sekimoto, T., Schreiner, E. P., Yoneda, Y., Yanagida, M., et al. (1998). Leptomycin B Inhibition of Signal-Mediated Nuclear Export by Direct Binding to CRM1. *Exp. Cell Res.* 242, 540–547. doi: 10.1006/excr.1998.4136

Kudo, N., Matsumori, N., Taoka, H., Fujiwara, D., Schreiner, E. P., Wolff, B., et al. (1999a). Leptomycin B inactivates CRM1/exportin 1 by covalent modification at a cysteine residue in the central conserved region. *Proc. Natl. Acad. Sci. U. S. A.* 96, 9112–9117. doi: 10.1073/pnas.96.16.9112

Kudo, N., Matsumori, N., Taoka, H., Fujiwara, D., Schreiner, E. P., Wolff, B., et al. (1999b). Leptomycin B inactivates CRM1/exportin 1 by covalent modification at a cysteine residue in the central conserved region. *Proc. Natl. Acad. Sci. U. S. A.* 96, 9112–9117. doi: 10.1073/pnas.96.16.9112

Lapalombella, R., Sun, Q., Williams, K., Tangeman, L., Jha, S., Zhong, Y., et al. (2012). Selective inhibitors of nuclear export show that CRM1/XPO1 is a target in chronic lymphocytic leukemia. *Blood* 120, 4621–4634. doi: 10.1182/blood-2012-05-429506

Li, F. F., Yi, S., Wen, L., He, J., Yang, L. J., Zhao, J., et al. (2014). Oridonin induces NPM mutant protein translocation and apoptosis in NPM1c+ acute myeloid leukemia cells in vitro. *Acta Pharmacol. Sin.* 35, 806–813. doi: 10.1038/aps.2014.25

Liu, X., Niu, M., Xu, X., Cai, W., Zeng, L., Zhou, X., et al. (2014). CRM1 is a direct cellular target of the natural anti-cancer agent plumbagin. *J. Pharmacol. Sci.* 124, 486–493. doi: 10.1254/jphs.13240FP

Machado, S., Raposo, C., Ferreira, B. I., and Link, W. (2019). Image-based Identification of Chemical Compounds Capable of Trapping FOXO in the Cell Nucleus. *Methods Mol. Biol.* 1890, 163–170. doi: 10.1007/978-1-4939-8900-3_14

Monecke, T., Güttler, T., Neumann, P., Dickmanns, A., Görlich, D., and Ficner, R. (2009). Crystal structure of the nuclear export receptor CRM1 in complex with snurportin1 and RanGTP. *Sci. (80-.).* 324, 1087–1091. doi: 10.1126/science.1173388

Monecke, T., Haselbach, D., Voß, B., Russek, A., Neumann, P., Thomson, E., et al. (2013). Structural basis for cooperativity of CRM1 export complex formation. *Proc. Natl. Acad. Sci. U. S. A.* 110, 960–965. doi: 10.1073/pnas.1215214110

Monovich, L., Koch, K. A., Burgis, R., Osimboni, E., Mann, T., Wall, D., et al. (2009). Suppression of HDAC nuclear export and cardiomyocyte hypertrophy by novel irreversible inhibitors of CRM1. *Biochim. Biophys. Acta Gene Regul. Mech.* 1789, 422–431. doi: 10.1016/j.bbagrm.2009.04.001

Murakami, N., Ye, Y., Kawanishi, M., Aoki, S., Kudo, N., Yoshida, M., et al. (2002). New Rev–transport inhibitor with anti–HIV activity from Valerianae Radix. *Bioorg. Med. Chem. Lett.* 12, 2807–2810. doi: 10.1016/S0960-894X(02)00624-8

Mutka, S. C., Yang, W. Q., Dong, S. D., Ward, S. L., Craig, D. A., Timmermans, P. B. M. W. M., et al. (2009). Identification of nuclear export inhibitors with potent anticancer activity in vivo. *Cancer Res.* 69, 510–517. doi: 10.1158/0008-5472.CAN-08-0858

Newlands, E. S., Rustin, G. J., and Brampton, M. H. (1996). Phase I trial of elactocin. *Br. J. Cancer* 74, 648–649. doi: 10.1038/bjc.1996.415

Niu, M., Wu, S., Mao, L., and Yang, Y. (2013). CRM1 Is a Cellular Target of Curcumin: New Insights for the Myriad of Biological Effects of an Ancient Spice. *Traffic* 14, 1042–1052. doi: 10.1111/tra.12090

Niu, M., Chong, Y., Han, Y., and Liu, X. (2015a). Novel reversible selective inhibitor of nuclear export shows that CRM1 is a target in colorectal cancer cells. *Cancer Biol. Ther.* 16, 1110–1118. doi: 10.1080/15384047.2015.1047569

Niu, M., Xu, X., Shen, Y., Yao, Y., Qiao, J., Zhu, F., et al. (2015b). Piperlongumine is a novel nuclear export inhibitor with potent anticancer activity. *Chem. Biol. Interact.* 237, 66–72. doi: 10.1016/j.cbi.2015.05.016

Noske, A., Weichert, W., Niesporek, S., Röske, A., Buckendahl, A.-C., Koch, I., et al. (2008). Expression of the nuclear export protein chromosomal region maintenance/exportin 1/Xpo1 is a prognostic factor in human ovarian cancer. *Cancer* 112, 1733–1743. doi: 10.1002/cncr.23354

Ossareh-Nazari, B., Bachelerie, F., and Dargemont, C. (1997). Evidence for a role of CRM1 in signal-mediated nuclear protein export. *Sci. (80-.).* 278, 141–144. doi: 10.1126/science.278.5335.141

Parikh, K., Cang, S., Sekhri, A., and Liu, D. (2014). Selective inhibitors of nuclear export (SINE)-A novel class of anti-cancer agents. *J. Hematol. Oncol.* 7, 78. doi: 10.1186/s13045-014-0078-0

Puente, X. S., Pinyol, M., Quesada, V., Conde, L., Ordóñez, G. R., Villamor, N., et al. (2011). Whole-genome sequencing identifies recurrent mutations in chronic lymphocytic leukaemia. *Nature* 475, 101–105. doi: 10.1038/nature10113

Ranganathan, P., Yu, X., Na, C., Santhanam, R., Shacham, S., Kauffman, M., et al. (2012). Preclinical activity of a novel CRM1 inhibitor in acute myeloid leukemia. *Blood* 120, 1765–1773. doi: 10.1182/blood-2012-04-423160

Saito, N., and Matsuura, Y. (2013). A 2.1-Å-resolution crystal structure of unliganded CRM1 reveals the mechanism of autoinhibition. *J. Mol. Biol.* 425, 350–364. doi: 10.1016/j.jmb.2012.11.014

Sakakibara, K., Saito, N., Sato, T., Suzuki, A., Hasegawa, Y., Friedman, J. M., et al. (2011). CBS9106 is a novel reversible oral CRM1 inhibitor with CRM1 degrading activity. *Blood* 118, 3922–3931. doi: 10.1182/blood-2011-01-333138

Santiago, A., Li, D., Zhao, L. Y., Godsey, A., and Liao, D. (2013). P53 SUMOylation promotes its nuclear export by facilitating its release from the nuclear export receptor CRM1. *Mol. Biol. Cell* 24, 2739–2752. doi: 10.1091/mbc.E12-10-0771

Schmidt, J., Braggio, E., Kortuem, K. M., Egan, J. B., Zhu, Y. X., Xin, C. S., et al. (2013). Genome-wide studies in multiple myeloma identify XPO1/CRM1 as a critical target validated using the selective nuclear export inhibitor KPT-276. *Leukemia* 27, 2357–2365. doi: 10.1038/leu.2013.172

Sendino, M., Omaetxebarria, M. J., and Rodríguez, J. A. (2018). Hitting a moving target: inhibition of the nuclear export receptor XPO1/CRM1 as a therapeutic approach in cancer. *Cancer Drug Resist* 1, 139–163. doi: 10.20517/cdr.2018.09

Shen, A., Wang, Y., Zhao, Y., Zou, L., Sun, L., and Cheng, C. (2009). Expression of crm1 in human gliomas and its significance in p27 expression and clinical prognosis. *Neurosurgery* 65, 153–160. doi: 10.1227/01.NEU.0000348550.47441.4B

Sun, Q., Carrasco, Y. P., Hu, Y., Guo, X., Mirzaei, H., MacMillan, J., et al. (2013). Nuclear export inhibition through covalent conjugation and hydrolysis of

Leptomycin B by CRM1. *Proc. Natl. Acad. Sci. U. S. A.* 110, 1303–1308. doi: 10.1073/pnas.1217203110

Sun, Q., Chen, X., Zhou, Q., Burstein, E., Yang, S., and Jia, D. (2016). Inhibiting cancer cell hallmark features through nuclear export inhibition. *Signal Transduction Targeting Ther.* 1, 16010. doi: 10.1038/sigtrans.2016.10

Tai, Y. T., Landesman, Y., Acharya, C., Calle, Y., Zhong, M. Y., Cea, M., et al. (2014). CRM1 inhibition induces tumor cell cytotoxicity and impairs osteoclastogenesis in multiple myeloma: Molecular mechanisms and therapeutic implications. *Leukemia* 28, 155–165. doi: 10.1038/leu.2013.115

Turner, J., and Sullivan, D. (2008). CRM1-Mediated Nuclear Export of Proteins and Drug Resistance in Cancer. *Curr. Med. Chem.* 15, 2648–2655. doi: 10.2174/092986708786242859

Turner, J. G., Dawson, J., and Sullivan, D. M. (2012). Nuclear export of proteins and drug resistance in cancer. *Biochem. Pharmacol.* 83, 1021–1032. doi: 10.1016/j.bcp.2011.12.016

van der Watt, P. J., Maske, C. P., Hendricks, D. T., Parker, M. I., Denny, L., Govender, D., et al. (2009). The Karyopherin proteins, Crm1 and Karyopherin β1, are overexpressed in cervical cancer and are critical for cancer cell survival and proliferation. *Int. J. Cancer* 124, 1829–1840. doi: 10.1002/ijc.24146

Van Der Watt, P. J., Zemanay, W., Govender, D., Hendricks, D. T., Parker, M. I., and Leaner, V. D. (2014). Elevated expression of the nuclear export protein, Crm1 (exportin 1), associates with human oesophageal squamous cell carcinoma. *Oncol. Rep.* 32, 730–738. doi: 10.3892/or.2014.3231

Wach, J. Y., Güttinger, S., Kutay, U., and Gademann, K. (2010). The cytotoxic styryl lactone goniothalamin is an inhibitor of nucleocytoplasmic transport. *Bioorg. Med. Chem. Lett.* 20, 2843–2846. doi: 10.1016/j.bmcl.2010.03.049

Wang, A. Y., and Liu, H. (2019). The past, present, and future of CRM1/XPO1 inhibitors. *Stem Cell Investig.* 6, 6. doi: 10.21037/sci.2019.02.03

Watanabe, K., Takatsuki, H., Sonoda, M., Tamura, S., Murakami, N., and Kobayashi, N. (2011). Anti-influenza viral effects of novel nuclear export inhibitors from Valerianae Radix and *Alpinia galanga*. *Drug Discovery Ther.* 5, 26–31. doi: 10.5582/ddt.v5.1.26

Yao, Y., Dong, Y., Lin, F., Zhao, H., Shen, Z., Chen, P., et al. (2009). The expression of CRM1 is associated with prognosis in human osteosarcoma. *Oncol. Rep.* 21, 229–235. doi: 10.3892/or_00000213

Yashiroda, Y., and Yoshida, M. (2003). Nucleo-Cytoplasmic Transport of Proteins as a Target for Therapeutic Drugs. *Curr. Med. Chem.* 10, 741–748. doi: 10.2174/0929867033457791

Ye, Y., and Li, B. (2006). 1′S-1′-acetoxychavicol acetate isolated from Alpinia galanga inhibits human immunodeficiency virus type 1 replication by blocking Rev transport. *J. Gen. Virol.* 87, 2047–2053. doi: 10.1099/vir.0.81685-0

Yoshimura, M., Ishizawa, J., Ruvolo, V., Dilip, A., Quintás-Cardama, A., McDonnell, T. J., et al. (2014). Induction of p53-mediated transcription and apoptosis by exportin-1 (XPO1) inhibition in mantle cell lymphoma. *Cancer Sci.* 105, 795–801. doi: 10.1111/cas.12430

Zanella, F., Lorens, J. B., and Link, W. (2010). High content screening: seeing is believing. *Trends Biotechnol.* 28, 237–245. doi: 10.1016/j.tibtech.2010.02.005

Zheng, Y., Gery, S., Sun, H., Shacham, S., Kauffman, M., and Koeffler, H. P. (2014). KPT-330 inhibitor of XPO1-mediated nuclear export has anti-proliferative activity in hepatocellular carcinoma. *Cancer Chemother. Pharmacol.* 74, 487–495. doi: 10.1007/s00280-014-2495-8

Zhou, F., Qiu, W., Yao, R., Xiang, J., Sun, X., Liu, S., et al. (2013). CRM1 is a novel independent prognostic factor for the poor prognosis of gastric carcinomas. *Med. Oncol.* 30 (726). doi: 10.1007/s12032-013-0726-1

Conflict of Interest: The authors declare that the research was conducted in the absence of any commercial or financial relationships that could be construed as a potential conflict of interest.

frontiers in Pharmacology

ORIGINAL RESEARCH
published: 08 May 2020
doi: 10.3389/fphar.2020.00599

Epoxylathyrane Derivatives as MDR-Selective Compounds for Disabling Multidrug Resistance in Cancer

Mariana Alves Reis[1†‡], *Ana M. Matos*[1‡], *Noélia Duarte*[1], *Omar Bauomy Ahmed*[2], *Ricardo J. Ferreira*[1,3], *Hermann Lage*[2] *and Maria-José U. Ferreira*[1*]

[1] Faculty of Pharmacy, Research Institute for Medicines (iMed.ULisboa), Universidade de Lisboa, Lisbon, Portugal, [2] Institute of Pathology, University Hospital Charité, Berlin, Germany, [3] Science for Life Laboratory, Department of Cell and Molecular Biology, Uppsala University, Uppsala, Sweden

Background: Multidrug resistance (MDR) has been regarded as one of the major hurdles for the successful outcome of cancer chemotherapy. The collateral sensitivity (CS) effect is one the most auspicious anti-MDR strategies. Epoxylathyrane derivatives **1–16** were obtained by derivatization of the macrocyclic diterpene epoxyboetirane A (**17**), a lathyrane-type macrocyclic diterpene isolated from *Euphorbia boetica.* Some of these compounds were found to strongly modulate P-glycoprotein (P-gp/ABCB1) efflux.

Purpose: The main goal was to develop lathyrane-type macrocyclic diterpenes with improved MDR-modifying activity, by targeting more than one anti-MDR mechanism.

Study design/methods: In this study, the potential CS effect of compounds **1**–**16** was evaluated against gastric (EPG85-257), pancreatic (EPP85-181), and colon (HT-29) human cancer cells and their drug-resistant counterparts, respectively selected against mitoxantrone (EPG85-257RNOV; EPP85-181RNOV; HT-RNOV) or daunorubicin (EPG85-257RDB; EPP85-181RDB; HT-RDB). The most promising compounds (**8**, **15**, and **16**) were investigated as apoptosis inducers, using the assays annexin V/PI and active caspase-3.

Results: The compounds were more effective against the resistant gastric cell lines, being the CS effect more significant in EPG85-257RDB cells. Taking together the IC_{50} values and the CS effect, compounds **8**, **15**, and **16** exhibited the best results. Epoxyboetirane P (**8**), with the strongest MDR-selective antiproliferative activity against gastric carcinoma EPG85-257RDB cells (IC_{50} of 0.72 μM), being 10-fold more active against this resistant subline than in sensitive gastric carcinoma cells. The CS effect elicited by compounds **15** and **16** appeared to be by inducing apoptosis *via* caspase-3 activation. Structure-activity relationships of the compounds were additionally obtained through regression models to clarify the structural determinants associated to the CS effect.

Conclusions: This study reinforces the importance of lathyrane-type diterpenes as lead molecules for the research of MDR-modifying agents.

Keywords: multidrug resistance, collateral sensitivity, apoptosis, *Euphorbia*, macrocyclic diterpenes, lathyrane, regression models

OPEN ACCESS

Edited by:
Cyril Corbet, Fonds National de la Recherche Scientifique (FNRS), Belgium

Reviewed by:
Krystyna Małgorzata Michalak, Wroclaw Medical University, Poland
Chin-Chuan Hung, China Medical University, Taiwan

***Correspondence:**
Maria-José U. Ferreira
mjuferreira@ff.ulisboa.pt

[†]***Present address:***
Mariana Alves Reis, Interdisciplinary Centre of Marine and Environmental Research (CIIMAR/CIMAR), University of Porto, Matosinhos, Portugal

[‡]*These authors share first authorship*

Specialty section:
This article was submitted to Pharmacology of Anti-Cancer Drugs, a section of the journal Frontiers in Pharmacology

Received: *31 January 2020*
Accepted: *17 April 2020*
Published: *08 May 2020*

Citation:
Reis MA, Matos AM, Duarte N, Ahmed OB, Ferreira RJ, Lage H and Ferreira M-JU (2020) Epoxylathyrane Derivatives as MDR-Selective Compounds for Disabling Multidrug Resistance in Cancer. Front. Pharmacol. 11:599. doi: 10.3389/fphar.2020.00599

INTRODUCTION

Multidrug resistance (MDR) is among the main clinical hurdles to successful cancer chemotherapy. It is defined by the development of cell resistance to a large variety of structurally unrelated drugs with diverse mechanisms of action. There is a great consensus that cancer cells might become resistant to anticancer drugs by several mechanisms that are still not completely understood and could occur simultaneously. Some of the most common cellular factors attributed to MDR include: changes in membrane transport through reduced drug uptake or augmented drug efflux; changes in drug targets and metabolism; increased DNA damage repair; and failure of apoptotic events. However, the most known and characterized MDR mechanism is owing to an increased efflux of the anticancer drugs as a result of the overexpression of ATP-binding cassette (ABC) transporter proteins, namely, P-glycoprotein (P-gp/ABCB1), multidrug resistance protein 1 (MRP1/ABCC1), and breast cancer resistance protein (BCRP/ABCG2) that act as extrusion pumps. From these mechanisms, P-gp still constitutes one of the biggest challenges for medicinal chemistry (Gottesman et al., 2002; Gottesman and Ling, 2006; Gottesman et al., 2016).

Several approaches have been developed to eradicate MDR in cancer. The most general has been the development of P-gp inhibitors to co-administer with anticancer drugs. However, despite great *in vitro* success, there is no P-gp inhibitor currently available for clinical use. The development of collateral sensitizing compounds is also included on the set of the most encouraging approaches to tackle MDR (Callaghan et al., 2014; Szakács et al., 2014). The collateral sensitivity (CS) effect is characterized by an increased sensitivity or hypersensitivity of resistant cells to certain compounds. The phenomenon was firstly recognized in the early 1950s, when it was observed that resistant *Escherichia coli* was hypersensitive to several drugs at the same time (Szybalski and Bryson, 1952). Based on this concept, which presently is considered a strong anti-MDR strategy, alterations of cancer cells that confer resistance to certain agents might simultaneously generate weaknesses that may rend drug-resistant cells more sensitive to alternative drugs than the corresponding parental cells. CS is thought to be highly correlated with the overexpression of one of the three major efflux proteins (P-gp, MRP1 or BCRP) in resistant cancer cells, therefore representing a new strategy to circumvent ABC transporters-mediated MDR (Gottesman et al., 2016). Thus, these vulnerabilities developed by cancer cells can be targeted for improving chemotherapy by developing compounds that are selective against resistant-phenotypes (MDR-selective compounds) and thus able to re-sensitize resistant tumors and reestablish drugs effectiveness. Several compounds have been reported to exert CS. However, although many hypotheses have been proposed, the mechanism of collateral sensitizing compounds remains unclear (Callaghan et al., 2014; Szakács et al., 2014). In this way, while in P-gp-overexpressing cancer cells, CS agents seem to be related to diverse biochemical mechanisms, in MRP1-overexpressing cancer cells, CS agents appeared to behave as stimulators of glutathione efflux, altering redox balance and thus triggering apoptosis of multi-resistant cells (Klukovits and Krajcsi, 2015).

Natural products have been of crucial importance for drug research and development. Concerning cancer, since the beginning of chemotherapy in the 1940s to date, about 75% of anticancer drugs approved world-wide are natural products or their synthetic derivatives (Newman and Cragg, 2012). In an effort to find out anticancer compounds from plants, for targeting MDR cancer cells, our group has been given particular attention on the development of MDR reversal compounds (Reis et al., 2015; Paterna et al., 2016; Ramalhete et al., 2016; Reis et al., 2016; Reis et al., 2017; Ferreira et al., 2018a; Ferreira et al., 2018b; Paterna et al., 2018; Ramalhete et al., 2018). Duo to the high and unusual chemical diversity of their metabolites, many of which coupled with strong biological properties, we have given particular attention to *Euphorbia* species (Euphorbiaceae), which are well known since ancient times for their use in folk medicine worldwide, namely, to cure cancer, tumors, and warts (Hartwell, 1969; Ernst et al., 2015). Other significant reported uses included treatment of respiratory and digestive disorders and inflammation (Ernst et al., 2015). Most importantly, in 2012, Food and Drug Administration (FDA) and European Medicines Agency (EMA) approved ingenol 3-angelate (Picato®), isolated from *Euphorbia peplus,* for the treatment of actinic keratosis. This diterpene ester, with a dual and unique mechanism of action embracing a rapid cellular necrosis and a specific immune response (Rosen et al., 2012), is a valuable example of the strong bioactivity and pharmacological importance of some *Euphorbia* genus metabolites.

Jatrophane and lathyrane-type diterpenes, from *Euphorbia* species, have revealed a significant MDR modulatory activity through reversion of the ABCB1 MDR phenotype (Ferreira et al., 2014). Aiming at optimizing their structures for improving their MDR reversal activity, *in silico* and structure-activity relationship studies were performed (Ferreira et al., 2011; Reis et al., 2012; Sousa et al., 2012; Ferreira et al., 2013; Reis et al., 2013; Baptista et al., 2016). In this regard, *Euphorbia boetica* Boiss. (Euphorbiacae) was a fruitful source of novel compounds and prototypes for the design of MDR reversers (Vieira et al., 2014; Matos et al., 2015). Macrocyclic diterpene derivatives with the lathyrane skeleton, obtained from this species, were found promising ABCB1 efflux modulators (Vieira et al., 2014; Matos et al., 2015).

Therefore, the present work aimed at assessing the ability of the macrocyclic diterpene derivatives **1–16** (**Figure 1**) for their potential as collateral sensitizing compounds, using the human tumor gastric (EPG85-257), pancreatic (EPP85-181), and colon (HT-29) cell models (drug-sensitive and drug-resistant sublines),

Abbreviations: ABC, ATP binding cassette; ABCB1, ATP-binding cassette, sub-family B; CS, collateral sensitivity; EPG85- 257P, parental gastric cancer cells; EPG85- 257RDB, gastric cancer cells selected against daunorubicin; EPG85-257RNOV, gastric cancer cells selected against mitoxantrone; EPP-181 RDB, pancreatic cancer cells selected against daunorubicin; EPP-181P, parental pancreatic cancer cells; EPP-181RNOV, pancreatic cancer cells selected against mitoxantrone; MDR, multidrug resistance; *MDR1*, multidrug resistance gene 1; RR, relative resistance; NB, Naïve Bayes; RT, random trees.

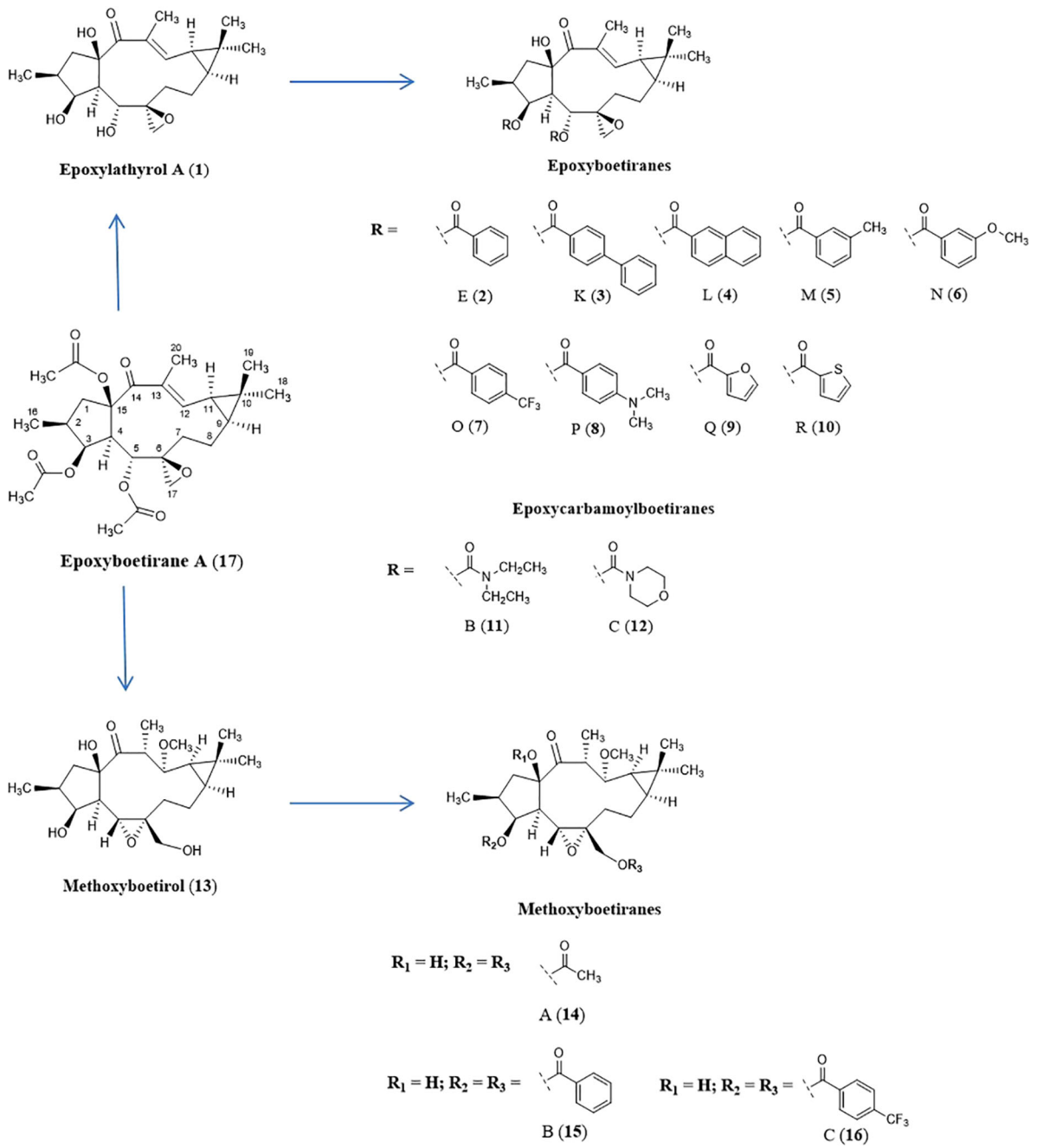

FIGURE 1 | Structures of compounds **1**–**17**.

well described for MDR (**Table S2**; Lage et al., 2010; Hilgeroth et al., 2013; Reis et al., 2014). Additionally, the MDR-selective antiproliferative activity mode of action of compounds **8**, **15**, and **16** was assessed towards apoptosis and caspase-3 activation, using the same cell lines. From the obtained results, and to better understand which structural features are correlated with the observed CS effect, regression models were further obtained from molecular descriptors calculated for a small library of macrocyclic diterpenes.

MATERIALS AND METHODS

Tested Compounds

Epoxylathyrane derivatives (**1**–**16**), namely, epoxylathyrol (**1**), epoxyboetirane E (**2**), epoxyboetirane L (**4**), epoxyboetirane M (**5**), epoxyboetirane N (**6**), epoxyboetirane O (**7**), epoxyboetirane P (**8**), epoxyboetirane Q (**9**), epoxyboetirane R (**10**), epoxycarbamoylboetirane B (**11**), epoxycarbamoylboetirane C (**12**), methoxyboetirane B (**15**), and methoxyboetirane C (**16**),

were obtained by derivatization of the macrocyclic diterpene epoxyboetirane A (**17**), isolated from *Euphorbia boetica* (Vieira et al., 2014; Matos et al., 2015). Briefly, epoxyboetirane A, was firstly hydrolyzed, yielding mostly epoxylathyrol (**1**). Methoxyboetirol (**13**), resulting from a Payne-rearranged Michael adduct, was also obtained as minor product. Compound **2–12** and **14–16** were obtained by acylation reactions of epoxylathyrol (**1**) and methoxyboetirol (**13**), respectively (Vieira et al., 2014; Matos et al., 2015).

Cell Lines, Cell Culture

The establishment and characterization of the cell lines EPG85-257P (gastric); EPP85-181P (pancreatic); and HT-29P (colon) and their drug-resistant sublines (EPG85-257RNOV, EPG85-257RDB, EPP85-181RNOV, EPP85-181RDB, HT-29RNOV, HT-29RDB used have been described previously (Reis et al., 2014). More experimental details at supplementary material and **Table S2**.

Cell Proliferation Assay, Annexin V/PI Staining, and Active Caspase-3 Assay

The antiproliferative activity of compounds was evaluated using a proliferation assay based on sulforhodamine B (SRB) staining, as previously described (Reis et al., 2014). More experimental details at supplementary material.

For detection of cytotoxic drug-induced apoptosis, a FITC Annexin V apoptosis detection kit (BD Pharmingen, BD Biosciences) was used. Detection of intracellular presence of active caspase-3 was also performed using FITC active Caspase-3 Apoptosis Kit (BD Pharmingen, BD Biosciences). Both assays followed the same experimental design, described at supplementary material.

Regression Models

For a given set of molecules obtained in the present and previous works ($N = 42$, **Table S1**) (Reis et al., 2014; Reis et al., 2016; Reis et al., 2017), a comprehensive database of molecular descriptors (constitutional, topological, and geometrical) was obtained from E-DRAGON, PaDEL, and MOE as in a previous work (Baptista et al., 2016). Afterward, relative resistant (RR) values obtained in the EPG-257RDB cell line were added to the dataset and transformed into a binary classification of 1 ($RR \leq 0.5$) or 0 ($RR > 0.5$) for the presence or absence of CS, respectively. All QSAR models were built using WEKA v3.8.3 (Hall et al., 2009) software as previously reported (Baptista et al., 2016), with only minor modifications. The CfsSubsetEval algorithm with the BestFirst search method was applied as default prior to model classification. All models were generated using WEKA's default options. The robustness of the generated models (NB and RT) were assessed by a 10-fold cross-validation and their predictive power by splitting the dataset into training and test sets (66:34). All models were analysed using several parameters, among which true positive rate (TP), false positive rate (FP), precision, Matthews Correlation Coefficient (MCC), and Receiver Operating Characteristics (ROC) area under the curve. Other parameters as the mean absolute error (MAE), root mean squared error (RMSE), and Kappa statistic (k) were also used to assess the reliability of the model.

RESULTS AND DISCUSSION

Collateral Sensitivity Effect

Aiming at optimizing macrocyclic diterpenes with lathyrane scaffold as active MDR reversal agents, the phytochemical investigation of *Euphorbia boetica* aerial parts (methanolic extract) was conducted, yielding several compounds with the lathyrane scaffold (Vieira et al., 2014). Epoxylathyrane A (**17**), a lathyrane polyester isolated in large amount, was hydrolyzed, in an alkaline methanolic solution, giving rise to epoxylathyrol (**1**), as main product, and a Payne-rearranged Michael adduct named methoxyboetirol (**13**) (Matos et al., 2015). In this previous work, compounds **1** and **13** were acylated, yielding the derivatives **2–12** and **14–16**, respectively. The potential of epoxylathyrane derivatives **1–16** as P-gp-mediated MDR reversers, was evaluated at non-cytotoxic doses in L5178Y *ABCB1*-transfected mouse T-lymphoma cells, by the accumulation rhodamine-123 assay. Most of the tested derivatives exhibited strong P-gp modulating activities and, in addition, they were able to enhance the cytotoxicity of doxorubicin in a synergistic mode, restoring its sensitivity by reversion of the ABCB1-MDR phenotype. By structure-activity relationships studies, it was concluded that the presence of an aromatic moiety on those structures improved significantly the inhibition of rhodamine-123 efflux (Matos et al., 2015).

Taking into account that targeting more than one MDR mechanism could be a way to provide a good therapeutic outcome, in the course of the development of epoxylathyrane derivatives as MDR reversal agents, it is also important to consider other potential anti-MDR mechanisms of action (Fojo, 2008; Gottesman et al., 2016). Therefore, the epoxylathyrane derivatives **1–16** were investigated for their potential CS effect against gastric (EPG85-257), pancreatic (EPP85-181), and colon (HT-29) human cancer cells and their drug-resistant counterparts, respectively selected against mitoxantrone (RNOV) or daunorubicin (RDB), using a proliferation assay (Reis et al., 2014). The MDR-selective activity was assessed by the relative resistance ratio ($RR = IC_{50(resistant)}/IC_{50(parental)}$). Values of $RR < 1$ indicate that the compound kills MDR cells more effectively than parental cells, but if $RR \leq 0.5$, then a CS effect is taking place (Hall et al., 2009). The cytotoxic agents etoposide and cisplatin were used as positive controls. The antiproliferative activity and CS effects of compounds **1–16** are presented in **Tables 1–4**. The heat map represented in **Table 1** allows the recognition of compounds that exhibit MDR-selective activity at a specific IC_{50} level.

As showed in **Tables 2–4**, the strongest antiproliferative effect in drug-sensitive cell lines was observed for epoxyboetirane P (**8**), bearing *p*-(dimethylamino)benzoyl acyl groups, that exhibited an $IC_{50} < 10$ μM in the three cell lines tested (EPG85-257P, EPP85-181P, and HT-29P, $IC_{50} = 7.81 \pm 2.01$, 4.88 ± 0.11, and 8.24 ± 0.47, respectively). An $IC_{50} < 10$ μM was also found for

TABLE 1 | Heat map table summarizing the antiproliferative and collateral sensitivity results against gastric carcinoma cells (EPG85-257P, EPG85-257RNOV, and EPG85-257RDB), and pancreatic carcinoma cells (EPP85-181P, EPP85-181RNOV, and EPP85-181RDB). This representation allows finding compounds that present MDR-selective activity at a determined IC_{50} level. CS values (RR ≤ 0.5) are presented.

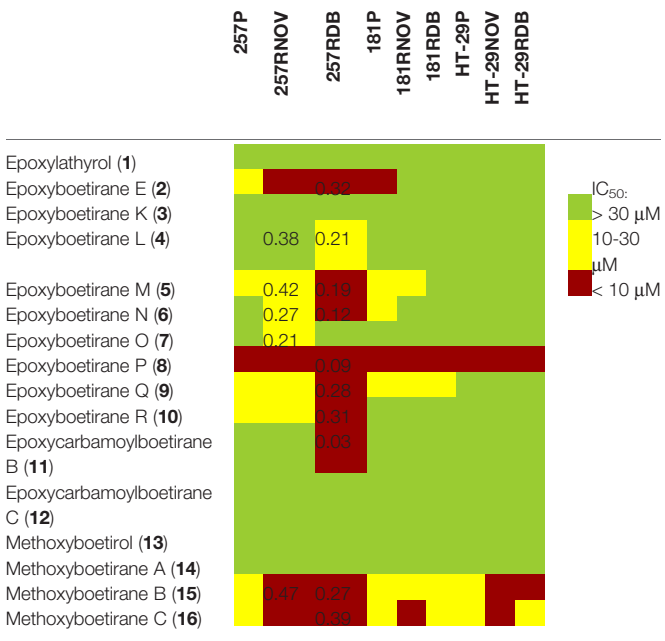

epoxyboetirane E (**2**) but only in pancreatic parental cells (EPP85-181P, IC_{50} = 9.52 ± 0.40). Significant IC_{50} values were also observed for methoxyboetiranes B (**15**) and C (**16**), in gastric parental cells (EPG85-257P, IC_{50} = 12.52 ± 1.15 and 10.12 ± 0.68, respectively), exhibiting the former (**15**) also an IC_{50} = 12.08 ± 1.84, against pancreatic cells. The other compounds were inactive or barely active, displaying a moderate/weak antiproliferative activity in parental drug-sensitive cell lines (**Tables 2**–**4**).

When analyzing the results against MDR sublines, several compounds were found to be more active against multidrug-resistant cells than in parental cells (**Tables 2**–**4**), exhibiting relative resistance values lower than 1.0. Moreover, as it can be observed, some compounds showed CS effect (RR ≤ 0.5), being more effective toward the resistant gastric cell lines, and more pronounced in EPG85-257RDB cells (**Tables 1** and **2**), which are characterized by ABCB1 overexpression (Dietel et al., 1990). Taking together the IC_{50} and RR values, the best results were found for epoxyboetirane P (**8**), which showed an antiproliferative effect 10-fold higher against the MDR subline of gastric carcinoma EPG85-257RDB than in parental drug-sensitive cells (IC_{50} = 0.72 ± 0.08; RR = 0.09). A selective IC_{50} value was also obtained with this compound against the resistant EPG85-257 RNOV subline (IC_{50} = 5.91 ± 1.15), although without CS effect (RR = 0.76). CS effect, associated with potent antiproliferative activity, was also registered for methoxyboetiranes B (**15**), (IC_{50} = 3.39 ± 0.44; RR = 0.27), and C (**16**) (IC_{50} = 3.98 ± 0.31; RR = 0.39), against the gastric EPG85-257 RDB subline, whose IC_{50} values were comparable to those of the positive controls etoposide and cisplatin and (IC_{50} = 6.2 ± 0.3 and 4.0 ± 0.3, respectively). Compound **15**, having unsubstituted benzoyl moieties, showed also CS effect in EPG85-257 RNOV subline (IC_{50} = 5.89 ± 0.62; RR = 0.47), whereas compound **16**, having trifluoromethyl substituents at *para*-position, exhibited slightly higher relative resistance and IC_{50} values (IC_{50} = 8.25 ± 1.49; RR = 0.82). Furthermore, epoxyboetyranes E, M, N, O, R (**2**, **5**, **6**, **9,** and **10**) and epoxycarbamoylboetirane B (**11**) also exhibited CS effect (RR ≤ 0.5) coupled with high selective antiproliferative activity (IC_{50} values ranging from 2.59 ± 0.39 to 7.15 ± 1.24) against the gastric EPG85-257 RDB subline. Excepting for compound **11**, comparable results were also

TABLE 2 | Antiproliferative activity of compounds **1–16** in gastric carcinoma cells: EPG85-257P (parental), EPG85-257RNOV (multidrug resistance [MDR] phenotype), and EPG85-257RDB (multidrug resistance [MDR] phenotype).

Compound	EPG85-257P	EPG85-257RNOV		EPG85-257RDB	
	IC_{50} ± SD (µM)	IC_{50} ± SD (µM)	RR[a]	IC_{50} ± SD (µM)	RR[a]
Epoxylathyrol (**1**)	>100	> 100	—	70.53 ± 6.24	< 0.70
Epoxyboetirane E (**2**)	19.67 ± 1.56	9.97 ± 0.38	0.50	6.40 ± 0.68	0.32
Epoxyboetirane L (**4**)	>100	38.17 ± 2.39	<0.38	21.13±1.76	< 0.21
Epoxyboetirane M (**5**)	>25 [b]	10.53 ± 0.44	<0.42	4.74 ± 0.21	< 0.19
Epoxyboetirane N (**6**)	39.67 ± 4.88	10.62 ± 0.64	0.27	4.56 ± 0.47	0.12
Epoxyboetirane O (**7**)	>100	21.41 ± 1.35	<0.21	50.91 ± 4.95	< 0.50
Epoxyboetirane P (**8**)	7.81 ± 2.01	5.91 ± 1.15	0.76	0.72 ± 0.08	0.09
Epoxyboetirane Q (**9**)	>25 [b]	>25 [b]	—	7.15 ± .1.24	< 0.28
Epoxyboetirane R (**10**)	21.08. ± 2.53	10.73 ± 1.36	0.50	6.63 ± 0.97	0.31
Epoxycarbamoylboetirane B (**11**)	>100	78.13 ± 3.69	<0.78	2.59 ± 0.39	< 0.03
Methoxyboetirane B (**15**)	12.52 ± 1.15	5.89 ± 0.62	0.47	3.39 ± 0.44	0.27
Methoxyboetirane C (**16**)	10.12 ± 0.68	8.25 ± 1.49	0.82	3.98 ± 0.31	0.39
Etoposide	0.105 ± 0.0	1.55 ± 0.1	14.8	6.2 ± 0.3	59
Cisplatin	4.4 ± 0.4	2.6 ± 0.2	0.6	4.0 ± 0.3	1
DMSO (2%)	>100	>100	—	>100	—

*[a]Relative resistance ratio, RR = $IC_{50(resistant)}/IC_{50(parental)}$; [b]above this concentration the compound crystallized in the culture medium. For compounds **3**, **12, 13** and **14** the IC_{50} values were found to be above 100 µM against the parental and both resistant cells. Each IC_{50} value indicates the mean ± SD of n = 3 to 4 independent experiments (each concentration was performed in triplicate per experiment).*

TABLE 3 | Antiproliferative activity of **1–16** in in pancreatic carcinoma cells: EPP85-181P (parental), EPP85-181RNOV (multidrug resistance [MDR] phenotype), and EPP85-181RBD (multidrug resistance [MDR] phenotype).

Compound	EPP85-181P	EPP85-181RNOV		EPP85-181RDB	
	IC_{50} ± SD (μM)	IC_{50} ± SD (μM)	RR[a]	IC_{50} ± SD (μM)	RR[a]
Epoxyboetirane E (**2**)	9.52 ± 0,40	41.24 ± 3.54	4.33	13.18 ± 1.65	1.38
Epoxyboetirane M (**5**)	17.49 ± 0.08	> 25 [b]	> 1.43	21.07 ± 2.06	1.20
Epoxyboetirane N (**6**)	20.63 ± 0.90	57.33 ± 4.90	2.78	14.17 ± 2.34	0.69
Epoxyboetirane P (**8**)	4.88 ± 0.11	5.42 ± 0.49	1.11	2.57 ± 0.30	0.53
Methoxyboetirane B (**15**)	12.08 ± 1.84	10.01 ± 0.42	0.83	10.18 ± 0.81	0.84
Methoxyboetirane C (**16**)	16.51 ± 1.97	8.72 ± 0.43	0.53	20.95 ± 1.79	1.27
Etoposide	0.58 ± 0.0	4.5 ± 0.7	7.8	62.0 ± 4.2	106.9
Cisplatin	0.08 ± 0.0	2.6 ± 0.2	34	0.09 ± 0.0	1.2
DMSO (2%)	> 100	> 100	—	> 100	—

*[a]Relative resistance ratio, RR = $IC_{50(resistant)}/IC_{50(parental)}$ [b]above this concentration the compound crystallized in the culture medium. For all the other compounds (**1 3**, **4**, **7** and **11-14**), the IC_{50} values were found to be above 100 μM, except for epoxyboetiranes Q (**9**) and R (**10**) which was above 25 μM and 50 μM, respectively, the maximum tested concentrations for each due to lower water solubility. Each IC_{50} value indicates the mean ± SD of n = 3 to 4 independent experiments (each concentration was performed in triplicate per experiment).*

observed for this set of compounds in the EPG85-257 RNOV subline, although associated with a lower antiproliferative effect (**Table 2**).

The tested compounds were less active and showed no CS effect in pancreatic cancer cell lines (**Tables 1** and **3**). Epoxyboetirane P (**8**) was once more the most active (IC_{50} < 10 μM) in parental and both resistant sublines, exhibiting MDR-selective antiproliferative effects (RR < 1) in resistant EPP85-181RRDB subline (EPP85-181P, IC_{50} = 4.88 ± 0.11; EPP85-181RDB, IC_{50} = 2.57 ± 0.30, RR = 0.53; EPP85-181RNOV, IC_{50} = 5.42 ± 0.49, RR = 1.11). When comparing with the positive controls, methoxyboetirane B (**15**) also showed significant antiproliferative activity in both resistant sublines associated with RR < 1 (EPP85-181RDB, IC_{50} = 10.18 ± 0.81, RR = 0.84; EPP85-181RNOV, IC_{50} = 10.01 ± 0.42, RR = 0.83).

In turn, the best results revealed by methoxyboetirane C (**16**) were in EPP85-181RNOV subline, showing an IC_{50} = 8.72 ± 0.43. (RR = 0.53).

Epoxyboetirane P (**8**) also showed the lowest IC_{50} values in colon cancer cell lines (**Table 4**), (HT-29RDB, IC_{50} = 5.25 ± 0.07 μM, RR = 0.64; HT-29RNOV; IC_{50} = 5.00 ± 0.16 μM, RR = 0.61). However, in colon cancer cells, CS effect (RR ≤ 5), associated with significant antiproliferative activity (IC_{50}≤ 10), was only observed for methoxyboetirane B (**15**), with similar results in both resistant variants (HT-29RDB, IC_{50} = 9.61 ± 0.10, RR = 0.47; HT-29RNOV IC_{50} = 9.40 ± 0.30, RR = 0.46). Methoxyboetirane C (**16**) showed comparable IC_{50} values against HT-29RNOV variant (9.39 ± 0.37, RR = 0.55). Indeed, it exhibited RR< 1 in HT-29RDB subline although with lower antiproliferative activity (IC_{50} = 13.12 ± 1.15, RR = 0.76).

When analyzing the results, it could be concluded that the antiproliferative activity depends on the acylation patterns. Thus, in both epoxylathyrol (**1**) and methoxyboetirol (**13**) derivatives, (**2–12** and **13–16**, respectively), acyl moieties bearing simple aromatic moieties, including benzoyl (**2**, **5**, **6–8**, **15**, **16**) furoyl (**9**), and thiophenecarbonyl (**10**) groups, were generally favorable for the antiproliferative activity. Conversely, compounds with biphenylcarbonyl (**3**) and naphthoyl substituents (**4**) were inactive or barely active in the three human cancer parental cells and corresponding MDR-sublines. No significant activity was observed for the parent compounds epoxylathyrol (**1**) and methoxyboetirol (**13**), without ester moieties, and for compounds **11**, **12,** and **14,** bearing aliphatic acyl moieties.

As already mentioned, this set of macrocyclic diterpenes (**1–16**) was previously evaluated for their ability to reverse P-gp-mediated MDR, using a functional assay (Vieira et al., 2014;

TABLE 4 | Antiproliferative activity of compounds **1–16** in colon carcinoma cells HT-29P (parental), HT-29RNOV (multidrug resistance [MDR] phenotype), and HT-29RBD (multidrug resistance [MDR] phenotype).

Compound	HT-29P	HT-29RNOV		HT-29RDB	
	IC_{50} ± SD (μM)	IC_{50} ± SD (μM)	RR[a]	IC_{50} ± SD (μM)	RR[a]
Epoxyboetirane E (**2**)	> 50[b]	32.27 ± 4.69	< 0.65	47.21 ± 5.17	< 0.94
Epoxyboetirane N (**6**)	> 100	48.92 ± 4.92	< 0.49	31.16 ± 0.53	< 0.31
Epoxyboetirane P (**8**)	8.24 ± 0.47	5.00 ± 0.16	0.61	5.25 ± 0.07	0.64
Epoxyboetirane R (**10**)	> 50[b]	30.20 ± 4.05	< 0.60	> 50[b]	—
Methoxyboetirane B (**15**)	20.40 ± 1.83	9.40 ± 0.30	0.46	9.61 ± 0.10	0.47
Methoxyboetirane C (**16**)	17.20 ± 2.62	9.39 ± 0.37	0.55	13.12 ± 1.15	0.76
Cisplatin	3.8 ± 0.1	3.8 ± 0.1	1	2.7 ± 0.1	0.7
Etoposide	2.3 ± 0.3	35.0 ± 2.6	15.2	26.0 ± 1.7	11.3
DMSO (2%)	> 100	> 100	—	> 100	—

*[a]Relative resistance ratio, RR = $IC_{50(resistant)}/IC_{50(parental)}$; [b]Above this concentration the compound crystallized in the culture medium. For all the other compounds, the IC_{50} was found to be above 100 μM, except for epoxyboetiranes M (**5**) and Q (**9**) which was above 25 μM – the maximum tested concentration due to lower water solubility. Each IC_{50} value indicates the mean ± SD of n = 3 to 4 independent experiments (each concentration was performed in triplicate per experiment).*

Matos et al., 2015). In this study, it is noteworthy that compounds with significant MDR-selective antiproliferative activities (**2**, **5**, **6**, **8**–**11**, **15,** and **16)**, mostly in drug-resistant gastric sublines, were also found to be strong P-gp modulators in a concentration-dependent manner.

Apoptosis Induction Activity

The ability of compounds **8**, **15,** and **16** as apoptosis inducers was evaluated using as models gastric and pancreatic cancer cells. The apoptotic process usually occurs through the extrinsic or intrinsic pathways. Despite their mechanistic differences, both converge on the same execution pathway, which is initiated by the activation of caspase-3. This cysteine protease takes a fundamental part in apoptosis, being pro-caspase-3, the penultimate enzyme for accomplishment of the apoptotic process (Tan et al., 2009). Therefore, the active caspase-3 was quantified by flow cytometry after 48 h of exposure at 20 μM of the compounds **8**, **15**, **16** (**Figure 2**). The results were expressed as fold increase (ratio between treated samples and untreated samples).

The subsequent apoptotic events include exposure of phosphatidylserine on the external surface of the plasma membrane, which is used as marker of apoptosis. As this phospholipid is shifted from the inner to the outer leaflet of the plasma membrane in early apoptosis, the annexin V/propidium iodide (PI) staining permits to identify both early and late apoptotic cells (PI negative, annexin V positive, and PI positive, annexin V positive, respectively) (Chen, 2009). Hence, the annexin V/PI assay was used to evaluate the induction of apoptosis by compounds **8**, **15,** and **16** (20 μM) (**Figure 2**). The results were presented as total apoptosis (early and late apoptotic events) and the effects were expressed as fold increase (ratio between treated samples and untreated samples).

As described above, epoxyboetirane P (**8**) not only presented a highly antiproliferative profile against EPG85-257 gastric cells, but also produced a CS effect for EPG85-257RDB (**Table 1**). After 48 h incubation, compound **8** elicited the activation of caspase-3 in EPG85-257P, EPG85-257RNOV and EPG85-257RDB (**Figure 2A**). Contrary to what would be expected this effect was significantly more pronounced (7-fold) on the parental cell line. With such results, it was expected to observe early and late apoptotic events, after 72 h incubation; however significant results were only obtained for the EPG85-257RNOV cells (**Figure 2A**). Furthermore, epoxyboetirane P (**8**) induced a different response in EPP85-181 pancreatic cells in respect to active caspase-3 (**Figure 2B**). Statistically significant discrimination between resistant pancreatic cell lines and EPP85-181P cells was observed (**Figure 2B**). Compound **8** produced an 8- and 5-fold increase of active caspase-3 in EPP85-181RNOV and EPP85-181RDB cells, respectively. Nonetheless, this compound was not able to induce early or late apoptotic events that would be quantifiable by the annexin V/PI assay, after 72 h incubation.

On our previous studies, methoxyboetirane B (**15**) was highlighted as a promising lead compound for MDR-reversal, since it showed a remarkable ABCB1 modulatory activity potential through a competitive mechanism of action (Matos et al., 2015). Herein, it presented an interesting CS effect on both gastric MDR phenotypes (RR = 0.47 and 0.27, respectively, to EPG85-257RNOV and EPG85-257RDB. These observations were also reflected in the results obtained from the annexin V/PI assays, where a significant stimulation of apoptotic events was recorded in the MDR phenotypes but not in the parental (**Figure 2C**). Compound **15** caused a 3- and 5-fold increase of total apoptosis in EPG85-257RNOV and EPG85-257RDB, respectively. Moreover, the active caspase-3 assays quantified induction of these proteins on about 5.5 to 7-fold, but without significant phenotypic discrimination (**Figure 2C**). In light of these experimental data it might be inferred that the selective antiproliferative activity of methoxyboetirane B (**15**) proceeded through caspase-dependent apoptosis. Regarding the pancreatic cancer cells, compound **15** did not presented CS effect despite the strong antiproliferative effect. Nevertheless, methoxyboetirane B (**15**) showed to be able to provoke differential activation of capase-3 in the MDR phenotypes, but not in the parental (**Figure 2D**). Though, no significant apoptotic events were recorded.

Methoxyboetirane C (**16**) differs from methoxyboetirane B (**15**) on the benzoyl ester substituent, where compound **16** bears a *p*-trifluoromethyl group. This structural variance had impact on reducing the ABCB1 modulatory efficacy of methoxyboetirane C (**16**), when compared with compound **15** (Matos et al., 2015). However, in the present study, structure activity effects were not observed. Both compounds presented comparable antiproliferative profiles against the tested cell lines. Likewise, in the apoptosis induction assays similar effects can be observed (**Figures 2E, F** versus **Figures 2C, D**). Therefore, on gastric EPG85-257RNOV and EPG85-257RDB cells methoxyboetirane C (**16**) modulated a MDR-selective cell death through capase-3-dependent apoptosis (**Figure 2E**). Besides, compound **16** triggered differential activation of capase-3 on pancreatic EPP85-181RNOV and EPP85-181RDB cells, but not in the parental (**Figure 2F**), without significant phosphatidylserine translocation and/or membrane damage.

Regression Models

In an attempt to identify which molecular descriptors explain the CS effect by the compounds, a computational approach was undertaken by developing regression models, which are powerful tools that allow further insights on the molecular determinants underlying any observed biological activity. They were calculated for a small library of macrocyclic diterpenes, including compounds **1**–**16** along with compounds **17**–**42** (Supporting Information, **Table S1**). For classification purposes, a binary classification identifying the presence (RR ≤ 0.5) or absence (RR > 0.5) of CS was used. Two models were built: the first using a Näive Bayes (NB) classification scheme, a simple probabilistic classifier that examines all samples independently and calculates the individual probability of each particular compound to belong to a distinct cluster (John and Langley, 1995); and a Random Tree (RT) model in which an

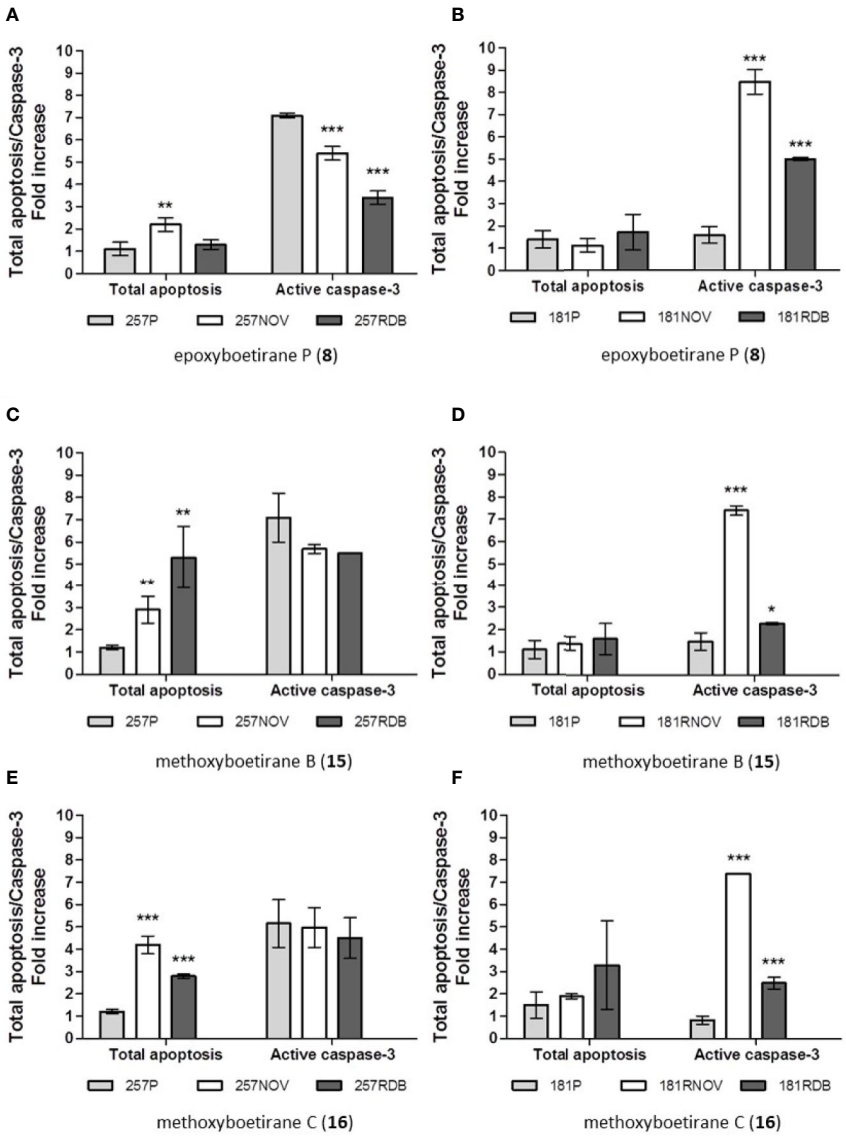

FIGURE 2 | Cell death mechanism measurements: apoptosis induction and active caspase-3 activation in gastric (**A, C, E**) and pancreatic (**B, D, F**) cancer cell lines after 72 h incubation with epoxyboetirane P (**8**), methoxyboetirane B (**15**), and methoxyboetirane C (**16**) (30 μM). Apoptosis induction: representative flow cytometry analysis after annexin V-FITC/PI staining. The FL1 and FL2 axis represent the fluorescence intensities of Annexin V-FITC and PI, respectively. Camptothecin (1 μM) was used as internal positive control. Total apoptosis was considered the sum of early and late apoptotic events (cells annexin V-FITC positive/PI negative plus cells annexin V-FITC positive/PI positive). The results were expressed as the ratio between treated samples with untreated. Each column represents the mean ± SD of three independent experiments. Statistical significance was calculated for the difference between treated resistant cell lines and treated parental cells using a two-tailed unpaired Student's t test. Level of significance *, $p < 0.05$. **, $p < 0.01$. ***, $p < 0.001$. Active caspase-3: the results were expressed as the ratio between treated samples with untreated. Each column represents the mean ± SD (n = 3). Statistical significance was calculated for the difference between treated resistant cell lines and treated parental cells using a two-tailed unpaired Student's t test. Level of significance *, $p < 0.05$. **, $p < 0.01$. ***, $p < 0.001$.

algorithm constructs trees with K randomly chosen attributes at each node to estimate class probabilities (Breiman, 2001). Herein, both models performed well in predicting which compounds trigger CS in EPG85-257RDB cells, with RT correctly classifying 100% of the compounds against 92.86% with the NB classifier. However, from both the 10-fold cross-validation and internal test (66% training, remaining test set) validations, the NB model provides increased robustness when compared with the RT approach, correctly classifying 85.71% in both validations (MAE, 0.1574 and 0.1106; RMSE, 0.3769 and 0.2685, respectively) against 80.95% (MAE, 0.1905; RMSE, 0.4364) and 85.71% (MAE 0.1429; RMSE, 0.3780) for the RT classifier, respectively (**Table 5**). At the end, we

TABLE 5 | Data obtained from the herein developed Regression Models.

		TP rate	FP Rate	Precision	Recall	F-Measure	MCC	ROC Area	PRC Area	Class*
NB	Train	0.923	0.069	0.857	0.923	0.889	0.973	0.973	0.940	0
		0.931	0.077	0.964	0.931	0.947	0.838	0.973	0.990	1
	10-fold	0.769	0.103	0.769	0.769	0.769	0.666	0.854	0.737	0
		0.897	0.231	0.897	0.897	0.897	0.666	0.854	0.927	1
	Test	0.800	0.111	0.800	0.800	0.800	0.689	0.978	0.967	0
		0.889	0.200	0.889	0.889	0.889	0.689	0.978	0.989	1
RT	Train	1.000	0.000	1.000	1.000	1.000	1.000	1.000	1.000	0
		1.000	0.000	1.000	1.000	1.000	1.000	1.000	1.000	1
	10-fold	0.538	0.069	0.778	0.538	0.636	0.529	0.735	0.562	0
		0.931	0.462	0.818	0.931	0.871	0.529	0.735	0.809	1
	Test	0.600	0.000	1.000	0.600	0.750	0.701	0.800	0.743	0
		1.000	0.400	0.818	1.000	0.900	0.701	0.800	0.818	1

Class 0: RR > 0.5; Class 1: RR ≤ 0.5.

concluded that both models are reliable in predicting which compounds are able to induce CS in the tested P-gp-expressing resistant cancer cell line.

To further improve the ability of the compounds in inducing such a biological response, the identification of the underlying molecular features is of the utmost importance. As in the Naïve Bayes all attributes are assumed to be equally important *a priori* (Lee et al., 2011), from the RT model it is possible to infer which molecular descriptors have the greatest weight in the decision tree. The first and most important descriptor was R4p (R autocorrelation of lag 4/weighted by polarizabilities), followed by MATS8m (Moran autocorrelation of lag 8/weighted by mass) at its first branch and X1A (Average connectivity index of order 1) on the second branch. Together, they are responsible for the classification of 24 compounds with RR ≤ 0.5 (**Figure S1**). For the classification of the remaining compounds, the second branch is further divided by using E2m (2^{nd} component accessibility directional WHIM index/weighted by mass), MDEC-22 (Molecular distance edge between all secondary carbons) and Mor03m (signal 03/weighted by mass) (Todeschini and Consonni, 2009; Devinyak et al., 2014). Herein, it is worth noticing that the E2m descriptor alone is responsible for the classification of 13 compounds (**Figure S1**). All these are geometrical descriptors encode information about the molecular size, shape, geometry, and symmetry. Therefore, it appears that the spatial position of the structural fragments and atom distribution within the molecular scaffold, together with its axial symmetry, are the most important structural determinants ruling CS effects.

Therefore, the aromaticity of the substituent increases the polarizability within the scaffold while promoting CS, in opposition to non-aromatic substituents as in compounds **12**–**14** and **39** (**Table S1**). However, substituents with higher mass ratios, obtained through the quotient between the substituents' and the molecules molecular weight (as in compounds **3**, **4, 20**, **21**, **37**, and **38**) or with a *meta* substitution pattern most (particularly in mono-substituted compounds **18** and **32**) (**Table S1**) are expected to perturb the axial symmetry of the molecular scaffold and thus impairing its biological activity. Yet, from the data it is also inferred that π-π stacking (**9**, **10**, and **15**) or the presence of additional hydrogen-bond acceptor moieties (as in compounds **8**, **11**, and **16**) are also important for the observed activity.

Overall, the achieved results hints that the substitution pattern and the presence of heteroatoms in an aromatic substituent are the strongest determinants relating to the observed CS effect. Furthermore, as the presence of substituents at positions C-15 and C-17 also impairs CS in a greater extent, the data suggests that future derivatives will have improved CS activities if i) the hydroxyl (or acetyl) group remains unchanged at position C-15 and ii) if only positions C-3 and/or C-5 are substituted but not C-17.

CONCLUSION

Targeting more than one anti-MDR mechanism has been considered a realistic strategy for overcoming the complex and multifactorial phenomenon of MDR. In a previous work, some epoxylathyrane derivatives were identified as strong P-glycoprotein efflux modulators. Consequently, aiming at improving their MDR-modifying activity, in this work the CS effect, one of the most hopeful anti-MDR strategies, was addressed. Derivatives **8**, **15**, and **16** were found to be very promising compounds, being many-fold more effective against MDR sublines, mainly in relation to gastric carcinoma cells. In these drug resistant counterparts compounds **15** and **16** significantly induced cell death through apoptosis.

The development of regression models emphasized axial symmetry of the overall molecular scaffold and, more particularly, its substitution pattern as the most determinant features related to the observed CS effect. Furthermore, while the hydroxyl function at position C-15 (or a small acetyl moiety) seems to be determinant, the aromaticity of the substituent together with the presence of heteroatoms was also inferred to be relevant for the observed activity.

All in all, this study reinforces the potential of macrocyclic diterpenes as leads for the development of MDR-modifying agents.

DATA AVAILABILITY STATEMENT

All datasets generated for this study are included in the article/ **Supplementary Material**.

AUTHOR CONTRIBUTIONS

All authors have participated and contributed substantially to this manuscript. HL and M-JF designed and supervised the study. MR, AM, and OA carried out the experiments. RF performed the regression models. M-JF, MR, ND, and RF wrote the manuscript. M-JF, MR, and ND revised the manuscript.

FUNDING

This study was financially supported by the FCT (Fundação para a Ciência e a Tecnologia) under the project PTDC/MED-QUI/ 30591/2017 and SAICTPAC/0019/2015.

SUPPLEMENTARY MATERIAL

The Supplementary Material for this article can be found online at: https://www.frontiersin.org/articles/10.3389/fphar.2020.00599/ full#supplementary-material

REFERENCES

Baptista, R., Ferreira, R. J., dos Santos, D. J., Fernandes, M. X., and Ferreira, M. J. U. (2016). Optimizing the macrocyclic diterpenic core toward the reversal of multidrug resistance in cancer. *Future Med. Chem.* 8, 629–645. doi: 10.4155/ fmc.16.11

Breiman, L. (2001). Random forests. *Mach. Learn.* 45, 5–32. doi: 10.1023/ A:1010933404324

Callaghan, R., Luk, F., Bebawy, M., Cuperus, F. J. C., Claudel, T., Gautherot, J., et al. (2014). Inhibition of the multidrug resistance P-glycoprotein: time for a change of strategy? *Drug Metab. Dispos.* 42, 623–631. doi: 10.1124/ dmd.113.056176

Chen, T. (2009). *A Practical Guide to Assay Development and High-Throughput Screening in Drug Discovery* (Boca Raton, Florida: CRC Press).

Devinyak, O., Havrylyuk, D., and Lesyk, R. (2014). 3D-MoRSE descriptors explained. *J. Mol. Graph. Model.* 54, 194–203. doi: 10.1016/j.jmgm.2014.10.006

Dietel, M., Arps, H., Lage, H., and Niendorf, A. (1990). Membrane vesicle formation due to acquired mitoxantrone resistance in human gastric carcinoma cell line EPG85-257. *Cancer Res.* 50, 6100–6106.

Ernst, M., Grace, O. M., Saslis-Lagoudakis, C. H., Nilsson, N., Simonsen, H. T., and Rønsted, N. (2015). Global medicinal uses of Euphorbia L. (Euphorbiaceae). *J. Ethnopharmacol.* 176, 90–101. doi: 10.1016/j.jep.2015.10.025

Ferreira, R. J., dos Santos, D. J. V., Ferreira, M. J. U., and Guedes, R. C. (2011). Toward a better pharmacophore description of P-glycoprotein modulators, based on macrocyclic diterpenes from *Euphorbia* species. *J. Chem. Inf. Model.* 51, 1315–1324. doi: 10.1021/ci200145p

Ferreira, R. J., Ferreira, M. J. U., and dos Santos, D. J. V. (2013). Molecular docking characterizes substrate-binding sites and efflux modulation mechanisms within P-glycoprotein. *J. Chem. Inf. Model.* 53, 1747–1760. doi: 10.1021/ci400195v

Ferreira, M. J. U., Duarte, N., Reis, M., Madureira, A. M., and Molnár, J. (2014). *Euphorbia* and *Momordica* metabolites for overcoming multidrug resistance. *Phytochem. Rev.* 13, 915–935. doi: 10.1007/s11101-014-9342-8

Ferreira, R. J., Baptista, R., Moreno, A., Madeira, P. G., Khonkarn, R., Baubichon-Cortay, H., et al. (2018a). Optimizing the flavanone core toward new selective nitrogen-containing modulators of ABC transporters. *Future Med. Chem.* 10, 725–741. doi: 10.4155/fmc-2017-0228

Ferreira, R. J., Kincses, A., Gajdács, M., Spengler, G., Dos Santos, D. J., Molnár, J., et al. (2018b). Terpenoids from *Euphorbia pedroi* as multidrug-resistance reversers. *J. Nat. Prod.* 81, 2032–2040. doi: 10.1021/acs.jnatprod.8b00326

Fojo, T. (2008). Commentary: Novel therapies for cancer: why dirty might be better. *Oncologist* 13, 277–283. doi: 10.1634/theoncologist.2007-0090

Gottesman, M. M., and Ling, V. (2006). The molecular basis of multidrug resistance in cancer: the early years of P-glycoprotein research. *FEBS Lett.* 580, 998–1009. doi: 10.1016/j.febslet.2005.12.060

Gottesman, M. M., Fojo, T., and Bates, S. E. (2002). Multidrug resistance in cancer: role of ATP-dependent transporters. *Nat. Rev. Cancer* 2, 48–58. doi: 10.1038/ nrc706

Gottesman, M. M., Lavi, O., Hall, M. D., and Gillet, J. P. (2016). Toward a Better Understanding of the Complexity of Cancer Drug Resistance. *Annu. Rev. Pharmacol. Toxicol.* 56, 85–102. doi: 10.1146/annurev-pharmtox-010715-103111

Hall, M. D., Handley, M. D., and Gottesman, M. M. (2009). Is resistance useless? Multidrug resistance and collateral sensitivity. *Trends Pharmacol. Sci.* 30, 546–556. doi: 10.1016/j.tips.2009.07.003

Hall, M., Frank, E., Holmes, G., Pfahringer, B., Reutemann, P., and Witten, I. H. (2009). The WEKA data mining software: an update. *ACM SIGKDD Explor.* 11, 10–18. doi: 10.1145/1656274.1656278

Hartwell, J. (1969). Plants used against cancer. A survey. *Lloydia* 32, 153–205.

Hilgeroth, A., Baumert, C., Coburger, C., Seifert, M., Krawczyk, S., Hempel, C., et al. (2013). Novel structurally varied N-alkyl 1,4-dihydropyridines as ABCB1 inhibitors: structure-activity relationships, biological activity and first bioanalytical evaluation. *Med. Chem.* 9, 487–493. doi: 10.2174/ 1573406411309040002

John, G. H., and Langley, P. (1995).Estimating continuous distributions in Bayesian classifiers, in: *Proceedings of the UAI'95 Eleventh Conference on Uncertainty in Artificial Intelligence*, Montréal, QC, Canada, 18–20 August. pp. 338–345.

Klukovits, A., and Krajcsi, P. (2015). Mechanisms and therapeutic potential of inhibiting drug efflux transporters. *Expert Opin. Drug Metab. Toxicol.* 11, 907–920. doi: 10.1517/17425255.2015.1028917

Lage, H., Duarte, N., Coburger, C., Hilgeroth, A., and Ferreira, M. J. U. (2010). Antitumor activity of terpenoids against classical and atypical multidrug resistant cancer cells. *Phytomedicine* 17, 441–448. doi: 10.1016/j.phymed.2009.07.009

Lee, C., Gutierrez, F., and Dou, D. (2011).Calculating feature weights in Naive Bayes with Kullback-Leibler measure, in: *2011 IEEE 11th International Conference on Data Mining*, Vancouver, BC. pp. 1146–1151.

Matos, A. M., Reis, M., Duarte, N., Spengler, G., Molnár, J., and Ferreira, M. J. U. (2015). Epoxylathyrol derivatives: modulation of ABCB1-mediated multidrug resistance in human colon adenocarcinoma and mouse T-Lymphoma cells. *J. Nat. Prod.* 78, 2215–2228. doi: 10.1021/acs.jnatprod.5b00370

Newman, D. J., and Cragg, G. M. (2012). Natural products as sources of new drugs over the 30 years from 1981 to 2010. *J. Nat. Prod.* 75, 311–335. doi: 10.1021/np200906s

Paterna, A., Kincses, A., Spengler, G., Mulhovo, S., Molnár, J., and Ferreira, M. J. U. (2016). Dregamine and tabernaemontanine derivatives as ABCB1 modulators on resistant cancer cells. *Eur. J. Med. Chem.* 128, 247–257. doi: 10.1016/j.ejmech.2017.01.044

Paterna, A., Khonkarn, R., Mulhovo, S., Moreno, A., Madeira, G., Baubichon-Cortay, H., et al. (2018). Monoterpene indole alkaloid azine derivatives as MDR reversal agents. *Bioorg. Med. Chem.* 26, 421–443. doi: 10.1016/j.bmc.2017.11.052

Ramalhete, C., Mulhovo, S., Molnar, J., and Ferreira, M. J. U. (2016). Triterpenoids from *Momordica balsamina*: Reversal of ABCB1-mediated multidrug resistance. *Bioorg. Med. Chem.* 24, 5061–5067. doi: 10.1016/j.bmc.2016.08.022

Ramalhete, C., Mulhovo, S., Molnar, J., and Ferreira, M. J. U. (2018). Triterpenoids from *Momordica balsamina* with a collateral sensitivity effect for tackling multidrug resistance in cancer cells. *Planta Med.* 84, 1372–1379. doi: 10.1055/ a-0651-8141

Reis, M., Ferreira, R., Serly, J., Duarte, N., Madureira, A., Santos, D. J., et al. (2012). Colon adenocarcinoma multidrug resistance reverted by *Euphorbia* diterpenes: structure-activity relationships and pharmacophore modeling. *Anticancer Agents Med. Chem.* 12, 1015–1024. doi: 10.2174/187152012803529655

Reis, M., Ferreira, R. J., Santos, M. M. M., dos Santos, D. J. V., Molnár, J., and Ferreira, M. J. U. (2013). Enhancing macrocyclic diterpenes as multidrug-resistance reversers: structure-activity studies on jolkinol D derivatives. *J. Med. Chem.* 56, 748–760. doi: 10.1021/jm301441w

Reis, M. A., Paterna, A., Ferreira, R. J., Lage, H., and Ferreira, M. J. U. (2014). Macrocyclic diterpenes resensitizing multidrug resistant phenotypes. *Bioorg. Med. Chem.* 22, 3696–3702. doi: 10.1016/j.bmc.2014.05.006

Reis, M. A., André, V., Duarte, M. T., Lage, H., and Ferreira, M. J. U. (2015). 12,17-Cyclojatrophane and Jatrophane Constituents of *Euphorbia welwitschii*. *J. Nat. Prod.* 78, 2684–2690. doi: 10.1021/acs.jnatprod.5b00631

Reis, M. A., Ahmed, O. B., Spengler, G., Molnár, J., Lage, H., and Ferreira, M. J. U. (2016). Jatrophane diterpenes and cancer multidrug resistance - ABCB1 efflux modulation and selective cell death induction. *Phytomedicine* 23, 968–978. doi: 10.1016/j.phymed.2016.05.007

Reis, M. A., Ahmed, O. B., Spengler, G., Molnár, J., Lage, H., and Ferreira, M. J. U. (2017). Exploring Jolkinol D derivatives to overcome multidrug resistance in cancer. *J. Nat. Prod.* 80, 1411–1420. doi: 10.1021/acs.jnatprod.6b01084

Rosen, R. H., Gupta, A. K., and Tyring, S. K. (2012). Dual mechanism of action of ingenol mebutate gel for topical treatment of actinic keratoses: Rapid lesion necrosis followed by lesion-specific immune response. *J. Am. Acad. Dermatol.* 66, 486–493. doi: 10.1016/j.jaad.2010.12.038

Sousa, I. J., Ferreira, M. J. U., Molnár, J., and Fernandes, M. X. (2012). QSAR studies of macrocyclic diterpenes with P-glycoprotein inhibitory activity. *Eur. J. Pharm. Sci.* 48, 542–553. doi: 10.1016/j.ejps.2012.11.012

Szakács, G., Hall, M. D., Gottesman, M. M., Boumendjel, A., Kachadourian, R., Day, B. J., et al. (2014). Targeting the achilles heel of multidrug-resistant Cancer by exploiting the fitness cost of resistance. *Chem. Rev.* 114, 5753–5774. doi: 10.1021/cr4006236

Szybalski, W., and Bryson, V. (1952). Genetic studies on microbial cross resistance to toxic agents I, cross resistance of *Escherichia coli* to fifteen antibiotics. *J. Bacteriol.* 64, 489–499. doi: 10.1128/JB.64.4.489-499.1952

Tan, M. L., Ooi, J. P., Ismail, N., Moad, A. I. H., and Muhammad, T. S. T. (2009). Programmed cell death pathways and current antitumor targets. *Pharm. Res.* 26, 1547–1560. doi: 10.1007/s11095-009-9895-1

Todeschini, R., and Consonni, V. (2009). "Molecular Descriptors for Chemoinformatics," in *Methods and Principles in Medicinal Chemistry* (Weinheim: Wiley-VCH Verlag GmbH & Co. KGaA).

Vieira, C., Duarte, N., Reis, M. A., Spengler, G., Madureira, A. M., Molnár, J., et al. (2014). Improving the MDR reversal activity of 6,17-epoxylathyrane diterpenes. *Bioorg. Med. Chem.* 22, 6392–6400. doi: 10.1016/j.bmc.2014.09.041

Conflict of Interest: The authors declare that the research was conducted in the absence of any commercial or financial relationships that could be construed as a potential conflict of interest.

frontiers in Pharmacology

REVIEW
published: 19 June 2020
doi: 10.3389/fphar.2020.00832

Phytochemicals: Potential Lead Molecules for MDR Reversal

Boshra Tinoush[1], *Iman Shirdel*[2] *and Michael Wink*[1]*

[1] Institute of Pharmacy and Molecular Biotechnology, Heidelberg University, Heidelberg, Germany, [2] Marine Sciences Faculty, Tarbiat Modares University, Noor, Iran

Multidrug resistance (MDR) is one of the main impediments in the treatment of cancers. MDR cancer cells are resistant to multiple anticancer drugs. One of the major mechanisms of MDR is the efflux of anticancer drugs by ABC transporters. Increased activity and overexpression of these transporters are important causes of drug efflux and, therefore, resistance to cancer chemotherapy. Overcoming MDR is a fundamental prerequisite for developing an efficient treatment of cancer. To date, various types of ABC transporter inhibitors have been employed but no effective anticancer drug is available at present, which can completely overcome MDR. Phytochemicals can reverse MDR in cancer cells via affecting the expression or activity of ABC transporters, and also through exerting synergistic interactions with anticancer drugs by addressing additional molecular targets. We have listed numerous phytochemicals which can affect the expression and activity of ABC transporters in MDR cancer cell lines. Phytochemicals in the groups of flavonoids, alkaloids, terpenes, carotenoids, stilbenoids, lignans, polyketides, and curcuminoids have been examined for MDR-reversing activity. The use of MDR-reversing phytochemicals with low toxicity to human in combination with effective anticancer agents may result in successful treatment of chemotherapy-resistant cancer. In this review, we summarize and discuss published evidence for natural products with MDR modulation abilities.

Keywords: cancer, ABC-transporter, drug efflux, multidrug resistance, secondary metabolites, synergism

OPEN ACCESS

Edited by:
Maria José U. Ferreira,
University of Lisbon, Portugal

Reviewed by:
Olga Wesolowska,
Wroclaw Medical University, Poland
Mariana A. Reis,
University of Porto, Portugal

***Correspondence:**
Michael Wink
wink@uni-heidelberg.de

Specialty section:
This article was submitted to Ethnopharmacology, a section of the journal Frontiers in Pharmacology

Received: *20 December 2019*
Accepted: *20 May 2020*
Published: *19 June 2020*

Citation:
Tinoush B, Shirdel I and Wink M (2020) Phytochemicals: Potential Lead Molecules for MDR Reversal. Front. Pharmacol. 11:832. doi: 10.3389/fphar.2020.00832

INTRODUCTION

Besides surgery and radiation, chemotherapy is one of the standard treatments of cancer. Drugs used in chemotherapy usually disturb cell division by inhibition of microtubule formation or disassembly (vinca alkaloids, paclitaxel), DNA topoisomerase (camptothecin and derivatives) or they intercalate or alkylate DNA (doxorubicin, cisplatin) (Wink, 2007; Wink et al., 2012). Furthermore, chemotherapy often causes extreme side effects as these drugs also affect the division of normal cells or they cause mutations, which can lead to secondary cancers. This additionally leads to restriction of the therapeutic applications; both dosage and application interval must be kept limited. When chemotherapeutic agents are used, it is often a matter of time before the

Abbreviations: ADR, adriamycin; CPT, camptothecin; DOX, doxorubicin; DNR, daunorubicin; DTN, digitonin; EGC, epigallocatechin; EGCG, epigallocatechin gallate; MDR, multidrug resistance; MTX, mitoxantrone; P-gp, P-glycoprotein; PTX, paclitaxel; Rh-123, rhodamine 123; VBL, vinblastine; VCR, vincristine; BCRP, breast cancer resistance protein; MRP, multidrug resistance protein.

cancer cells develop resistance against them. One of the major resistance mechanisms is the overexpression of ABC transporters, which can pump out the chemotherapeutic from cancer cells. Because these ABC transporters have a wide substrate spectrum, they not only confer resistance to a single drug but to several others, therefore, the term Multidrug Resistance (MDR). Since multiple drug resistance is a major issue in tumor therapy, new strategies are necessary to overcome this obstacle. One strategy involves the combination of anti-cancer drugs with modulators of ABC transporters. Our review presents a summary about various modulating effects of phytochemicals.

Multidrug Resistance in Cancer

One of the major difficulties in suppressing growth and survival of cancer cells is multidrug resistance. MDR is the resistance of cancer cells to various types of anticancer drugs which may have an intrinsic or acquired origin. Acquired resistance is induced after the administration of chemotherapy, whereas, intrinsic resistance already exists prior to drug application in cancer cells (Wang et al., 2019). Several mechanisms in cancer cells can lead to MDR (Coley, 2008). These include changes in target enzymes, such as DNA topoisomerases (Brown et al., 1995), alteration in microtubule-associated proteins (Zhang et al., 1998), mutations or changes in tubulin (Kamath et al., 2005; Wang and Cabral, 2005), alteration in microtubules (Kavallaris et al., 2001), mitotic arrest (Kamath et al., 2005), mutated protein p53 (O'Connor et al., 1997), disruption in DNA repair due to the damaging effect of an anticancer drug (Bernstein et al., 2002) and the impairment of apoptosis or genes involved in apoptosis and necrosis (Tanaka et al., 2000; Simstein et al., 2003).

A widespread mechanism of MDR is drug efflux via transmembrane transporters known as ATP-binding cassette transporters (ABC transporter). Overexpression of these transporters is the most important cause of drug resistance in many cancer cells. The family of ABC transporter proteins has 48 members in humans and far more in nature (Chen et al., 2016). The most well-known and widely-studied ABC transporters include P-Glycoprotein (P-gp), multidrug resistance protein 1 (MRP1), and breast cancer resistance protein (BCRP). These transporters are expressed in healthy cells of various mammalian tissues having physiological tasks for translocating small molecules. They are found especially in intestinal epithelial cells, endothelial cells of blood capillaries and epithelia of renal proximal tubules being involved in the excretion and clearance of endogenous and exogenous cytotoxic substances (Borst et al., 2000; Durmus et al., 2015; Chen et al., 2016). ABC transporters evolved in nature millions of years ago to eliminate toxic phytochemicals that herbivores would obtain from their plant diet (Wink, 2007). Anticancer drugs also can be substrates of these transporters and if being considered as foreign they get exported to the extracellular space by cells expressing ABC transporters. Cancer cells which are not resistant to anticancer agents yet can develop the ability by overexpressing these transporters for saving themselves from the substances being toxic to them. This leads to an increased efflux, leading to low intracellular drug concentrations, insufficient to kill a cancer cell. Once this overexpression has occurred, the efflux also affects other chemotherapeutics and thus, makes the cancer cell resistant to chemotherapy (Coley, 2008; Durmus et al., 2015).

P-gp (ABCB1)

P-gp is a 170 kDa protein which is encoded by the *MDR1* gene. This transporter is found in normal cells of various tissues including the brain, liver, kidney, gastrointestinal tract and pancreas. P-gp transports anticancer drugs such as paclitaxel, doxorubicin, daunorubicin, epirubicin, mitoxantrone, vincristine, and vinblastine against the concentration gradient using energy derived from hydrolysis of ATP (Chen et al., 2016). Chemotherapeutic agents can stimulate P-gp expression in cancer cells and thereby cause resistance to chemotherapy. Chemotherapy has been reported to increase the proportion of P-gp-expressing tumors by approximately 1.8-fold in breast cancer. Moreover, in patients with activated P-gp transporter in their tumors, the risk of failure of chemotherapy is 3 times higher than in patients who do not express P-gp transporter (Trock et al., 1997).

Multidrug Resistance Proteins (MRPs)

Another class of membrane transporters which causes MDR is MRPs. Nine members of this class have been identified so far (König et al., 2005; Coley, 2008). MRPs are found in normal cells of some mammalian tissues and expel drugs as a complex with glutathione, glucuronate, or sulfate (Borst et al., 2000; Coley, 2008). Among the MRP transporters, MRP1 (ABCC1) is the most important and most studied one regarding MDR. The MRP1 protein has a molecular weight of 190 kDa. Similar to P-gp, MRP1 expression has been reported to be considerably higher expressed in cancer cells after chemotherapy than before chemotherapy (Trock et al., 1997). Therefore, MRP1 enhances resistance to chemotherapy and to anticancer drugs such as doxorubicin, daunorubicin, epirubicin, vincristine, and vinblastine (Coley, 2008).

BCRP (ABCG2)

Breast cancer resistance protein, also called mitoxantrone transporter (MXR1), has a molecular weight of 72 kDa. BCRP is extensively expressed in MCF-7 breast cancer cells (Doyle et al., 1998). This protein is also expressed in other tissues including the liver, kidney, and intestine (Chen et al., 2016). The anticancer drugs doxorubicin, daunorubicin, epirubicin and mitoxantrone have been described as substrates of BCRP transporter (Coley, 2008). Thus, cancer cells overexpressing BCRP transporter become resistant to these drugs.

MDR Modulators

One of the essential requirements for developing better anti-cancer therapies is overcoming multidrug resistance. Much research has been carried out on cancer treatment and development of anticancer drugs in recent years but MDR to cytostatics is still a great impediment. Although our knowledge about the mechanisms of multidrug resistance has increased, there is no effective drug which can completely overcome or reverse resistance at non-toxic concentrations. Since ABC

transporters play a fundamental role in resistance to chemotherapy, the ability to inhibit them in a combination with conventional treatments will greatly help to treat cancer (Chen et al., 2016).

Until now, different types of ABC transporter inhibitors have been examined. The use of the first generation of these compounds, including verapamil and cyclosporine A, in combination with anticancer drugs had poor clinical success and toxic effects (Daenen et al., 2004). Second generation of MDR modulators included dexverapamil, valspodar, and dexniguldipine. Even though less toxic and with a higher therapeutic index than the first generation, this group of modulators is not well suited for a therapy either, both because of its interactions with other drugs and ABC transporters, as well as due to the inhibition of enzymes like CYP3A (Wandel et al., 1999; Syed and Coumar, 2016). The third-generation ABC transporter modulators do not have the disadvantages of the first and second generation. They are potent and non-competitive inhibitors of P-gp, and also less toxic. Tariquidar (XR9576) and zosuquidar are members of the third generation of MDR modulators but unfortunately they were not efficative in clinical trials (Cripe et al., 2010; Kelly et al., 2011).

Phytochemicals

Alkaloids (**Figure 1**) are the most widely studied group of secondary metabolites in terms of MDR, not only because of their quantity but also because of their great diversity (Wink, 2007; Wink et al., 2012). As alkaloids have a wide distribution among angiosperms (Wink, 2020) and represent a diversity of structures, they differ in pharmacological and toxicological properties. Alkaloids contain heterocyclic nitrogen, which mostly has its origin in amino acids (Cseke et al., 2006). Alkaloids are subdivided into many subcategories of special functional groups, similarities of skeleton or biosynthetic pathways.

Quinoline and isoquinoline alkaloids for example have a benzopyridine ring differing in the position of their nitrogen. Quinazoline alkaloids have a similar aromatic structure but with two nitrogen atoms instead of one. Each of these structures has found several uses depending on molecular structure. There are many examples for quinoline alkaloids such as mefloquine as antimalarial agent, fluoroquinolone antibiotics and topotecan as anticancer drug, just to name a few (Collin and Höke, 2000; Tiwary et al., 2015). The latter two work as inhibitors of different DNA topoisomerases (Lemmer and Brune, 2004).

Quinolizidines also are cyclic nitrogen-containing compounds but unlike the previously mentioned subgroups they are not aromatic. A natural representative is sparteine, which is used as an antiarrhythmic agent blocking sodium channels (Ruenitz and Mokler, 1977; Körper et al., 1998; Gawali et al., 2017).

Among other groups of alkaloids, indole, monoterpene indole and β-carboline alkaloids show many pharmacological activities (Gilbert, 2001). A typical basic structure of β-carboline alkaloids consists of benzene fused with a five-membered pyrrole and is consequently similarly structured to some endogenous hormones and neurotransmitters such as serotonin and melatonin. In addition to benzene, the pyrrole ring of β-carboline is fused to a pyridine, another six-membered nitrogen-containing ring. This structure by itself is an inverse agonist of GABA-receptors, which involves psychological influence on humans (Aktories et al., 2017). Substrates among the indoles target many receptors, for example PDE-receptors e.g. by tadalafil, 5-HT receptors e.g. by naratriptane and HMG-CoA reductases e.g. by fluvastatin (Wink, 2000; de Sa et al.,

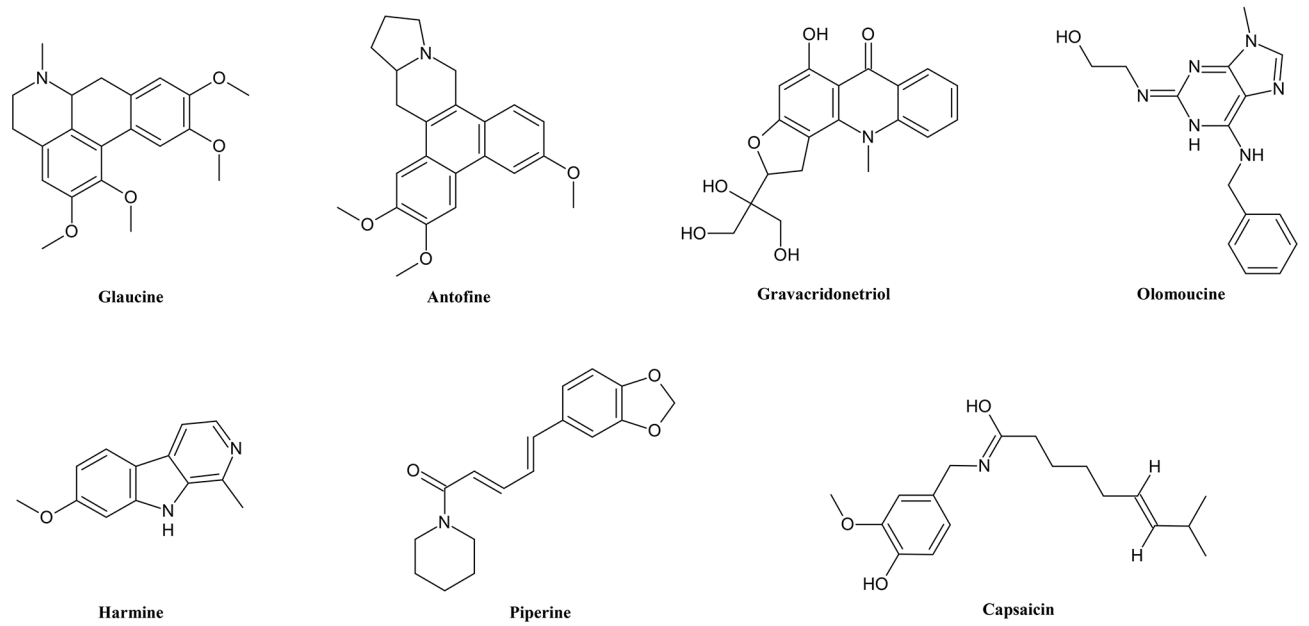

FIGURE 1 | Chemical structures of some selected alkaloids with MDR reversal effects.

2009). Several indole alkaloids have stimulant and hallucinogenic properties (Wink, 2000; Wink and van Wyk, 2008).

As the nitrogen of steroidal alkaloids does not originate from amino acids they belong to pseudoalkaloids. A member of steroidal alkaloids is the teratogenic cyclopamine, which can cause cyclopean eyes in vertebrates (Roberts and Wink, 1998; Incardona et al., 1998).

Piperidine and diketopiperazine are six-membered non-aromatic moieties in alkaloids whereby diketopiperazine is a cyclic dipeptide having two oppositely located nitrogen. Pyrazine has the same position of nitrogen, though aromatic. Here we also can find medicinal use of active ingredients such as the oxytocin antagonist retosiban and plinabulin which is still in clinical trial against multiple drug resistant non-small cell lung cancer (Borthwick and Liddle, 2011; Mohanlal et al., 2019).

Tropane alkaloids are widespread and their plants one of the oldest medicines to use because of spasmolytic, mydriatic and hallucinogenic properties (Wink and van Wyk, 2008; van Wyk and Wink, 2017). They contain a special bicyclic moiety which is made of a seven-membered ring and a nitrogen atom which is linked to its C-1 and C-5 and forms the second ring (Osman et al., 2013). Due to their spasmolytic effect nowadays we use tropane alkaloids such as scopolamine or atropine for digestive tract spastic conditions and for ophthalmological purposes (Kukula-Koch and Widelski, 2017).

The most popular alkaloid caffeine belongs to purine alkaloids, which are consumed by many people on all continents. Theobromine, theophylline and caffeine are common members found as main ingredients in chocolate, mate, cola, green and black tea or coffee (Baumann and Frischknecht, 1988). By inhibiting adenosine receptors and cAMP phosphodiesterase they can mediate a stimulant effect (van Wyk and Wink, 2017).

Flavonoids (**Figure 2**) are another complex but also often colored group of secondary metabolites. Unlike alkaloids, we can make a general statement about their common origin and basic skeleton. Flavonoids can be classified as polyphenols which share a common biosynthesis. They contain aromatic rings with phenolic hydroxyl groups. These phenolic hydroxyl groups can dissociate under physiological condition and form negatively charged phenolate ions. Because of these properties flavonoids and polyphenols can interact with proteins forming multiple

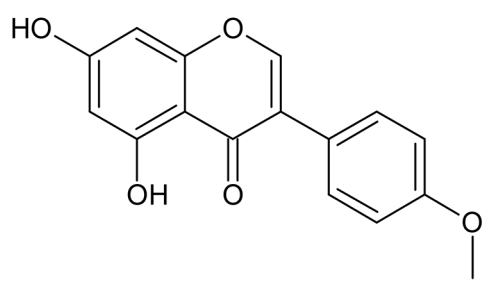

Biochanin A

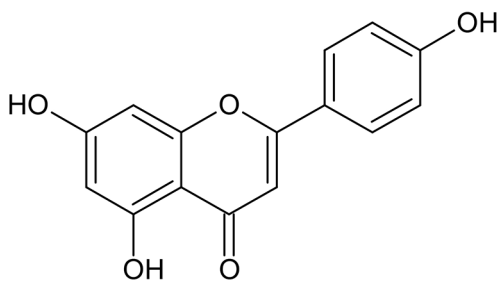

Apigenin

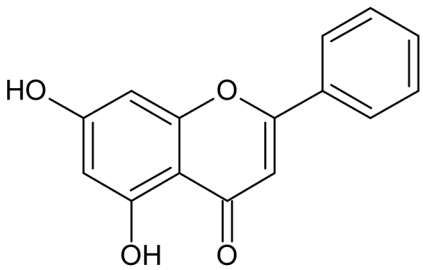

Chrysin

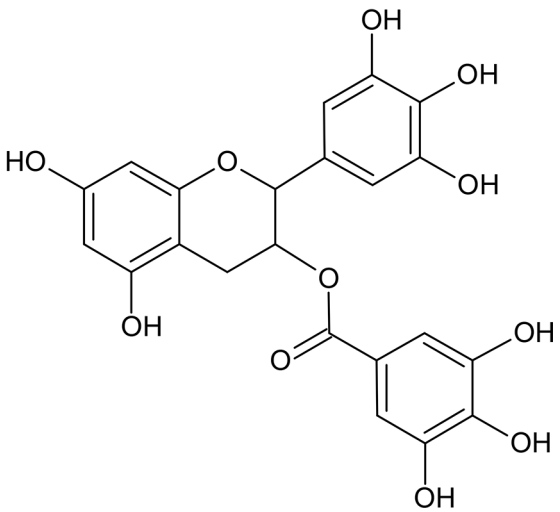

Epigallocatechin gallate

FIGURE 2 | Chemical structures of some selected flavonoids with MDR reversal effects.

hydrogen and ionic bonds (Wink, 2015). Flavonoids are widely distributed in plants and are responsible, inter alia, for their pollinator attracting colors, ultraviolet light protection, antioxidant and antimicrobial functions, and mediating symbiosis with bacteria. Including the main subgroups flavones, isoflavones, flavonols, flavanones, anthocyanins, chalcones and catechins, they derive from flavan, a benzopyran structure with a phenyl ring in position 2. Flavonoids with a phenyl ring in position 3 and 4 are called iso- and neoflavonoids, respectively. The variety of flavonoids comes from many functional groups and different states of oxidation of the heterocycle (Koes et al., 1994; Wink and van Wyk, 2008; Hänsel and Sticher, 2009). Although there has been a lot of research on the antioxidant capacity of flavonoids, the mechanism is not fully understood yet. Many studies have reported anti-inflammatory, anti-carcinogenic, anti-mutagenic, antiviral, anti-allergic and osteogenetic potentials of flavonoids in vitro. There is evidence, that polyphenols are also important for the pharmacological activity of many medicinal plants (van Wyk and Wink, 2017). Still there is a lack of information about how the necessary bioavailability is achieved in the human body as polyphenols are polar compounds (Panche et al., 2016). Most common representatives in food are luteolin and apigenin. Isoflavones are known for their estrogenic properties (Wink, 2015).

In addition to flavonoids, there are smaller but also important groups of polyphenols, for example stilbenoid with resveratrol as its main member known for its potential as anti-cancer (Huang et al., 2014), antioxidant and anti-aging agent (Alamolhodaei et al., 2017). Curcuminoids (**Figure 3**) have been widely studied and have been found to have many functions such as antioxidative, anti-cancer, anti-microbial and anti-inflammatory effects in humans. They can interact with many targets (Fantini et al., 2015).

Terpenes (**Figure 4**) are widely distributed in plants, fungi and animals. They are composed of different numbers of isoprene units, forming mono- (C10), di- (C20), sesqui- (C15), tetra- (C40) and triterpenes (C30). Many mono- and sequiterpenes are volatile and aromatic and typical ingredient of essential oils. These compounds are often lipophilic and can thus modulate the fluidity and permeability of biomembranes in animals and microbes. Many plants with essential oil have been used in traditional medicine for treatment of microbial infections and inflammation (Wink, 2015; van Wyk and Wink, 2017).

Known for their skin permeation enhancing ability, terpenes have been used as moieties of synthetic structures for topical

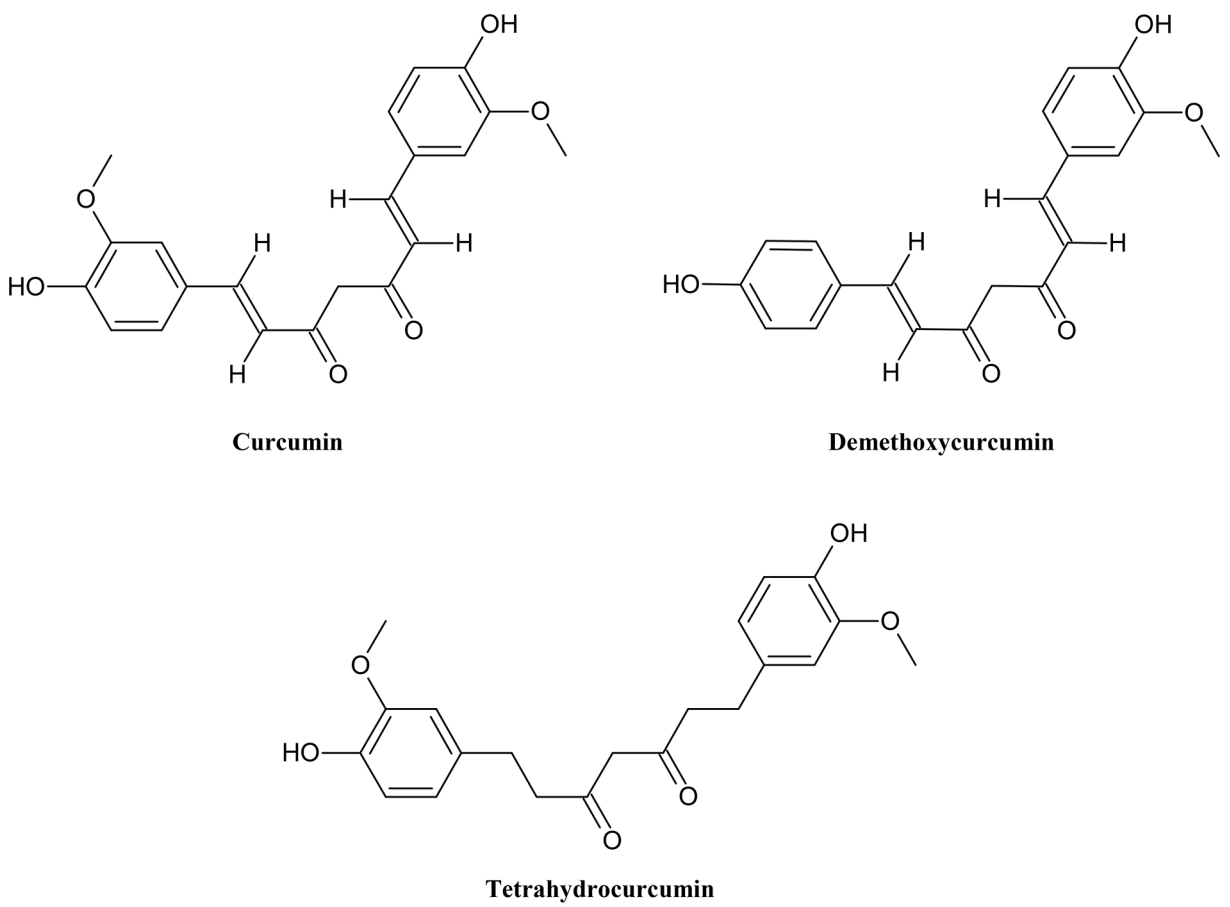

FIGURE 3 | Chemical structures of some selected curcuminoids with MDR reversal effects.

use (Smith and Maibach, 1995). In vitro studies have shown anti-cancer, antimicrobial and antioxidant activities but for practice and use in humans this class of secondary metabolites must be further investigated (Lu et al., 2012; Cör et al., 2018). Squalene is a standard triterpene produced in plants and animals, and it is the precursor for steroid synthesis. Glycosides of steroids or triterpenes, so-called saponins have one or more polysaccharides attached saponins are amphiphilic and react as a detergent. They generally form stable foams and complex cholesterol in biomembranes. As a consequence, saponins can lyse biomembranes (Bloch, 1983). In traditional medicine they have been used for example as expectorants and anti-infectants (Wink, 2015). As effective components of vaccine adjuvants they enhance the cellular immune response (Sun et al., 2009).

Carotenoids are tetraterpenes with many conjugated double bonds. They often exhibit yellow to purple colors and can function as anti-oxidants and precursors for vitamin A.

As the name implies polyketides contain carbonyl groups positioned between methylene groups. Still they vary in shape and volume. Although they appear with an impressive structural variety, they have their source from the same biosynthetic pathway. The most famous members among drugs may be the antibiotic erythromycin or the antifungal amphotericin B.

Phytochemicals Modulating MDR Targeting ABC-Transporters

A considerable number of secondary metabolites, which affect ABC transporters has already been discovered (**Table 1**) and several of them will be discussed in the following; glaucine (an isoquinoline alkaloid) increased the efflux of substrates such as ADR and MTX in the P-gp over-expressing cell lines of MCF-7/ADR and reduced DOX resistance in Caco-2 and CEM/ADR5000 (Eid et al., 2013; Lei et al., 2013). Tetrandrine (a benzolisoquinoline alkaloid) also caused an inhibition of efflux in Caco-2 and CEM/ADR5000 cells (Sun and Wink, 2014). A 5-substituted derivative of it named PY35 was tested for the MDR reversal activity, and showed more MDR reversal than the natural compound in resistant K562/ADM and MCF-7/ADM cells (Cao et al., 2014). Hernandezine, a bisbenzyl-isoquinoline, is a potent inhibitor of P-gp in MDR19-HEK293 cells and was able to resensitize MDR19-HEK293 and KB-V-1 cells to DOX after entering the cell membrane (Hsiao et al., 2016). High MDR-reversing activities of the quinoline derivatives were linked to the

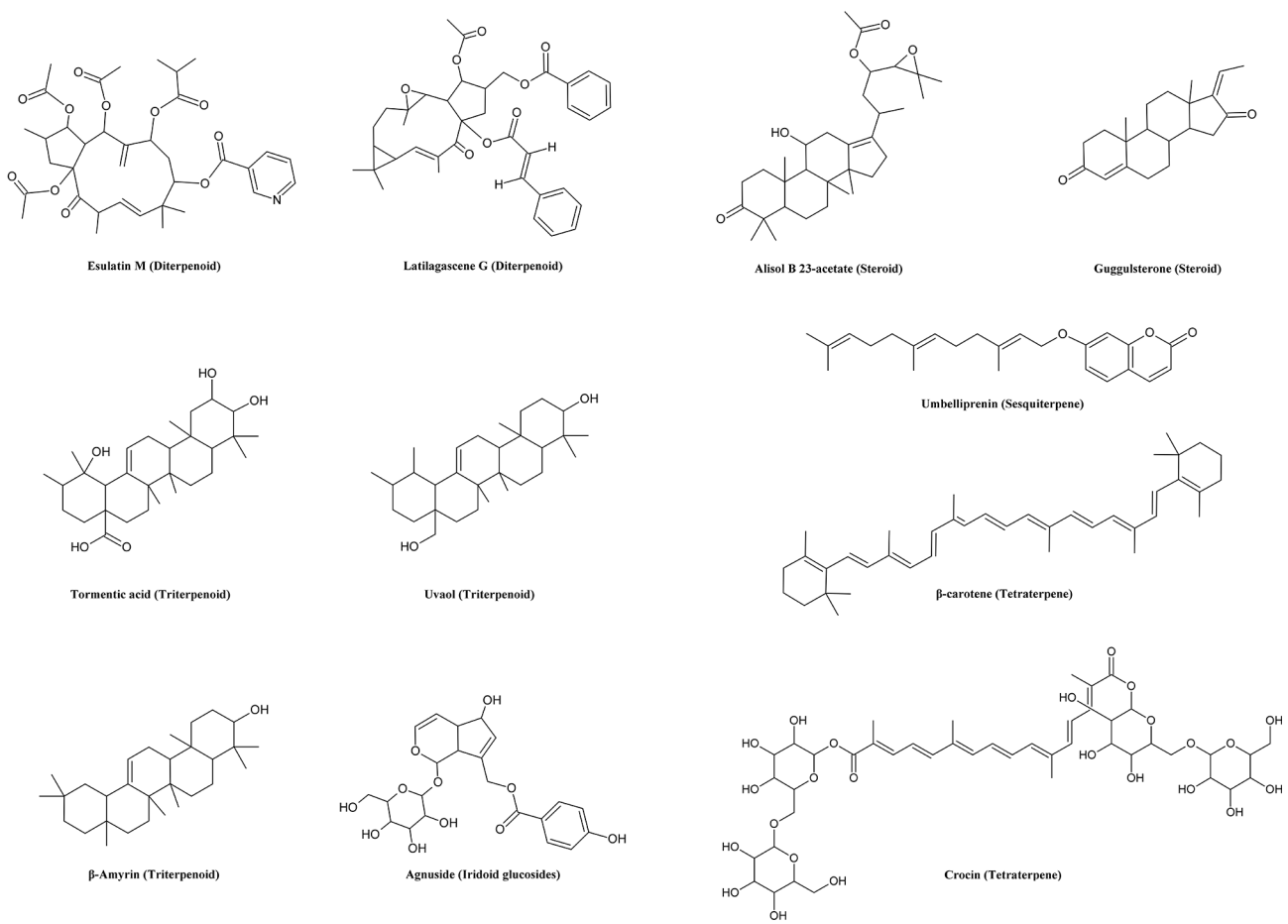

FIGURE 4 | Chemical structures of some selected terpenes with MDR reversal effects.

TABLE 1 | Phytochemicals modulating MDR via ABC-transporters.

The effects of secondary metabolites on different cell lines expressing ABC-transporters – Transporters targeted directly

	Substance	Cell line	Assay system	Result	Reference
Alkaloids					
Quinolines, Isoquinolines, Quinazolines	Dauriporphine	MES-SA/DX5 and HCT15	MDR reversing activity (cytotoxicity assay in the presence and absence of an anticancer drug, PTX)	Increase in cytotoxicity of PTX (inhibition of P-gp MDR)	Min et al. (2006)
	Fangchinoline	MDR1-MDCK II	MDR reversing activity	Decrease in substrate (PTX) efflux, inhibition of the multidrug resistance of antitumor drug PTX	He et al. (2010)
	Glaucine	Caco-2, CEM/ADR5000	MTT assay, Rh-123 accumulation assay using fluorospectroscopy	Reversal of DOX resistance in both cell lines with very high effect, synergism with DOX	Eid et al. (2013)
		Caco-2, CEM/ADR5000	MTT assay, Rh-123 accumulation assay using fluorospectroscopy	Sensitization of cell lines, enhancement of cytotoxicity, strong reduction of the IC_{50} value of DOX and consequently increase of efficacy, synergism with DOX and DTN	Eid et al. (2013)
		MCF-7/ADR	MDR reversing activity, ADR and MTX efflux assay, real-time RT-PCR, P-gp and MRP1 ATPase activity assay	Inhibition of P-gp and *MRP1*-mediated efflux, suppression of the expression of *MDR1* and *MRP1* genes, reversion of the resistance of MCF-7/ADR to ADR and MTX, increase in P-gp and MRP1 ATPase activities	Lei et al. (2013)
	Hernandezine	MDR19-HEK293, KB-V-1, NCI-ADR-RES	MDR reversing activity, fluorescent drug (calcein-AM and pheophorbide A) accumulation assay,	Inhibition of the transport function of ABCB1 (P-gp), increase in calcein-AM accumulation in MDR19-HEK293 cells, resensitizing of MDR19-HEK293 cells to DOX, resensitizing of KB-V-1 cells to DOX, colchicine and VCR, resensitizing of NCI-ADR-RES cells to DOX, colchicine and vincristine	Hsiao et al. (2016)
	Roemerine	MDR KB-V1	Cytotoxicity assay with VBL	Cytotoxicity synergism	You et al. (1995)
	Sanguinarine	Caco-2, CEM/ADR5000	MTT assay, Rh-123 accumulation assay using fluorospectroscopy	Reversal of DOX resistance in both cell lines with very high effect, synergism with DOX	Eid et al. (2013)
		Caco-2, CEM/ADR5000	MTT assay, Rh-123 accumulation assay using fluorospectroscopy	Sensitization of cell lines to DOX	Eid et al. (2013)
	Tetrandrine	Caco-2, CEM/ADR5000	Rh-123 accumulation	Increased accumulation of substrate, inhibited efflux in both cell lines, reduction of P-gp expression	Sun and Wink (2014)
	Quinidine homodimer	MCF-7/DX1	Radioactive substrate ([^{3}H] PTX) accumulation assay, flow cytometric accumulation assay, confocal microscopy	Inhibition of the efflux of Rh-123, DOX, BODIPY-FL-prazosin, PTX and MTX,	Pires et al. (2009)
Steroidal alkaloids	Verabenzoamine	L5178/*MDR1* (human *MDR1*-gene-transfected mouse lymphoma cells)	Flow cytometric assay of Rh-123 accumulation	Increase in accumulation	Ivanova et al. (2011)
	Veralosine	L5178/*MDR1*	Flow cytometric assay of Rh-123 accumulation	Increase in accumulation	Ivanova et al. (2011)
	Veralosinine + Veranigrine	L5178/*MDR1*	Flow cytometric assay of Rh-123 accumulation	Increase in accumulation	Ivanova et al. (2011)
Indoles and β-carbolines	Antofine	A549-PA (PTX-resistant human lung cancer cell line)	P-gp expression using western blot, *MDR-1* mRNA expression using RT-PCR, Rh-123 accumulation by FACS	Reduction of P-gp and *MDR-1* mRNA expression, increase in intracellular Rh-123 content, synergism with PTX	Kim et al. (2012)
	Arboloscine	KB/VJ300	MDR reversing activity	Moderate to weak activity in reversing MDR	Gan et al. (2014)
	Conoduramine	KB-V1	Binding assay (VBL binding to KB-V1 vesicles)	Inhibition of drug-binding, resulting in circumventing multi-drug resistance	You et al. (1994)
	Coronaridine	KB-V1	Binding assay (VBL binding to KB-V1 vesicles)	Inhibition of drug-binding resulting in circumventing multi-drug resistance	You et al. (1994)

(Continued)

TABLE 1 | Continued

The effects of secondary metabolites on different cell lines expressing ABC-transporters – Transporters targeted directly

	Substance	Cell line	Assay system	Result	Reference
	Harmine	MDA-MB-231 (BCRP), CEM/ADR5000 (P-gp)	Rh-123 accumulation assay, cytotoxicity assay using MTT, MTX efflux assay	Reversal of MTX and CPT resistance in cell line with BCRP-mediated efflux, no effect on P-gp mediated efflux	Ma and Wink (2010)
		Caco-2, CEM/ADR5000	MTT assay	Reversal of DOX resistance in both cell lines, synergism with DOX	Eid et al. (2013)
		Caco-2, CEM/ADR5000	MTT assay, Rh-123 accumulation assay using fluorospectroscopy	Sensitization of cell lines to DOX	Eid et al. (2013)
	Kopsamine	KB/VJ300	MDR reversing activity	Appreciable activity in reversing MDR	Kam et al. (1998)
	Kopsiflorine	KB/VJ300	MDR reversing activity	Appreciable activity in reversing MDR	Kam et al. (1998)
	Lahadinine A	KB/VJ300	MDR reversing activity	Appreciable activity in reversing MDR	Kam et al. (1998)
	Leuconicine (types A - E)	KB/VJ300	MDR reversing activity	Reversal of multidrug resistance	Gan et al. (2009)
	11-Methoxykopsilongine	KB/VJ300	MDR reversing activity	Appreciable activity in reversing MDR	Kam et al. (1998)
	N-methoxycarbonyl-11,12-methylene-dioxykopsinine	KB/VJ300	MDR reversing activity	Appreciable activity in reversing MDR	Kam et al. (1998)
	Pleiocarpine	KB/VJ300	MDR reversing activity	Appreciable activity in reversing MDR	Kam et al. (1998)
	Reserpine	CEM/VLB100	MDR reversing activity	Increase in cytotoxicity, synergism with VBL	Pearce et al. (1989)
	Tryptanthrin	Caco-2	Transport across the Caco-2 cell monolayers, *MDR1* & *2* gene expression	Decrease in the efflux transport of the P-gp and MRP2 substrates (potential inhibitor of P-gp and MRP2)	Zhu et al. (2011)
	Vocamine	KB-V1	Binding assay (VBL binding to KB-V1 vesicles)	Inhibition of drug-binding resulting in circumventing multi-drug resistance	You et al. (1994)
	Yohimbine	CEM/VLB100	MDR reversing activity	Increase in cytotoxicity synergism with VBL	Pearce et al. (1989)
Piperidines, Pyrazines, Diketopiperazines	11E-didehydrostemofoline, 11Z-didehydrostemofoline	K562/Adr	MTT assay; fluorescent substrates accumulation assays	Increase in sensitivity to DOX and PTX; increase in the intracellular concentrations of Rh-123 and calcein-AM	Umsumarng et al. (2017)
	Isostemofoline	K562/Adr	MTT assay; fluorescent substrates accumulation assays	Increase in sensitivity to DOX and PTX; increase in the intracellular concentrations of Rh-123 and calcein-AM	Umsumarng et al. (2017)
	Lobeline	Caco-2, CEM/ADR5000	Rh-123 accumulation assay, cytotoxicity assay using MTT, MTX efflux assay	Inhibition of P-gp mediated efflux, accumulation of Rh-123, increase of DOX sensitivity of both cell lines	Ma and Wink (2008)
	Oxystemokerrine	KB-V1	MDR reversing activity	Slight increase in sensitivity	Chanmahasathien et al. (2011)
	Piperine	MCF-7/DOX, A-549/DDP	MDR reversing activity, Rh-123 accumulation assay, MTX efflux assay, RT-PCR	Reversal of resistance, decrease in ABCB1 and ABCG2 genes expression in MCF-7/DOX cells, decrease in ABCC1 gene expression in A-549/DDP cells	Li et al. (2011)
		Caco-2, CEM/ADR 5000	Cytotoxicity assay using MTT, Rh-123 and calcein-AM retention assay	Substrate, synergistic enhancement of cytotoxicity, inhibition of efflux and consequently accumulation of Rh-123 and calcein-AM	Li et al. (2018a)
	Stemocurtisine	KB-V1	MDR reversing activity	Slight increase of sensitivity	Chanmahasathien et al. (2011)
	Stemofoline	KB-V1	MDR reversing activity	Increase in cell sensitivity	Chanmahasathien et al. (2011)
	Tetramethylpyrazine	MCF-7/Dox	Flow cytometric evaluation of DOX accumulation, P-gp expression	Inhibition of efflux, decrease in P-gp expression	Zhang et al. (2012)
Tropane alkaloids	Pervilleine A	MDR KB-V1	Intracellular VBL accumulation, cytotoxicity	Cytotoxicity synergism with VBL, increase in VBL accumulation	Mi et al. (2001)
	Pervilleine B, C	MDR KB-V1	Cytotoxicity assay	Cytotoxicity synergism with VBL	Mi et al. (2002)
Acridone alkaloids	Acrimarine E	K562/R7	DNR accumulation assay	Inhibition of P-gp-mediated drug efflux	Bayet et al. (2007)
	Gravacridonediol	L5178/*MDR1*	Rh-123 accumulation assay, MTT assay, *MDR1* mRNA expression	Increase in Rh-123 accumulation, increase in DOX toxicity (synergism)	Rethy et al. (2008)

(Continued)

TABLE 1 | Continued

The effects of secondary metabolites on different cell lines expressing ABC-transporters – Transporters targeted directly

	Substance	Cell line	Assay system	Result	Reference
	Gravacridonediol monomethyl ether	L5178/*MDR1*	Rh-123 accumulation assay, MTT assay, *MDR1* mRNA expression	Increase in Rh-123 accumulation, cytotoxicity, synergism with DOX, decrease in *MDR1* mRNA	Rethy et al. (2008)
	Gravacridonetriol	L5178/*MDR1*	Rh-123 accumulation assay, MTT assay, *MDR1* mRNA expression	Increase in Rh-123 accumulation, cytotoxicity, synergism with DOX, decrease in *MDR1* mRNA	Rethy et al. (2008)
	2-Methoxycitpressine I	K562/R7	DNR accumulation assay	Inhibition of p-glycoprotein-mediated drug efflux	Bayet et al. (2007)
	Rutacridone	L5178/*MDR1*	Rh-123 accumulation assay, MTT assay, *MDR1* mRNA expression	Increase in Rh-123 accumulation	Rethy et al. (2008)
Purine alkaloids	Olomoucine II	MDCKII-ABCB1, HCT-8 and HepG2	Hoechst 33342 and DNR accumulation assay	Synergism with DNR (increase in intracellular retention of DNR)	Cihalova et al. (2013}
	Purvalanol A	MDCKII-ABCB1, HCT-8 and HepG2	Hoechst 33342 and DNR accumulation assay	Synergism with DNR (increase in intracellular retention of DNR)	Cihalova et al. (2013)
	Roscovitine	MDCKII-ABCB1, HCT-8 and HepG2	Hoechst 33342 and DNR accumulation assay	Synergism with DNR (increase in intracellular retention of DNR)	Cihalova et al. (2013)
Further alkaloids	Anandamine	HK-2	Fluorimetric measurement of the intracellular accumulation of calcein	Inhibition efflux (increase in the intracellular accumulation of calcein)	Nieri et al. (2006)
	Capsaicin	KB-C2	Determination of DNR and Rh-123 accumulation	Increase in the accumulation of DNR and Rh-123	Nabekura et al. (2005)
		Caco-2	[^{3}H]-digoxin transport assay	At non-cytotoxic concentrations, inhibition of P-gp mediated efflux transport of [^{3}H]-digoxin	Han et al. (2006)
		Caco-2, CEM/ADR 5000	Cytotoxicity assay using MTT, Rh-123 and calcein-AM retention assay	Substrate, synergistic enhancement of cytotoxicity, inhibition of efflux and consequently accumulation of Rh-123 and calcein-AM	Li et al. (2018a)
	Galantamine dimer	MCF-7/DX1	Measuring Rh-123 and DOX accumulation	Inhibition of efflux (increased accumulation)	Namanja et al. (2009)
Polyphenols					
Flavonoids	Acacetin	K562/BCRP	Cytotoxicity assay	Increase in cytotoxicity of SN-38 and MTX, strong reversing activity of BCRP-mediated drug resistances	Imai et al. (2004)
		MDA-MB-231	BCECF accumulation assay	Inhibition of the efflux of MRP1 fluorescent substrate (BCECF) from breast cancer cells	Wesołowska et al. (2009)
	Afrormosin	L5178/*MDR1*	Cytotoxicity assay, Rh-123 accumulation assay	Moderately effective on the human *MDR1*-transfected mouse lymphoma cell line	Gyémánt et al. (2005)
		MDA-MB-231	Cytotoxicity assay, BCECF-AM accumulation assay	MRP-mediated efflux pump modifiers, additive effect in combination with epirubicin	Gyémánt et al. (2005)
	Amorphigenin	L5178/*MDR1*	Cytotoxicity assay, Rh-123 accumulation assay	P-gp-mediated efflux pump modifier (strong MDR-reversal effects), strong antiproliferative effects, synergistic effects in combination with epirubicin	Gyémánt et al. (2005)
	Apigenin	MCF-7 MX100	MTX accumulation, cytotoxicity assay	Increasing accumulation and inhibition of BCRP in combination with other flavonoids e.g. biochanin A, and chrysin	Zhang et al. (2004)
		K562/BCRP	Cytotoxicity assay	Strong reversing activity of BCRP-mediated drug resistances	Imai et al. (2004)
	Ampelopsin	K562/ADR	MTT assay, P-gp expression assay using PE-labeled antibody, ADR accumulation assay	Decreasing P-gp expression, reversal of MDR to ADR, increase in cytotoxicity and the intracellular ADR accumulation	Ye et al. (2009)
	7,8-Benzoflavon	MCF-7 MX100	Topotecan accumulation studies	Inhibition of the efflux, increasing the accumulation of topotecan	Zhang et al. (2005)
		MCF-7/ADR	Daunomycin accumulation assay	Decrease of daunomycin efflux, increase in [^{3}H]-daunomycin accumulation, strongly potentiated cytotoxicity of daunomycin	Chung et al. (2005)

(Continued)

TABLE 1 | Continued

The effects of secondary metabolites on different cell lines expressing ABC-transporters – Transporters targeted directly

Substance	Cell line	Assay system	Result	Reference
Biochanin A	MDA435/LCC6, MCF-7/ADR, MDA435/ LCCMDR1	Daunomycin accumulation, DOX cytotoxicity	Increase in [^{3}H]-daunomycin accumulation, potentiation of DOX cytotoxicity, inhibition of P-gp-mediated cellular efflux	Zhang and Morris (2003)
	Panc-1	Determination of daunomycin and VBL accumulation	Increase in accumulation of daunomycin and VBL in Panc-1 cells, inhibiting MRP1-mediated drug transport	Nguyen et al. (2003)
	MCF-7 MX100	MTX accumulation, cytotoxicity assay	Increasing accumulation and inhibiting BCRP in combination with other flavonoids e.g. apigenin or chrysin	Zhang et al. (2004)
	Caco-2	Ochratoxin A (OTA) accumulation assay	Increase in OTA accumulation, impairing OTA efflux through competitive inhibition of MRP-2 pump	Sergent et al. (2005)
Catechin	Rats jejunal membrane in vitro	P-gp stimulation/inhibition profiles using a P-gp-dependent ATPase assay	Inhibitory effect on P-gp ATPase activity	Najar et al. (2010)
	NIH-3T3-G185	Intracellular retention of Rh-123 or LDS-751 (P-gp marker substrate)	Slight facilitation of the efflux of LDS-751 (providing a chemoprotective role)	Wang et al. (2002)
Chalcone	Panc-1	Determination of daunomycin and VBL accumulation	Increasing the accumulation of daunomycin and VBL in Panc-1 cells, inhibiting MRP1-mediated drug transport	Nguyen et al. (2003)
Chrysin	CaCo-2	Ochratoxin A (OTA) accumulation assay	Increase in OTA accumulation, impairing OTA efflux through competitive inhibition of MRP-2 pump	Sergent et al. (2005)
	MCF-7 MX100	MTX accumulation, topotecan accumulation studies, cytotoxicity assay	Increasing accumulation and inhibiting BCRP in combination with other flavonoids e.g. Biochanin A, increase in accumulation of topotecan (inhibition of the BCRP-mediated transport of topotecan)	Zhang et al. (2004; 2005)
	K562/BCRP	Cytotoxicity assay	Strong reversing activity of BCRP-mediated drug resistances	Imai et al. (2004)
	L5178/*MDR1*	Cytotoxicity assay, Rh-123 accumulation assay	P-gp-mediated efflux pump modifiers (increase in Rh-123 accumulation), strong antiproliferative effects, synergistic effects in combination with epirubicin	Gyémánt et al. (2005)
Chrysosplenol D	Staphylococcus aureus	S. aureus growth inhibition assay	Synergism with berberine and norfloxacin (Potentiated the activity of berberine and norfloxacin against a resistant strain of S. aureus), MDR pump inhibitor	Stermitz et al. (2002)
Diosmetin	K562/BCRP	Cytotoxicity assay	Strong reversing activity of BCRP-mediated drug resistances	Imai et al. (2004)
Diosmin	Caco-2	Accumulation of Rh-123	Increase in accumulation of Rh-123	Yoo et al. (2007a)
(+)Epicatechin	NIH-3T3-G185	Intracellular retention of Rh-123 or LDS-751 (P-gp marker substrate)	Slightly facilitated active transport (efflux) of LDS-751 (providing a chemoprotective role)	Wang et al. (2002)
(-)Epicatechin	NIH-3T3-G185	Intracellular retention of Rh-123 or LDS-751 (P-gp marker substrate)	Significant enhance of the active transport (efflux) of LDS-751 (providing a chemoprotective role)	Wang et al. (2002)
	KB-C2	Rh-123 and DNR accumulation	No effect on P-gp efflux	Kitagawa et al. (2004)
(-)Epicatechin gallate	NIH-3T3-G185	Intracellular retention of Rh-123 or LDS-751 (P-gp marker substrate)	Slight inhibition of LDS efflux	Wang et al. (2002)
Epicatechin gallate	KB-C2	Rh-123 and DNR accumulation	Increase in cellular accumulation of Rh-123 and DNR	Kitagawa et al. (2004)
	Bel-7404/DOX, mouse models	Cell proliferation, Rh-123 and DOX (DOX) accumulation assay, semi-quantitative RT-PCR	At higher doses a slight inhibitory effect on cell proliferation, administration of DOX with ECG at lower doses significant inhibition of cell proliferation in vitro and hepatoma growth in a xenograft mouse model, increase in DOX and Rh-	Liang et al. (2010)

(Continued)

TABLE 1 | Continued

The effects of secondary metabolites on different cell lines expressing ABC-transporters – Transporters targeted directly

Substance	Cell line	Assay system	Result	Reference
		analysis of *MDR1* mRNA expression	123 accumulations, decreasing P-gp in cells concurrently treated by DOX and ECG, reduction of the expression of *MDR1* mRNA in BEL-7404/DOX cells treated by DOX and ECG	
(-)Epigallocatechin	NIH-3T3-G185	Intracellular retention of Rh-123 or LDS-751 (P-gp marker substrate)	Inhibition of LDS efflux	Wang et al. (2002)
Epigallocatechin	KB-C2	Rh-123 and DNR accumulation	Increasing the accumulation of DNR	Kitagawa et al. (2004)
	MDA-MB-231	BCECF-AM accumulation assay	MRP-mediated efflux pump modifiers	Gyémánt et al. (2005)
Epigallocatechin gallate	NIH-3T3-G185	Intracellular retention of Rh-123 or LDS-751 (P-gp marker substrate)	Slight inhibition of the efflux of Rh-123, enhancing the efflux of LDS	Wang et al. (2002)
	KB-C2	Rh-123 and DNR accumulation	Increase in Rh-123 and DNR accumulation, decrease in the efflux of Rh-123	Kitagawa et al. (2004)
	Bel-7404/DOX, mouse models	Cell proliferation, Rh-123 and DOX (DOX) accumulation assay, Semi-quantitative RT-PCR analysis of *MDR1* mRNA expression	Slight inhibitory effect on cell proliferation at higher doses, significant inhibition of cell proliferation and hepatoma growth by the administration of DOX with EGCG at lower doses in vitro in a xenograft mouse model, increasing DOX and Rh-123 accumulations, decrease of P-gp in cells concurrently treated by DOX and EGCG, expression of *MDR1* mRNA in BEL-7404/DOX cells treated by DOX and EGCG reduced	Liang et al. (2010)
	CEM/ADR5000	MTT assay, Rh-123 accumulation assay using fluorospectroscopy	Reversal of DOX resistance in the cancer cell line	Eid et al. (2013)
	Caco-2, CEM/ADR5000	MTT assay, Rh-123 accumulation assay using fluorospectroscopy	Sensitization of cell lines to DOX	Eid et al. (2013)
	MCF-7	Cytotoxicity using MTS assay, P-gp protein expression using western blot and immunofluorescence microscopy, Rh-123 accumulation	Increase in intracellular Rh-123 accumulation, decrease in P-gp protein expression, reduction of cell viability	Reyes-Esparza et al. (2015)
	Caco-2, CEM/ADR5000	Cytotoxicity determination using MTT assay after combining with DOX, Rh-123 assay and Calcein-AM assay testing P-gp activity	DOX sensitization, synergistic effect on the leukemia cell line	Li et al. (2018b)
	Caco-2, CEM/ADR5000	Cytotoxicity determination using MTT assay after combining with DOX + DTN, Rh-123 assay and Calcein-AM assay testing P-gp activity	DOX sensitization, synergism in both cell lines	Li et al. (2018b)
Formononetin	L5178/*MDR1*	Cytotoxicity assay, Rh-123 accumulation assay	P-gp-mediated efflux pump modifier (strong MDR-reversal effects)	Gyémánt et al. (2005)
	MDA-MB-231	Cytotoxicity assay, BCECF-AM accumulation assay	MRP-mediated efflux pump modifier, synergistic effects in combination with epirubicin	Gyémánt et al. (2005)
Genistein	K562/BCRP	Topotecan and [^{3}H]Genistein accumulation, cytotoxicity assay	Increasing cytotoxicity of SN-38 and MTX, increasing accumulation of [^{3}H]Genistein and topotecan, inhibition of BCRP-mediated drug efflux	Imai et al. (2004)
	Panc-1	Determination of daunomycin and VBL accumulation	Increasing the accumulation of DNM and VBL in Panc-1 cells, inhibiting MRP1-mediated drug transport	Nguyen et al. (2003)

(Continued)

TABLE 1 | Continued

The effects of secondary metabolites on different cell lines expressing ABC-transporters – Transporters targeted directly

Substance	Cell line	Assay system	Result	Reference
	CaCo2	Ochratoxin A (OTA) accumulation assay	Increase in OTA accumulation, impairing OTA efflux through competitive inhibition of MRP-2 pump	Sergent et al. (2005)
Glabridin	MDCKII	Transport of [^{3}H]digoxin	Inhibition of P-gp-mediated transport of digoxin	Cao et al. (2007)
	KB-C2	DNR accumulation	Increase of DNR accumulation (inhibition of the P-gp-mediated efflux of DNR)	Nabekura et al. (2008a)
3,3',4',5,6,7,8-Heptamethoxyflavone	K562/ADM	Uptake of [^{3}H]vincristine	Increasing the uptake of [^{3}H]vincristine (inhibition of P-gp mediated efflux of [^{3}H]vincristine)	Ikegawa et al. (2000)
Kaempferol	Panc-1	Determination of daunomycin and VBL accumulation	Increase in accumulation of DNM and VBL in Panc-1 cells, inhibiting MRP1-mediated drug transport	Nguyen et al. (2003)
	KB-C2	Rh-123 and DNR accumulation	Increase in the accumulation of Rh-123 and DNR (inhibition of substrate efflux)	Kitagawa et al. (2005)
	K562/BCRP	Cytotoxicity assay	Increasing cytotoxicity of SN-38 and MTX, strong reversing activity of BCRP-mediated drug resistances	Imai et al. (2004)
	MDA-MB-231	Cytotoxicity assay, BCECF-AM accumulation assay	MRP-mediated efflux pump modifier, synergistic effects in combination with epirubicin	Gyémánt et al. (2005)
Luteolin	K562/BCRP	Cytotoxicity assay	Strong reversing activity of BCRP-mediated drug resistances	Imai et al. (2004)
Morin	MDA435/LCC6, MCF-7/ADR, MDA435/LCCMDR1	Daunomycin (DNM) accumulation, P-gp ATPase activity assay, [^{3}H]azidopine photoaffinity labeling	Increase in DNM accumulation, inhibition of P-gp ATPase activity, inhibition of P-gp-mediated cellular efflux, inhibition of [^{3}H]azidopine photoaffinity labeling of P-gp suggesting a direct interaction with P-gp substrate binding	Zhang and Morris (2003)
	Panc-1	Determination of daunomycin and VBL accumulation	Increasing the accumulation of DNM and VBL in Panc-1 cells, inhibiting MRP1-mediated drug transport	Nguyen et al. (2003)
Myricetin	MDCKII-MRP1, MDCKII-MRP2	Efflux of calcein (inhibition of MRP1 and MRP2 activity was studied using the fluorescent calcein as a model substrate	Inhibition of MRP1 and MRP2 activity (inhibition of calcein efflux)	van Zanden et al. (2005)
Naringenin	MCF-7/ADR	[^{3}H]-Daunomycin (DNM) accumulation, [^{3}H]-Daunomycin efflux study	Increase in accumulation of DNM, decrease in efflux of DNM	Chung et al. (2005)
	Caco-2	The flux of talinolol across Caco-2 cell monolayers	Reduction of P-gp mediated secretory transport of talinolol (inhibition of P-gp)	De Castro et al. (2008)
	K562/BCRP	Cytotoxicity assay, topotecan accumulation	Increase in cytotoxicity of SN-38 and MTX, increase in accumulation of topotecan	Imai et al. (2004)
Naringenin-7-glucosid	K562/BCRP	Cytotoxicity assay	Inhibition of BCRP-mediated drug resistance	Imai et al. (2004)
Nobiletin	KB-C2, KB/MRP	Accumulation assay of DNR in KB-C2 cells and calcein in KB/MRP cells, P-gp ATPase activity	Increase in the accumulation of DNR in KB-C2 cells, increase in calcein accumulation in KB/MRP cells, stimulation of ATPase activity of P-gp	Nabekura et al. (2008b)
	K562/ADM	Uptake of [^{3}H]vincristine	Increase in the uptake of [^{3}H]vincristine (inhibition of P-gp mediated efflux of [^{3}H]vincristine)	Ikegawa et al. (2000)
	A2780/T, A549/T	Cytotoxicity assay (SRB assay); intracellular accumulation of Rh-123, DOX and Flutax-2 using flow cytometry	Sensitization of cells to chemotherapeutic drugs PTX, DOX, DNR and docetaxel; synergism with PTX; increase in intracellular accumulation of Rh-123, DOX and Flutax-2	Ma et al. (2015)
Phloretin	MDA435/LCC6, MCF-7/ADR	Daunomycin (DNM) accumulation	Increase in DNM accumulation, inhibition of P-gp-mediated cellular efflux	Zhang and Morris (2003)
	Panc-1	Determination of daunomycin and VBL accumulation	Increase in the accumulation of DNM and VBL in Panc-1 cells, inhibiting MRP1-mediated drug transport	Nguyen et al. (2003)
	Mouse lymphoma/MDR1 cells	Rh-123 accumulation	Moderate inhibition of efflux	Molnár et al., 2010 (review)

(Continued)

TABLE 1 | Continued

The effects of secondary metabolites on different cell lines expressing ABC-transporters – Transporters targeted directly

	Substance	Cell line	Assay system	Result	Reference
	Procyanidine	Rat brain microvessel endothelial cells (RBMECs)	Rh-123 intracellular accumulation assay, Rh-123 efflux assay, P-gp ATPase activity measurement	Increase in the accumulation of Rh-123, decrease in Rh-123 efflux, inhibition of the P-gp ATPase activity	He et al. (2009)
	Quercetin	Panc-1	Determination of daunomycin and VBL accumulation	Increase in the accumulation of DNM and VBL in Panc-1 cells, inhibition of MRP1-mediated drug transport	Nguyen et al. (2003)
		CaCo2	Ochratoxin A (OTA) accumulation assay	Increase of OTA accumulation, impairing OTA efflux through competitive inhibition of MRP-2 pump	Sergent et al. (2005)
		BEL/5-FU	Cytotoxicity assay; Rh-123 and ADR accumulation using flow cytometry; ABCB1, ABCC1, ABCC2 mRNA and protein expression using real-time PCR and western blot	Increase in sensitivity to chemotherapeutic drugs 5-FU, MMC and ADR; increase in intracellular Rh-123 and ADR accumulation; decrease in ABCB1, ABCC1 and ABCC2 mRNAs and proteins expression	Chen et al. (2018)
	Robinetin	MDCKII-MRP1, MDCKII-MRP2	Efflux of calcein (inhibition of MRP1 and MRP2 activity was studied using the fluorescent calcein as a model substrate	Inhibition of MRP1 and MRP2 activity (inhibited calcein efflux)	van Zanden et al. (2005)
	Robinin	MDA-MB-231	Cytotoxicity assay, BCECF-AM accumulation assay	MRP-mediated efflux pump modifiers, additive effects in combination with epirubicin	Gyémánt et al. (2005)
	Rotenone	Mouse lymphoma/ MDR1, COLO320/ MDR1	Rh-123 accumulation	Inhibited efflux, increased Rh-123 accumulation	Molnár et al., 2010 (review)
		L5178/*MDR1*	Cytotoxicity assay, Rh-123 accumulation assay	P-gp-mediated efflux pump modifier (MDR modulating activity), strong antiproliferative effects, additive effects in combination with epirubicin	Gyémánt et al. (2005)
	Silymarin	MCF-7/ADR	[^{3}H]-Daunomycin (DNM) accumulation, [^{3}H]-Daunomycin efflux study	Increase in the accumulation of DNM, decrease in efflux of DNM	Chung et al. (2005)
		MDA435/LCC6, MCF-7/ADR, MDA435/ LCCMDR1	Daunomycin (DNM) accumulation, P-gp ATPase activity assay, [^{3}H]azidopine photoaffinity labeling	Increase in DNM accumulation, inhibition of P-gp ATPase activity, inhibition of P-gp-mediated cellular efflux, inhibition of [^{3}H]azidopine photoaffinity labeling of P-gp suggesting a direct interaction with the P-gp substrate binding	Zhang and Morris (2003)
		Panc-1	Determination of daunomycin and VBL accumulation	Increase in the accumulation of DNM and VBL in Panc-1 cells, inhibition of MRP1-mediated drug transport	Nguyen et al. (2003)
	Tangeretin	K562/ADM	Uptake of [^{3}H]vincristine	Increase in the uptake of [^{3}H]vincristine (inhibition of P-gp mediated efflux of [^{3}H]vincristine)	Ikegawa et al. (2000)
Stilbenoids	Resveratrol	KB-C2	Determination of DNR and Rh-123 accumulation	Increase in the accumulation of DNR, decrease in the efflux of Rh-123	Nabekura et al. (2005)
		CaCo2	Ochratoxin A (OTA) accumulation assay	Increase of OTA accumulation, impairing OTA efflux through competitive inhibition of MRP-2 pump	Sergent et al. (2005)
		Caco-2, CEM/ ADR5000	Cytotoxicity assay using MTT, Rh-123 accumulation assay	Increase in Rh-123 accumulation, enhancement of DOX cytotoxicity	El-Readi et al. (2019)
Curcuminoids	Curcumin	SGC7901/VCR	Analysis of apoptosis by propidium iodide (PI)-stained flow cytometry (FCM) and a morphological assay using acridine orange (AO)/ethidium bromide (EB) dual staining, accumulation and efflux of Rh123 as measured by flow cytometry, expression of P-	Promotion of VCR-mediated apoptosis, increase in Rh-123 accumulation and inhibition of the efflux of Rh-123, downregulation of P-gp expression	Tang et al. (2005)

(Continued)

TABLE 1 | Continued

The effects of secondary metabolites on different cell lines expressing ABC-transporters – Transporters targeted directly

	Substance	Cell line	Assay system	Result	Reference
			gp by FCM using fluorescein isothiocyanate (FITC)-conjugated anti-P-gp		
		KBV20C	VCR, PTX	Increasing cytotoxicity	Um et al. (2008)
		KB-C2	Determination of DNR and Rh-123 accumulation	Increase in the accumulation of DNR and Rh-123	Nabekura et al. (2005)
		Caco-2, LLC-PK1, LLC-GA5-COL300	DNR transport (apical to basolateral (a-b) and basolateral to apical (b-a)) across Caco-2 cell monolayers, calcein-AM uptake in LLC-PK1 and LLC-GA5-COL300 cells	Decrease in the efflux ratio of DNR, increase of calcein-AM accumulation in LLC-GA5-COL300	Ampasavate et al. (2010)
		Caco-2, CEM/ADR5000	Cytotoxicity determination using MTT assay after combining with DOX, Rh-123 assay and Calcein-AM assay testing P-gp activity	DOX sensitization, synergistic effect on the colon cancer cell line	Li et al. (2018b)
		Caco-2, CEM/ADR5000	Cytotoxicity determination using MTT assay after combining with DOX + DTN, Rh-123 assay and Calcein-AM assay testing P-gp activity	DOX sensitization, synergism in both cell lines	Li et al. (2018b)
	Bisdemethoxycurcumin	Caco-2, LLC-PK1, LLC-GA5-COL300	DNR transport (apical to basolateral (a-b) and basolateral to apical (b-a)) across Caco-2 cell monolayers, calcein-AM uptake in LLC-PK1 and LLC-GA5-COL300 cells	Decrease in the efflux ratio of DNR	Ampasavate et al. (2010)
	Demethoxycurcumin,	Caco-2, LLC-PK1, LLC-GA5-COL300	DNR transport (apical to basolateral (a-b) and basolateral to apical (b-a)) across Caco-2 cell monolayers, calcein-AM uptake in LLC-PK1 and LLC-GA5-COL300 cells	Decrease in the efflux ratio of DNR, increase of calcein-AM accumulation in LLC-GA5-COL300	Ampasavate et al. (2010)
	Tetrahydrocurcumin	KB-V1, MCF-7 MDR	Rh-123 and calcein-AM accumulation assay by FACS in KB-V1 cells, radiolabeled drug ([^{3}H]-VBL) accumulation for MCF-7 MDR	Increase in the accumulation of Rh-123 and calcein-AM in KB-V-1 cells, increase in the accumulation and inhibition of the [^{3}H]-VBL efflux in MCF-7 MDR	Limtrakul et al. (2007)
Others	Tannic acid	Caco-2, CEM/ADR5000	Cytotoxicity determination using MTT assay after combining with DOX, Rh-123 assay and Calcein-AM assay testing P-gp activity	DOX sensitization, synergistic effect on the colon cancer cell line	Li et al. (2018b)
		Caco-2, CEM/ADR5000	Cytotoxicity determination using MTT assay after combining with DOX + DTN, Rh-123 assay and Calcein-AM assay testing P-gp activity	DOX sensitization, synergism in both cell lines	Li et al. (2018b)
Phenylpropanoids					
Neo-/lignans	Arctigenin	Caco-2	Cytotoxicity determination using MTT assay after combining with DOX, Rh-123 accumulation assay testing P-gp activity	Synergism in Caco-2 cells and slight synergistic effect in CEM/ADR5000, increase in Rh-123 accumulation	Su et al. (2015)

(Continued)

TABLE 1 | Continued

The effects of secondary metabolites on different cell lines expressing ABC-transporters – Transporters targeted directly

	Substance	Cell line	Assay system	Result	Reference
		Caco-2, CEM/ ADR5000	Cytotoxicity determination using MTT assay after combining with DOX + DTN, Rh-123 accumulation assay testing P-gp activity	Significant increase in synergism of combination with DOX by DTN, increase in Rh-123 accumulation	Su et al. (2015)
	Arctiin	Caco-2, CEM/ ADR 5000	Cytotoxicity determination using MTT assay after combining with DOX, Rh-123 accumulation assay testing P-gp activity	Moderate synergistic effect in CEM/ADR (concentration-dependent) and in Caco-2 cells, increase in Rh-123 accumulation	Su et al. (2015)
			Cytotoxicity determination using MTT assay after combining with DOX + DTN, Rh-123 accumulation assay testing P-gp activity	Significant increase in synergism of combination with DOX by DTN, increase in Rh-123 accumulation	Su et al. (2015)
	Epimagnolin A	Flp-In-293/ ABCB1	MTT assay; calcein assay	Enhancement of sensitivity to anti-cancer drugs DNR, DOX, VBL and VCR; inhibition of calcein efflux	Mitani et al. (2018)
	Iso-/lappaol A	Caco-2	Cytotoxicity determination using MTT assay after combining with DOX, Rh-123 accumulation assay testing P-gp activity	Slight synergistic effect in Caco-2 cells, additive effect in CEM/ADR cells, increase in Rh-123 accumulation	Su et al. (2015)
		Caco-2, CEM/ ADR5000	Cytotoxicity determination using MTT assay after combining with DOX + DTN, Rh-123 accumulation assay testing P-gp activity	Significant increase in synergism of combination with DOX by DTN, increase in Rh-123 accumulation	Su et al. (2015)
	Lappaol C	Caco-2, CEM/ ADR 5000	Cytotoxicity determination using MTT assay after combining with DOX, Rh-123 accumulation assay testing P-gp activity	Synergistic effect in CEM/ADR (concentration-dependent) and in Caco-2 cells	Su et al. (2015)
		Caco-2, CEM/ ADR 5000	Cytotoxicity determination using MTT assay after combining with DOX + DTN, Rh-123 accumulation assay testing P-gp activity	Significant increase in synergism of combination with DOX by DTN	Su et al. (2015)
	Lappaol F	Caco-2, CEM/ ADR 5000	Cytotoxicity determination using MTT assay after combining with DOX, Rh-123 accumulation assay testing P-gp activity	Moderate synergism in CEM/ADR 5000 cells with concentration-dependent activity, stronger effect in Caco-2 cells, increase in Rh-123 accumulation	Su et al. (2015)
			Cytotoxicity determination using MTT assay after combining with DOX + DTN, Rh-123 accumulation assay testing P-gp activity	Significant increase in synergism of combination with DOX by DTN, increase in Rh-123 accumulation	Su et al. (2015)
	Matairesinol	KB-C2, KB/ MRP	DNR and calcein accumulation assay	Increasing accumulation of DNR (inhibits the P-gp-mediated efflux of DNR) and calcein (inhibits the MRP1-mediated efflux of calcein)	Nabekura et al. (2008a)
		Caco-2, CEM/ ADR 5000	Cytotoxicity determination using MTT assay after combining with DOX, Rh-123 accumulation assay testing P-gp activity	Synergistic effect in Caco-2 cells, increase in Rh-123 accumulation, reversal of multidrug resistance	Su et al. (2015)
		Caco-2, CEM/ ADR 5000	Cytotoxicity determination using MTT assay after combining with DOX + DTN, Rh-123 accumulation assay testing P-gp activity	Significant increase in synergism of combination with DOX by DTN, increase in Rh-123 accumulation	

(Continued)

TABLE 1 | Continued

The effects of secondary metabolites on different cell lines expressing ABC-transporters – Transporters targeted directly

	Substance	Cell line	Assay system	Result	Reference
	Sesamin	KB-C2	DNR accumulation assay	Increase in DNR accumulation (inhibition of the P-gp-mediated efflux of DNR)	Nabekura et al. (2008a)
Dibenzocyclo-octadienelignans	Gomisin A	HepG2-DR	Cellular Rh-123 accumulation assay by flow cytometry, determination of P-gp-associated ATPase activity, photoaffinity labeling of P-gp with [^{125}I] iodoarylazidoprazosin	Restoration of the cytotoxicity of VBL and DOX, inhibition of the P-gp ATPase activity, additive effect with verapamil and vanadate on the inhibition of Rh-123 efflux, inhibition of [^{125}I]IAAP photo-crosslinking of P-gp	Wan et al. (2006)
	Schisandrin A (Deoxyschizandrin)	Caco-2	Rh-123 uptake assay, bidirectional transports of digoxin and Rh-123	Increase in Rh-123 accumulation, increase in apical-to-basal transports of digoxin and Rh-123, decrease in basal-to-apical transports	Yoo et al. (2007b)
		COR-L23/R	MTT assay, DOX accumulation assay	Restoration of the cytotoxic action of DOX to COR-L23/R cells, increase in the accumulation of DOX	Slaninová et al. (2009)
	Schisandrin B/γ-Schizandrin	COR-L23/R	MTT assay, DOX accumulation assay	Restoration of the cytotoxic action of DOX to COR-L23/R cells, increase in the accumulation of DOX	Slaninová et al. (2009)
	Schisandrol A	HepG2-DR	Flow cytometry analyses of cell cycle and Rh-123 efflux, P-gp-ATPase activity assay	Strong synergistic effect (enhanced cytotoxicity) with DOX, VBL and taxol, restoration VBL-induced G2/M arrest, increase in cellular retention of Rh-123, stimulation of basal P-gp-ATPase	Fong et al. (2007)
Others	Chlorogenic acid	Rats jejunal membrane in vitro	P-gp stimulation/inhibition profiles using a P-gp-dependent ATPase assay	Inhibitory effect on P-gp ATPase activity	Najar et al. (2010)
	Ginkgolic acid	KB-C2	DNR accumulation	Increase of DNR accumulation (inhibiting the P-gp-mediated efflux of DNR)	Nabekura et al. (2008a)
Terpenes					
Monoterpenes	Citronellal	LLC-GA5-COL150	Intracellular accumulation of [^{3}H]digoxin	Increase in [^{3}H]digoxin accumulation	Yoshida et al. (2005)
	(R)-(+)-citronellal	LLC-GA5-COL150	Intracellular accumulation of [^{3}H]digoxin	Increase in [^{3}H]digoxin accumulation	Yoshida et al. (2005)
	(S)-(–) β-citronellol	LLC-GA5-COL150	Intracellular accumulation of [^{3}H]digoxin	Increase in [^{3}H]digoxin accumulation	Yoshida et al. (2005)
	Cineole	LLC-GA5-COL150	Intracellular accumulation of [^{3}H]digoxin	Increase in [^{3}H]digoxin accumulation	Yoshida et al. (2005)
	DL-citronellol	LLC-GA5-COL150	Intracellular accumulation of [^{3}H]digoxin	Increase in [^{3}H]digoxin accumulation	Yoshida et al. (2005)
	Menthol	Caco-2, CEM/ADR5000	MTT assay, Rh-123 accumulation assay using fluorospectroscopy	Reversal of DOX resistance in both cell lines, synergism with DOX	Eid et al. (2013)
		Caco-2, CEM/ADR5000	MTT assay, Rh-123 accumulation assay using fluorospectroscopy	Synergism with DOX	Eid et al. (2013)
	Thymol	Caco-2, CEM/ADR5000	MTT assay, Rh-123 accumulation assay using fluorospectroscopy	Synergism with DOX	Eid et al. (2013)
		Caco-2, CEM/ADR5000	MTT assay, Rh-123 accumulation assay using fluorospectroscopy	Synergism with DOX	Eid et al. (2013)
Iridoid glucosides	Agnuside	Rats jejunal membrane in vitro	P-gp stimulation/inhibition profiles using a P-gp-dependent ATPase assay	Inhibitory effect on P-gp ATPase activity	Najar et al. (2010)
	Negundoside	Rats jejunal membrane in vitro	P-gp stimulation/inhibition profiles using a P-gp-dependent ATPase assay	Stimulatory effect on P-gp ATPase activity	Najar et al. (2010)
	Picroside-I	Rats jejunal membrane in vitro	P-gp stimulation/inhibition profiles using a P-gp-dependent ATPase assay	Stimulatory effect on P-gp ATPase activity	Najar et al. (2010)

(Continued)

TABLE 1 | Continued

The effects of secondary metabolites on different cell lines expressing ABC-transporters – Transporters targeted directly

	Substance	Cell line	Assay system	Result	Reference
	Picroside-II	Rats jejunal membrane in vitro	P-gp stimulation/inhibition profiles using a P-gp-dependent ATPase assay	Inhibitory effect on P-gp ATPase activity	Najar et al. (2010)
Sesquiterpenes	Aromadendrene	Caco-2, CEM/ADR5000	MTT assay using, Rh-123 accumulation assay using fluorospectroscopy	Synergism with DOX	Eid et al. (2013)
		Caco-2, CEM/ADR5000	MTT assay using, Rh-123 accumulation assay using fluorospectroscopy	Synergism with DOX	Eid et al. (2013)
	Farnesiferol B	MCF-7/Adr	Cytotoxicity using alamar blue assay, accumulation of Rh-123 using flow cytometry	Increase in cytotoxicity of DOX, increase in intracellular accumulation of Rh-123	Kasaian et al. (2015)
	Farnesiferol C	MCF-7/Adr	Cytotoxicity using alamar blue assay, accumulation of Rh-123 using flow cytometry	Increase in cytotoxicity of DOX, increase in intracellular accumulation of Rh-123	Kasaian et al. (2015)
	Lehmferin	MCF-7/Adr	Cytotoxicity using alamar blue assay, accumulation of Rh-123 using flow cytometry	Increase in cytotoxicity of DOX, increase in intracellular accumulation of Rh-123	Kasaian et al. (2015)
	Santonin	Rats jejunal membrane in vitro	P-gp stimulation/inhibition profiles using a P-gp-dependent ATPase assay	Inhibitory effect on P-gp ATPase activity	Najar et al. (2010)
	Umbelliprenin	MCF-7/Adr	Cytotoxicity using alamar blue assay, accumulation of Rh-123 using flow cytometry	Increase in cytotoxicity of DOX, increase in intracellular accumulation of Rh-123	Kasaian et al. (2015)
Diterpenes	Andrographolide	Rats jejunal membrane in vitro	P-gp stimulation/inhibition profiles using a P-gp-dependent ATPase assay	Biphasic effect (stimulation at low concentration and inhibition at high concentration)	Najar et al. (2010)
	Carnosic acid	KB-C2, KB/MRP	Accumulation assay of DNR and Rh-123 in KB-C2 and calcein in KB/MRP cells, ATPase activity assay, resistance to VBL cytotoxicity by a calorimetric assay	Increase in the accumulation of DNR and Rh-123 in KB-C2 cells, stimulation of the P-gp ATPase activity, sensitization of KB-C2 cells to VBL cytotoxicity	Nabekura et al. (2010)
	Carnosol	KB-C2, KB/MRP	Accumulation assay of DNR and Rh-123 in KB-C2 and calcein in KB/MRP cells, ATPase activity assay, resistance to VBL cytotoxicity by a calorimetric assay	Increase in the accumulation of DNR and Rh-123 in KB-C2 cells, stimulation of P-gp ATPase activity	Nabekura et al. (2010)
	Esulatin M	L5178Y-MDR	MTT assay; Rh-123 accumulation assay	Synergistic interaction with DOX; increase in intracellular accumulation of Rh-123	Reis et al. (2016)
	Epoxywelwitschene	L5178Y-MDR	MTT assay; Rh-123 accumulation assay	Synergistic interaction with DOX; increase in intracellular accumulation of Rh-123	Reis et al. (2016)
	Euphoboetirane A, C, D, E, F, G and I	L5178Y-MDR	MTT assay; Rh-123 accumulation assay	Increase in intracellular Rh-123 accumulation; synergism with DOX	Neto et al. (2019)
	Euphotuckeyanol	L5178/*MDR1*	Rh-123 accumulation assay, in vitro antiproliferative effect in combination with epirubicin using checkerboard microplate method	Inhibition of Rh-123 efflux (increase in accumulation), exhibition of a synergistic interaction with epirubicin and enhancement of the antiproliferative effect of epirubicin	Duarte et al. (2008)
	Euphowelwitschine A, B	L5178Y-MDR	MTT assay; Rh-123 accumulation assay	Synergistic interaction with DOX; increase in intracellular accumulation of Rh-123	Reis et al. (2016)
	12-Hydroxyboetirane A, B and C	L5178Y-MDR	MTT assay; Rh-123 accumulation assay	Increase in intracellular Rh-123 accumulation; synergism with DOX	Neto et al. (2019)
	Latilagascene A, B, C	L5178/*MDR1*	Assay for Rh-123 accumulation	Inhibition of Rh-123 efflux (increase in accumulation)	Duarte et al. (2006)
	Latilagascene G, H, I	L5178/*MDR1*	Rh-123 accumulation assay, in vitro antiproliferative effect in combination with epirubicin using checkerboard microplate method	Inhibition of Rh-123 efflux (increase in accumulation), exhibition of a synergistic interaction by all compounds with epirubicin and enhancement of the antiproliferative effect of epirubicin	Duarte et al. (2008)

(Continued)

TABLE 1 | Continued

The effects of secondary metabolites on different cell lines expressing ABC-transporters – Transporters targeted directly

	Substance	Cell line	Assay system	Result	Reference
	Totarol	*Staphylococcus aureus* SA-K3092 (Totarol-resistant mutant overexpressing norA)	Checkerboard combination studies using ethidium bromide (EtBr) and totarol, EtBr efflux assay, modulatory activity of totarol at half the MIC	Reduction of the MICs of selected antibiotics by subinhibitory concentrations (suggesting that it may be an efflux pump inhibitor), reduction of ethidium efflux and ethidium MIC in SA-K3092	Smith et al. (2007)
	Tuckeyanol A, B	L5178/*MDR1*	Rh-123 accumulation assay, in vitro antiproliferative effect in combination with epirubicin using checkerboard microplate method	Inhibition of Rh-123 efflux (increase in accumulation), exhibition of a synergistic interaction by both compounds with epirubicin and enhancement of the antiproliferative effect of epirubicin	Duarte et al. (2008)
	Welwitschene	L5178Y-MDR	MTT assay; Rh-123 accumulation assay	Increase in intracellular accumulation of Rh-123	Reis et al. (2016)
Triterpenoids, Saponins*	β-Amyrin	*MDR1*-transfected mouse lymphoma cells	Accumulation of Rh-123, accumulation of ethidium bromide (semi-automated ethidium bromide fluorometric method)	Increase in the accumulation of ethidium bromide (inhibitory activity against the P-gp transporter)	Martins et al. (2010)
	Cumingianol A, B, D	KB-C2	Cytotoxicity assay (MTT)	Enhancement of cytotoxicity against KB-C2 cells in the presence of colchicine	Kurimoto et al. (2011a)
	Cumingianol D	MCF7	Cytotoxicity assay (MTT)	Moderate cytotoxicity	Kurimoto et al. (2011a)
	Deacetylnomilin	CEM/ADR5000, Caco-2	Measurement of DOX cytotoxicity (reversal assay), Rh-123 efflux assay	Inhibition of Rh-123 efflux in CEM/ADR5000 cells, increase in DOX cytotoxicity in Caco-2 cells	El-Readi et al. (2010)
	Dyscusin A	KB-C2	Cytotoxicity assay (MTT)	Enhancement of cytotoxicity against KB-C2 cells in the presence of colchicine	Kurimoto et al. (2011b)
	Glycyrrhetinic acid (Enoxolone)	KB-C2, KB/MRP	DNR and calcein accumulation	Increasing DNR (inhibits the P-gp-mediated efflux of DNR) and calcein (inhibits the MRP1-mediated efflux of calcein) accumulation	Nabekura et al. (2008a)
	Glycyrrhizin*	Rats jejunal membrane in vitro	P-gp stimulation/inhibition profiles using a P-gp-dependent ATPase assay	Biphasic effect (stimulation at low concentration and inhibition at high concentration)	Najar et al. (2010)
	Limonin	CEM/ADR5000, Caco-2	Measurement of DOX cytotoxicity (reversal assay), Rh-123 efflux assay	Inhibition of Rh-123 efflux in CEM/ADR5000 cells, enhancement of DOX cytotoxicity in CEM/ADR5000 and Caco-2 cells	El-Readi et al. (2010)
	Obacunone	MES-SA/DX5, HCT15	Cytotoxicity assay in the presence of PTX	Significant inhibition of the P-gp MDR activity	Min et al. (2007)
	Oleanolic acid	Rats jejunal membrane in vitro	P-gp stimulation/inhibition profiles using a P-gp-dependent ATPase assay	Stimulatory effect on P-gp ATPase activity	Najar et al. (2010)
		MDR1-transfected mouse lymphoma cells	Accumulation of Rh-123, accumulation of ethidium bromide (semi-automated ethidium bromide fluorometric method)	Increase in the accumulation of ethidium bromide (inhibitory activity against the P-gp transporter)	Martins et al. (2010)
	Sinocalycanchinensin E	KB-C2	Cytotoxicity assay (MTT)	Enhancement of the cytotoxicity against KB-C2 cells in the presence of colchicine	Kashiwada et al. (2011)
	Ursolic Acid	KB-C2, KB/MRP	Accumulation assay of DNR and Rh-123 in KB-C2 and calcein in KB/MRP cells, ATPase activity assay, resistance to VBL cytotoxicity by a calorimetric assay	Increase in the accumulation of DNR and Rh-123 in KB-C2 cells, stimulation of P-gp ATPase activity	Nabekura et al. (2010)
	Uvaol	*MDR1*-transfected mouse lymphoma cells	Accumulation of Rh-123, accumulation of ethidium bromide (semi-automated ethidium bromide fluorometric method), checker-board assay (for the study of synergism between uvaol and DOX)	Increase in the accumulation of Rh-123 and ethidium bromide (inhibitory activity against the P-gp transporter), synergism with DOX cytotoxicity	Martins et al. (2010)

(Continued)

TABLE 1 | Continued

The effects of secondary metabolites on different cell lines expressing ABC-transporters – Transporters targeted directly

	Substance	Cell line	Assay system	Result	Reference
Steroids, Saponins*	Alisol B 23-acetate	HepG2-DR, K562-DR	Cellular Rh-123 and DOX accumulation, photoaffinity labeling of P-gp with [^{125}I] iodoarylazidoprazosin, P-gp ATPase activity,	Enhancement of VBL toxicity, restoration of the activity of VBL in causing G2/M arrest, increase in DOX accumulation, delay of Rh-123 efflux, inhibition of the photoaffinity labeling of P-gp by [^{125}I]IAAP, stimulation of the P-gp ATPase activity	Wang et al. (2004)
	11α-O-benzoyl-12β-O-acetyltenacigenin B	HepG2/DOX	MDR reversing potential evaluation (comparing IC_{50} values of an anticancer drug in the absence or presence of 11-Alpha-O-benzoyl-12β-O-acetyl-tenacigenin B)	Increase in the sensitivity of HepG2/Dox cells to the antitumor drugs DOX, VBL, puromycin, and PTX	Hu et al. (2008)
	DTN	Caco-2, CEM/ADR5000	MTT assay using, Rh-123 accumulation assay using fluorospectroscopy	Reversal of DOX resistance, reduction of the IC_{50} value of DOX	Eid et al. (2013)
	Ginsenoside M1, M4 and M12 (hydrolyzed metabolites of ginsenoside)	KB-C2	DNR accumulation, verapamil-induced ATPase activity (for M4)	Increase in DNR accumulation by M1, M4 and M12; decrease of ATPase activity by M4 (most potent substance in this study)	Kitagawa et al. (2007)
	Ginsenoside Rc and Rd	Multidrug resistant mouse lymphoma cells	–	Moderate reduction of the activity of the efflux pump	Berek et al. (2001)
	Ginsenoside Rg_3*	KBV20C	Rh-123 retention assay, photo-affinity labeling with [^{3}H]azidopine, [^{3}H]VBL accumulation, cytotoxicity assay using Sulforhodamine B cell staining method	Increase in accumulation of Rh-123, inhibition of [^{3}H]VBL efflux, prevention of binding of [^{3}H] azidopine to P-gp, restoration of the sensitivity of KBV20C cells to DOX, COL, VCR, and VP-16	Kim et al. (2003)
	Ginsenosides Rg1, Rc, Rd, Re*	Multidrug resistant mouse lymphoma cells	–	Moderate inhibitory effect on the drug efflux pump	Molnár et al. (2000)
	Guggulsterone	KB-C2, KB/MRP	Accumulation assay of DNR and Rh-123 in KB-C2 cells and calcein in KB/MRP cells, ATPase activity of P-gp and MRP1	Increase in Rh-123 and DNR accumulation in KB-C2 cells, inhibition of Rh-123 efflux from KB-C2 cells, increase in the accumulation of calcein in KB/MRP cells, stimulation of ATPase activities of P-gp and MRP1	Nabekura et al. (2008c)
	Methylprototribestin*	L5178/*MDR1*	Rh-123 accumulation, checkerboard microplate method to study the interaction (MDR reversal effect) between the methylprototribestin and DOX	Increase in Rh-123 accumulation, synergistic interaction between methylprototribestin and DOX	Ivanova et al. (2009)
	Protopanaxatriol ginsenosides*	AML-2/D100	Accumulation assay of DNR, [^{3}H]-azidopine photolabeling of P-gp	Reversing the resistance to DNR, increase in DNR accumulation, inhibition of [^{3}H]-azidopine photolabeling of P-gp	Choi et al. (2003)
	β-sitosterol-O-glucoside*	CEM/ADR5000, Caco-2	Measurement of DOX cytotoxicity (reversal assay), Rh-123 efflux assay	Inhibition of Rh-123 efflux in CEM/ADR5000 cells, increase in the cytotoxicity of DOX in Caco-2 cells	El-Readi et al. (2010)
		Caco-2, CEM/ADR5000	MTT assay, Rh-123 accumulation assay using fluorospectroscopy	Reversal of DOX resistance in both cell lines, synergism	Eid et al. (2013)
		Caco-2, CEM/ADR5000	MTT assay, Rh-123 accumulation assay using fluorospectroscopy	Sensitization of cell lines, enhancement of cytotoxicity, light reduction of the IC_{50} value of DOX, synergism in the Caco-2 cells	Eid et al. (2013)
	Stigmasterol	Caco-2, CEM/ADR5000	Measurement of DOX cytotoxicity (reversal assay), Rh-123 efflux assay	Inhibition of Rh-123 efflux in CEM/ADR5000 cells, increase in the cytotoxicity of DOX in Caco-2 cells	El-Readi et al. (2010)
	Tenacigenin B: P8, P26 and P27	SW620/Ad300 (P-gp-overexpressing) MCF-7/VP (MRP-1-	MDR reversal effect on cytotoxicity of anticancer drugs DOX (substrate of P-gp and MRP1) and MTX (substrate of ABCG2), flow	Effective in circumventing MDR mediated by P-gp, MRP1 and ABCG2, inhibition of P-gp efflux activity, increase in intracellular concentration of the substrate drugs through the inhibition of MRP1- and ABCG2-mediated efflux	To et al. (2017)

(Continued)

TABLE 1 | Continued

The effects of secondary metabolites on different cell lines expressing ABC-transporters – Transporters targeted directly

	Substance	Cell line	Assay system	Result	Reference
		overexpressing) MCF-7/ FLV1000 (ABCG2-overexpressing)	cytometry-based efflux assay of Rh-123 (P-gp substrate), calcein AM (MRP1 substrate) and PhA (ABCG2 substrate)		
	Tenacigenin B: P2, P3 and P6	SW620/Ad300 (P-gp-overexpressing), MCF-7/VP (MRP-1-overexpressing), MCF-7/ FLV1000 (ABCG2-overexpressing)	MDR reversal effect on cytotoxicity of anticancer drugs DOX (substrate of P-gp and MRP1) and MTX (substrate of ABCG2), flow cytometry-based efflux assay of Rh-123 (P-gp substrate), calcein AM (MRP1 substrate) and PhA (ABCG2 substrate)	Effective in circumventing MDR mediated by P-gp and MRP1, inhibition of P-gp efflux activity by P2 and P6, increase in the intracellular concentration of the substrate drug via inhibition of MRP1-mediated efflux	To et al. (2017)
	Tenacigenin B: P1, P4, P5, P9 and P28	SW620/Ad300 (P-gp-overexpressing) MCF-7/VP (MRP-1-overexpressing) MCF-7/ FLV1000 (ABCG2-overexpressing)	MDR reversal effect on cytotoxicity of anticancer drugs DOX (substrate of P-gp and MRP1) and MTX (substrate of ABCG2), flow cytometry-based efflux assay of Rh-123 (P-gp substrate), calcein AM (MRP1 substrate) and PhA (ABCG2 substrate)	Effective in circumventing P-gp-mediated MDR, P1 and P5 inhibition of P-gp efflux activity	To et al. (2017)
	Tenacissimoside A*	HepG2/DOX	DOX accumulation, Rh-123 and Hoechst 33342 efflux assay, cell cycle analysis, MDR reversing potential evaluation (comparing IC_{50} values of an anticancer drug in the absence or presence of Tenacissimoside A)	Increase in the sensitivity of HepG2/Dox cells to the antitumor drugs DOX, VBL, puromycin, and PTX, increase in DOX accumulation, enhancement of the action of DOX in causing G2/M arrest, inhibition of the efflux of Rh-123 and Hoechst 33342	Hu et al. (2008)
Tetraterpenes	Aurochrome	L5178/*MDR1*	Rh-123 accumulation assay	Moderate inhibition of P-gp	Gyémánt et al. (2006)
	Canthaxanthin	Caco-2, CEM/ ADR5000	MTT assay, activity determination using Rh-123- and Calcein-AM retention assay	Significant enhancement of cytotoxicity and synergism using the following drugs: PTX, Cycloheximide, DOX, VBL, amphotericin-B, 5-FU, etoposide and cisplatine	Eid et al. (2012)
	Capsanthin	*MDR1* gene-transfected mouse lymphoma (L1210) cells	Rh-123 accumulation assay	Inhibition of the efflux, very active in MDR reversal effect	Molnár et al. (2006)
	Capsorubin	Human *MDR1*-gene-transfected mouse lymphoma (L1210) cells	Rh-123 accumulation assay	MDR reversal activity, enhancement of Rh-123 accumulation	Molnár et al. (2006)
	β-carotene	Caco-2, CEM/ ADR5000	MTT assay, activity determination using Rh-123- and Calcein-AM retention assay	Synergism, significant enhancement of cytotoxicity of DOX, VBL, amphotericin-B, 5-FU, etoposide and cisplatine; substrate	Eid et al. (2012)
		Caco-2, CEM/ ADR5000	MTT assay using, Rh-123 accumulation assay using fluorospectroscopy	Sensitization of cell lines, enhancement of cytotoxicity, strong reduction of the IC_{50} value of DOX and consequently increase of efficacy, synergism	Eid et al. (2013)
		Caco-2, CEM/ ADR5000		Reversal of DOX resistance in both cell lines, synergism	Eid et al. (2013)

(Continued)

TABLE 1 | Continued

The effects of secondary metabolites on different cell lines expressing ABC-transporters – Transporters targeted directly

	Substance	Cell line	Assay system	Result	Reference
			MTT assay using, Rh-123 accumulation assay using fluorospectroscopy		
		ABCB1/Flp-In™-293	MTT assay; calcein-AM accumulation assay	Increase in cytotoxicity of DOX; increase in intracellular concentration of calcein	Teng et al. (2016)
	Crocin	Caco-2, CEM/ADR5000	MTT assay, activity determination using Rh-123- and Calcein-AM retention assay	Synergism, enhancement of cytotoxicity of DOX, VBL, cisplatine; substrate	Eid et al. (2012)
	Diepoxycarotene	L5178/*MDR1*	Rh-123 accumulation assay	Moderate inhibition of P-gp	Gyémánt et al. (2006)
	Fucoxanthin	Caco-2, CEM/ADR5000	MTT assay, activity determination using Rh-123- and Calcein-AM retention assay	Significant enhancement of cytotoxicity and synergism using the following drugs: PTX, Cycloheximide, DOX, VBL, amphotericin-B, 5-FU, etoposide and cisplatine	Eid et al. (2012)
	Mutatochrome	L5178/*MDR1*	Rh-123 accumulation assay	Moderate inhibition of P-gp	Gyémánt et al. (2006)
	Retinoic acid	Caco-2, CEM/ADR5000	MTT assay, activity determination using Rh-123- and Calcein-AM retention assay	Significant enhancement of cytotoxicity and synergism using the following drugs: DOX, VBL, 5-FU, etoposide and cisplatine	Eid et al. (2012)
Benzopyrones					
Coumarins/ coumaric acids	Auraptene	KB-C2 and KB/MRP	Accumulation assay of DNR in KB-C2 cells and calcein in KB/MRP cells, P-gp ATPase activity	Increase in the accumulation of DNR in KB-C2 cells, stimulation of the P-gp ATPase activity	Nabekura et al. (2008b)
		HT29	Cytotoxicity assay (MTT), real-time RT-PCR	Synergic effects with cisplatin, DOX and VCR, increase in the toxicity of applied radiations in auraptene pretreated cells, overexpression of p21 in auraptene pretreated cells after radiotherapy	Moussavi et al. (2017)
	Bergamottin	K562/ADM	[^{3}H]vincristine uptake	Increase in [^{3}H]vincristine uptake, weak MDR reversal activity	Ikegawa et al. (2000)
	Clausarin	K562/R7	DNR accumulation assay	Inhibition of P-gp-mediated drug efflux	Bayet et al. (2007)
	Dicynnamoyl-cis-khellactone	HepG2/Dox, K562/Dox	DOX accumulation and efflux assay, MDR reversing activity (cytotoxicity assay in the presence and absence of an anticancer drug), cell cycle distribution	Increase in DOX uptake and reduction of DOX efflux in HepG2/Dox cells, increase in cytotoxicity of anticancer drugs VBL, DOX, puromycin and PTX in HepG2/Dox and K562/Dox cells, enhancement of DOX-induced G2/M arrest in HepG2/Dox cells	Shen et al. (2006)
	Dihydroxybergamottin	K562/ADM	[^{3}H]vincristine uptake	Increase in [^{3}H]vincristine uptake, weak MDR reversal activity	Ikegawa et al. (2000)
	Phyllodulcin	KB-C2	DNR accumulation	Increase in DNR accumulation (inhibition of P-gp-mediated efflux of DNR)	Nabekura et al. (2008a)
	Praeruptorin A	HepG2/Dox, K562/Dox	MDR reversing activity (cytotoxicity assay in the presence and absence of an anticancer drug)	Increase in cytotoxicity of anticancer drugs VBL, DOX, puromycin and PTX in HepG2/Dox and K562/Dox cells	Shen et al. (2006)
Others					
Dibenzopyran	Magniferin	Rats jejunal membrane in vitro	P-gp stimulation/inhibition profiles using a P-gp-dependent ATPase assay	Biphasic effect (stimulation at low concentration and inhibition at high concentration)	Najar et al. (2010)
Phenols	[6]-Gingerol	KB-C2	Determination of DNR and Rh-123 accumulation	Increase in accumulation of DNR and Rh-123	Nabekura et al. (2005)
Glucoside	Parishin C	Lymphoma cells	–	Moderate reduction of the activity of the efflux pump	Berek et al. (2001)
Phenyl propanoid	Acteoside (Verbascosine)	Rats jejunal membrane in vitro	P-gp stimulation/inhibition profiles using a P-gp-dependent ATPase assay	Inhibitory effect on P-gp ATPase activity	Najar et al. (2010)

**Saponins are marked with asterisks.*

presence of two aryl rings in the hydrophobic moiety, deviation of the aryl rings from a common plane, basicity of nitrogen atom in piperazine, as well as to the distance between the hydrophobic moiety and the basic nitrogen of piperazine which must be no less than 5 Å (Suzuki et al., 1997). The quinolyl group was also suggested to have a key role in the activity of quinolines, because substitution of a quinoline ring by a naphthyl ring or a phenyl ring resulted in the reduction of MDR-reversing activity of the compounds (Suzuki et al., 1997). Among indole alkaloids, antofine showed synergistic effects with PTX in A549-PA cells and overcame resistance to PTX (Kim et al., 2012). The β-carboline harmine reversed the resistance of MTX and CPT in MDA-MB-231 cells with BCRP as overexpressed transporter but it could not affect the P-gp over-expressing CEM/ADR5000 cells the same way in this study (Ma and Wink, 2010). Not only has harmine been tested in combination with DOX but also as three-drug-combination with DTN both of which showed here an increase of effect on cells and a reduction of DOX resistance in Caco-2 and CEM/ADR5000 cells (Eid et al., 2013). As an N-acylpiperidine, piperine inhibited the efflux of the tested substrate which led to an increase of its concentration in Caco-2 and CEM/ADR5000 cells (Li et al., 2018a). Tests of piperine on MCF-7/DOX and A-549/DDP cells resulted in an increase in cytotoxicity of MTX and DOX (Li et al., 2011). Gravacridonetriol, gravacridonediol and its monomethyl ether, all had an inhibitive effect on P-gp L5178/MDR1 cells, which also led to a higher cytotoxicity of DOX (Rethy et al., 2008). Substitution of methyl groups at the positions C-2 and C-4 of acridone led to the increased lipophilicity, which can enhance the binding affinity of acridone derivatives to P-gp (Mayur, 2015). Murahari et al. (2017) studied on 2,4-dimethylacridone derivatives and showed that these compounds were potential modulators of P-gp-mediated MDR. 2,4-dimethylacridones are tricyclic and hydrophobic and have methyl groups at C-2 and C-4 positions with a propyl or butyl side chain containing terminally substituted tertiary amino groups. They found that an alkyl side chain and hydroxyl substituted secondary amine are necessary for the acridones to reverse the P-gp-mediated multidrug resistance. Moreover, an alkyl side chain of length four (butyl) was found to have higher biological activity (Murahari et al., 2017). Hegde et al. (2004) reported that replacing the hydrogen atom at position C-4 by a methoxy group slightly enhanced the lipophilicity of the acridone derivatives. Furthermore, they investigated the MDR-reversing activity of N-10-substituted acridones and N-10-substituted 4-methoxyacridones relative to their corresponding unsubstituted counterparts where the C-4 positions of the acridone rings are occupied by a hydrogen atom and a methoxy group, respectively. The parent acridone and 4-methoxyacridone had the least effect in inhibiting drug efflux suggesting that N-10-substitution is necessary for an ideal activity. It was also found that 4-methoxyacridone derivatives are more efficient than their acridone derivatives' counterparts in increasing drug accumulation. Several N-10-substituted acridones and N-10-substituted-4-methoxyacridones showed MDR-reversing activity greater than the P-gp inhibitor verapamil (Hegde et al., 2004). In another study eighteen N-10-substituted-2-bromoacridones were examined for the anti-MDR activity and compared to the parent compound 2-bromo-10H-acridin-9-one. N-10-substitution was suggested to be necessary for optimal activity of 2-bromoacridones because the parent compound had the least effect in efflux inhibiting activity (Mayur et al., 2006).

Research on olomoucine, purvalanol and roscovitine revealed amongst other things the inhibitive potential of purine alkaloids on P-gp in the form of MDCKII-ABCB1 cells and human HCT-8 and HepG2 cells while olomoucine had the strongest effect of all (Cihalova et al., 2013). Several groups have run experiments with the benzazepine alkaloid capsaicin on different cell lines such as KB-C2, Caco-2 and CEM/ADR5000. The most relevant result was the inhibition of P-gp efflux in the presence of digoxin as substrate at non-toxic concentrations (Nabekura et al., 2005; Han et al., 2006; Li et al., 2018a).

Isoflavonoids and some flavonoids often act as phytoestrogens. Investigations revealed that hydroxyl groups at position C-5 and C-7 are an important property for the P-gp inhibitory effect of flavonoids, although hydrophobicity usually promotes the affinity (Sheu et al., 2010). Acacetin, genistein, kaempferol and naringenin, were examined by Imai et al. (2004) and it resulted in positive effects on K562 cells expressing BCRP. The cytotoxicity of MTX and 7-ethyl-10-hydroxycamptothecin was enhanced using phytoestrogens. In addition, genistein and naringenin enhanced the accumulation of topotecan in K562/BCRP cells. Also apigenin had strong reversal effect on BCRP-mediated MDR (Imai et al., 2004). In MCF-7 MX100 cells, which also overexpressed BCRP, apigenin had similar effect on the accumulation of the anticancer agent MTX (Zhang et al., 2004). However, naringenin, which differs from apigenin only in the saturation of C-2 and C-3, had a significant loss of potency in comparison to the latter due to the lack of a double bond (Conseil et al., 1998). Several groups experimented with the isoflavone and phytoestrogen biochanin A and its outcome on BCRP and P-gp in cell lines such as Panc-1, MCF-7 MX100, MDA435/LCC6, MCF-7/ADR, MDA435/LCCMDR1 and Caco-2. In all studies, an inhibition of drug efflux, an increase of accumulation and a potentiation of cytotoxicity were observed. A combination of biochanin A with some other flavonoids yielded additive effects (Nguyen et al., 2003; Zhang and Morris, 2003; Zhang et al., 2004; Sergent et al., 2005). Nobiletin and tangeretin prevented the P-gp mediated efflux of [^{3}H]vincristine (Ikegawa et al., 2000). Among other flavones with methoxyls they were examined by Ohtani et al. (2007) for the uptake potential of [^{3}H]vincristine as a P-gp substrate. The MDR-reversing effect increased with the number of methoxyl moieties but with the exception of both at C-3′ and C-5′ position on B-ring. In this case there was even a decrease of MDR-reversing potency. Chrysin is a hydroxyflavone with simple structure which has also been examined by a number of groups. The competitive inhibition of the MRP-2 pumps in Caco-2 cells and an antiproliferative effect of chrysin are certain (Gyémánt et al., 2005; Sergent et al., 2005). Moreover, a prevention of BCRP and P-gp mediated efflux took place in MCF-7 MX100 cells and L5178 cells, respectively (Zhang et al., 2004; Zhang et al., 2005;

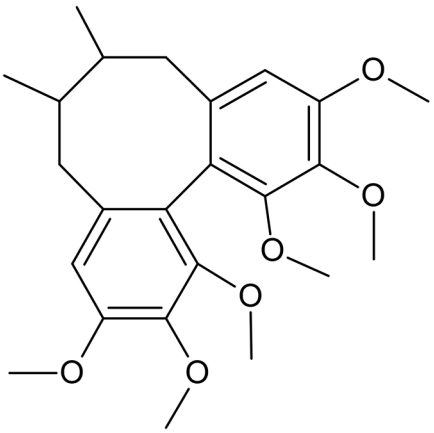

Schisandrin A

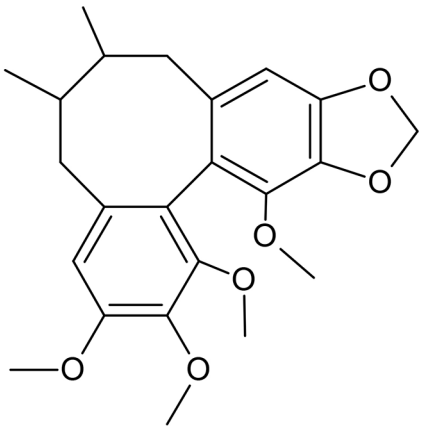

Schisandrin B

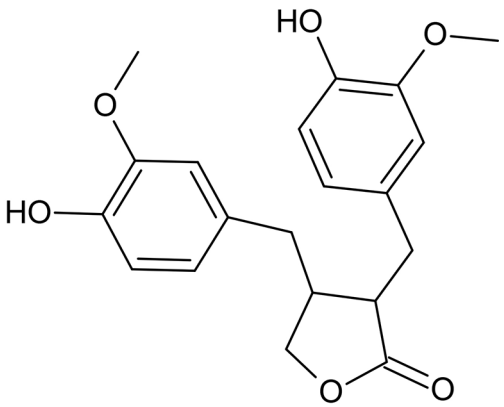

Matairesinol

FIGURE 5 | Chemical structures of some selected lignans with MDR reversal effects.

Gyémánt et al., 2005). A prenyl or geranyl group at C-6 and C-8 of chrysin, and a prenyl in both positions ensured an improvement of the binding affinity to P-gp. In addition, there was more potency for inhibition after geranylation than prenylation which could be due to its level of lipophilicity (Di Pietro et al., 2002). In contrast, glycosylation taking place at any position tested, dramatically decreased the binding affinity of flavonoids (Sheu et al., 2010). Another way to gain binding affinity toward the C-terminal nucleotide-binding domain of P-gp, were other kinds of alkylation of chrysin including methyl, benzyl, isopropyl and 3,3-dimethylallyl (Boumendjel et al., 2002).

Several experiments have been carried out for the flavan epigallocatechin gallate (EGCG), a derivative of epigallocatechin (EGC) abundant in green tea. EGCG has been tested on different cells such as liver cancer cells Bel-7404/DOX, the colon cancer cell line Caco-2, leukemia cells CEM/ADR5000, endocervical adenocarcinoma cells KB-C2 and others. An increase of drug accumulation and sensitization in these and several other cell lines was observed (Kitagawa et al., 2004; Liang et al., 2010; Eid et al., 2013; Reyes-Esparza et al., 2015). Particularly substitutions at D-ring had positive effect on EGC and derivatives. A derivative of EGC with three methoxy groups in cis-configuration at D-ring and an oxycarbonylvinyl as its connection to C-3 led to a higher potency. This structure only regulated P-gp and could not affect BCRP or MRP1 (Wong et al., 2015).

While curcumin is a promising agent for liver protection and inhibition of cancerous cell growth, other curcuminoids like demethoxycurcumin and tetrahydrocurcumin have being studied more closely. They inhibited the efflux of chemptherapeutics and consequently increased cellular accumulation of drugs (Limtrakul et al., 2007; Ampasavate et al., 2010).

TABLE 2 | Phytochemicals Modulating Transporter or Protein Expression.

The effects of secondary metabolites on different cell lines expressing ABC-transporters – Regulation of the expression

	Substance	Cell line	Assay system	Result	Reference
Alkaloids					
Quinolines, Isoquinolines, Quinazolines	Berbamine	K562/ADR	P-gp expression using flow cytometry, mdr-1 gene expression using RT-PCR	Reduction of *MDR1* gene expression	Dong et al. (2004)
	Berberine	OC2 and KB (oral-), SC-M1 and NUGC-3 (gastric-), COLO 205 (colon cancer cell line)	Pgp-170 protein expression using flow cytometry	Upregulation of P-gp expression in tested cell lines, decrease in retention of Rh-123	Lin et al. (1999a)
		Hep3B, HepG2, HA22T/VGH	Rh-123 retention and MDR1 transporter level using flow cytometry	Increase in MDR1 transporter level in HepG2, Hep3B, and HA22T/VGH cells, decrease in retention of Rh-123 in HepG2	Lin et al. (1999b)
		A10 (rat vascular smooth muscle cells)	*MDR1a* and *MDR1b* gene expression by RT-PCR	Increase in expression of *MDR1a* and *MDR1b* mRNA	Suzuki et al. (2010)
		3Y1, dRLh-84, B16	Rh-123 retention using flow cytometry, MDR1a and MDR1b protein expression using western blot	Increase in MDR1a and MDR1b protein level, decrease in intracellular Rh-123 concentration	Suzuki et al. (2010)
	Coptisine	A10	*MDR1a* and *MDR1b* gene expression by RT-PCR, MDR1a and MDR1b protein expression using western blot, Rh-123 retention using flow cytometry	Increase in MDR1a and MDR1b mRNA and protein level, decrease in intracellular Rh-123 content	Suzuki et al. (2010)
		3Y1, dRLh-84, B16	Rh-123 retention using flow cytometry, MDR1a and MDR1b protein expression using western blot	Increase in the level of MDR1a and MDR1b protein, decrease in intracellular Rh-123 concentration	Suzuki et al. (2010)
	Fangchinoline	Caco-2, CEM/ADR5000	MDR reversal assay (effect on DOX cytotoxicity), Rh-123 accumulation assay, western blot (P-gp expression level)	Increase in intracellular Rh-123 accumulation, decrease in P-gp expression, synergism in combination with DOX	Sun and Wink (2014)
	Glaucine	MCF-7/ADR	MDR reversing activity, ADR and MTX efflux assay, real-time RT-PCR, P-gp and MRP1 ATPase activity assay	Inhibition of P-gp and *MRP1*-mediated efflux, suppression of the expression of *MDR1* and *MRP1* genes, reversion of the resistance of MCF-7/ADR to ADR and MTX, increase in P-gp and MRP1 ATPase activities	Lei et al. (2013)
	O-(4-ethoxyl-butyl)-berbamine	MCF-7/ADR	MCF-7/ADR sensitivity to ADR (MTT assay), Rh-123 retention using flow cytometry, expression of mdr-1gene using RT-PCR	Sensitization to ADR, increase in the accumulation of Rh-123, reduction of *MDR1* gene expression	Cheng et al. (2006)
	Palmatine	A10	*MDR1a* and *MDR1b* gene expression by RT-PCR	Increase in the expression of *MDR1a* and *MDR1b* mRNA	Suzuki et al. (2010)
		3Y1, dRLh-84, B16	MDR1a and MDR1b protein expression using western blot, Rh-123 retention using flow cytometry	Increase in the level of MDR1a and MDR1b protein, increase in intracellular Rh-123 content	Suzuki et al. (2010)
	Tetrandrine	Caco-2, CEM/ADR5000	MDR reversal assay (effect on DOX cytotoxicity), Rh-123 accumulation assay, western blot (P-gp expression level)	Increase in intracellular Rh-123 accumulation, decrease in P-gp expression, synergism in combination with DOX	Sun and Wink (2014)
		K562 (DOX-treated vs. tetrandrine+DOX-treated group)	mRNA expression using RT-PCR, detecting P-gp expression as well as Rh-123 accumulation by FACS	Decrease in DOX-induced *MDR1* mRNA expression, inhibition of DOX-induced P-gp expression, increase in Rh-123 accumulation	Shen et al. (2010)
Quinolizidine alkaloids	Matrine	MCF-7/ADR	Western blot for labelling P-gp and MRP1 proteins, fluorospectrophotometry for ADR accumulation assay	Reduction of P-gp expression, increase in intracellular accumulation of ADR, decrease in cell growth	Zhou et al. (2017)
Indoles and β-carbolines	Antofine	A549-PA	P-gp expression using western blot, *MDR-1* mRNA expression using RT-PCR, Rh-123 accumulation by FACS	Reduction of P-gp and *MDR-1* mRNA expression, increase in intracellular Rh-123 content, synergism with PTX	Kim et al. (2012)
	Ephedrine	K562/A02	*MDR1* gene expression using semi-quantitative RT-PCR, P-gp expression using western blot	Decrease in *MDR1* mRNA and P-gp expression	Gao et al. (2008)
	Indole-3-carbinol	Hepatocytes of mouse treated with combination of indole-3-	P-gp expression using western blot, quantitative stereology using immunohistochemical staining with anti-P-gp antibody	Inhibition of VBL/VCR-induced P-gp expression	Arora and Shukla (2003)

(Continued)

TABLE 2 | Continued

The effects of secondary metabolites on different cell lines expressing ABC-transporters – Regulation of the expression

	Substance	Cell line	Assay system	Result	Reference
		carbinol and VBL/VCR (*in vivo*)			
	Staurosporine	MDR KB-V1	Cytotoxicity, P-gp expression using western blot, *MDR1* gene expression by northern blot	Cytotoxicity synergism with verapamil, sensitization of cells to VBL when co-treated with verapamil, decrease in P-gp and *MDR1* gene expression	Sampson et al. (1993)
	Vauqueline	K562/A02	*MDR1* gene expression using semi-quantitative RT-PCR, P-gp expression using western blot	Decrease in *MDR1* mRNA and P-gp expression	Gao et al. (2008)
Piperidines, Pyrazines, Diketopiperazines	Piperine	MCF-7/Dox	*ABCB1* and *ABCG2* mRNA expression by semi-quantitative RT-PCR; fluorescent dye efflux assay, cytotoxicity assay (MTT)	Decrease in *ABCB1* and *ABCG2* mRNA expression, increase in intracellular Rh-123 and MTX accumulation, reversal of resistance to DOX and MTX	Li et al. (2011)
		A-549/DDP	*ABCC1* mRNA expression by semi-quantitative RT-PCR; fluorescent dye efflux assay, cytotoxicity assay (MTT)	Decrease in *ABCC1* mRNA expression, increase in intracellular DOX accumulation, reversal of resistance to DOX	
	Tetramethylpyrazine	MCF-7/Dox	DOX retention by flow cytometry, P-gp expression using western blot, *MDR1* expression using RT-PCR	Increase in DOX retention, reversal of resistance to PTX, VCR and DOX; decrease in P-gp and *MDR1* mRNA expression	Zhang et al. (2012)
		Pumc-91/ADM, T24/DDP	Cell viability assay using Cell Counting Kit-8, qRT-PCR for *MRP1* mRNA, western blot and immunofluorescence assay for MRP1 protein expression	Decrease in MRP1 protein and mRNA expression, reversal of MDR (increase in cytotoxicity of ADR and DDP)	Wang et al. (2016)
		BEL-7402/ADM	ADR accumulation by flow cytometry and HPLC, gene expression using RT-PCR, protein expression by western blot	Decrease in *MDR1*, *MRP2*, *MRP3* and *MRP5* mRNA and proteins expression, increase in ADR intracellular accumulation, increase in ADR cytotoxicity (MDR reversal effect)	Wang et al. (2010)
Acridone alkaloids	Gravacridonetriol	L5178/*MDR1*	Rh-123 retention, MTT antiproliferative assay, *MDR1* expression by RT-PCR	Decrease in Rh-123 efflux, increase in DOX cytotoxicity (synergism), decrease in *MDR1* mRNA expression	Rethy et al. (2008)
	Gravacridonediol monomethyl ether	L5178/*MDR1*	Rh-123 retention, MTT antiproliferative assay, *MDR1* expression by RT-PCR	Decrease in Rh-123 efflux, increase in DOX cytotoxicity (synergism), decrease in *MDR1* mRNA expression	Rethy et al. (2008)
Nucleosides	Clitocine	R-HepG2, MES-SA/Dx5	DOX retention by flow cytometry, western blot for P-gp and qRT-PCR for *MDR1* expression	Decrease in *MDR1* mRNA and P-gp expression, reversal of MDR (enhancement of DOX cytotoxicity), increase in DOX accumulation	Sun et al. (2012)
	Sulfinosine	NCI-H460/R, U87-TxR	DOX retention by flow cytometry, western blot for P-gp and RT-PCR for *MDR1* mRNA expression	Decrease in *MDR1* mRNA and P-g expression, increase in DOX accumulation, decrease in resistance to DOX (enhancement of DOX cytotoxicity)	Dačević et al. (2013)
Further alkaloids	Capsaicin	Caco-2	[^{3}H]-digoxin retention, western blot for P-gp and RT-PCR for *MDR1* mRNA expression	Increase in P-gp and *MDR1* mRNA expression, increase in [^{3}H]-digoxin efflux	Han et al. (2006)
	Homoharringtonine	CEM/E1000	MTT assay	Decrease in cell viability, modulation of MRP1-mediated MDR	Efferth et al. (2002)
Polyphenols					
Flavonoids	Ampelopsin	K562/ADR	MTT assay, P-gp expression by PE-labeled antibody, ADR accumulation using flow cytometry	Decrease in P-gp expression, increase in ADR cytotoxicity and intracellular accumulation, synergism with ADR	Ye et al. (2009)
	Baicalein	LS174T, HepG2	MTT assay, *MDR1* expression using real-time PCR	Decrease in cell viability, increase in *MDR1* expression in LS174T	Li et al. (2010)
	Epicatechingallate	Bel-7404/DOX	MTT assay, Rh-123 retention by flow cytometry, intracellular DOX content using fluorospectrophotometry, semi-quantitative RT-PCR, P-gp expression by FACS using anti-P-gp monoclonal antibody	Increase in DOX and Rh-123 accumulation, and DOX cytotoxicity (synergism), decrease in *MDR1* and P-gp expression	Liang et al. (2010)
	Epigallocatechin gallate	Bel-7404/DOX			

(Continued)

TABLE 2 | Continued

The effects of secondary metabolites on different cell lines expressing ABC-transporters – Regulation of the expression

	Substance	Cell line	Assay system	Result	Reference
			MTT assay, Rh-123 retention by flow cytometry, intracellular DOX content using fluorospectrophotometry, semi-quantitative RT-PCR, P-gp expression by FACS using anti-P-gp monoclonal antibody	Increase in DOX and Rh-123 accumulation, and DOX cytotoxicity (synergism),decrease in *MDR1* and P-gp expression	Liang et al. 2010)
		MCF-7Tam	MTT assay, RT-PCR, western blot for P-gp and BCRP protein expression, Rh-123 and MTX accumulation	Reduction of cell proliferation, decrease in P-gp and BCRP expression, increase in MTX accumulation	Farabegoli et al. (2010)
		MCF-7	Cytotoxicity using MTS assay, P-gp protein expression using western blot and immunofluorescence microscopy, Rh-123 accumulation	Increase in Rh-123 accumulation, decrease in P-gp protein expression, reduction of cell viability	Reyes-Esparza et al. (2015)
	Quercetin	HL-60/ADM, K562/ADM	MDR reversal by MTT assay, RT-PCR, flow cytometry	Sensitization to DNR, decrease in MRP1 gene and protein expression	Cai et al. (2004; 2005)
		BEL/5-FU	Cytotoxicity assay; Rh-123 and ADR accumulation using flow cytometry; ABCB1, ABCC1, ABCC2 mRNA and protein expression using real-time PCR and western blot	Increase in sensitivity to chemotherapeutic drugs 5-FU, MMC and ADR; increase in Rh-123 and ADR accumulation; decrease in ABCB1, ABCC1 and ABCC2 mRNAs and proteins expression	Chen et al. (2018)
Curcuminoids	Bisdemethoxycurcumin	KB-V1	RT-PCR, western blot	Decrease in *MDR1* and P-gp expression	Limtrakul et al. (2004)
	Curcumin	SKOV3(TR)	Cytotoxicity in combination with PTX, western blot	Enhancement of PTX cytotoxic activity, reduction of P-gp expression	Ganta and Amiji (2009)
		HCT-8/VCR	MTT assay, Rh-123 retention, *MDR1* and *survivin* genes expression by RT-PCR	Reversal of MDR, decrease in *MDR1* expression, increase in substrate accumulation	Lu et al. (2013)
Neo-/lignans	Honokiol	MCF-7/ADR	MTT assay, Rh-123 retention, qPCR, P-gp expression by FACS	Increase in Rh-123 retention, reduction of *MDR1* and P-gp expression, increase in ADR cytotoxicity	Xu et al. (2006)
Dibenzocyclo-octadienelignans	Schisandrin A (Deoxyschizandrin)	KBV200, MCF-7/Dox, Bel7402	MTT assay (cytotoxicity in combination with DOX, VCR and PTX), DOX and Rh-123 retention, RT-PCR, western blot for P-gp expression	Increase in Dox and Rh-123 retention, reduction of *MDR1* and P-gp expression, sensitization to cytotoxic drugs	Huang et al. (2008)
		COR-L23/R	MTT assay, DOX retention by flow cytometry	Elevation of DOX cytotoxicity, increase in DOX accumulation	Slaninová et al. (2009)
	Schisandrin B/γ-Schizandrin	COR-L23/R	MTT assay, DOX retention by flow cytometry	Elevation of DOX cytotoxicity, increase in DOX accumulation	Slaninová et al. (2009)
Terpenoids					
Sesquiterpenes	Artesunate	CEM/E1000, CEM/VLB100	MTT assay, DNR retention assay by flow cytometry	Decrease in cell viability, increase in DNR accumulation, modulation of MDR1- and MRP1-mediated MDR	Efferth et al. (2002)
	EGb761	HepG2	*MDR1* expression by real-time RT-PCR	Induction of *MDR1* expression	Li et al. (2009)
Diterpenes	Ginkgolide A and B	HepG2	*MDR1* expression by real-time RT-PCR	Induction of *MDR1* expression	Li et al. (2009)
	Triptolide	In vitro (KB-7D, KB-tax) In vivo (KB-7D-, KB-tax-bearing mouse)	In vitro growth inhibition assay, western blot for MDR1 and MRP1 protein expression, in vivo tumor weight evaluation	Inhibition of cell growth, decrease in MDR1 and MRP1 protein expression, inhibition of tumor growth, decrease in tumor weight when combined with 5-fluorouracil (synergism effect)	Chen et al. (2010)
		DU145/ADM	MTT assay, RT-PCR, western blot	Increase in ADR cytotoxicity, reduction of *MDR1* mRNA and protein expression	Guo et al. (2013)
Benzopyrones					
Coumarins/ coumaric acids	Pyranocoumarins	KB-V1	Sulforhodamine B cytotoxicity assay, DOX retention by flow cytometry, *MDR1* mRNA	Synergism with DOX, VCR, puromycin and PTX; increase in intracellular accumulation of	Wu et al. (2003)

(Continued)

TABLE 2 | Continued

The effects of secondary metabolites on different cell lines expressing ABC-transporters – Regulation of the expression

	Substance	Cell line	Assay system	Result	Reference
			Expression using RT-PCR, P-gp expression by western blot	DOX; decrease in P-gp and *MDR1* mRNA expression	
Phenols					
	6-Gingerol, 10-Gingerol	PC3R	Cytotoxicity assay, MRP-1 protein expression using western blot	Reduction of cell survival, decrease in MRP-1 protein expression	Liu et al. (2017)
	6-Shogaol, 10-Shogaol	PC3R	Cytotoxicity assay, MRP-1 protein expression using western blot	Reduction of cell survival, decrease in MRP-1 protein expression	Liu et al. (2017)

Among phenylpropanoids, some lignans (**Figure 5**) showed an inhibitory effect on P-gp. Schisandrin A was used on Caco-2 cells resulting in an increase in apical-to-basal transport and cytotoxicity Yoo et al. (2007b). A study which examined the structure activity of lignans showed the benefit of the absence of a hydroxyl group in position C-8 as in schisandrin A and γ-schizandrin for the function as p-gp inhibitor. In addition, a higher effect was seen in R-configurated biaryl than in the S-configuration (Slaninová et al., 2009). The reversal of cytotoxicity in CEM/ADR 5000 and Caco-2 cells was moreover successful by using menthol or thymol, monoterpenes obtained from volatile oils. They could reduce the IC_{50} value of doxorubicin which enhances the effectiveness of the drug (Eid et al., 2013).

Reis et al. (2016) reported that jatrophane diterpenes including esulatin M, epoxywelwitschene, welwitschene, and euphowelwitschine A were more efficative in MDR cells than the positive control verapamil. In comparison to the known MDR modifier verapamil, euphoboetirane C, D, E, F, and G extracted from *Euphorbia boetica* showed multifold P-gp modulatory activity in L5178Y-MDR cells (Neto et al., 2019). Three types of latilagascenes (G, H and I), macrocyclic diterpene esters, were effective in L5178 cells expressing P-gp as transport inhibitors (Duarte et al., 2008). All successfully tested diterpenes mentioned above had a cyclopentane moiety in their structure. An enormous increase of activity was observed due to their saturation. Moreover, there was lower MDR-reversing activity mostly when the number of three hydroxyls was exceeded, especially in position 5, 7, 9 and 12. Nevertheless hydropxyls at C-1, C-13, C-14 and C-15 had not any negative effect on their function (Zhu et al., 2016). Vasas et al. (2011) observed that the lack of oxygenation at C-2 increased the MDR-reversing activity in diterpene jatrophanes such as 3β,5α,15β-triacetoxy-7β-isobutanoyloxyjatropha-6(17),11E-diene-9,14-dione and 3β,5α,15β-triacetoxy-7β-isobutanoyloxy-9α-nicotinoyloxyjatropha-6(17),11-dien-14-one. Furthermore, they stated that the presence of benzoyl or nicotinoyl group at C-2 instead of an acetyl group increases the potency of jatrophane diterpenes. The reversal of MDR was noticed in some triterpenoids including ursolic acid tested in KB-C2 cells (Nabekura et al., 2010), and deacteylnomilin and limonin in CEM/ADR5000 cells (El-Readi et al., 2010). A study on triterpenoids such as tormentic acid and derivatives suggests that an acetylation of C-2 of a terpenoid can cause an increase of activity, while this is not the case with the acetylation of C-3 (da Graça Rocha et al., 2007). Carotenoids, a group derived from tetraterpenes, are substrates for ABC transporters and can effectively modulate MDR in cancer cells (Eid et al., 2012). A few types such as β-carotene (Eid et al., 2013) or the xanthophyll member capsorubin showed MDR reversal activity (Molnár et al., 2006). To mention another important group with aromatic members, coumarins and coumaric acids are benzopyrones which we presented in **Tables 1** and **2**. Auraptene for example not only caused an enhancement of drug uptake (Nabekura et al., 2008b); its effect even was of a synergistic kind with drugs such as cisplatin and VCR (Moussavi et al., 2017). Kasaian et al. (2015) examined fifteen sesquiterpene coumarins. Considering the structure-activity relationship they described that ring-opened drimane-type sesquiterpene coumarins such as lehmferin, farnesiferol B and farnesiferol C showed the best P-gp inhibitory effects. Their study also revealed that farnesiferol C inhibited the Rh-123 efflux even more than the positive control verapamil.

The studies introduced phytochemicals with completely different basic structures, each showing both strong and ineffective members in targeting ABC-transporters. The molecules mentioned were a selection chosen due to their effectiveness, especially in relation to the substances to which they were compared.

Phytochemicals Modulating Transporter or Protein Expression

The following discussion focusses on the question how far phytochemicals affect the expression of ABC transporters or proteins in cancer cell lines. A list of relevant publications is documented in **Table 2**. Although many investigations addressed the inhibitory effect of secondary metabolites on transporter activity, many phytochemicals regulate the expression of corresponding genes, including alkaloids, polyphenols, lignans, terpenes and benzopyrones. Berbamine caused a downregulation of *Mdr-1* expression in K562/ADR cells (Dong et al., 2004), and so did its derivative O-(4-ethoxylbutyl)-berbamine (Cheng et al., 2006). Glaucine not only functioned as inhibitor of transporters but also reduced the expression of *MDR1* and *MRP1* (Lei et al., 2013) while the isoquinoline alkaloids berberine and coptisine, mediated the expression of P-gp (Lin et al., 1999a). Tetramethylpyrazine downregulated the expression of MDR1, MRP2, MRP3 and MRP5 in BEL-7402/ADM cells (Wang et al., 2010). It has also reduced the expression of MDR1 and MRP1 in MCF-7/Dox and Pumc-91/ADM cells, respectively (Zhang et al., 2012; Wang et al., 2016). *MDR1* mRNA and P-gp expression were reduced in response to clitocine and sulfinosine in several cell

lines, such as R-HepG2, MES-SA/Dx5, NCI-H460/R and U87-TxR (Sun et al., 2012; Dačević et al., 2013). Among polyphenols, EGCG mediated a reduction of P-gp and BCRP expression resulting in drug accumulation (Farabegoli et al., 2010). Curcumin enhanced the cytotoxicity of PTX and ADR, respectively against SKOV3(TR) and K562/A02 cells by reducing the expression of P-gp in both cell lines (Chang et al., 2006; Ganta and Amiji, 2009). While some diterpenes and sesquiterpenes induced the transporter expression (Li et al., 2009), others like triptolide suppressed the expression of MDR1 and MRP1 proteins in KB-7D and KB-tax cells (Chen et al., 2010). Beside the positive effect of some coumarins on the activity of ABC transporters, pyranocoumarin was tested on KB-V1 cells and showed a reduction of P-gp protein and MDR1 expression (Wu et al., 2003).

Athough no clear relationship could be established between the structure of a modulator with thre expression of a transporter protein, these findings can be relevant for clinical applications.

Synergistic Combinations of Chemotherapeutics With Phytochemicals

In addition to affecting the activity or expression of transporters, phytochemicals can also reverse MDR in cancer cells through synergism. Phytochemicals causing synergistic interactions with anticancer drugs are documented in **Tables 1** and **2**. The two-drug combination of harmine with DOX not only showed an enhancement of cytotoxicity but a synergistic effect. Glaucine potentiated DOX toxicity in Caco-2 and CEM/ADR5000 cells and reversed their resistance to anticancer drugs. Glaucine exerted synergistic interaction with DOX and even more in a three drug combination with DTN (Eid et al., 2013). Euphoboetirane C, D, F, G, H and I extracted from *Euphorbia boetica* showed strong synergistic interactions with DOX in L5178Y-MDR cells (Neto et al., 2019). Nobiletin and antofine showed synergistic interactions with PTX (Kim et al., 2012; Ma et al., 2015). Jatrophane diterpenes including euphowelwitschine A, euphowelwitschine B, epoxywelwitschene, esulatin M isolated from *Euphorbia welwitschii* demonstrated synergism with DOX in L5178Y-MDR cells (Reis et al., 2016). Fangchinoline, tetrandrine, and pyranocoumarins has been shown to synergistically increase the cytotoxicity of DOX (Wu et al., 2003; Sun and Wink, 2014). These synergistic effects are probably caused by interference of the phytochemicals with ABC transporters and additional molecular targets in cancer cells (Wink et al., 2012). These studies show that a combination of substances can have a great advantage over using single drugs against cancer cells by exploiting synergism.

In Silico Analysis of Phytochemicals as MDR Reversing Agents

In Silico experiments are promising methods for making predictions about interactions of molecules to the drug-binding site of a target such as P-gp, BCRP and MRP1. Molecular docking studies can help finding the phytochemicals with best affinity for the drug-binding site which should be used as lead molecules for further studies. The nucleotide-binding domains (NBD) of these ABC-Transporters are hydrophilic protein parts (Jones and George, 2002). In addition to essential hydrogen bonds which play a crucial role in maintaining the stability and function of biomolecules, modulators with hydrophobic moieties often show affinties to NBDs.

The benzolisoquinoline alkaloid tetrandrine was confirmed to have inhibitory capability. Its binding affinity is close to verapamil and their docking positions are similar. Main part of tetrandrine is fixed in a lipophilic pocket formed by the amino acids Ala729, Ala987, Ileu306, Ileu340, Leu339, Leu65, Leu975, Met69, Met986, Phe303, Phe336, Phe343, Phe728, Phe732, Phe983, Tyr307, Tyr310. Moreover, the positively charged methylamine moiety of tetrandrine formed a cation-π interaction with Phe343 and an aryl ether got into a π-π interaction with Phe336 (Liao et al., 2019).

Regarding in silico investigations, another subtype of alkaloids, piperine was examined by Syed et al. (2017) revealing that hydrophobic interactions with P-gp took place in following positions: Leu339, Met69, Met986, Phe72, Phe336, Phe728, Phe983, Tyr953 and Val982. Moreover, an H-bond with Tyr307 was established. Two piperine analogs were designed which showed better hydrophobic interaction with most of the amino acids mentioned (Syed et al., 2017).

Pharmacophore modeling which was carried out for acridones indicated that three aromatic rings and two H–acceptors which are given in position C-9 bearing a carbonyl group and N-10 were conducive for stable docking. Including designed analogs of acridone the oxygen of a morpholine moiety at a phenyl ring built a water bridge with Ser309 of P-gp and a carboxamide at C-4 helped docking with Phe343. This analog showed hydrophobic interactions with Ala229, Ala302, Ala342, Ile218, Ile221, Ile299, Ile306, Leu225 with even more than two interactions, Leu339, Phe343, and Val345 of P-gp (Gade et al., 2018).

Badhan and Penny (2006) worked on the main characteristics of the pharmacophore of flavonoids by in silico modeling. Flavonoids tested get located within the C-terminal NBD of P-gp binding to amino acids of the ATP pocket such as Tyr1044. The hydroxyl moiety at C-5 of natural flavonoids can form a water bridge with Lys1076 while the hydroxyl group in position 3 and the carbonyl group get into hydrogen bonds within the NBD. Hydroxyl groups at position C-7 led to important hydrogen bonds with amino acids for several flavonoids such as EGC and chrysin (Wongrattanakamon et al., 2017). Ring B gets involved in π- π interaction with Tyr1044. If benzyl, geranyl or prenyl groups added at C-6 and several substitutes added at C-8 position, the docking capability was enhanced. Molecular docking analysis demonstrated that apigenin binds to the ATP-binding site of P-gp through a hydrogen bond with LYS408 and therefore, interferes with binding and cleavage of ATP which are vital for the function of ABC transporters (Saeed et al., 2015). Comparing flavonols to their corresponding flavones such as kaempferol to apigenin, better docking properties have been found in flavonols due to the number of

hydrogen bonds (Badhan and Penny, 2006). A number of naringenin derivatives such as hydrazones and azines were produced by Ferreira et al. (2018) to achieve an improved MDR reversal in P-gp and BCRP. There was a high selectivity for most members of these two groups. It has been shown that the active compounds bind to hydrophobic residues such as transmembrane helix 4 and 5 in the center of an active pocket of BCRP similar to fumitremorgin C, a common inhibitor of BCRP. The hydrazone of these derivatives, a continuation of imine, is located in a pocket in π- π interaction with Phe515 and a dipole-dipole interaction with Met541. The B-ring is in another lipophilic bag made of Phe545, Pro574 and Val516. An improvement in the interaction between the transporter MRP1 and the carbohydrazide derivatives of flavonones due to the resulting flexibility was also observed (Ferreira et al., 2018).

Conclusions and Future Perspectives

Due to the increase of cancer cases and restrictions in therapy owing to the degree of harmfulness, effectiveness and the associated high costs, the development of new substances with less side effects and higher efficacy is required. So far, many structures from the plant kingdom have been discovered and used, such as, diterpene derivatives as taxanes and vinca alkaloids are prime examples with regard to antitumor therapy. Therefore, numerous secondary metabolites which already had positive effect on cell lines should be taken into account for further investigations, which is why we have tried to list them extensively in our tables.

Many phytochemicals including alkaloids, flavonoids, curcuminoids, stilbenoids, terpenes, carotenoids, lignans, and polyketides were examined for their pharmacological activity against MDR. In most of the studies it was possible to differentiate between more effective and less effective molecules. As the next step these molecules must be further studied to determine molecular mechanisms and to identify the pharmacophores. Some valuable results have been provided by structure-activity relationship studies or in silico modeling as shown in this article. Subtances which were superior to others should be selected for further research, so possible lead molecules can be developed. A further step to increase efficacy could be the use of new drug delivery methods and controlled release as with nanotechnologies. As shown in this review, the combination of two and more modulators of differing structures and mode of actions together with chemotherapeutics is another interesting approach. The resulting additive, but above all synergistic effects can be of great importance. They would allow reducing the dose of chemotherapeutics resulting in less side effects and a higher compliance of patients.

Summin up, many phytochemicals in the group of alkaloids, flavonoids, curcuminoids, stilbenoids, terpenes, carotenoids, lignans, and polyketides have been investigated for MDR-reversing activity. Phytochemicals can be a promising source of adjuvant chemicals against cancer, not at least because of their generally low cytotoxicity in the human body. The adjuvant uses of MDR reversing phytochemicals in combination with anticancer drugs may improve the treatment of multidrug resistant cancer types. The present review summarized reports of several secondary metabolites that are capable of synergistically reversing MDR and inhibiting chemotherapy-resistant cancer cells by affecting transporter activity and the expression of ABC transporter genes. Synergism would allow reducing the dose of chemotherapeutics resulting in less side effects and a higher compliance of patients. The efficacy of phytochemicals needs to be confirmed clinically, but nevertheless they already can be considered as the fourth generation of ABC transporter modulators.

AUTHOR CONTRIBUTIONS

BT and IS performed the literature search and wrote the first draft of the manuscript. MW revised and edited the manuscript. All the authors approved the final version of the manuscript.

FUNDING

Ruprecht-Karls-Universität Heidelberg provided financial support within Open-Access Publishing Program.

REFERENCES

Aktories, K., Förstermann, U., Hofmann, F. B., and Starke, K. (2017). *Allgemeine und spezielle Pharmakologie und Toxikologie: Begründet von W. Forth*. Eds. D. Henschler and W. Rummel (München, Germany: Urban & Fischer Verlag/ Elsevier GmbH).

Alamolhodaei, N. S., Tsatsakis, A. M., Ramezani, M., Hayes, A. W., and Karimi, G. (2017). Resveratrol as MDR reversion molecule in breast cancer: An overview. *Food Chem. Toxicol.* 103, 223–232. doi: 10.1016/j.fct.2017.03.024

Ampasavate, C., Sotanaphun, U., Phattanawasin, P., and Piyapolrungroj, N. (2010). Effects of *Curcuma* spp. on P-glycoprotein function. *Phytomedicine* 17, 506–512. doi: 10.1016/j.phymed.2009.09.004

Arora, A., and Shukla, Y. (2003). Modulation of vinca-alkaloid induced P-glycoprotein expression by indole-3-carbinol. *Canc. Lett.* 189, 167–173. doi: 10.1016/S0304-3835(02)00550-5

Badhan, R., and Penny, J. (2006). In silico modelling of the interaction of flavonoids with human P-glycoprotein nucleotide-binding domain. *Eur. J. Med. Chem.* 41, 285–295. doi: 10.1016/j.ejmech.2005.11.012

Baumann, T. W., and Frischknecht, P. M. (1988). "Purines," in *Phytochemicals in Plant Cell Cultures* (San Diego, USA: Academic Press), 403–417.

Bayet, C., Fazio, C., Darbour, N., Berger, O., Raad, I., Chaboud, A., et al. (2007). Modulation of P-glycoprotein activity by acridones and coumarins from *Citrus sinensis*. *Phytother. Res.* 21, 386–390. doi: 10.1002/ptr.2081

Berek, L., Szabo, D., Petri, I. B., Shoyama, Y., Lin, Y. H., and Molnár, J. (2001). Effects of naturally occurring glucosides, solasodine glucosides, ginsenosides and parishin derivatives on multidrug resistance of lymphoma cells and leukocyte functions. *Vivo* 15, 151–156.

Bernstein, C., Bernstein, H., Payne, C. M., and Garewal, H. (2002). DNA repair/pro-apoptotic dual-role proteins in five major DNA repair pathways: fail-safe protection against carcinogenesis. *Mutat. Res. Rev. Mutat.* 511, 145–178. doi: 10.1016/S1383-5742(02)00009-1

Bloch, K. E. (1983). Sterol, structure and membrane function. *Crit. Rev. Biochem.* 14, 47–92. doi: 10.3109/10409238309102790

Borst, P., Evers, R., Kool, M., and Wijnholds, J. (2000). A family of drug transporters: the multidrug resistance-associated proteins. *J. Natl. Canc. Inst.* 92, 1295–1302. doi: 10.1093/jnci/92.16.1295

Borthwick, A. D., and Liddle, J. (2011). The design of orally bioavailable 2, 5-diketopiperazine oxytocin antagonists: from concept to clinical candidate for premature labor. *Med. Res. Rev.* 31, 576–604. doi: 10.1002/med.20193

Boumendjel, A., Di Pietro, A., Dumontet, C., and Barron, D. (2002). Recent advances in the discovery of flavonoids and analogs with high-affinity binding to P-glycoprotein responsible for cancer cell multidrug resistance. *Med. Res. Rev.* 22, 512–529. doi: 10.1002/med.10015

Brown, G. A., McPherson, J. P., Gu, L., Hedley, D. W., Toso, R., Deuchars, K. L., et al. (1995). Relationship of DNA topoisomerase IIα and β expression to cytotoxicity of antineoplastic agents in human acute lymphoblastic leukemia cell lines. *Canc. Res.* 55, 78–82.

Cai, X., Chen, F. Y., Han, J. Y., Gu, C. H., Zhong, H., and Ouyang, R. R. (2004). Restorative effect of quercetin on subcellular distribution of daunorubicin in multidrug resistant leukemia cell lines K562/ADM and HL-60/ADM. *Chin. J. Canc.* 23, 1611–1615.

Cai, X., Chen, F. Y., Han, J. Y., Gu, C. H., Zhong, H., Teng, Y., et al. (2005). Reversal of multidrug resistance of HL-60 adriamycin resistant leukemia cell line by quercetin and its mechanisms. *Chin. J. Oncol.* 27, 326–329.

Cao, J., Chen, X., Liang, J., Yu, X. Q., Xu, A. L., Chan, E., et al. (2007). Role of P-glycoprotein in the intestinal absorption of glabridin, an active flavonoid from the root of *Glycyrrhiza glabra*. *Drug Metabol. Dispos.* 35, 539–553. doi: 10.1124/dmd.106.010801

Cao, Z., Wright, M., Cheng, J., Huang, X., Liu, L., Wu, L., et al. (2014). The novel bis-benzylisoquinoline PY35 reverses P-glycoprotein-mediated multidrug resistance. *Oncol. Rep.* 32, 1211–1217. doi: 10.3892/or.2014.3326

Chanmahasathien, W., Ampasavate, C., Greger, H., and Limtrakul, P. (2011). Stemona alkaloids, from traditional Thai medicine, increase chemosensitivity via P-glycoprotein-mediated multidrug resistance. *Phytomedicine* 18, 199–204. doi: 10.1016/j.phymed.2010.07.014

Chang, H. Y., Pan, K. L., Ma, F. C., Jiao, X. Y., Zhu, H. F., Liu, J. H., et al. (2006). The Study on Reversing Mechanism of Multidrug Resistance of K562/A02 Cell Line by Curcumin and Erythromycin. *Chin. J. Hematol.* 27, 254–258.

Chen, Y. W., Lin, G. J., Chuang, Y. P., Chia, W. T., Hueng, D. Y., Lin, C. K., et al. (2010). Triptolide circumvents drug-resistant effect and enhances 5-fluorouracil antitumor effect on KB cells. *Anti Canc. Drugs* 21, 502–513. doi: 10.1097/CAD.0b013e328337337c

Chen, Z., Shi, T., Zhang, L., Zhu, P., Deng, M., Huang, C., et al. (2016). Mammalian drug efflux transporters of the ATP binding cassette (ABC) family in multidrug resistance: A review of the past decade. *Canc. Lett.* 370, 153–164. doi: 10.1016/j.canlet.2015.10.010

Chen, Z., Huang, C., Ma, T., Jiang, L., Tang, L., Shi, T., et al. (2018). Reversal effect of quercetin on multidrug resistance via FZD7/β-catenin pathway in hepatocellular carcinoma cells. *Phytomedicine* 43, 37–45. doi: 10.1016/j.phymed.2018.03.040

Cheng, Y. H., Qi, J., Xiong, D. S., Liu, J. W., Qi, S. L., Pan, B., et al. (2006). Reversal of multidrug resistance in drug-resistant human breast cancer cell line MCF-7/ADR by calmodulin antagonist O-(4-ethoxyl-butyl)-berbamine. *Acta Academiae Medicinae Sinicae* 28, 164–168.

Choi, C. H., Kang, G., and Min, Y. D. (2003). Reversal of P-glycoprotein-mediated multidrug resistance by protopanaxatriol ginsenosides from Korean red ginseng. *Planta Med.* 69, 235–240. doi: 10.1055/s-2003-38483

Chung, S. Y., Sung, M. K., Kim, N. H., Jang, J. O., Go, E. J., and Lee, H. J. (2005). Inhibition of P-glycoprotein by natural products in human breast cancer cells. *Arch. Pharmacal Res.* 28, 823–828. doi: 10.1007/BF02977349

Cihalova, D., Hofman, J., Ceckova, M., and Staud, F. (2013). Purvalanol A, olomoucine II and roscovitine inhibit ABCB1 transporter and synergistically potentiate cytotoxic effects of daunorubicin in vitro. *PloS One* 8, e83467. doi: 10.1371/journal.pone.0083467

Coley, H. M. (2008). Mechanisms and strategies to overcome chemotherapy resistance in metastatic breast cancer. *Canc. Treat. Rev.* 34, 378–390. doi: 10.1016/j.ctrv.2008.01.007

Collin, G., and Höke, H. (2000). "Quinoline and isoquinoline," in *Ullmann"s Encyclopedia of Industrial Chemistry* (New Jersey, USA: Wiley-VCH).

Conseil, G., Baubichon-Cortay, H., Dayan, G., Jault, J. M., Barron, D., and Di Pietro, A. (1998). Flavonoids: a class of modulators with bifunctional interactions at vicinal ATP-and steroid-binding sites on mouse P-glycoprotein. *Proc. Natl. Acad. Sci.* 95, 9831–9836. doi: 10.1073/pnas.95.17.9831

Cör, D., Knez, Ž., and Knez Hrnčič, M. (2018). Antitumour, antimicrobial, antioxidant and antiacetylcholinesterase effect of *Ganoderma lucidum* terpenoids and polysaccharides: A review. *Molecules* 23, 649. doi: 10.3390/molecules23030649

Cripe, L. D., Uno, H., Paietta, E. M., Litzow, M. R., Ketterling, R. P., Bennett, J. M., et al. (2010). Zosuquidar, a novel modulator of P-glycoprotein, does not improve the outcome of older patients with newly diagnosed acute myeloid leukemia: a randomized, placebo-controlled trial of the Eastern Cooperative Oncology Group 3999. *Blood* 116, 4077–4085. doi: 10.1182/blood-2010-04-277269

Cseke, L. J., Kirakosyan, A., Kaufman, P. B., Warber, S. L., Duke, J. A., and Brielmann, H. L. (2006). *Natural Products from Plants. 2nd Ed* (Boca Raton, USA: CRC Press), ISBN: .

da Graça Rocha, G., Simoes, M., Lucio, K. A., Oliveira, R. R., Kaplan, M. A. C., and Gattass, C. R. (2007). Natural triterpenoids from *Cecropia lyratiloba* are cytotoxic to both sensitive and multidrug resistant leukemia cell lines. *Bioorg. Med. Chem.* 15, 7355–7360. doi: 10.1016/j.bmc.2007.07.020

Dačević, M., Isaković, A., Podolski-Renić, A., Isaković, A. M., Stanković, T., Milošević, Z., et al. (2013). Purine nucleoside analog-sulfinosine modulates diverse mechanisms of cancer progression in multi-drug resistant cancer cell lines. *PloS One* 8, e54044. doi: 10.1371/journal.pone.0054044

Daenen, S., van der Holt, B., Verhoef, G. E., Löwenberg, B., Wijermans, P. W., Huijgens, P. C., et al. (2004). Addition of cyclosporin A to the combination of mitoxantrone and etoposide to overcome resistance to chemotherapy in refractory or relapsing acute myeloid leukaemia: A randomised phase II trial from HOVON, the Dutch–Belgian Haemato-Oncology Working Group for adults. *Leuk. Res.* 28, 1057–1067. doi: 10.1016/j.leukres.2004.03.001

De Castro, W. V., Mertens-Talcott, S., Derendorf, H., and Butterweck, V. (2008). Effect of grapefruit juice, naringin, naringenin, and bergamottin on the intestinal carrier-mediated transport of talinolol in rats. *J. Agr. Food Chem.* 56, 4840–4845. doi: 10.1021/jf0728451

de Sa, A., Fernando, R., Barreiro, E. J., Fraga, M., and Alberto, C. (2009). From nature to drug discovery: the indole scaffold as a 'privileged structure'. *Mini Rev. Med. Chem.* 9, 782–793. doi: 10.2174/138955709788452649

Di Pietro, A., Conseil, G., Perez-Victoria, J. M., Dayan, G., Baubichon-Cortay, H., Trompier, D., et al. (2002). Modulation by flavonoids of cell multidrug resistance mediated by P-glycoprotein and related ABC transporters. *Cell. Mol. Life Sci.* 59, 307–322. doi: 10.1007/s00018-002-8424-8

Dong, Q. H., Zheng, S., Xu, R. Z., Lu, Q., and He, L. (2004). Study on effect of berbamine on multidrug resistance leukemia K562/Adr cells. *Chin. J. Integrated Tradit. West. Med.* 24, 820–822.

Doyle, L. A., Yang, W., Abruzzo, L. V., Krogmann, T., Gao, Y., Rishi, A. K., et al. (1998). A multidrug resistance transporter from human MCF-7 breast cancer cells. *Proc. Natl. Acad. Sci.* 95, 15665–15670. doi: 10.1073/pnas.95.26.15665

Duarte, N., Gyémánt, N., Abreu, P. M., Molnár, J., and Ferreira, M. J. U. (2006). New macrocyclic lathyrane diterpenes, from *Euphorbia lagascae*, as inhibitors of multidrug resistance of tumour cells. *Planta Med.* 72, 162–168. doi: 10.1055/s-2005-873196

Duarte, N., Járdánházy, A., Molnár, J., Hilgeroth, A., and Ferreira, M. J. U. (2008). Synergistic interaction between p-glycoprotein modulators and epirubicine on resistant cancer cells. *Bioorg. Med. Chem.* 16, 9323–9330. doi: 10.1016/j.bmc.2008.08.071

Durmus, S., Hendrikx, J. J., and Schinkel, A. H. (2015). "Apical ABC transporters and cancer chemotherapeutic drug disposition," in *Advances in Cancer Research* (San Diego, USA: Academic Press), 1–41.

Efferth, T., Davey, M., Olbrich, A., Rücker, G., Gebhart, E., and Davey, R. (2002). Activity of drugs from traditional Chinese medicine toward sensitive and MDR1-or MRP1-overexpressing multidrug-resistant human CCRF-CEM leukemia cells. *Blood Cells Mol. Dis.* 28, 160–168. doi: 10.1006/bcmd.2002.0492

Eid, S. Y., El-Readi, M. Z., and Wink, M. (2012). Carotenoids reverse multidrug resistance in cancer cells by interfering with ABC-transporters. *Phytomedicine* 19, 977–987. doi: 10.1016/J.PHYMED.2012.05.010

Eid, S. Y., El-Readi, M. Z., Eldin, E. E. M. N., Fatani, S. H., and Wink, M. (2013). Influence of combinations of digitonin with selected phenolics, terpenoids, and alkaloids on the expression and activity of P-glycoprotein in leukaemia and colon cancer cells. *Phytomedicine* 21, 47–61. doi: 10.1016/J.PHYMED.2013.07.019

El-Readi, M. Z., Hamdan, D., Farrag, N., El-Shazly, A., and Wink, M. (2010). Inhibition of P-glycoprotein activity by limonin and other secondary metabolites from *Citrus* species in human colon and leukaemia cell lines. *Eur. J. Pharmacol.* 626, 139–145. doi: 10.1016/j.ejphar.2009.09.040

El-Readi, M. Z., Eid, S., Abdelghany, A. A., Al-Amoudi, H. S., Efferth, T., and Wink, M. (2019). Resveratrol mediated cancer cell apoptosis, and modulation of multidrug resistance proteins and metabolic enzymes. *Phytomedicine* 55, 269–281. doi: 10.1016/J.PHYMED.2018.06.046

Fantini, M., Benvenuto, M., Masuelli, L., Frajese, G. V., Tresoldi, I., Modesti, A., et al. (2015). In vitro and in vivo antitumoral effects of combinations of polyphenols, or polyphenols and anticancer drugs: Perspectives on cancer treatment. *Int. J. Mol. Sci.* 16, 9236–9282. doi: 10.3390/ijms16059236

Farabegoli, F., Papi, A., Bartolini, G., Ostan, R., and Orlandi, M. (2010). (-)-Epigallocatechin-3-gallate downregulates P-gp and BCRP in a tamoxifen resistant MCF-7 cell line. *Phytomedicine* 17, 356–362. doi: 10.1016/j.phymed.2010.01.001

Ferreira, R. J., Baptista, R., Moreno, A., Madeira, P. G., Khonkarn, R., Baubichon-Cortay, H., et al. (2018). Optimizing the flavanone core toward new selective nitrogen-containing modulators of ABC transporters. *Future Med. Chem.* 10, 725–741. doi: 10.4155/fmc-2017-0228

Fong, W. F., Wan, C. K., Zhu, G. Y., Chattopadhyay, A., Dey, S., Zhao, Z., et al. (2007). Schisandrol A from *Schisandra chinensis* reverses P-glycoprotein-mediated multidrug resistance by affecting Pgp-substrate complexes. *Planta Med.* 73, 212–220. doi: 10.1055/s-2007-967120

Gade, D. R., Makkapati, A., Yarlagadda, R. B., Peters, G. J., Sastry, B. S., and Prasad, V. R. (2018). Elucidation of chemosensitization effect of acridones in cancer cell lines: Combined pharmacophore modeling, 3D QSAR, and molecular dynamics studies. *Comput. Biol. Chem.* 74, 63–75. doi: 10.1016/j.compbiolchem.2018.02.014

Gan, C. Y., Low, Y. Y., Etoh, T., Hayashi, M., Komiyama, K., and Kam, T. S. (2009). Leuconicines A– G and (–)-Eburnamaline, Biologically Active Strychnan and Eburnan Alkaloids from Leuconotis. *J. Nat. Prod.* 72, 2098–2103. doi: 10.1021/np900576b

Gan, C. Y., Yoganathan, K., Sim, K. S., Low, Y. Y., Lim, S. H., and Kam, T. S. (2014). Corynanthean, eburnan, secoleuconoxine, and pauciflorine alkaloids from *Kopsia pauciflora*. *Phytochemistry* 108, 234–242. doi: 10.1016/j.phytochem.2014.09.014

Ganta, S., and Amiji, M. (2009). Coadministration of paclitaxel and curcumin in nanoemulsion formulations to overcome multidrug resistance in tumor cells. *Mol. Pharm.* 6, 928–939. doi: 10.1021/mp800240j

Gao, N., Zhang, Y., Mao, J. Q., Li, G. Q., Zhou, W., Gao, B., et al. (2008). Effects of some traditional Chinese drugs on Mdr1 gene and its expression product in K562/A02 cells. *J. Exp. Hematol.* 16, 785–789.

Gawali, V. S., Simeonov, S., Drescher, M., Knott, T., Scheel, O., Kudolo, J., et al. (2017). C2-modified sparteine derivatives are a new class of potentially long-acting sodium channel blockers. *ChemMedChem* 12, 1819–1822. doi: 10.1002/cmdc.201700568

Gilbert, K. (2001). Review of Plant Secondary Metabolism, by David S. Seigler. *Plant Growth Regul.* 34, 149. doi: 10.1023/A:1013354907356

Guo, Q., Nan, X. X., Yang, J. R., Yi, L., Liang, B. L., Wei, Y. B., et al. (2013). Triptolide inhibits the multidrug resistance in prostate cancer cells via the downregulation of MDR1 expression. *Neoplasma* 60, 598–604. doi: 10.4149/neo_2013_077

Gyémánt, N., Tanaka, M., Antus, S., Hohmann, J., Csuka, O., Mándoky, L., et al. (2005). andIn vitro search for synergy between flavonoids and epirubicin on multidrug-resistant cancer cells. *Vivo* 19, 367–374.

Gyémánt, N., Tanaka, M., Molnár, P., Deli, J., Mándoky, L., and Molnár, J. (2006). Reversal of multidrug resistance of cancer cells in vitro: modification of drug resistance by selected carotenoids. *Anticancer Res.* 26, 367–374.

R. Hänsel and O. Sticher (Eds.) (2009). *Pharmakognosie-Phytopharmazie* (Heidelberg, Germany: Springer-Verlag).

Han, Y., Tan, T. M. C., and Lim, L. Y. (2006). Effects of capsaicin on P-gp function and expression in Caco-2 cells. *Biochem. Pharmacol.* 71, 1727–1734. doi: 10.1016/j.bcp.2006.03.024

He, L., Zhao, C., Yan, M., Zhang, L. Y., and Xia, Y. Z. (2009). Inhibition of P-glycoprotein function by procyanidine on blood–brain barrier. *Phytother. Res.* 23, 933–937. doi: 10.1002/ptr.2781

He, L., Yang, J., and Hu, L. (2010). Transmembrane transport activity of paclitaxel regulated by fangchinoline in MDR1-mDCK II cells. *China J. Chin. Materia Med.* 35, 1478–1481.

Hegde, R., Thimmaiah, P., Yerigeri, M. C., Krishnegowda, G., Thimmaiah, K. N., and Houghton, P. J. (2004). Anti-calmodulin acridone derivatives modulate vinblastine resistance in multidrug resistant (MDR) cancer cells. *Eur. J. Med. Chem.* 39, 161–177. doi: 10.1016/j.ejmech.2003.12.001

Hsiao, S. H., Lu, Y. J., Yang, C. C., Tuo, W. C., Li, Y. Q., Huang, Y. H., et al. (2016). Hernandezine, a bisbenzylisoquinoline alkaloid with selective inhibitory activity against multidrug-resistance-linked ATP-binding cassette drug transporter ABCB1. *J. Nat. Prod.* 79, 2135–2142. doi: 10.1021/acs.jnatprod.6b00597

Hu, Y. J., Shen, X. L., Lu, H. L., Zhang, Y. H., Huang, X. A., Fu, L. C., et al. (2008). Tenacigenin B derivatives reverse P-glycoprotein-mediated multidrug resistance in HepG2/Dox cells. *J. Nat. Prod.* 71, 1049–1051. doi: 10.1021/np070458f

Huang, M., Jin, J., Sun, H., and Liu, G. T. (2008). Reversal of P-glycoprotein-mediated multidrug resistance of cancer cells by five schizandrins isolated from the Chinese herb *Fructus schizandrae*. *Canc. Chemother. Pharmacol.* 62, 1015–1026. doi: 10.1007/s00280-008-0691-0

Huang, F., Wu, X. N., Chen, J. I. E., Wang, W. X., and Lu, Z. F. (2014). Resveratrol reverses multidrug resistance in human breast cancer doxorubicin-resistant cells. *Exp. Ther. Med.* 7, 1611–1616. doi: 10.3892/etm.2014.1662

Ikegawa, T., Ushigome, F., Koyabu, N., Morimoto, S., Shoyama, Y., Naito, M., et al. (2000). Inhibition of P-glycoprotein by orange juice components, polymethoxyflavones in adriamycin-resistant human myelogenous leukemia (K562/ADM) cells. *Canc. Lett.* 160, 21–28. doi: 10.1016/S0304-3835(00)00549-8

Imai, Y., Tsukahara, S., Asada, S., and Sugimoto, Y. (2004). Phytoestrogens/flavonoids reverse breast cancer resistance protein/ABCG2-mediated multidrug resistance. *Canc. Res.* 64, 4346–4352. doi: 10.1158/0008-5472.CAN-04-0078

Incardona, J. P., Gaffield, W., Kapur, R. P., and Roelink, H. (1998). The teratogenic *Veratrum* alkaloid cyclopamine inhibits sonic hedgehog signal transduction. *Development* 125, 3553–3562.

Ivanova, A., Serly, J., Dinchev, D., Ocsovszki, I., Kostova, I., and Molnár, J. (2009). Screening of some saponins and phenolic components of *Tribulus terrestris* and *Smilax excelsa* as MDR modulators. *Vivo* 23, 545–550.

Ivanova, A., Serly, J., Christov, V., Stamboliyska, B., and Molnaár, J. (2011). Alkaloids derived from genus *Veratrum* and *Peganum* of Mongolian origin as multidrug resistance inhibitors of cancer cells. *Fitoterapia* 82, 570–575. doi: 10.1016/J.FITOTE.2011.01.015

Jones, P. M., and George, A. M. (2002). Mechanism of ABC transporters: a molecular dynamics simulation of a well characterized nucleotide-binding subunit. *Proc. Natl. Acad. Sci.* 99, 12639–12644. doi: 10.1073/pnas.152439599

Kam, T. S., Subramaniam, G., Sim, K. M., Yoganathan, K., Koyano, T., Toyoshima, M., et al. (1998). Reversal of multidrug resistance (MDR) by aspidofractinine-type indole alkaloids. *Bioorg. Med. Chem. Lett.* 8, 2769–2772. doi: 10.1016/S0960-894X(98)00486-7

Kamath, K., Wilson, L., Cabral, F., and Jordan, M. A. (2005). βIII-tubulin induces paclitaxel resistance in association with reduced effects on microtubule dynamic instability. *J. Biol. Chem.* 280, 12902–12907. doi: 10.1074/jbc.M414477200

Kasaian, J., Mosaffa, F., Behravan, J., Masullo, M., Piacente, S., Ghandadi, M., et al. (2015). Reversal of P-glycoprotein-mediated multidrug resistance in MCF-7/Adr cancer cells by sesquiterpene coumarins. *Fitoterapia* 103, 149–154. doi: 10.1016/j.fitote.2015.03.025

Kashiwada, Y., Nishimura, K., Kurimoto, S., and Takaishi, Y. (2011). New 29-nor-cycloartanes with a 3,4-seco- and a novel 2,3-seco-structure from the leaves of *Sinocalycanthus chinensis*. *Bioorg. Med. Chem.* 19, 2790–2796. doi: 10.1016/j.bmc.2011.03.055

Kavallaris, M., Tait, A. S., Walsh, B. J., He, L., Horwitz, S. B., Norris, M. D., et al. (2001). Multiple microtubule alterations are associated with *Vinca* alkaloid resistance in human leukemia cells. *Canc. Res.* 61, 5803–5809.

Kelly, R. J., Draper, D., Chen, C. C., Robey, R. W., Figg, W. D., Piekarz, R. L., et al. (2011). A pharmacodynamic study of docetaxel in combination with the P-glycoprotein antagonist tariquidar (XR9576) in patients with lung, ovarian, and cervical cancer. *Clin. Canc. Res.* 17, 569–580. doi: 10.1158/1078-0432.CCR-10-1725

Kim, S. W., Kwon, H. Y., Chi, D. W., Shim, J. H., Park, J. D., Lee, Y. H., et al. (2003). Reversal of P-glycoprotein-mediated multidrug resistance by ginsenoside Rg3. *Biochem. Pharmacol.* 65, 75–82. doi: 10.1016/S0006-2952(02)01446-6

Kim, E.-H., Min, H.-Y., Chung, H.-J., Song, J., Park, H.-J., Kim, S., et al. (2012). Anti-proliferative activity and suppression of P-glycoprotein by (–)-antofine, a natural phenanthroindolizidine alkaloid, in paclitaxel-resistant human lung cancer cells. *Food Chem. Toxicol.* 50, 1060–1065. doi: 10.1016/J.FCT.2011.11.008

Kitagawa, S., Nabekura, T., and Kamiyama, S. (2004). Inhibition of P-glycoprotein function by tea catechins in KB-C2 cells. *J. Pharm. Pharmacol.* 56, 1001–1005. doi: 10.1211/0022357044003

Kitagawa, S., Nabekura, T., Takahashi, T., Nakamura, Y., Sakamoto, H., Tano, H., et al. (2005). Structure–activity relationships of the inhibitory effects of flavonoids on P-glycoprotein-mediated transport in KB-C2 cells. *Biol. Pharm. Bull.* 28, 2274–2278. doi: 10.1248/bpb.28.2274

Kitagawa, S., Takahashi, T., Nabekura, T., Tachikawa, E., and Hasegawa, H. (2007). Inhibitory effects of ginsenosides and their hydrolyzed metabolites on daunorubicin transport in KB-C2 cells. *Biol. Pharm. Bull.* 30, 1979–1981. doi: 10.1248/bpb.30.1979

Koes, R. E., Quattrocchio, F., and Mol, J. N. (1994). The flavonoid biosynthetic pathway in plants: function and evolution. *BioEssays* 16, 123–132. doi: 10.1002/bies.950160209

König, J., Hartel, M., Nies, A. T., Martignoni, M. E., Guo, J., Büchler, M. W., et al. (2005). Expression and localization of human multidrug resistance protein (ABCC) family members in pancreatic carcinoma. *Int. J. Canc.* 115, 359–367. doi: 10.1002/ijc.20831

Körper, S., Wink, M., and Fink, R. H. (1998). Differential effects of alkaloids on sodium currents of isolated single skeletal muscle fibers. *FEBS Lett.* 436, 251–255. doi: 10.1016/S0014-5793(98)01135-1

Kukula-Koch, W. A., and Widelski, J. (2017). "Alkaloids," in *Pharmacognosy* (San Diego, USA: Academic Press), 163–198.

Kurimoto, S. I., Kashiwada, Y., Lee, K. H., and Takaishi, Y. (2011a). Triterpenes and a triterpene glucoside from *Dysoxylum cumingianum*. *Phytochemistry* 72, 2205–2211. doi: 10.1016/j.phytochem.2011.08.002

Kurimoto, S. I., Kashiwada, Y., Morris-Natschke, S. L., Lee, K. H., and Takaishi, Y. (2011b). Dyscusins A—C, three new steroids from the leaves of *Dysoxylum cumingianum*. *Chem. Pharm. Bull.* 59, 1303–1306. doi: 10.1248/cpb.59.1303

Lei, Y., Tan, J., Wink, M., Ma, Y., Li, N., and Su, G. (2013). An isoquinoline alkaloid from the Chinese herbal plant *Corydalis yanhusuo* W.T. Wang inhibits P-glycoprotein and multidrug resistance-associate protein 1. *Food Chem.* 136, 1117–1121. doi: 10.1016/j.foodchem.2012.09.059

Lemmer, B., and Brune, K. (2004). *Pharmakotherapie* (Heidelberg, Germany: Springer-Verlag).

Li, L., Stanton, J. D., Tolson, A. H., Luo, Y., and Wang, H. (2009). Bioactive terpenoids and flavonoids from *Ginkgo biloba* extract induce the expression of hepatic drug-metabolizing enzymes through pregnane X receptor, constitutive androstane receptor, and aryl hydrocarbon receptor-mediated pathways. *Pharmaceut. Res.* 26, 872. doi: 10.1007/s11095-008-9788-8

Li, Y., Wang, Q., Yao, X., and Li, Y. (2010). Induction of CYP3A4 and MDR1 gene expression by baicalin, baicalein, chlorogenic acid, and ginsenoside Rf through constitutive androstane receptor-and pregnane X receptor-mediated pathways. *Eur. J. Pharmacol.* 640, 46–54. doi: 10.1016/j.ejphar.2010.05.017

Li, S., Lei, Y., Jia, Y., Li, N., Wink, M., and Ma, Y. (2011). Piperine, a piperidine alkaloid from *Piper nigrum* re-sensitizes P-gp, MRP1 and BCRP dependent multidrug resistant cancer cells. *Phytomedicine* 19, 83–87. doi: 10.1016/j.phymed.2011.06.031

Li, H., Krstin, S., Wang, S., and Wink, M. (2018a). Capsaicin and piperine can overcome multidrug resistance in cancer cells to doxorubicin. *Molecules* 23, 557. doi: 10.3390/molecules23030557

Li, H., Krstin, S., and Wink, M. (2018b). Modulation of multidrug resistant in cancer cells by EGCG, tannic acid and curcumin. *Phytomedicine* 50, 213–222. doi: 10.1016/j.phymed.2018.09.169

Liang, G., Tang, A., Lin, X., Li, L., Zhang, S., Huang, Z., et al. (2010). Green tea catechins augment the antitumor activity of doxorubicin in an in vivo mouse model for chemoresistant liver cancer. *Int. J. Oncol.* 37, 111–123. doi: 10.3892/ijo_00000659

Liao, D., Zhang, W., Gupta, P., Lei, Z. N., Wang, J. Q., Cai, C. Y., et al. (2019). Tetrandrine Interaction with ABCB1 Reverses Multidrug Resistance in Cancer Cells Through Competition with Anti-Cancer Drugs Followed by Downregulation of ABCB1 Expression. *Molecules* 24, 4383. doi: 10.3390/molecules24234383

Limtrakul, P., Anuchapreeda, S., and Buddhasukh, D. (2004). Modulation of human multidrug-resistance MDR-1 gene by natural curcuminoids. *BMC Canc.* 4, 13. doi: 10.1186/1471-2407-4-13

Limtrakul, P., Chearwae, W., Shukla, S., Phisalphong, C., and Ambudkar, S. V. (2007). Modulation of function of three ABC drug transporters, P-glycoprotein (ABCB1), mitoxantrone resistance protein (ABCG2) and multidrug resistance protein 1 (ABCC1) by tetrahydrocurcumin, a major metabolite of curcumin. *Mol. Cell. Biochem.* 296, 85–95. doi: 10.1007/s11010-006-9302-8

Lin, H. L., Liu, T. Y., Lui, W. Y., and Chi, C. W. (1999a). Up-regulation of multidrug resistance transporter expression by berberine in human and murine hepatoma cells. *Canc. Interdiscipl. Int. J. Am. Canc. Soc* 85, 1937–1942. doi: 10.1002/(SICI)1097-0142(19990501)85:9<1937::AID-CNCR9>3.0.CO;2-F

Lin, H.-L., Liu, T.-Y., Wu, C.-W., and Chi, C.-W. (1999b). Berberine modulates expression of MDR1 gene product and the responses of digestive track cancer cells to paclitaxel. *Br. J. Canc.* 81, 416–422. doi: 10.1038/sj.bjc.6690710

Liu, C. M., Kao, C. L., Tseng, Y. T., Lo, Y. C., and Chen, C. Y. (2017). Ginger phytochemicals inhibit cell growth and modulate drug resistance factors in docetaxel resistant prostate cancer cell. *Molecules* 22, 1477. doi: 10.3390/molecules22091477

Lu, J. J., Dang, Y. Y., Huang, M., Xu, W. S., Chen, X. P., and Wang, Y. T. (2012). Anti-cancer properties of terpenoids isolated from *Rhizoma curcumae* – a review. *J. Ethnopharmacol.* 143, 406–411. doi: 10.1016/j.jep.2012.07.009

Lu, W. D., Qin, Y., Yang, C., and Li, L. (2013). Effect of curcumin on human colon cancer multidrug resistance in vitro and in vivo. *Clinics* 68, 694–701. doi: 10.6061/clinics/2013(05)18

Ma, Y., and Wink, M. (2008). Lobeline, a piperidine alkaloid from *Lobelia* can reverse P-gp dependent multidrug resistance in tumor cells. *Phytomedicine* 15, 754–758. doi: 10.1016/j.phymed.2007.11.028

Ma, Y., and Wink, M. (2010). The beta-carboline alkaloid harmine inhibits BCRP and can reverse resistance to the anticancer drugs mitoxantrone and camptothecin in breast cancer cells. *Phytother. Res.* 24, 146–149. doi: 10.1002/ptr.2860

Ma, W., Feng, S., Yao, X., Yuan, Z., Liu, L., and Xie, Y. (2015). Nobiletin enhances the efficacy of chemotherapeutic agents in ABCB1 overexpression cancer cells. *Sci. Rep.* 5, 18789. doi: 10.1038/srep18789

Martins, A., Vasas, A., Schelz, Z., Viveiros, M., Molnár, J., Hohmann, J., et al. (2010). Constituents of *Carpobrotus edulis* inhibit P-glycoprotein of MDR1-transfected mouse lymphoma cells. *Anticancer Res.* 30, 829–835.

Mayur, Y. C., Padma, T., Parimala, B. H., Chandramouli, K. H., Jagadeesh, S., Gowda, N. M., et al. (2006). Sensitization of multidrug resistant (MDR) cancer cells to vinblastine by novel acridones: correlation between anti-calmodulin activity and anti-MDR activity. *Med. Chem.* 2, 63–77. doi: 10.2174/157340606775197732

Mayur, Y. C. (2015). "Designing of drug molecules for reversing P-glycoprotein (Pgp) mediated drug resistance in cancer cells," in *Frontiers in Anti-Cancer Drug Discovery*. Eds. R. Ata-ur- and M. I. Chaudhary (Sharjah, UAE: Bentham Science Publishers), 157–198.

Mi, Q., Cui, B., Silva, G. L., Lantvit, D., Lim, E., Chai, H., et al. (2001). Pervilleine A, a novel tropane alkaloid that reverses the multidrug-resistance phenotype. *Canc. Res.* 61, 4030–4037.

Mi, Q., Cui, B., Silva, G. L., Lantvit, D., Lim, E., Chai, H., et al. (2002). Pervilleines B and C, new tropane alkaloid aromatic esters that reverse the multidrug-resistance in the hollow fiber assay. *Canc. Lett.* 184, 13–20. doi: 10.1016/S0304-3835(02)00202-1

Min, Y. D., Choi, S. U., and Lee, K. R. (2006). Aporphine alkaloids and their reversal activity of multidrug resistance (MDR) from the stems and rhizomes

of *Sinomenium acutum*. *Arch. Pharm. Res.* 29, 627–632. doi: 10.1007/BF02968246

Min, Y. D., Kwon, H. C., Yang, M. C., Lee, K. H., Choi, S. U., and Lee, K. R. (2007). Isolation of limonoids and alkaloids from *Phellodendron amurense* and their multidrug resistance (MDR) reversal activity. *Arch. Pharmacal Res.* 30, 58–63. doi: 10.1007/BF02977779

Mitani, Y., Satake, K., Tsukamoto, M., Nakamura, I., Kadioglu, O., Teruya, T., et al. (2018). Epimagnolin A, a tetrahydrofurofuranoid lignan from *Magnolia fargesii*, reverses ABCB1-mediated drug resistance. *Phytomedicine* 51, 112–119. doi: 10.1016/j.phymed.2018.06.030

Mohanlal, R., Sun, Y., Kloecker, G., Feinstein, T., Shi, Y., Han, B., et al. (2019). P2. 01-23 DUBLIN-3, a phase (Ph) III trial comparing the plinabulin (P)/docetaxel (D) combination with D alone in stage IIIb/IV NSCLC. *J. Thorac. Oncol.* 14, S647–S648. doi: 10.1016/j.jtho.2019.08.1367

Molnár, J., Szabo, D., Pusztai, R., Mucsi, I., Berek, L., Ocsovszki, I., et al. (2000). Membrane associated antitumor effects of crocine-, ginsenoside-and cannabinoid derivates. *Anticancer Res.* 20, 861–867.

Molnár, J., Gyémánt, N., Tanaka, M., Hohmann, J., Bergmann-Leitner, E., Molnár, P., et al. (2006). Inhibition of multidrug resistance of cancer cells by natural diterpenes, triterpenes and carotenoids. *Curr. Pharmaceut. Des.* 12, 287–311. doi: 10.2174/138161206775201893

Molnár, J., Engi, H., Hohmann, J., Molnár, P., Deli, J., Wesolowska, O., et al. (2010). Reversal of multidrug resistance by natural substances from plants. *Curr. Top. Med. Chem.* 10, 1757–1768. doi: 10.2174/156802610792928103

Moussavi, M., Haddad, F., Rassouli, F. B., Iranshahi, M., and Soleymanifard, S. (2017). Synergy between auraptene, ionizing radiation, and anticancer drugs in colon adenocarcinoma cells. *Phytother. Res.* 31, 1369–1375. doi: 10.1002/ptr.5863

Murahari, M., Kharkar, P. S., Lonikar, N., and Mayur, Y. C. (2017). Design, synthesis, biological evaluation, molecular docking and QSAR studies of 2, 4-dimethylacridones as anticancer agents. *Eur. J. Med. Chem.* 130, 154–170. doi: 10.1016/j.ejmech.2017.02.022

Nabekura, T., Kamiyama, S., and Kitagawa, S. (2005). Effects of dietary chemopreventive phytochemicals on P-glycoprotein function. *Biochem. Biophys. Res. Commun.* 327, 866–870. doi: 10.1016/j.bbrc.2004.12.081

Nabekura, T., Yamaki, T., Ueno, K., and Kitagawa, S. (2008a). Inhibition of P-glycoprotein and multidrug resistance protein 1 by dietary phytochemicals. *Canc. Chemother. Pharmacol.* 62, 867–873. doi: 10.1007/s00280-007-0676-4

Nabekura, T., Yamaki, T., and Kitagawa, S. (2008b). Effects of chemopreventive citrus phytochemicals on human P-glycoprotein and multidrug resistance protein 1. *Eur. J. Pharmacol.* 600, 45–49. doi: 10.1016/j.ejphar.2008.10.025

Nabekura, T., Yamaki, T., Ueno, K., and Kitagawa, S. (2008c). Effects of plant sterols on human multidrug transporters ABCB1 and ABCC1. *Biochem. Biophys. Res. Commun.* 369, 363–368. doi: 10.1016/j.bbrc.2008.02.026

Nabekura, T., Yamaki, T., Hiroi, T., Ueno, K., and Kitagawa, S. (2010). Inhibition of anticancer drug efflux transporter P-glycoprotein by rosemary phytochemicals. *Pharmacol. Res.* 61, 259–263. doi: 10.1016/j.phrs.2009.11.010

Najar, I. A., Sachin, B. S., Sharma, S. C., Satti, N. K., Suri, K. A., and Johri, R. K. (2010). Modulation of P-glycoprotein ATPase activity by some phytoconstituents. *Phytother. Res.* 24, 454–458. doi: 10.1002/ptr.2951

Namanja, H. A., Emmert, D., Pires, M. M., Hrycyna, C. A., and Chmielewski, J. (2009). Inhibition of human P-glycoprotein transport and substrate binding using a galantamine dimer. *Biochem. Biophys. Res. Commun.* 388, 672–676. doi: 10.1016/J.BBRC.2009.08.056

Neto, S., Duarte, N., Pedro, C., Spengler, G., Molnár, J., and Ferreira, M. J. U. (2019). Effective MDR reversers through phytochemical study of Euphorbia boetica. *Phytochem. Anal.* 30, 498–511. doi: 10.1002/pca.2841

Nguyen, H., Zhang, S., and Morris, M. E. (2003). Effect of flavonoids on MRP1-mediated transport in Panc-1 cells. *J. Pharmaceut. Sci.* 92, 250–257. doi: 10.1002/jps.10283

Nieri, P., Romiti, N., Adinolfi, B., Chicca, A., Massarelli, I., and Chieli, E. (2006). Modulation of P-glycoprotein activity by cannabinoid molecules in HK-2 renal cells. *Br. J. Pharmacol.* 148, 682. doi: 10.1038/sj.bjp.0706778

O'Connor, P. M., Jackman, J., Bae, I., Myers, T. G., Fan, S., Mutoh, M., et al. (1997). Characterization of the p53 tumor suppressor pathway in cell lines of the National Cancer Institute anticancer drug screen and correlations with the growth-inhibitory potency of 123 anticancer agents. *Canc. Res.* 57, 4285–4300.

Ohtani, H., Ikegawa, T., Honda, Y., Kohyama, N., Morimoto, S., Shoyama, Y., et al. (2007). Effects of various methoxyflavones on vincristine uptake and multidrug resistance to vincristine in P-gp-overexpressing K562/ADM cells. *Pharmaceut. Res.* 24, 1936–1943. doi: 10.1007/s11095-007-9320-6

Osman, A. M. G., Chittiboyina, A. G., and Khan, I. A. (2013). "Foodborne infections and intoxications: Chapter 32," in *Plant Toxins* (San Diego, USA: Academic Press).

Panche, A. N., Diwan, A. D., and Chandra, S. R. (2016). Flavonoids: an overview. *J. Nutr. Sci.* 5 (E47), 1–15. doi: 10.1017/jns.2016.41

Pearce, H. L., Safa, A. R., Bach, N. J., Winter, M. A., Cirtain, M. C., and Beck, W. T. (1989). Essential features of the P-glycoprotein pharmacophore as defined by a series of reserpine analogs that modulate multidrug resistance. *Proc. Natl. Acad. Sci. U.S.A.* 86, 5128–5132. doi: 10.1073/PNAS.86.13.5128

Pires, M. M., Emmert, D., Hrycyna, C. A., and Chmielewski, J. (2009). Inhibition of P-glycoprotein-mediated paclitaxel resistance by reversibly linked quinine homodimers. *Mol. Pharmacol.* 75, 92–100. doi: 10.1124/mol.108.050492

Reis, M. A., Ahmed, O. B., Spengler, G., Molnár, J., Lage, H., and Ferreira, M. J. U. (2016). Jatrophane diterpenes and cancer multidrug resistance–ABCB1 efflux modulation and selective cell death induction. *Phytomedicine* 23, 968–978. doi: 10.1016/j.phymed.2016.05.007

Rethy, B., Hohmann, J., Minorics, R., Varga, A., Ocsovszki, I., Molnár, J., et al. (2008). Antitumour properties of acridone alkaloids on a murine lymphoma cell line. *Anticancer Res.* 28, 2737–2743.

Reyes-Esparza, J., Morales, A. I. G., González-Maya, L., and Rodríguez-Fragoso, L. (2015). (-)-Epigallocatechin-3-gallate modulates the activity and expression of P-glycoprotein in breast cancer cells. *J. Pharmacol. Clin. Toxicol.* 3, 1044.

Roberts, M. F., and Wink, M. (1998). *Alkaloids: Biochemistry, Ecology, and Medicinal Applications* (New York, USA: Plenum Press).

Ruenitz, P. C., and Mokler, C. M. (1977). Analogs of sparteine. 5. antiarrhythmic activity of selected N, N'-disubstituted bispidines. *J. Med. Chem.* 20, 1668–1671. doi: 10.1021/jm00222a026

Saeed, M., Kadioglu, O., Khalid, H., Sugimoto, Y., and Efferth, T. (2015). Activity of the dietary flavonoid, apigenin, against multidrug-resistant tumor cells as determined by pharmacogenomics and molecular docking. *J. Nutr. Biochem.* 26, 44–56. doi: 10.1016/j.jnutbio.2014.09.008

Sampson, K. E., Wolf, C. L., and Abraham, I. (1993). Staurosporine reduces P-glycoprotein expression and modulates multidrug resistance. *Canc. Lett.* 68, 7–14. doi: 10.1016/0304-3835(93)90213-S

Sergent, T., Garsou, S., Schaut, A., De Saeger, S., Pussemier, L., Van Peteghem, C., et al. (2005). Differential modulation of ochratoxin A absorption across Caco-2 cells by dietary polyphenols, used at realistic intestinal concentrations. *Toxicol. Lett.* 159, 60–70. doi: 10.1016/j.toxlet.2005.04.013

Shen, X., Chen, G., Zhu, G., and Fong, W. F. (2006). (±)-3′-O, 4′-O-dicynnamoyl-cis-khellactone, a derivative of (±)-praeruptorin A, reverses P-glycoprotein mediated multidrug resistance in cancer cells. *Bioorg. Med. Chem.* 14, 7138–7145. doi: 10.1016/j.bmc.2006.06.066

Shen, H., Xu, W., Chen, Q., Wu, Z., Tang, H., and Wang, F. (2010). Tetrandrine prevents acquired drug resistance of K562 cells through inhibition of MDR1 gene transcription. *J. Canc. Res. Clin. Oncol.* 136, 659–665. doi: 10.1007/s00432-009-0704-3

Sheu, M. T., Liou, Y. B., Kao, Y. H., Lin, Y. K., and Ho, H. O. (2010). A quantitative structure–activity relationship for the modulation effects of flavonoids on P-glycoprotein-mediated transport. *Chem. Pharmaceut. Bull.* 58, 1187–1194. doi: 10.1248/cpb.58.1187

Simstein, R., Burow, M., Parker, A., Weldon, C., and Beckman, B. (2003). Apoptosis, chemoresistance, and breast cancer: insights from the MCF-7 cell model system. *Exp. Biol. Med.* 228, 995–1003. doi: 10.1177/153537020322800903

Slaninová, I., Březinová, L., Koubíková, L., and Slanina, J. (2009). Dibenzocyclooctadiene lignans overcome drug resistance in lung cancer cells–study of structure–activity relationship. *Toxicol. Vitro* 23, 1047–1054. doi: 10.1016/j.tiv.2009.06.008

Smith, E. W., and Maibach, H. I. (1995). *Percutaneous Penetration Enhancers* (Boca Raton, USA: CRC Press).

Smith, E. C., Kaatz, G. W., Seo, S. M., Wareham, N., Williamson, E. M., and Gibbons, S. (2007). The phenolic diterpene totarol inhibits multidrug efflux pump activity in *Staphylococcus aureus*. *Antimicrob. Agents Chemother.* 51, 4480–4483. doi: 10.1128/AAC.00216-07

Stermitz, F. R., Scriven, L. N., Tegos, G., and Lewis, K. (2002). Two flavonols from *Artemisa annua* which potentiate the activity of berberine and norfloxacin against a resistant strain of *Staphylococcus aureus*. *Planta Med.* 68, 1140–1141. doi: 10.1055/s-2002-36347

Su, S., Cheng, X., and Wink, M. (2015). Natural lignans from *Arctium lappa* modulate P-glycoprotein efflux function in multidrug resistant cancer cells. *Phytomedicine* 22, 301–307. doi: 10.1016/J.PHYMED.2014.12.009

Sun, Y. F., and Wink, M. (2014). Tetrandrine and fangchinoline, bisbenzylisoquinoline alkaloids from *Stephania tetrandra* can reverse multidrug resistance by inhibiting P-glycoprotein activity in multidrug resistant human cancer cells. *Phytomedicine* 21, 1110–1119. doi: 10.1016/J.PHYMED.2014.04.029

Sun, H. X., Xie, Y., and Ye, Y. P. (2009). Advances in saponin-based adjuvants. *Vaccine* 27, 1787–1796. doi: 10.1016/j.vaccine.2009.01.091

Sun, J., Yeung, C. A., Tsang, T. Y., Yau, E., Luo, K., Wu, P., et al. (2012). Clitocine reversal of P-glycoprotein associated multi-drug resistance through down-regulation of transcription factor NF-κB in R-HepG2 cell line. *PloS One* 7, e40720. doi: 10.1371/journal.pone.0040720

Suzuki, T., Fukazawa, N., San-nohe, K., Sato, W., Yano, O., and Tsuruo, T. (1997). Structure– activity relationship of newly synthesized quinoline derivatives for reversal of multidrug resistance in cancer. *J. Med. Chem.* 40, 2047–2052. doi: 10.1021/jm960869l

Suzuki, H., Tanabe, H., Mizukami, H., and Inoue, M. (2010). Selective regulation of multidrug resistance protein in vascular smooth muscle cells by the isoquinoline alkaloid coptisine. *Biol. Pharm. Bull.* 33, 677–682. doi: 10.1248/bpb.33.677

Syed, S. B., and Coumar, M. S. (2016). P-Glycoprotein mediated multidrug resistance reversal by phytochemicals: a review of SAR & future perspective for drug design. *Curr. Top. Med. Chem.* 16, 2484–2508. doi: 10.2174/1568026616666160212123814

Syed, S. B., Arya, H., Fu, I. H., Yeh, T. K., Periyasamy, L., Hsieh, H. P., et al. (2017). Targeting P-glycoprotein: Investigation of piperine analogs for overcoming drug resistance in cancer. *Sci. Rep.* 7, 1–18. doi: 10.1038/s41598-017-08062-2

Tanaka, K., Iwamoto, S., Gon, G., Nohara, T., Iwamoto, M., and Tanigawa, N. (2000). Expression of survivin and its relationship to loss of apoptosis in breast carcinomas. *Clin. Canc. Res.* 6, 127–134.

Tang, X., Bi, H., Feng, J., and Cao, J. (2005). Effect of curcumin on multidrug resistance in resistant human gastric carcinoma cell line SGC7901/VCR. *Acta Pharmacol. Sin.* 26, 1009–1016. doi: 10.1111/j.1745-7254.2005.00149.x

Teng, Y. N., Sheu, M. J., Hsieh, Y. W., Wang, R. Y., Chiang, Y. C., and Hung, C. C. (2016). β-carotene reverses multidrug resistant cancer cells by selectively modulating human P-glycoprotein function. *Phytomedicine* 23, 316–323. doi: 10.1016/j.phymed.2016.01.008

Tiwary, B. K., Pradhan, K., Nanda, A. K., and Chakraborty, R. (2015). Implication of quinazoline-4(3H)-ones in medicinal chemistry: a brief review. *J. Chem. Biol. Ther.* 1, 104. doi: 10.4172/2572-0406.1000104

To, K. K., Wu, X., Yin, C., Chai, S., Yao, S., and Kadioglu, O. (2017). Reversal of multidrug resistance by *Marsdenia tenacissima* and its main active ingredients polyoxypregnanes. *J. Ethnopharmacol.* 203, 110–119. doi: 10.1016/j.jep.2017.03.051

Trock, B. J., Leonessa, F., and Clarke, R. (1997). Multidrug resistance in breast cancer: A Meta-analysis of MDR1/gp170 expression and its possible functional significance. *J. Natl. Canc. Inst.* 89, 917–931. doi: 10.1093/jnci/89.13.917

Um, Y., Cho, S., Woo, H. B., Kim, Y. K., Kim, H., Ham, J., et al. (2008). Synthesis of curcumin mimics with multidrug resistance reversal activities. *Bioorg. Med. Chem.* 16, 3608–3615. doi: 10.1016/j.bmc.2008.02.012

Umsumarng, S., Pitchakarn, P., Yodkeeree, S., Punfa, W., Mapoung, S., and Ramli, R. A. (2017). Modulation of P-glycoprotein by Stemona alkaloids in human multidrug resistance leukemic cells and structural relationships. *Phytomedicine* 34, 182–190. doi: 10.1016/j.phymed.2017.08.004

van Wyk, B. E., and Wink, M. (2017). *Medicinal Plants of the World* (Wallingford, UK: CABI).

van Zanden, J. J., Wortelboer, H. M., Bijlsma, S., Punt, A., Usta, M., Bladeren, v., et al. (2005). Quantitative structure activity relationship studies on the flavonoid mediated inhibition of multidrug resistance proteins 1 and 2. *Biochem. Pharmacol.* 69, 699–708. doi: 10.1016/j.bcp.2004.11.002

Vasas, A., Sulyok, E., Rédei, D., Forgo, P., Szabó, P., Zupkó, I., et al. (2011). Jatrophane diterpenes from *Euphorbia esula* as antiproliferative agents and potent chemosensitizers to overcome multidrug resistance. *J. Nat. Prod.* 74, 1453–1461. doi: 10.1021/np200202h

Wan, C. K., Zhu, G. Y., Shen, X. L., Chattopadhyay, A., Dey, S., and Fong, W. F. (2006). Gomisin A alters substrate interaction and reverses P-glycoprotein-mediated multidrug resistance in HepG2-DR cells. *Biochem. Pharmacol.* 72, 824–837. doi: 10.1016/j.bcp.2006.06.036

Wandel, C., Kim, R. B., Kajiji, S., Guengerich, F. P., Wilkinson, G. R., and Wood, A. J. (1999). P-glycoprotein and cytochrome P-450 3A inhibition: dissociation of inhibitory potencies. *Canc. Res.* 59, 3944–3948.

Wang, Y., and Cabral, F. (2005). Paclitaxel resistance in cells with reduced β-tubulin. *Biochim. Biophys. Acta Mol. Cell Res.* 1744, 245–255. doi: 10.1016/j.bbamcr.2004.12.003

Wang, E. J., Barecki-Roach, M., and Johnson, W. W. (2002). Elevation of P-glycoprotein function by a catechin in green tea. *Biochem. Biophys. Res. Commun.* 297, 412–418. doi: 10.1016/S0006-291X(02)02219-2

Wang, C., Zhang, J. X., Shen, X. L., Wan, C. K., Tse, A. K. W., and Fong, W. F. (2004). Reversal of P-glycoprotein-mediated multidrug resistance by Alisol B 23-acetate. *Biochem. Pharmacol.* 68, 843–855. doi: 10.1016/j.bcp.2004.05.021

Wang, X. B., Wang, S. S., Zhang, Q. F., Liu, M., Li, H. L., Liu, Y., et al. (2010). Inhibition of tetramethylpyrazine on P-gp, MRP2, MRP3 and MRP5 in multidrug resistant human hepatocellular carcinoma cells. *Oncol. Rep.* 23, 211–215. doi: 10.3892/or_00000625

Wang, S., Lei, T., and Zhang, M. (2016). The reversal effect and its mechanisms of tetramethylpyrazine on multidrug resistance in human bladder cancer. *PloS One* 11, e0157759. doi: 10.1371/journal.pone.0157759

Wang, X., Zhang, H., and Chen, X. (2019). Drug resistance and combating drug resistance in cancer. *Canc. Drug Resist.* 2, 141–160. doi: 10.20517/cdr.2019.10

Wesołowska, O., Hendrich, A. B., Łania-Pietrzak, B., Wiśniewski, J., Molnár, J., Ocsovszki, I., et al. (2009). Perturbation of the lipid phase of a membrane is not involved in the modulation of MRP1 transport activity by flavonoids. *Cell. Mol. Biol. Lett.* 14, 199. doi: 10.2478/s11658-008-0044-3

Wink, M., and van Wyk, B. E. (2008). *Mind-Altering and Poisonous Plants of the World* (Portland, USA: Timber Press).

Wink, M., Ashour, M. L., and El-Readi, M. Z. (2012). Secondary metabolites inhibiting ABC transporters and reversing resistance of cancer cells and fungi to cytotoxic and antimicrobial agents. *Front. Microbiol.* 3, 130. doi: 10.3389/fmicb.2012.00130

Wink, M. (2000). "Interference of alkaloids with neuroreceptors and ion channels," in *Studies in Natural Products Chemistry*. Ed. R. Ata-ur- (Amsterdam, Netherlands: Elsevier), 3–122.

Wink, M. (2007). "Molecular modes of action of cytotoxic alkaloids: from DNA intercalation, spindle poisoning, topoisomerase inhibition to apoptosis and multiple drug resistance," in *The Alkaloids: Chemistry and Biology*, vol. 64. (San Diego, USA: Academic Press), 1–47.

Wink, M. (2015). Modes of action of herbal medicines and plant secondary metabolites. *Medicines* 2, 251–286. doi: 10.3390/medicines2030251

Wink, M. (2020). *Evolution of the angiosperms and co-evolution of secondary metabolites, especially of Alkaloids. Reference Series in Phytochemistry. Co-Evolution of Secondary Metabolites* (Cham, Switzerland: Springer Nature).

Wong, I. L., Wang, B. C., Yuan, J., Duan, L. X., Liu, Z., Liu, T., et al. (2015). Potent and nontoxic chemosensitizer of P-glycoprotein-mediated multidrug resistance in cancer: synthesis and evaluation of methylated epigallocatechin, gallocatechin, and dihydromyricetin derivatives. *J. Med. Chem.* 58, 4529–4549. doi: 10.1021/acs.jmedchem.5b00085

Wongrattanakamon, P., Lee, V. S., Nimmanpipug, P., Sirithunyalug, B., Chansakaow, S., and Jiranusornkul, S. (2017). Insight into the molecular mechanism of p-glycoprotein mediated drug toxicity induced by bioflavonoids: An integrated computational approach. *Toxicol. Mech. Meth.* 27, 253–271. doi: 10.1080/15376516.2016.1273428

Wu, J. Y. C., Fong, W. F., Zhang, J. X., Leung, C. H., Kwong, H. L., Yang, M. S., et al. (2003). Reversal of multidrug resistance in cancer cells by pyranocoumarins isolated from *Radix peucedani*. *Eur. J. Pharmacol.* 473, 9–17. doi: 10.1016/S0014-2999(03)01946-0

Xu, D., Lu, Q., and Hu, X. (2006). Down-regulation of P-glycoprotein expression in MDR breast cancer cell MCF-7/ADR by honokiol. *Canc. Lett.* 243, 274–280. doi: 10.1016/j.canlet.2005.11.031

Ye, J., Zheng, Y., and Liu, D. (2009). Reversal effect and its mechanism of ampelopsin on multidrug resistance in K562/ADR cells. *China J. Chin. Materia Med.* 34, 761–765.

Yoo, H. H., Lee, M., Chung, H. J., Lee, S. K., and Kim, D. H. (2007a). Effects of diosmin, a flavonoid glycoside in citrus fruits, on P-glycoprotein-mediated drug efflux in human intestinal Caco-2 cells. *J. Agr. Food Chem.* 55, 7620–7625. doi: 10.1021/jf070893f

Yoo, H. H., Lee, M., Lee, M. W., Lim, S. Y., Shin, J., and Kim, D. H. (2007b). Effects of *Schisandra* lignans on P-glycoprotein-mediated drug efflux in human intestinal Caco-2 cells. *Planta Med.* 53, 444–450. doi: 10.1055/s-2007-967178

Yoshida, N., Takagi, A., Kitazawa, H., Kawakami, J., and Adachi, I. (2005). Inhibition of P-glycoprotein-mediated transport by extracts of and monoterpenoids contained in *Zanthoxyli fructus*. *Toxicol. Appl. Pharmacol.* 209, 167–173. doi: 10.1016/j.taap.2005.04.001

You, M., Ma, X., Mukherjee, R., Farnsworth, N. R., Cordell, G. A., Kinghorn, A. D., et al. (1994). Indole alkaloids from *Peschiera laeta* that enhance vinblastine-mediated cytotoxicity with multidrug-resistant cells. *J. Nat. Prod.* 57, 1517–1522. doi: 10.1021/np50113a007

You, M., Wickramaratne, D. M., Silva, G. L., Chai, H., Chagwedera, T. E., Farnsworth, N. R., et al. (1995). (-)-Roemerine, an aporphine alkaloid from *Annona senegalensis* that reverses the multidrug-resistance phenotype with cultured cells. *J. Nat. Prod.* 58, 598–604. doi: 10.1021/np50118a021

Zhang, S., and Morris, M. E. (2003). Effects of the flavonoids biochanin A, morin, phloretin, and silymarin on P-glycoprotein-mediated transport. *J. Pharmacol. Exp. Therapeut.* 304, 1258–1267. doi: 10.1124/jpet.102.044412

Zhang, C. C., Yang, J. M., White, E., Murphy, M., Levine, A., and Hait, W. N. (1998). The role of MAP4 expression in the sensitivity to paclitaxel and resistance to vinca alkaloids in p53 mutant cells. *Oncogene* 16, 1617–1624. doi: 10.1038/sj.onc.1201658

Zhang, S., Yang, X., and Morris, M. E. (2004). Combined effects of multiple flavonoids on breast cancer resistance protein (ABCG2)-mediated transport. *Pharm. Res.* 21, 1263–1273. doi: 10.1023/B:PHAM.0000033015.84146.4c

Zhang, S., Wang, X., Sagawa, K., and Morris, M. E. (2005). Flavonoids chrysin and benzoflavone, potent breast cancer resistance protein inhibitors, have no significant effect on topotecan pharmacokinetics in rats or mdr1a/1b (−/−) mice. *Drug Metabol. Dispos.* 33, 341–348. doi: 10.1124/dmd.104.002501

Zhang, Y., Liu, X., Zuo, T., Liu, Y., and Zhang, J. H. (2012). Tetramethylpyrazine reverses multidrug resistance in breast cancer cells through regulating the expression and function of P-glycoprotein. *Med. Oncol.* 29, 534–538. doi: 10.1007/s12032-011-9950-8

Zhou, N., Li, J., Li, T., Chen, G., Zhang, Z., and Si, Z. (2017). Matrine-induced apoptosis in Hep3B cells via the inhibition of MDM2. *Mol. Med. Rep.* 15, 442–450. doi: 10.3892/mmr.2016.5999

Zhu, X., Zhang, X., Ma, G., Yan, J., Wang, H., and Yang, Q. (2011). Transport characteristics of tryptanthrin and its inhibitory effect on P-gp and MRP2 in Caco-2 cells. *J. Pharm. Pharmaceut. Sci.* 14, 325–335. doi: 10.18433/J3501W

Zhu, J., Wang, R., Lou, L., Li, W., Tang, G., Bu, X., et al. (2016). Jatrophane diterpenoids as modulators of P-glycoprotein-dependent multidrug resistance (MDR): advances of structure–activity relationships and discovery of promising MDR reversal agents. *J. Med. Chem.* 59, 6353–6369. doi: 10.1021/acs.jmedchem.6b00605

Conflict of Interest: The authors declare that the research was conducted in the absence of any commercial or financial relationships that could be construed as a potential conflict of interest.

frontiers in Pharmacology

ORIGINAL RESEARCH
published: 24 July 2020
doi: 10.3389/fphar.2020.01099

Dioscin Promotes Prostate Cancer Cell Apoptosis and Inhibits Cell Invasion by Increasing SHP1 Phosphorylation and Suppressing the Subsequent MAPK Signaling Pathway

Shuyun He[1,2], Jinrui Yang[1], Shaobo Hong[3], Haijian Huang[4], Qingguo Zhu[3], Liefu Ye[3], Tao Li[3], Xing Zhang[5], Yongbao Wei[1,3†] and Yunliang Gao[1*†]*

[1] Department of Urology, The Second Xiangya Hospital, Central South University, Changsha, China, [2] Department of Urology, The People's Hospital of Xiangtan Country, Xiangtan, China, [3] Shengli Clinical Medical College of Fujian Medical University and Department of Urology, Fujian Provincial Hospital, Fuzhou, China, [4] Shengli Clinical Medical College of Fujian Medical University and Department of Pathology, Fujian Provincial Hospital, Fuzhou, China, [5] Department of Urology, The Traditional Chinese Medicine Hospital of Yangzhou, Yangzhou University of Traditional Chinese Medicine, Yangzhou, China

Dioscin possesses antioxidant effects and has anticancer ability in many solid tumors including prostate cancer (PCa). Nevertheless, its effect and mechanism of anti-PCa action remain unclear. The tyrosine protein phosphatase SHP1, which contains an oxidation-sensitive domain, has been confirmed as a target for multicancer treatment. Further studies are needed to determine whether dioscin inhibits PCa through SHP1. We performed *in vitro* studies using androgen-sensitive (LNCaP) and androgen-independent (LNCaP -C81) cells to investigate the anticancer effects and possible mechanisms of dioscin after administering interleukin-6 (IL-6) and dihydrotestosterone (DHT). Our results show that dioscin inhibited cell growth and invasion by increasing SHP1 phosphorylation [p-SHP1 (Y536)] and inhibiting the subsequent P38 mitogen-activated protein kinase signaling pathway. Further *in vivo* studies confirmed that dioscin promoted caspase-3 and Bad-related cell apoptosis in these two cell lines. Our research suggests that the anticancer effects of dioscin on PCa may occur through SHP1. Dioscin may be useful to treat androgen-sensitive and independent PCa in the future.

Keywords: dioscin, prostate cancer, cell apoptosis, cell invasion, SHP1, mitogen-activated protein kinase

OPEN ACCESS

Edited by:
Patrícia Mendonça Rijo, Universidade Lusófona Research Center for Biosciences and Health Technologies, Portugal

Reviewed by:
Sheng-Yow Ho, Chi Mei Medical Center, Taiwan
Feng Wang, Affiliated Hospital of Nantong University, China

***Correspondence:**
Yongbao Wei
weiyb@fjmu.edu.cn
Yunliang Gao
yunliang.gao@csu.edu.cn

†These authors have contributed equally to this work

Specialty section:
This article was submitted to Pharmacology of Anti-Cancer Drugs, a section of the journal Frontiers in Pharmacology

Received: *16 March 2020*
Accepted: *06 July 2020*
Published: *24 July 2020*

Citation:
He S, Yang J, Hong S, Huang H, Zhu Q, Ye L, Li T, Zhang X, Wei Y and Gao Y (2020) Dioscin Promotes Prostate Cancer Cell Apoptosis and Inhibits Cell Invasion by Increasing SHP1 Phosphorylation and Suppressing the Subsequent MAPK Signaling Pathway. Front. Pharmacol. 11:1099. doi: 10.3389/fphar.2020.01099

INTRODUCTION

Interleukin-6 (IL-6) and androgen are two important factors that induce the occurrence and progression of prostate cancer (PCa) through activation of the P38 mitogen-activated protein kinase (MAPK) (extracellular regulated protein kinases 1/2, Erk1/2), phosphoinositide 3-kinase/protein kinase B (PI3K/AKT) and other signaling pathways to induce cancer cells and malignant transformation (Schafer and Brugge, 2007; Mukherjee and Mayer, 2008; Erdogan et al., 2018;

Johnson et al., 2018). Various plant extracts, such as dioscin, possess anticancer effects (Kim et al., 2014; Tao et al., 2018). Dioscin has antiinflammatory, immunomodulatory, hypolipidemic, antiviral, antifungal and antiallergic effects, and also shows anticancer antioxidant activity (Tao et al., 2018). Dioscin has significant antitumor effects and inhibits a variety of solid tumors (Wei et al., 2013; Chen et al., 2014; Kim et al., 2014; Tao et al., 2017; Zhou et al., 2019). Two studies have confirmed that dioscin promotes caspase-3 and Bcl-2-associated cell apoptosis and exhibits anticancer effects on PCa. These studies demonstrated that the anti-PCa effect of dioscin occurs *via* activation of estrogen receptor-beta (Chen et al., 2014; Tao et al., 2017). However, the role and mechanism of dioscin in PCa have not yet been fully elucidated. This study aimed to decipher the mechanism underlying the effect of dioscin on PCa.

SHP1, a member of the protein tyrosine phosphatase family, reversibly oxidizes active-site cysteine residues to sense reactive oxygen species and affect tyrosine phosphorylation-mediated cellular processes (Tonks, 2005; Dustin et al., 2019). Previous studies have reported that SHP1 is overexpressed in PCa cells (Wu et al., 2003) and that SHP1 knockdown causes cell-cycle arrest in the PC3 human prostate cancer cell line (Rodriguez-Ubreva et al., 2010). Another study confirmed that SHP1 predicts outcome after radical prostatectomy (Tassidis et al., 2010a). These results indicate that SHP1 may be a promising target to treat PCa and demonstrate that SHP1 is activated by plant extracts (Pesce et al., 2015). As dioscin is an herbal component, whether it activates SHP1 and plays a role in PCa deserves further investigation.

MATERIALS AND METHODS

Cell Culture and Transfection

LNCaP-C-33 (LNCaP) and LNCaP-C81 are androgen-sensitive and androgen-independent PCa cells, respectively (Igawa et al., 2002; Muniyan et al., 2015). The cells used in this study were purchased from the Chinese Academy of Sciences (Beijing, China). Cells were routinely cultured in a conventional medium containing phenol red-positive RPMI 1640 medium supplemented with 10% (v/v) fetal bovine serum (FBS), 2 mm glutamine, and 50 μg/ml gentamicin. Lipofectamine™ 2000 (Invitrogen, Carlsbad, CA, USA) was used to transfect small interfering RNA (siRNA). The diluted siRNA was mixed with Lipofectamine™ 3000 and the resulting siRNA-Lipofectamine™ 3000 complex was added to wells containing cells and culture medium for cell transfection. The four SHP1 siRNA sequences used were as follows:

SiR-1 (siRNA-893, F: 5'-GGUGAAUGCGGCUGACAU UTT-3', R: 5'-AAUGUCAGCCGCAUUCACCTT-3');SiR-2 (siRNA-666 F: 5'-CCUGGAGACUUCGUGCUUUTT-3', R: 5'-AAAGCACGAAGUCUCCAGGTT-3'); SiR-3 (siRNA-340, F: 5'-GCAAGAACCAGGGUGACUUTT-3', R: 5'-AAGUCACC CUGGUUCUUGCT-3'); SiR-NC (negative control, F: 5'-UU CUCCGAACGUGUCACGUTT-3', R: 5'-ACGUGACACG UUCGGAGAATT-3').

Cell Proliferation

A 100-μl aliquot of cells (about 1×10^4 cells) was added to each well of a 96-well plate and placed in a 37°C 5% CO_2 incubator for 24 h. An appropriate concentration of the drug was added and incubated. Then, 5× 3-(4,5-dimethylthiazol-2-yl)-2,5-diphenyltetrazolium bromide (MTT; Sigma, St. Louis, MO, USA) was diluted to 1× MTT with Dilution Buffer, and 50 μl was added to each well followed by a 4-h incubation. The supernatant was aspirated and 150 μl of dimethyl sulfoxide (Sigma) was added to each well. A microplate reader (Molecular Devices Sunnyvale, CA, USA) was used to detect the optical density of each well at 570 nm, and the cell survival rate was calculated.

Cell Apoptosis Assay

Annexin V-fluorescein isothiocyanate/propidium iodide (PI) (Mbchem M3021, Mumbai, India) was used to detect cell apoptosis. The cells were collected at room temperature, resuspended in 50 μl of prechilled 1× PBS (4°C) and centrifuged. Each sample (10^5–10^6 cells) was prepared with 100 μl of Annexin-V labeling solution. The cells were suspended and incubated for 15 min, and then 10 μl of PI was added. A prepared dilution (cold 400 μl of Binding Buffer) was added to 100 μl of incubation solution, and flow cytometry was performed within 15 min.

Cell Scratch Wound Repair Assay

A reference line was drawn on the back of a six-well plate, and 5×10^5 cells were added to each well. After the cells covered the bottom of the well, a 20-μl pipette tip was used to create an "I"-shaped scratch in the middle of the well as the 0-h control. Each well was washed three times with serum-free medium to remove the scratched cells. The plate was placed in a 5% CO_2 incubator at 37°C for 24 h and then removed to record relative scratch width.

Cell Formation Assay

Monolayer cells cultured in the logarithmic growth phase were digested with 0.25% trypsin, pipetted into single cells and counted. The cell concentration was adjusted to 1,000 per dish, and the drug was added. The cell suspension was inoculated into a dish containing 3 ml of 37°C prewarmed culture medium and gently rotated to uniformly disperse the cells. The cells were incubated at 37°C at 5% CO_2 with saturated humidity for 2–3 weeks. The number of cells contained in each dish was counted, and the cell formation rate was calculated.

Cell Invasion Assay

The lower and upper wells of a Transwell plate (Corning, Corning, NY, USA) were coated with a 60–80 μl dilution of Matrigel. The Matrigel was polymerized into a gel at 37°C for 30 min to prepare the Transwell plate. After the cells were digested, centrifuged, washed with PBS and resuspended, cell density was adjusted to 5×10^4/ml. Next, 1 ml of FBS-containing medium was added to the lower well and the cell suspension was added to the upper well. The cells were cultured for 24 h and the

basement membrane of the lower well was removed. The cells were wiped off the Matrigel and the upper well was fixed with 95% alcohol for 15–20 min and stained with hematoxylin for 10 min. The cells were then counted under an inverted microscope.

Tumor Formation Assay in Nude Mice

Normal cultured LNCaP and LNCaP-C81 cells were subgrouped and processed as follows: LNCaP-C81 tumor formation without any special treatment (group A: L-C81); LNCaP-C81 cells treated with the optimal dioscin dose (Cat. No.: HY-N0124, Purity: 98.33%, MedChemExpress LLC, Monmouth Junction, NJ, USA) (group B: L-C81 + D); SHP1 knockdown LNCaP-C81 cells treated with the same dioscin dose (Group C: L-C81 + KD + D); LNCaP tumor formation without any special treatment (Group D: LNCaP); LNCaP treated with the optimal dioscin dose (Group E: LNCaP + D); and SHP1 knockdown LNCaP cells treated with the same dioscin dose (Group F: LNCaP + KD + D). Each group of cells was adjusted to 1×10^6 cells. A cell suspension with a total volume of 0.2 ml was inoculated at each injection point. Tumor formation was induced near the extremities of 6-week-old BALB/c nude mice (purchased from Chinese Academy of Sciences). After 1 week of rearing, tumor size was measured (longest diameter: a; and shortest diameter: b; once every 3 days, six times in a row). A tumor growth curve was plotted, with time as the abscissa and tumor volume as the ordinate (tumor volume was calculated using the formula: $v = a \times b^2 \times 0.52$; volume unit: mm^3). Tumor tissues were obtained to detect Ki67 by immunohistochemistry and other proteins were also analyzed.

Western Blot

A radioimmunoprecipitation assay (RIPA) lysate [containing 1% NP-40, 0.1% SDS (Sigma), and 50 mM DTT] was used to extract the cell and tissue proteins. The proteins were separated by 10% sodium dodecyl sulfate-polyacrylamide gel electrophoresis, and 1 ml of primary antibody (**Supplementary Table 1**) was added. The primary antibody was discarded after a 2-h incubation. The gel was washed with 2–3 ml PBST followed by 1 ml of secondary antibody (**Supplementary Table 1**), and the gel was incubated at 4°C overnight. The gel signals were analyzed with Gel pro version 4.0 software (Media Cybernetics, Silver Spring, MD, USA).

Immunohistochemical Staining

Tissue sections were sliced at a thickness of 3 μm and baked at 60–65°C for 4 h. After the sections were dewaxed and hydrated, they were washed with 1× PBS buffer (0.01 M, pH 7.2). The paraffin section tissue antigen was repaired using the high-pressure method and the sections were rinsed with PBS. Next, 50 μl of primary antibody (Ki-67 GTX16667/rabbit antibody, dilution 1: 100; GeneTex Inc., Irvine, CA, USA) was added to each section, followed by an overnight incubation at 4°C. After washing with PBS, 50 μl of biotin-labeled secondary antibody was sequentially added and 50 μl of streptavidin-peroxidase solution was added for the incubation. After washing with PBS, 1–2 drops of freshly prepared 3,3′-diaminobenzidine (Cat. No: DAB-0031/1031) was added to each section and the tissues were observed under a microscope. After counterstaining with hematoxylin, dehydration through an alcohol gradient and neutral gum mounting, each section was analyzed at 200× and 400× magnification.

Statistical Analysis

Each set of experiments was performed in duplicate or triplicate in accordance with the experimental design and repeated at least two or three times. Representative data from one of three independent experiments were selected and shown in the figures. The average and standard error values of the experimental results were calculated. Student's *t*-test was used to compare the groups. A p-value < 0.05 was considered significant.

RESULTS

Screening for the Optimal Dioscin Dose and Duration

LNCaP-C81 cells were treated with different dioscin concentrations (0.1, 0.5, 1, 5, 10, 25, and 50 μg/ml) for 24 h. The cells were collected to detect SHP1 and its three known phosphorylation sites, namely two C-terminal tyrosine residues (Y536 and Y564) and serine 591 (S591) (Choi et al., 2017; Mkaddem et al., 2017). The results showed that the expression levels of SHP1 and p-SHP1 (Y536) were highest in LNCaP-C81 cells after treatment with 10 μg/ml dioscin for 24 h (**Figures S1A, B**) ($p < 0.001$). This finding indicates that p-SHP1 (Y536) could be used to measure SHP1 phosphorylation. Then, 10 μg/ml dioscin was applied for different durations (0, 3, 6, 12, 24, and 48 h). The expression of the SHP1 protein and p-SHP1 (Y536) was highest after 24 h of treatment (**Figures S1C, D**) ($p < 0.001$). Cell function experiments were performed, and the results showed that proliferation of LNCaP-C81 cells was significantly inhibited (**Figure S1E**) and cell apoptosis increased (**Figures S1F, G**) (both $p < 0.05$) after treatment with 10 μg/ml dioscin for 24 h. Thus, in subsequent experiments, LNCaP-C81 cells were treated with 10 μg/ml dioscin for 24 h.

The same methods were used with LNCaP cells to determine the optimal concentration and duration of dioscin treatment. The expression of the SHP1 protein and p-SHP1 (Y536) was highest after treatment with 10 μg/ml dioscin for 24 h ($p < 0.001$) (**Figures S2A–D**). Subsequently, the proliferation of LNCaP1 cells was significantly lower (**Figure 2E**) and the rate of cell apoptosis was relatively higher (**Figures S2F, G**) (both $p < 0.05$). Thus, we selected the 24-h treatment with 10 μg/ml dioscin for subsequent LNCaP cell studies.

Dioscin Regulates SHP1 to Reverse IL-6-Induced Proliferation and Invasion of PCa Cells

We determined the optimal SHP1 interfering sequence. We transfected LNCaP-c81 with the SiR-NC, SiR-1, SiR-2, and SiR-3 sequences and measured SHP1 expression 24 h later by western blotting. As a result, SiR-2 completely blocked the expression of SHP1, reducing the expression level to 0.

Therefore, SiR-2 was considered the optimal SHP1 interfering sequence (**Figures S3A, B**).

LNCaP-C81 was divided into four groups: routine culture (group A: L-C81); IL-6 intervention (group B: IL6); IL-6 and dioscin co-treatment (group C: IL6 + D) and SHP1 knockdown and co-treatment with IL-6 and dioscin (group D: KD + IL6 + D). The IL-6 dosage for these groups was set to 5 ng/ml (Hobisch et al., 2001). After a 24 h treatment, IL-6 significantly inhibited p-SHP1 (Y536) expression ($p < 0.01$) and the protein phosphorylation levels of subsequent signaling pathways were also significantly upregulated. The expression levels of p-Erk1/2 (T202/T204), p-P38 (T182) and p-AKT (T326) increased significantly (all $p < 0.01$). However, the inhibitory effects on p-Erk1/2(T177) and p-P38 (T180) were not significant (all $p > 0.05$) (**Figures 1A, B**). Dioscin reversed the regulatory effects of IL-6 on these phosphorylated proteins. Dioscin also significantly promoted the expression of p-SHP1 (Y536) ($p < 0.01$) and inhibited the proteins in the signaling pathways, specifically p-Erk1/2 (T202/T204), p-P38 (T182) and p-AKT (T326) (all $p < 0.05$) (**Figures 1A, B**). Cell function experiments revealed that IL-6 promoted LNCaP-C81 cell proliferation (**Figure 1C**) and formation (**Figures 1F, G**) after inhibiting p-SHP1 (Y536), and increased the capability of the cells for wound repair (**Figures 1H, I**) and migration (**Figures 1J, K**) (all $p < 0.01$). However, IL-6 had no significant effect on apoptosis (**Figures 1D, E**) ($p > 0.05$). In contrast, dioscin promoted the expression of p-SHP1 (Y536), inhibited cell proliferation (**Figure 1C**), increased apoptosis (**Figures 1D, E**), inhibited cell formation (**Figures 1F, G**) and reduced cell wound repair (**Figures 1H, I**) and cell migration ability (**Figures 1J, K**) (all $p < 0.05$). However, when SHP1 was knocked down, the effect of dioscin was significantly suppressed, suggesting that SHP1 may be a target gene of dioscin.

The same method was used to study the effects of IL-6 and dioscin on LNCaP cells. SiR-2 completely blocked SHP1 expression in LNCaP cells (**Figures S4A, B**) ($p < 0.01$). Further study revealed similar results as shown in LNCaP-C81 cells. IL-6 inhibited p-SHP1 (Y536) expression ($p < 0.01$), promoted expression of the signaling proteins p-Erk1/2 (T202/T204), p-P38 (T182) and p-P38 (Tyr180) (**Figures 2A, B**) (all $p < 0.01$), promoted cell proliferation (**Figure 2C**), inhibited apoptosis (**Figures 2D, E**), promoted cell formation (**Figures 2F, G**) and enhanced wound repair capability (**Figures 2H, I**) and migration (**Figures 2J, K**) (all $p < 0.01$). Dioscin reversed these effects of IL-6 in LNCaP1 cells and the effects of dioscin were significantly suppressed after SHP1 knockdown (all $p < 0.05$).

Dioscin Regulates SHP1 to Reverse Dihydrotestosterone (DHT)-Induced Proliferation and Invasion by PCa Cells

LNCaP-C81 cells were subjected to the following treatments: conventional culture (group A: L-C81), DHT intervention (group B: DHT), co-treatment with DHT and dioscin (group C: DHT + D) and SHP1 knockdown with DHT and dioscin co-treatment (group D: KD + DHT + D). The dosage and duration of DHT were in accordance with a previous report (Krongrad et al., 1991). After 24 h of treatment, p-SHP1 (Y536) expression decreased significantly after DHT was added ($p < 0.01$). The proteins for the subsequent signaling pathways, such as p-Erk1/2 (T202/T204), p-P38 (T182) and p-P38(T180), increased significantly (all $p < 0.01$), but p-Erk1/2 (T177) and p-AKT (T326) levels were not significantly inhibited (all $p > 0.05$) (**Figures 3A, B**). Dioscin reversed the effects of DHT on LNCaP-C81 cells. Dioscin significantly promoted the expression of p-SHP1 (Y536) ($p < 0.01$) and inhibited the expression of p-Erk1/2 (T202/T204), p-P38 (T182) and p-P38 (T180) (all $p < 0.05$) (**Figures 3A, B**). Cell function experiments revealed that after inhibiting p-SHP1 (Y536) expression, DHT significantly promoted LNCaP-C81 cell proliferation (**Figure 3C**), formation (**Figures 3F, G**) and wound repair ability (**Figures 3H, I**) (all $p < 0.05$). However, it had no significant effect on cell apoptosis (**Figures 3D, E**) or migration (**Figures 3J, K**) (both $p > 0.05$). Dioscin substantially promoted p-SHP1 (Y536) expression, inhibited cell proliferation (**Figure 3C**), promoted apoptosis (**Figures 3D, E**), inhibited cell formation (**Figures 3F, G**) and reduced wound repair ability (**Figures 3H, I**) and cell migration (**Figures 3J, K**) (all $p < 0.05$). Similarly, the effect of dioscin was significantly suppressed when SHP1 was knocked down.

The same method was used to study the effects of DHT on LNCaP cells and similar results were obtained as with LNCaP-C81. DHT inhibited the expression of p-SHP1 (Y536) ($p < 0.01$) and promoted the expression of p-Erk1/2 (T202/T204), p-P38 (T182), and p-P38 (Tyr180) (all $p < 0.01$) (**Figures 4A, B**), which in turn promoted cell formation (**Figures 4F, G**) ($p < 0.05$). DHT had no significant effect on cell proliferation (**Figure 4C**), apoptosis (**Figures 4D, E**), wound repair (**Figures 4H, I**) or migration (**Figures 4J, K**) (all $p > 0.05$). Dioscin reversed the effects of DHT on these phosphorylated proteins and significantly inhibited cell proliferation, promoted apoptosis, inhibited cell formation and reduced wound repair ability and cell migration (all $p < 0.05$). The effect of dioscin was consistently reduced significantly when SHP1 was knocked down.

In Vivo Experiments to Verify the Inhibitory Effects of Dioscin on PCa

After grouping BALB/c nude mice according to the methods described above, dioscin inhibited the growth of nude mice tumors consisting of LNCaP-C81 and LNCaP cells (**Figures 5A, B**) (both $p < 0.01$). Ki67 expression in tumor tissues was detected by immunohistochemical staining to assess tumor cell proliferation (Gerdes et al., 1984). The expression of Ki67 among the above groups did not change significantly (**Figures 5C, D**) ($p > 0.05$), suggesting that dioscin may not inhibit tumor cell proliferation *in vivo*. Phosphorylated protein detection revealed that dioscin promoted the expression of p-SHP1 (Y536) ($p < 0.05$) and inhibited the expression of p-Erk1/2 (T202/T204), p-P38 (T182), p-P38(T180), and caspase-3(35KD) proteins (**Figures 5E, F**) (all $p < 0.01$), but significantly promoted the expression of caspase-3 (17/19KD) and Bad (**Figures 5E, F**) (both $p < 0.01$). Dioscin had no significant effects on the expression of p-Erk1/2 (T177), p-AKT (T326), or p-AKT (S129) (all $p > 0.05$). The effect of dioscin was significantly

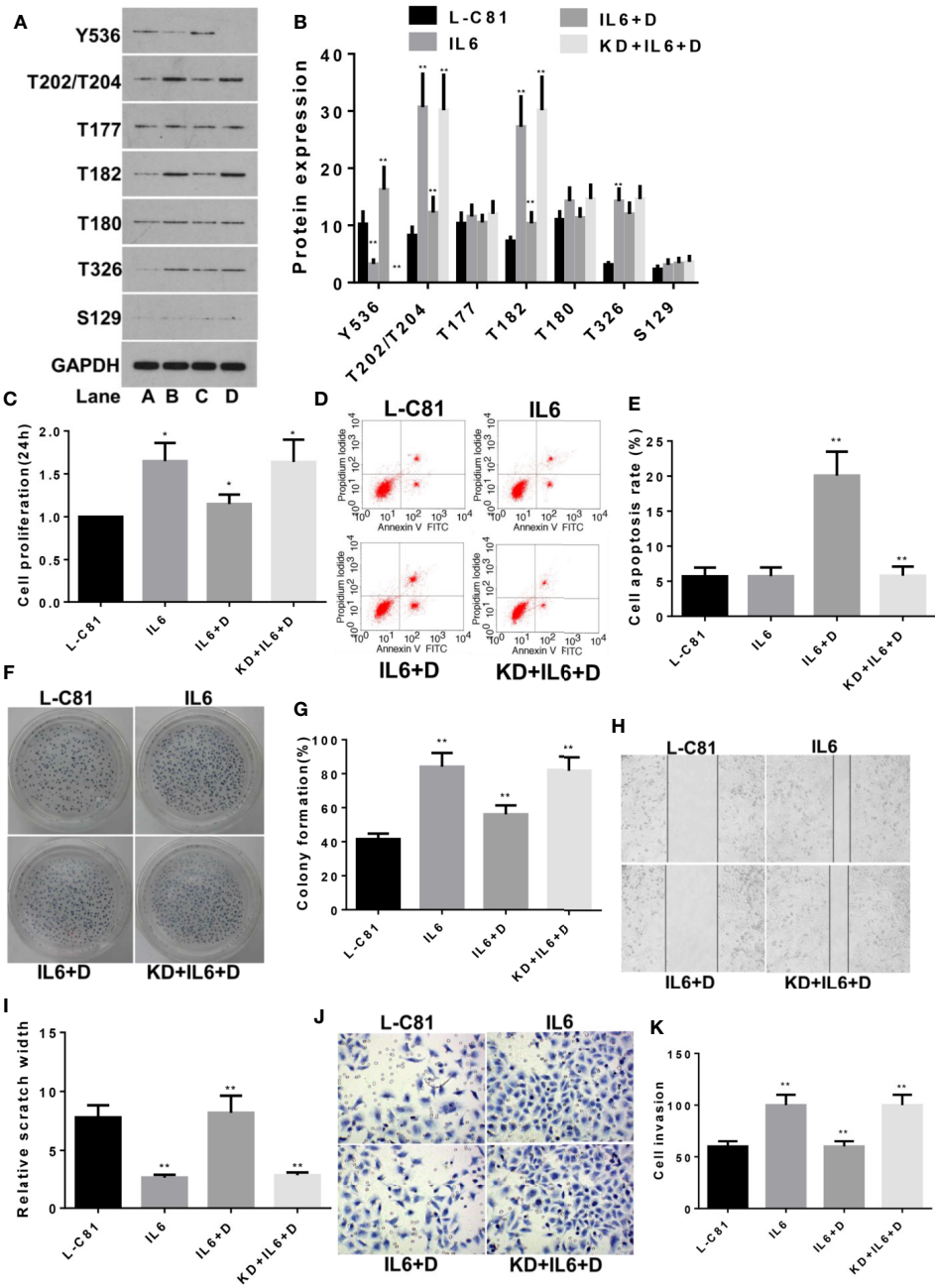

FIGURE 1 | Dioscin regulates SHP1 to reverse IL-6-induced LNCaP-c81 cell proliferation and invasion. **(A, B)** IL-6 significantly inhibits p-SHP1 (Y536) expression and increases the subsequent expression of the p-Erk1/2 (T202/T204), p-P38 (T182) and p-AKT (T326) proteins (all $p < 0.01$). Dioscin reversed the regulatory effect of IL-6 on these phosphorylated proteins. After inhibiting p-SHP1 (Y536), IL-6 promoted LNCaP-C81 cell proliferation **(C)** and formation **(F, G)** and increased cell wound repair **(H, I)** and migration **(J, K)** (all $p < 0.01$). However, it had no effect on cell apoptosis **(D, E)**. Dioscin reversed all of the effects of IL-6 on protein regulation and cell functions (all $p < 0.05$). Representative data from one of three independent experiments are shown in Figure 1 **(A, D, F, H, J)**. * on behalf of $p < 0.05$; ** on behalf of $p < 0.01$.

reduced after SHP1 was knocked down. Correspondingly, the expression of p-SHP1 (Y536) and its subsequent pathway proteins showed the opposite results. These results suggest that dioscin has potential as a targeted drug to promote SHP1 phosphorylation and promote caspase-3 and Bad-related apoptosis by inhibiting the downstream Erk1/2 and P38 signaling pathways (Gajewski and Thompson, 1996; Porter and Janicke, 1999); thus, presenting antitumor effects on PCa.

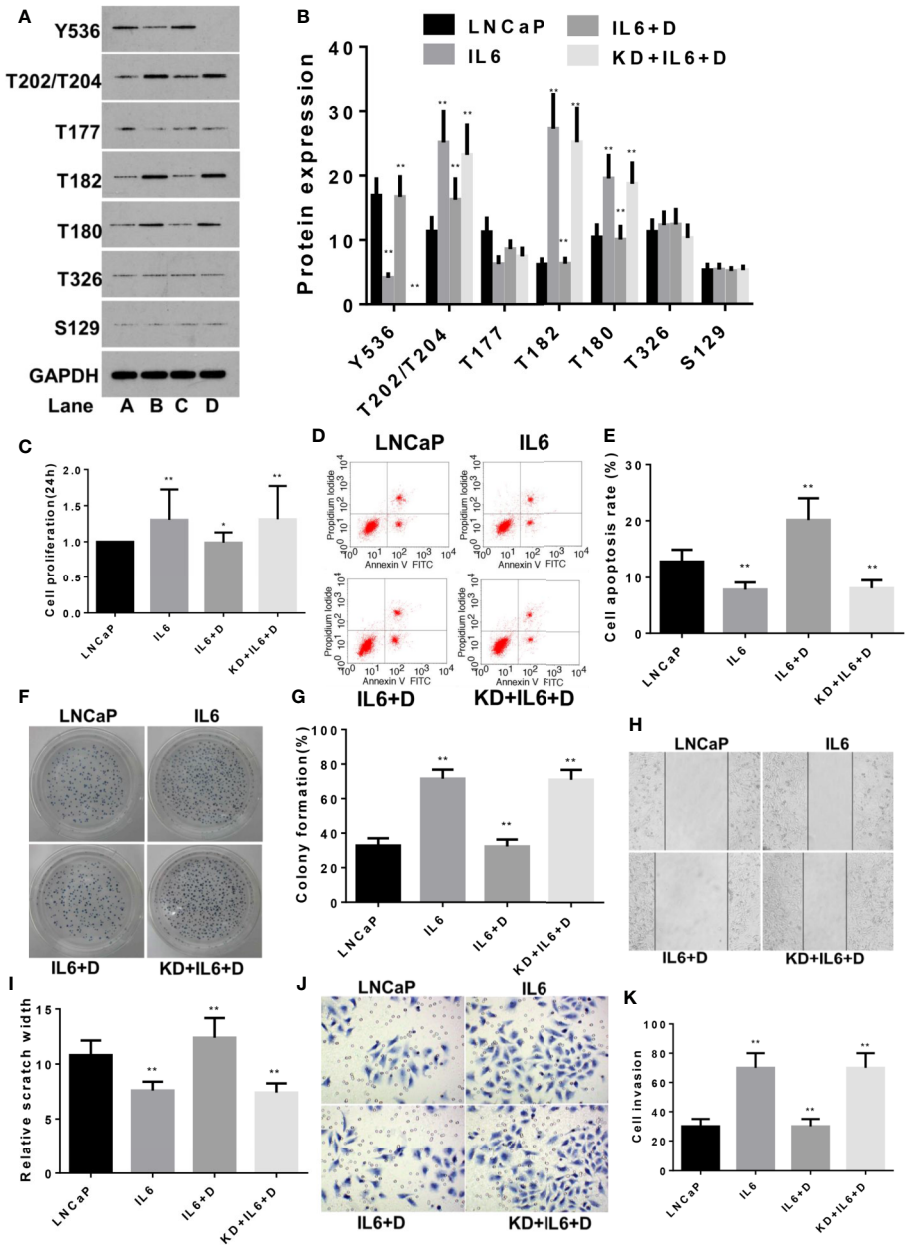

FIGURE 2 | Dioscin regulates SHP1 to reverse IL-6-induced LNCaP cell proliferation and invasion. **(A, B)** IL-6 significantly inhibits p-SHP1 (Y536) expression and increases the subsequent expression of the p-Erk1/2 (T202/T204), p-P38 (T182) and p-P38 (Tyr180) proteins (all $p < 0.01$). Dioscin reversed the regulatory effect of IL-6 on these phosphorylated proteins. After inhibiting p-SHP1 (Y536), IL-6 promoted LNCaP cell proliferation **(C)** and formation **(F, G)**, reduced apoptosis **(D, E)** and increased wound repair **(H, I)** and migration **(J, K)** (all $p < 0.01$). Dioscin reversed all of the IL-6 effects on protein regulation and cell functions (all $p < 0.05$). Representative data from one of three independent experiments are shown in Figure 2 **(A, D, F, H, J)**. * on behalf of $p < 0.05$; ** on behalf of $p < 0.01$.

DISCUSSION

Erk1/2 is an important subfamily of MAPKs, which control a wide range of cellular activities and physiological processes (Lu and Xu, 2006). MAPKs control the activity or abundance of BCL-2 protein family members (such as Bad) to promote cell survival (Balmanno and Cook, 2009). In addition, the MAPK signaling pathway is closely related to cancer progression (Wagner and Nebreda, 2009; Cuadrado and Nebreda, 2010) and activation of caspase-3 or Bad promotes cell apoptosis (Gajewski and Thompson, 1996; Porter and Janicke, 1999; Min et al., 2004). Dioscin increased apoptosis in PCa cells by promoting the expression of phosphorylated SHP1-p-SHP1 (Y536), inhibiting the expression of p-Erk1/2 (T202/T204), p-P38 (T182) and p-P38(T180) and promoting the expression of apoptosis-related proteins caspase-3 (17/19KD) and Bad. Our

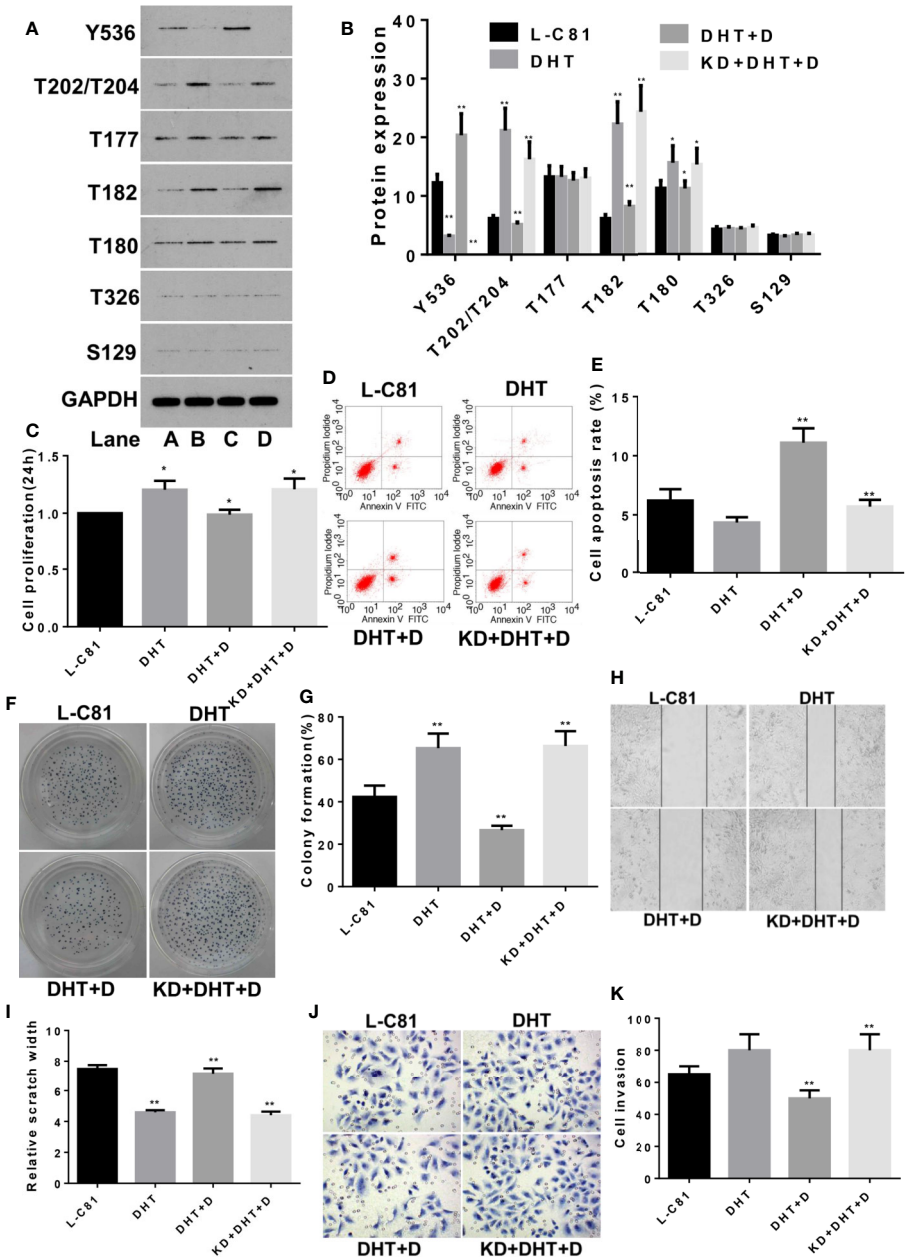

FIGURE 3 | Dioscin regulates SHP1 to reverse DHT-induced LNCaP-C81 cell proliferation and invasion. **(A, B)** DHT significantly reduces p-SHP1 (Y536) expression and increases subsequent expression of the p-Erk1/2 (T202/T204), p-P38 (T182) and p-P38 (T180) proteins (all $p < 0.01$). Dioscin reversed these effects of DHT on protein regulation in LNCaP-C81 cells (all $p < 0.05$). After inhibiting p-SHP1 (Y536) expression, DHT significantly promoted LNCaP-C81 cell proliferation **(C)**, formation **(F, G)** and wound repair ability **(H, I)** (all $p < 0.05$). However, it had no significant effect on cell apoptosis **(D, E)** or migration **(J, K)** (all $p > 0.05$). Dioscin promoted p-SHP1 (Y536) expression and reversed DHT-induced LNCaP-C81 cell functions (all $p < 0.05$). Representative data from one of three independent experiments are shown in Figure 3 **(A, D, F, H, J)**. * on behalf of $p < 0.05$; ** on behalf of $p < 0.01$.

study may provide a basis for understanding the mechanism of PCa development and exploring new therapeutic drugs for the disease.

IL-6 plays an important role in both the progression and treatment of PCa (Hobisch et al., 2001; Johnson et al., 2018). IL-6 is a pleiotropic pro-inflammatory cytokine involved in the development of PCa and plays a role mediated through autocrine and paracrine mechanisms (Adekoya and Richardson, 2020). Long-term application of IL-6 promotes PCa cell proliferation and thus can be used to establish *in vitro* models of advanced PCa (Hobisch et al., 2001). Several reports indicate that IL6 is produced by invasive PCa and the PC3 and

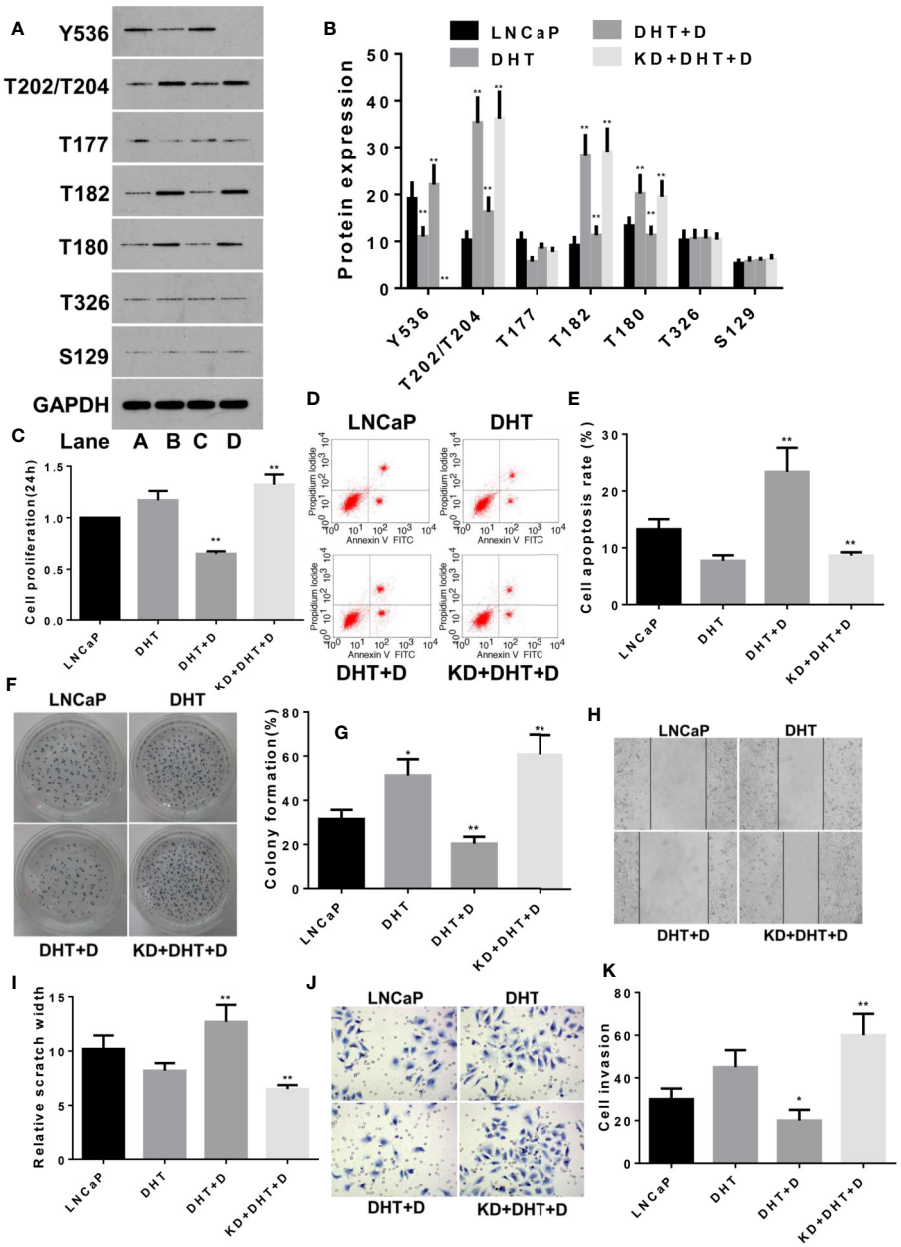

FIGURE 4 | Dioscin regulates SHP1 to reverse DHT-induced LNCaP cell proliferation and invasion. **(A, B)** DHT significantly reduces p-SHP1 (Y536) expression and increases subsequent expression of the p-Erk1/2 (T202/T204), p-P38 (T182) and p-P38 (T180) proteins (all $p < 0.01$). Dioscin reversed these effects of DHT on protein regulation in LNCaP cells (all $p < 0.01$). After inhibiting p-SHP1 (Y536) expression, DHT significantly promoted LNCaP cell formation **(F, G)** ($p < 0.05$), but had no significant effect on cell proliferation **(C)**, apoptosis **(D, E)**, wound repair ability **(H, I)** or migration **(J, K)** ($p > 0.05$). Dioscin promoted p-SHP1 (Y536) expression and reversed the DHT-induced LNCaP cell functions (all $p < 0.05$). Representative data from one of three independent experiments are shown in Figure 4 **(A, D, F, H, J)**. * on behalf of $p < 0.05$; ** on behalf of $p < 0.01$.

DU145 cell lines, while its production is low or non-existent in non-invasive PCa and LNCaP cells (Inoue et al., 2005; Giannoni et al., 2010). In our study, we used LNCaP and LNCaP-C81 cells to study the role of dioscin in PCa; we artificially reduced the uncontrollable endogenous or exocrine IL-6 expression levels from tumor cells that interfered with the results of this study. In addition, we found that dioscin inhibited cell proliferation and migration after applying IL-6. One study demonstrated that the IL-6/JAK/STAT3 pathway plays an important role in the tumor microenvironment and drug research. SHP1 has been identified as one of the most important negative regulators of STAT3 and increased expression of SHP1 inhibits STAT3 and present

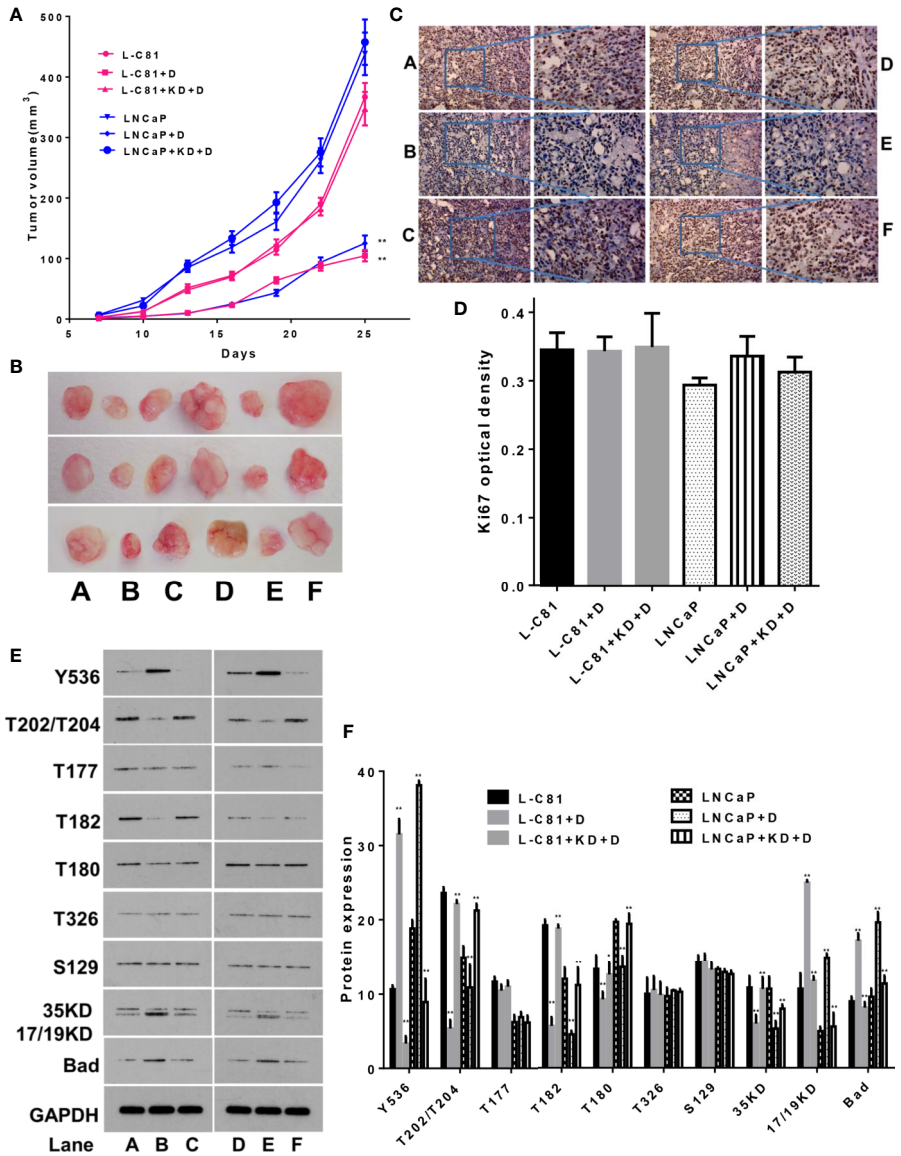

FIGURE 5 | *In vivo* experiments to verify the inhibitory effect of dioscin on prostate cancer. **(A, B)** Dioscin inhibits tumor growth in BALB/c nude mice after tumor implantation with LNCaP-C81 or LNCaP cells (both $p < 0.01$). **(C, D)** Ki67 was used to assess tumor cell proliferation but did not change significantly between the groups ($p > 0.05$). **(E, F)** Dioscin promoted the expression of p-SHP1 (Y536) ($p < 0.05$) and inhibited p-Erk1/2 (T202/T204), p-P38 (T182), p-P38 (T180) and caspase-3 (35 KD) protein expression (all $p < 0.01$). It also significantly promoted the expression of caspase-3 (17/19KD) and Bad (all $p < 0.01$). Representative data from one of three independent experiments are shown in Figure 5 **(C, E)**. * on behalf of $p < 0.05$; ** on behalf of $p < 0.01$.

antitumor effects (Johnson et al., 2018). Another study demonstrated that SHP1 inhibits the proliferation and apoptosis of LNCaP cells as well as IL-6-treated offspring LNCaP-IL6^{+} cell lines, suggesting that SHP1 may be a therapeutic target for PCa (Tassidis et al., 2010b). In our study, dioscin promoted SHP1 phosphorylation and thus exhibited anticancer effects through the MAPK signaling pathway.

DHT also plays an important role in the development and progression of PCa. DHT activated ErbB-2 and Erk1/2-mediated PCa cell proliferation. In contrast, ErbB-2-specific inhibitors inhibit DHT-stimulated cell proliferation by blocking Erk1/2 (Muniyan et al., 2015). In the present study, dioscin inhibited the proliferation and migration of cells after DHT treatment and increased apoptosis. This role of dioscin in cells treated with DHT may also be related to the Erk1/2 and P38 MAPK signaling pathways.

Dioscin is a natural steroid saponin. Increasing evidence shows that dioscin exhibits anticancer properties against a variety of cancers (Wang et al., 2019). Zhou et al. (2019) screened 88 natural products and found that only dioscin

significantly inhibited Skp2 and thus inhibited the progression of rectal cancer cells. After applying dioscin, A549, NCI-H446, and NCI-H460 lung cancer cells revealed DNA damage, mitochondrial structural changes, and blockage of the cell cycle in the S phase, indicating that dioscin increases lung cancer cell apoptosis (Wei et al., 2013). PCa changes from hormone dependence to hormone independence after treatment, which presents a significant challenge. It is thus of great importance to explore new drugs for treating hormone-independent PCa (Santer et al., 2015). Studies suggest that dioscin may be a potential treatment for PCa. Dioscin significantly inhibits cell viability, colony formation and motility and induces apoptosis in PC3 cells. Furthermore, dioscin reduces the levels of aldehyde dehydrogenase (ALDH) and CD133 (+)/CD44 (+) cells, suggesting that it also effectively inhibits PCa stem cells (Tao et al., 2017). In our study, dioscin effectively inhibited cell proliferation, reduced migration and exhibited antitumor effects on both hormone-sensitive PCa cells (LNCaP) and hormone-resistant PCa cells (LNCaP-C81).

The mechanism of how dioscin suppresses cancer remains unclear. Researchers have used inverse docking technology to screen potential cancer treatment drugs and discovered that only dioscin had the following properties for cancer treatment: it may be a TOP1 inhibitor, which halts the cancer cell cycle and DNA replication; it down-regulates epidermal growth factor receptor (EGFR) and EGF to inhibit growth of a vascular supply; it also has antiinflammatory activity by regulating the JNK signaling pathway to suppress cancer (Yin et al., 2015). Dioscin inhibits angiogenesis induced by the vascular endothelial growth factor receptor 2 (VEGF2) signaling and AKT/MAPK pathways, resulting in inhibition of cell proliferation, migration and invasion (Tong et al., 2014). The traditional herbal component verbascoside enhances phosphorylation of SHP1 by attenuating the TAK-1/JNK/AP-1 pathway, revealing an antiinflammatory effect by reducing the expression and activity of cyclooxygenase and nitric oxide synthase. However, depleting SHP1 eliminates the antiinflammatory effects of verbascoside (Pesce et al., 2015). Dioscin upregulates VEGF-A in osteoblast-like cells and increases angiogenesis to promote bone formation and fracture healing through hypoxia-inducible factor-1α activation of Src kinase, P38 MAPK and the Akt signaling pathways (Yen et al., 2005). Applying dioscin to A549 and H1299 lung cancer cells causes a dose-dependent increase in Erk1/2 and JNK1/2 activities, while reducing PI3K expression and Akt and mTOR phosphorylation (Hsieh et al., 2013). Our study demonstrated that dioscin promotes SHP1 phosphorylation, induces caspase-3 and Bad-related apoptosis and inhibits cell proliferation and invasion through the MAPK signaling pathway in PCa. In addition, we measured Ki67 expression in tumor tissues to assess tumor cell proliferation (Gerdes et al., 1984), but the Ki67 results were not different between the groups, suggesting that dioscin may not directly inhibit tumor cell proliferation. However, full-length caspase 3 (35 kD) is significantly inhibited by dioscin, whereas its cleaved forms (19 and 17 kD) increase significantly, indicating that dioscin may induce caspase 3-related apoptosis (Porter and Janicke, 1999; Min et al., 2004). We also found that dioscin promoted the expression of Bad, a pro-apoptotic BCL-2 family member, suggesting that dioscin induces cell apoptosis through the Bad pathway (Gajewski and Thompson, 1996). It should be noted that the antitumor effect of dioscin may be due to its hydrolysate diosgenin (Liu et al., 1995). Previous studies have revealed that in addition to diosgenin reducing cell proliferation and inducing apoptosis (Srinivasan et al., 2009), dioscin also inhibits angiogenesis, which inhibits tumor metastasis (Chen et al., 2015). Diosgenin reverses the multidrug resistance of cancer cells and make cancer cells sensitive to standard chemotherapy. Synthesis of diosgenin analogs and nano-formulations improve the anticancer efficacy and pharmacokinetic characteristics of the drug by enhancing the anticancer effects (Sethi et al., 2018). Therefore, future research on the active dioscin metabolites may be an important direction to study its anticancer effects.

SHP1 is a protein tyrosine phosphatase containing the Src homology 2 domain (SH2 domain). It has an oxidation sensitivity site and can be used as a target for antitumor therapy (Weibrecht et al., 2007). One study reported that the SHP1 protein is expressed in several non-lymphocytic cell lines, such as PCa, ovarian cancer and breast cancer cell lines, and that abnormal regulation of this protein causes abnormal cell proliferation and induces various cancers (Wu et al., 2003). Another study using PC3 cells revealed that SHP1 controls various factors necessary for normal functioning of the cell cycle through the PI3K-AKT pathway. Additionally, depleting SHP1 induced by siRNA causes G1 phase arrest, and SHP1 knockdown promotes nuclear localisation and p27 gene transcription (Rodriguez-Ubreva et al., 2010). SHP1 exhibits different expression levels and effects in different PCa cell lines. SHP1 is expressed at higher levels in LNCaP PCa cells than in PC3 cells and siRNA silencing of SHP1 increases LNCaP cell proliferation, while overexpression of SHP1 in PC3 cells decreases proliferation (Tassidis et al., 2010a). Clinical studies have shown that the expression of SHP1 in tumor cells is closely related to the timing of biochemical recurrence and clinical progression in PCa patients (Tassidis et al., 2010a). Reversing SHP1 gene silencing may be an attractive new strategy for cancer treatment (Zhang et al., 2005). Some natural antioxidants improve SHP1 expression. Several studies have reported that sylph verbascoside increases SHP1 expression, inhibits glioblastoma cell proliferation, migration and invasion and induces apoptosis. It also reduces tumor volume and growth in glioblastoma-planted nude mice (Jia et al., 2018). The SHP1 agonists SC-43 and SC-78 stimulate SHP1 to deactivate IL-6-induced STAT3 phosphorylation, thereby inhibiting colorectal cancer stem cells (Chung et al., 2018). Our study demonstrated that the antioxidant dioscin may have potential as a drug targeting SHP1. Dioscin promoted SHP1 phosphorylation and showed potential effects in the treatment of PCa.

In conclusion, the results of *in vitro* and *in vivo* studies have revealed that dioscin reversed IL-6 and DHT-stimulated PCa cell proliferation and invasion and increased apoptosis in these cells. These anticancer effects caused by dioscin may be due to its effects of increasing SHP1 phosphorylation and inhibiting the

subsequent MAPK signaling pathway. Our results suggest that dioscin may be a potential drug to treat both androgen-sensitive and androgen-independent PCa.

DATA AVAILABILITY STATEMENT

The datasets generated for this study are available on request to the corresponding authors.

ETHICS STATEMENT

The animal study was reviewed and approved by Ethics Committee of Fujian Provincial Hospital.

AUTHOR CONTRIBUTIONS

SHe wrote the manuscript. YG, XZ, and YW performed and designed the experiments. SHo and JY analyzed the data. HH performed the cell assays. QZ performed the WB assay. LY and TL performed *in vivo* experiments. YW, YG, and JY supervised the project.

FUNDING

The study was supported by the Joint Funds for the innovation of science and Technology, Fujian province (2017Y9064); high-level hospital foster grants from Fujian Provincial Hospital, Fujian province, China (2019HSJJ29) the Project of Science and Technology Plan of Xiangtan, China (SF-CP20173004) and the Natural Science Foundation of Jiangsu Province (no.BK20160481).

ACKNOWLEDGMENTS

The authors appreciate WELL BIOLOGICAL SCIENCE (http://www.wellbiology.com/, Changsha, China) greatly for their help in this study.

SUPPLEMENTARY MATERIAL

The Supplementary Material for this article can be found online at: https://www.frontiersin.org/articles/10.3389/fphar.2020.01099/full#supplementary-material

REFERENCES

Adekoya, T. O., and Richardson, R. M. (2020). Cytokines and chemokines as mediators ofprostate cancer metastasis. *Int. J. Mol. Sci.* 21, e4449. doi: 10.3390/ijms21124449

Balmanno, K., and Cook, S. J. (2009). Tumour cell survival signalling by the ERK1/2 pathway. *Cell Death Differ.* 16, 368–377. doi: 10.1038/cdd.2008.148

Chen, J., Li, H. M., Zhang, X. N., Xiong, C. M., and Ruan, J. L. (2014). Dioscin-induced apoptosis of human LNCaP prostate carcinoma cells through activation of caspase-3 and modulation of Bcl-2 protein family. *J. Huazhong Univ. Sci. Technolog. Med. Sci.* 34, 125–130. doi: 10.1007/s11596-014-1243-y

Chen, Y., Tang, Y. M., Yu, S. L., Han, Y. W., Kou, J. P., Liu, B. L., et al. (2015). Advances in the pharmacological activities and mechanisms of diosgenin. *Chin. J. Nat. Med.* 13, 578–587. doi: 10.1016/S1875-5364(15)30053-4

Choi, S., Warzecha, C., Zvezdova, E., Lee, J., Argenty, J., Lesourne, R., et al. (2017). THEMIS enhances TCR signaling and enables positive selection by selective inhibition of the phosphatase SHP-1. *Nat. Immunol.* 18, 433–441. doi: 10.1038/ni.3692

Chung, S. Y., Chen, Y. H., Lin, P. R., Chao, T. C., Su, J. C., Shiau, C. W., et al. (2018). Two novel SHP-1 agonists, SC-43 and SC-78, are more potent than regorafenib in suppressing the in vitro stemness of human colorectal cancer cells. *Cell Death Discovery* 4, 25. doi: 10.1038/s41420-018-0084-z

Cuadrado, A., and Nebreda, A. R. (2010). Mechanisms and functions of p38 MAPK signalling. *Biochem. J.* 429, 403–417. doi: 10.1042/BJ20100323

Dustin, C. M., Heppner, D. E., Lin, M. J., and van der Vliet, A. (2019). Redox regulation of tyrosine kinase signaling: More than meet the eye. *J. Biochem.* 167, 151–163. doi: 10.1093/jb/mvz085

Erdogan, S., Turkekul, K., Dibirdik, I., Doganlar, O., Doganlar, Z. B., Bilir, A., et al. (2018). Midkine downregulation increases the efficacy of quercetin on prostate cancer stem cell survival and migration through PI3K/AKT and MAPK/ERK pathway. *BioMed. Pharmacother.* 107, 793–805. doi: 10.1016/j.biopha.2018.08.061

Gajewski, T. F., and Thompson, C. B. (1996). Apoptosis meets signal transduction: Elimination of a BAD influence. *Cell* 87, 589–592. doi: 10.1016/s0092-8674(00)81377-x

Gerdes, J., Lemke, H., Baisch, H., Wacker, H. H., Schwab, U., and Stein, H. (1984). Cell cycle analysis of a cell proliferation-associated human nuclear antigen defined by the monoclonal antibody Ki-67. *J. Immunol.* 133, 1710–1715.

Giannoni, E., Bianchini, F., Masieri, L., Serni, S., Torre, E., Calorini, L., et al. (2010). Reciprocal activation of prostate cancer cells and cancer-associated fibroblasts stimulates epithelial-mesenchymal transition and cancer stemness. *Cancer Res.* 70, 6945–6956. doi: 10.1158/0008-5472.CAN-10-0785

Hobisch, A., Ramoner, R., Fuchs, D., Godoy-Tundidor, S., Bartsch, G., Klocker, H., et al. (2001). Prostate cancer cells (LNCaP) generated after long-term interleukin 6 (IL-6) treatment express IL-6 and acquire an IL-6 partially resistant phenotype. *Clin. Cancer Res.* 7, 2941–2948.

Hsieh, M. J., Tsai, T. L., Hsieh, Y. S., Wang, C. J., and Chiou, H. L. (2013). Dioscin-induced autophagy mitigates cell apoptosis through modulation of PI3K/Akt and ERK and JNK signaling pathways in human lung cancer cell lines. *Arch. Toxicol.* 87, 1927–1937. doi: 10.1007/s00204-013-1047-z

Igawa, T., Lin, F. F., Lee, M. S., Karan, D., Batra, S. K., Lin, M. F., et al. (2002). Establishment and characterization of androgen-independent human prostate cancer LNCaP cell model. *Prostate* 50, 222–235. doi: 10.1002/pros.10054

Inoue, H., Nishimura, K., Oka, D., Nakai, Y., Shiba, M., Tokizane, T., et al. (2005). Prostate cancer mediates osteoclastogenesis through two different pathways. *Cancer Lett.* 223, 121–128. doi: 10.1016/j.canlet.2004.09.053

Jia, W. Q., Wang, Z. T., Zou, M. M., Lin, J. H., Li, Y. H., Zhang, L., et al. (2018). Verbascoside inhibits glioblastoma cell proliferation, migration and invasion while promoting apoptosis through upregulation of protein tyrosine phosphatase SHP-1 and inhibition of STAT3 phosphorylation. *Cell Physiol. Biochem.* 47, 1871–1882. doi: 10.1159/000491067

Johnson, D. E., O'Keefe, R. A., and Grandis, J. R. (2018). Targeting the IL-6/JAK/STAT3 signalling axis in cancer. *Nat. Rev. Clin. Oncol.* 15, 234–248. doi: 10.1038/nrclinonc.2018.8

Kim, E. A., Jang, J. H., Lee, Y. H., Sung, E. G., Song, I. H., Kim, J. Y., et al. (2014). Dioscin induces caspase-independent apoptosis through activation of apoptosis-inducing factor in breast cancer cells. *Apoptosis* 19, 1165–1175. doi: 10.1007/s10495-014-0994-z

Krongrad, A., Wilson, C. M., Wilson, J. D., Allman, D. R., and McPhaul, M. J. (1991). Androgen increases androgen receptor protein while decreasing receptor mRNA in LNCaP cells. *Mol. Cell Endocrinol.* 76, 79–88. doi: 10.1016/0303-7207(91)90262-Q

Liu, B., Lockwood, G. B., and Gifford, L. A. (1995). Supercritical fluid extraction of diosgenin from tubers of Dioscorea nipponica. *J. Chromatogr.* 690, 250–253. doi: 10.1016/0021-9673(94)01117-W

Lu, Z., and Xu, S. (2006). ERK1/2 MAP kinases in cell survival and apoptosis. *IUBMB Life* 58, 621–631. doi: 10.1080/15216540600957438

Min, D. Y., Lee, Y. A., Ryu, J. S., Ahn, M. H., Chung, Y. B., Sim, S., et al. (2004). Caspase-3-mediated apoptosis of human eosinophils by the tissue-invading helminth Paragonimus westermani. *Int. Arch. Allergy Immunol.* 133, 357–364. doi: 10.1159/000077355

Mkaddem, S. B., Murua, A., Flament, H., Titeca-Beauport, D., Bounaix, C., Danelli, L., et al. (2017). Lyn and Fyn function as molecular switches that control immunoreceptors to direct homeostasis or inflammation. *Nat. Commun.* 8, 246. doi: 10.1038/s41467-017-00294-0

Mukherjee, B., and Mayer, D. (2008). Dihydrotestosterone interacts with EGFR/MAPKsignalling and modulates EGFR levels in androgen receptor-positive LNCaP prostate cancercells. *Int. J. Oncol.* 33, 623–629. doi: 10.3892/ijo_00000048

Muniyan, S., Chen, S. J., Lin, F. F., Wang, Z., Mehta, P. P., Batra, S. K., et al. (2015). ErbB-2 signaling plays a critical role in regulating androgen-sensitive and castration-resistant androgen receptor-positive prostate cancer cells. *Cell Signal* 27, 2261–2271. doi: 10.1016/j.cellsig.2015.08.002

Pesce, M., Franceschelli, S., Ferrone, A., De Lutiis, M. A., Patruno, A., Grilli, A., et al. (2015). Verbascoside down-regulates some pro-inflammatory signal transduction pathways by increasing the activity of tyrosine phosphatase SHP-1 in the U937 cell line. *J. Cell Mol. Med.* 19, 1548–1556. doi: 10.1111/jcmm.12524

Porter, A. G., and Janicke, R. U. (1999). Emerging roles of caspase-3 in apoptosis. *Cell Death Differ.* 6, 99–104. doi: 10.1038/sj.cdd.4400476

Rodriguez-Ubreva, F. J., Cariaga-Martinez, A. E., Cortes, M. A., Romero-De, P. M., Ropero, S., López-Ruiz, P., et al. (2010). Knockdown of protein tyrosine phosphatase SHP-1 inhibits G1/S progression in prostate cancer cells through the regulation of components of the cell-cycle machinery. *Oncogene* 29, 345–355. doi: 10.1038/onc.2009.329

Santer, F. R., Erb, H. H., and McNeill, R. V. (2015). Therapy escape mechanisms in the malignant prostate. *Semin. Cancer Biol.* 35, 133–144. doi: 10.1016/j.semcancer.2015.08.005

Schafer, Z. T., and Brugge, J. S. (2007). IL-6 involvement in epithelial cancers. *J. Clin. Invest.* 117, 3660–3663. doi: 10.1172/JCI34237

Sethi, G., Shanmugam, M. K., Warrier, S., Merarchi, M., Arfuso, F., Kumar, A. P., et al. (2018). Pro-Apoptotic and Anti-Cancer properties of diosgenin: A comprehensive and critical review. *Nutrients* 10, 645. doi: 10.3390/nu10050645

Srinivasan, S., Koduru, S., Kumar, R., Venguswamy, G., Kyprianou, N., and Damodaran, C. (2009). Diosgenin targets Akt-mediated prosurvival signaling in human breast cancer cells. *Int. J. Cancer* 125, 961–967. doi: 10.1002/ijc.24419

Tao, X., Xu, L., Yin, L., Han, X., Qi, Y., Xu, Y., et al. (2017). Dioscin induces prostate cancer cell apoptosis through activation of estrogen receptor-beta. *Cell Death Dis.* 8, e2989. doi: 10.1038/cddis.2017.391

Tao, X., Yin, L., Xu, L., and Peng, J. (2018). Dioscin: A diverse acting natural compound with therapeutic potential in metabolic diseases, cancer, inflammation and infections. *Pharmacol. Res.* 137, 259–269. doi: 10.1016/j.phrs.2018.09.022

Tassidis, H., Brokken, L. J., Jirstrom, K., Ehrnstrom, R., Ponten, F., Ulmert, D., et al. (2010a). Immunohistochemical detection of tyrosine phosphatase SHP-1 predicts outcome after radical prostatectomy for localized prostate cancer. *Int. J. Cancer* 126, 2296–2307. doi: 10.1002/ijc.24917

Tassidis, H., Culig, Z., Wingren, A. G., and Harkonen, P. (2010b). Role of the protein tyrosine phosphatase SHP-1 in Interleukin-6 regulation of prostate cancer cells. *Prostate* 70, 1491–1500. doi: 10.1002/pros.21184

Tong, Q., Qing, Y., Wu, Y., Hu, X., Jiang, L., and Wu, X. (2014). Dioscin inhibits colon tumor growth and tumor angiogenesis through regulating VEGFR2 and AKT/MAPK signaling pathways. *Toxicol. Appl. Pharmacol.* 281, 166–173. doi: 10.1016/j.taap.2014.07.026

Tonks, N. K. (2005). Redox redux: Revisiting PTPs and the control of cell signaling. *Cell* 121, 667–670. doi: 10.1016/j.cell.2005.05.016

Wagner, E. F., and Nebreda, A. R. (2009). Signal integration by JNK and p38 MAPK pathways in cancer development. *Nat. Rev. Cancer* 9, 537–549. doi: 10.1038/nrc2694

Wang, Y., Fu, M., Liu, J., Yang, Y., Yu, Y., Li, J., et al. (2019). Inhibition of tumor metastasis by targeted daunorubicin and dioscin codelivery liposomes modified with PFV for the treatment of non-small-cell lung cancer. *Int. J. Nanomed.* 14, 4071–4090. doi: 10.2147/IJN.S194304

Wei, Y., Xu, Y., Han, X., Qi, Y., Xu, L., Xu, Y., et al. (2013). Anti-cancer effects of dioscin on three kinds of human lung cancer cell lines through inducing DNA damage and activating mitochondrial signal pathway. *Food Chem. Toxicol.* 59, 118–128. doi: 10.1016/j.fct.2013.05.054

Weibrecht, I., Bohmer, S. A., Dagnell, M., Kappert, K., Ostman, A., and Böhmer, F.-D. (2007). Oxidation sensitivity of the catalytic cysteine of the protein-tyrosine phosphatases SHP-1 and SHP-2. *Free Radic. Biol. Med.* 43, 100–110. doi: 10.1016/j.freeradbiomed.2007.03.021

Wu, C., Sun, M., Liu, L., and Zhou, G. W. (2003). The function of the protein tyrosine phosphatase SHP-1 in cancer. *Gene* 306, 1–12. doi: 10.1016/s0378-1119(03)00400-1

Yen, M. L., Su, J. L., Chien, C. L., Tseng, K. W., Yang, C. Y., Chen, W. F., et al. (2005). Diosgenin induces hypoxia-inducible factor-1 activation and angiogenesis through estrogen receptor-related phosphatidylinositol 3-kinase/Akt and p38 mitogen-activated protein kinase pathways in osteoblasts. *Mol. Pharmacol.* 68, 1061–1073. doi: 10.1124/mol.104.010082

Yin, L., Zheng, L., Xu, L., Dong, D., Han, X., Qi, Y., et al. (2015). In-silico prediction of drug targets, biological activities, signal pathways and regulating networks of dioscin based on bioinformatics. *BMC Complement Altern. Med.* 15, 41. doi: 10.1186/s12906-015-0579-6

Zhang, Q., Wang, H. Y., Marzec, M., Raghunath, P. N., Nagasawa, T., and Wasik, M. A. (2005). STAT3- and DNA methyltransferase 1-mediated epigenetic silencing of SHP-1 tyrosine phosphatase tumor suppressor gene in malignant T lymphocytes. *Proc. Natl. Acad. Sci. U. S.* 102, 6948–6953. doi: 10.1073/pnas.0501959102

Zhou, L., Yu, X., Li, M., Gong, G., Liu, W., Li, T., et al. (2019). Cdh1-mediated Skp2 degradation by dioscinreprogrammes aerobic glycolysis and inhibits colorectal cancer cells growth. *EBioMedicine.* 51, 102570. doi: 10.1016/j.ebiom.2019.11.031

Conflict of Interest: The authors declare that the research was conducted in the absence of any commercial or financial relationships that could be construed as a potential conflict of interest.

frontiers in Pharmacology

ORIGINAL RESEARCH
published: 11 September 2020
doi: 10.3389/fphar.2020.552088

Squalenoylated Nanoparticle Pro-Drugs of Adjuvant Antitumor 11α-Hydroxyecdysteroid 2,3-Acetonides Act as Cytoprotective Agents Against Doxorubicin and Paclitaxel

Máté Vágvölgyi[1], Péter Bélteky[2], Dóra Bogdán[3,4], Márta Nové[5], Gabriella Spengler[5], Ahmed D. Latif[6†], István Zupkó[6,7], Tamás Gáti[8], Gábor Tóth[9], Zoltán Kónya[2,10] and Attila Hunyadi[1,7]*

[1] Institute of Pharmacognosy, Interdisciplinary Excellence Centre, University of Szeged, Szeged, Hungary, [2] Department of Applied and Environmental Chemistry, Interdisciplinary Excellence Centre, University of Szeged, Szeged, Hungary, [3] Department of Organic Chemistry, Semmelweis University, Budapest, Hungary, [4] Institute of Materials and Environmental Chemistry, Research Centre for Natural Sciences, Budapest, Hungary, [5] Department of Medical Microbiology and Immunobiology, University of Szeged, Szeged, Hungary, [6] Department of Pharmacodynamics and Biopharmacy, Faculty of Pharmacy, University of Szeged, Szeged, Hungary, [7] Interdisciplinary Centre for Natural Products, University of Szeged, Szeged, Hungary, [8] Servier Research Institute of Medicinal Chemistry (SRIMC), Budapest, Hungary, [9] NMR Group, Department of Inorganic and Analytical Chemistry, Budapest University of Technology and Economics, Budapest, Hungary, [10] MTA-SZTE Reaction Kinetics and Surface Chemistry Research Group, University of Szeged, Szeged, Hungary

Several ecdysteroid acetonides act as adjuvant chemo-sensitizing agents against various cancer cell lines, and they can be formulated to self-assembling nanoparticle (NP) pro-drugs through a hydrolysable conjugation with squalene. In the bloodstream such squalenoylated nanoparticles dissolve into low-density lipoprotein (LDL) that allows targeting tissues containing high levels of LDL-receptors. In this work, ajugasterone C 2,3;20,22-diacetonide (**3**) and 11α-hydroxypoststerone 2,3-acetonide (**4**) were squalenoylated to obtain two new ecdysteroid pro-drugs (**6** and **7**) and their nano-assemblies ($\mathbf{6_{NP}}$ and $\mathbf{7_{NP}}$). A complete NMR signal assignment of **6** and **7** was achieved. Interaction of compounds **3** and **4** with chemotherapeutics was studied by the Chou-Talalay method. Compound **3** showed strong synergism with doxorubicin on a multi-drug resistant lymphoma cell line. In contrast, its nanoassembly $\mathbf{6_{NP}}$ significantly decreased the cytotoxicity of doxorubicin on these MDR cells, strongly suggesting that at least the 2,3-acetonide group was cleaved by the acidic pH of lysosomes after endocytosis of the prodrug. Further, compound **4** acted in strong antagonism with paclitaxel on MCF-7 cells and its nanoassemby $\mathbf{7_{NP}}$ also protected MCF-7 cells from the effect of paclitaxel. Our results suggest that acid-resistant A-ring substitution would be crucial to design adjuvant antitumor squalenoylated ecdysteroid prodrugs. Additionally, our results may be considered as a serendipitous discovery of a novel way to deliver cytoprotective, adaptogen ecdysteroids to healthy tissues with upregulated LDL-R.

Keywords: ecdysteroid, squalene nanoparticle pro-drug, self-assembly, low-density lipoprotein targeting, cancer, multi-drug resistance

OPEN ACCESS

Edited by:
Maria José U. Ferreira, University of Lisbon, Portugal

Reviewed by:
Didier Desmaele, UMR8612 Institut Galien Paris Sud (IGPS), France
Junhua Mai, Houston Methodist Research Institute, United States

***Correspondence:**
Attila Hunyadi
hunyadi.a@pharm.u-szeged.hu

†On leave from Department of Pharmacology and Toxicology, Faculty of Medicine, Wasit University, Wasit, Iraq

Specialty section:
This article was submitted to Pharmacology of Anti-Cancer Drugs, a section of the journal Frontiers in Pharmacology

Received: *16 April 2020*
Accepted: *14 August 2020*
Published: *11 September 2020*

Citation:
Vágvölgyi M, Bélteky P, Bogdán D, Nové M, Spengler G, Latif AD, Zupkó I, Gáti T, Tóth G, Kónya Z and Hunyadi A (2020) Squalenoylated Nanoparticle Pro-Drugs of Adjuvant Antitumor 11α-Hydroxyecdysteroid 2, 3-Acetonides Act as Cytoprotective Agents Against Doxorubicin and Paclitaxel. Front. Pharmacol. 11:552088. doi: 10.3389/fphar.2020.552088

INTRODUCTION

Nanotechnology offers various perspectives to overcome the insufficient therapeutic efficacy of a biomolecule. Over the previous decades, a wide array of nano-sized delivery platforms had been developed in antitumor chemotherapy for a more efficient delivery of chemotherapeutic agents to the target cells (Li et al., 2017). Typically, the use of nanomaterials as *in vivo* transport systems serves more than one intention: a) by placing the drug in a biocompatible, protective matrix, we can modulate its physicochemical stability in the organism, therefore improving its pharmacokinetic and pharmacological properties, and b) by considering the tissue- or cell-specific delivery mechanism of nanoparticles (NPs) we can have a partial control over the accumulation and distribution of the drug, and, accordingly, directly or indirectly target the tumor (Xu et al., 2015; Shi et al., 2017).

One particularly simple, yet efficient way to design anticancer NPs is the preparation of self-assembling drug conjugates (Fumagalli et al., 2016). We can obtain these molecules through synthesis, by chemically linking the chosen chemotherapeutic agent to an essential functional unit, the so-called inducer. Organic molecules, such as terpenes, polysaccharides, or polymeric chains with high biocompatibility, are widely used as inducers, which can spontaneously self-assemble into NPs in an aqueous medium without the need for using any additional surfactants to stabilize their colloid suspensions (Bildstein et al., 2011; Delplace et al., 2014). In some instances, connecting the drug and the inducer can be achieved by using a so-called linker moiety, which may further enhance the *in vivo* release of the therapeutic agent from its conjugate (Borrelli et al., 2014). During the synthetic preparation of bioconjugates, components are coupled together through covalent bonds that are hydrolysable in a biological environment (e.g., esters), so that such self-assembled NPs will typically act as pro-drugs (Cheetham et al., 2017).

Among the possible inducers, squalene is a particularly attractive choice due to its biocompatibility, inertness, and the ease of transforming the terminal double bond to versatile functional groups that may be linked to the drug (Desmaele et al., 2012; Maksimenko et al., 2014). It has recently been revealed that NPs of squalene conjugates do not remain intact after getting into the bloodstream. Instead, they get dissolved into lipoproteins (whose most affected fraction depends on the species, in humans it is mainly low-density lipoprotein or rather LDL) that will transport them in the bloodstream, and this allows a unique targeting of cancer cells that commonly display high expression and activity of LDL receptors (LDL-R) (Sobot et al., 2017).

Ecdysteroids, analogs of the insect molting hormone ecdysone, exert a wide range of bioactivities in mammals (Lafont and Dinan, 2003; Dinan et al., 2020). We have previously reported that less polar ecdysteroid derivatives can strongly sensitize both multi-drug resistant (MDR) and drug-susceptible cancer cell lines to various chemotherapeutics (Martins et al., 2012; Martins et al., 2015). We have been exploring relevant structure-activity relationships over the years, and found that the most important is the presence of a 2,3-acetonide group (Hunyadi et al., 2017). This moiety is unfortunately also the most chemically sensitive part of these compounds, particularly in acidic environment. Therefore, nano-formulation of these compounds can not only serve as a relevant targeting strategy, but it may also significantly increase their stability. Previously, we reported the preparation and evaluation of squalene-conjugates obtained from poststerone 2,3-acetonide 20-oxime (Bogdan et al., 2018). These compounds, together with 25-squalenoylated analogs of 20-hydroxyecdysone 2,3;20,22-diacetonide (20DA), were subsequently formulated into doxorubicin-containing hetero-nanoparticles that could efficiently inhibit proliferation of adriamycin-resistant $A2780_{ADR}$ cancer cells (Fumagalli et al., 2018).

In the present work, we aimed to further expand the available chemical and pharmacological space by preparing further self-assembling conjugates and NPs from other, less abundant ecdysteroids containing an 11α-OH group for a convenient ester coupling, and to evaluate their effect on the chemoresistance of MDR and non-MDR cancer cell lines.

MATERIALS AND METHODS

Materials

Reagents and solvents were purchased from Sigma (Merck KGaA, Darmstadt, Germany) and were applied for the corresponding research purpose without any further purification. Each synthetic reaction was monitored by thin-layer chromatography (TLC) on Kieselgel $60F_{254}$ silica plates (Merck KGaA, Darmstadt, Germany). The characteristic spots of materials were examined under UV illumination at 254 and 366 nm. Ajugasterone C (**1**) was previously isolated from *Serratula wolffii* (Hunyadi et al., 2007).

Synthetic Procedures

Synthesis of Compound 2

Compound **2** was prepared according to our previously published method (Issaadi et al., 2019). Briefly, a 1 g aliquot of ajugasterone C (**1**) was dissolved in 80 ml of methanol. One equivalent of (diacetoxyiodo)benzene (PIDA) was added to the solution, and subsequently, the reaction mixture was left under stirring for 45 min at RT. Following this, the solution was neutralized with 10% aq. $NaHCO_3$ and then, the solvent was evaporated on a rotary evaporator. The obtained dry residue was re-dissolved in methanol, and silica gel (~4 g) was added to the solution. After this, the solvent was removed under reduced pressure allowing the preparation of the sample for dry loading flash chromatographic purification. This resulted in the successful isolation of compound **2** (0.59 g, 74.8%).

Synthesis of Compounds 3 and 4

Derivatization of the diols of ecdysteroids **1** and **2** was performed as published before (Martins et al., 2012). Briefly, a 500 mg aliquot of the corresponding substrate was dissolved in a concentration of 1 g/100 ml (50 ml) in acetone. To the obtained solution, 500 mg of phosphomolybdic acid (PMA) hydrate was added, and the mixture was sonicated for 25 min

at RT. Subsequently, the solution was neutralized with 10% aq. $NaHCO_3$ and then, the solvent was evaporated under reduced pressure. The obtained products were extracted from their aqueous residue using ethyl acetate (3 ml x 100 ml), and the organic fractions were combined and dried over Na_2SO_4. Following this, the drying agent was removed by filtration, and the solvent was evaporated on a rotary evaporator. The residue was subjected to flash chromatographic purification to yield ajugasterone C 2,3;20,22-diacetonide (**3**; 364 mg, 62.4%), or 11α-hydroxypoststerone 2,3-acetonide (**4**; 386 mg, 69.8%) in pure form.

Synthesis of Ecdysteroid Conjugates 6 and 7

Self-assembly inducer squalene was functionalized and conjugated with sebacic acid following previously published procedures, which had allowed us the preparation of compound **5** (Borrelli et al., 2014; Maksimenko et al., 2014). An aliquot of 0.2 mmol of ecdysteroid 3 (112.2 mg) or 4 (83.7 mg) and 142.7 mg of compound **5** (0.25 mmol, 1.25 equiv.) were dissolved in 10 ml of dry dichloromethane in a two-neck round-bottom flask. Later, 48.9 mg of 4-dimethylaminopyridine (DMAP; 0.4 mmol, two equiv.) and 115 mg of (3-dimethylaminopropyl)-N′-ethylcarbodiimide hydrochloride (EDC·HCl; 0.6 mmol, three equiv.) were added to the solution, and then, the reaction mixture was stirred under an argon atmosphere at RT for overnight. Following this, the solution was neutralized with 10% aq. $NaHCO_3$ and was diluted with brine (30 ml) allowing to perform an extraction with dichloromethane (4 ml x 30 ml). The collected organic fractions were combined and dried under Na_2SO_4, and subsequently, the drying agent was removed through filtration. The solvent of the sample was evaporated, and then, the residue was purified utilizing preparative NP-HPLC affording the isolation of compound **6** (180.9 mg, 81.2%) or the side chain-cleaved conjugate analogue **7** (97.9 mg, 58.9%), as a colorless oil.

Chromatographic Conditions

Following organic synthesis, chromatographic purification of substances was carried out on either a Combiflash Rf+ flash chromatographic instrument (TELEDYNE Isco, Lincoln, NE, USA) equipped with DAD-ELS detection using commercially available RediSep columns (TELEDYNE Isco, USA), or on an Armen Spot Prep II preparative HPLC purification system (Gilson, Middleton, WI, USA) equipped with a dual-wavelength UV-VIS detector. Flash chromatographic purifications were performed on 4–24 G silica columns with adequately chosen eluent ratios of dichloromethane—methanol. For preparative HPLC separations, a Phenomenex Luna® 5 µm Silica (2) 100 Å 250 mm x 21.2 mm column (Phenomenex Inc., Torrance, CA, USA) was used, typically in isocratic elution mode with adequately chosen eluent ratios of cyclohexane—isopropanol. In general, the applied flow rates were 15 ml/min, and the wavelengths of detection were 210 andd 250 nm. Purity of the isolated compounds was determined on a Jasco HPLC instrument (Jasco International Co. Ltd., Hachioji, Tokyo, Japan) equipped with LC capillary cables proper for analytical purposes. The analysis was carried out on a 250 mm x 4.6 mm analogue of the preparative silica column using the peak area % data of the PDA chromatogram recorded between 210 and 410 nm. During the analytical-scale HPLC measurements, the applied flow rate was a constant 1 ml/min.

Structure Elucidation

The compounds' mass spectra were recorded on an Agilent 1100 LC-MS instrument (Agilent Technologies, Santa Clara, CA, USA) coupled with Thermo Q-Exactive Plus orbitrap analyzer (Thermo Fisher Scientific, Waltham, MA, USA) used in positive mode.

^1H (800 and 500 MHz) and ^{13}C (200 and 125 MHz) NMR spectra were recorded at room temperature on Bruker Avance III spectrometers equipped with cryo probeheads. Amounts of approximately 3–5 mg of compounds were dissolved in 0.6 ml of chloroform-*d* and transferred to 5 mm NMR sample tubes. Chemical shifts are given on the δ-scale and are referenced to the solvent chloroform-*d*: δ_C = 77.00 and δ_H = 7.27 ppm). Pulse programs of all experiments (^1H, ^{13}C, DEPTQ, 1D sel-TOCSY, gs-HSQC, and gs-HMBC (optimized for 8 and 10 Hz respectively), band–selective–HSQC, –HMBC and HSQC–TOCSY were taken from the Bruker software library. For 1D measurements, 64K data points were used to yield the FID. For 2D measurements, on the 500 MHz spectrometer in case of the HSQC spectrum data points (t_2 x t_1) were acquired with 2 K x 128, in case of the HMBC spectrum data points (t_2 x t_1) were acquired with 2 K x 256, respectively. In the band-selective HMBC experiment, the used digital resolution was 1.04 Hz per point; in the band-selective HSQC experiment it was 0.13 Hz per point. For F_1 linear prediction was applied to enhance the resolution. Most ^1H assignments were accomplished using general knowledge of chemical shift dispersion with the aid of the proton-proton coupling pattern (^1H NMR spectra). The NMR signals of the products were assigned by comprehensive one- and two-dimensional NMR methods using widely accepted strategies (Duddeck et al., 1998; Pretsch et al., 2002).The ^1H and ^{13}C NMR data for the steroid moiety of compounds **6** and **7**, are compiled in **Table 1**, whereas the signals of the R-groups are summarized in **Table 2**. The characteristic NMR and HRMS spectra of compounds **6** and **7** are presented as supporting information.

Preparation of Self-Assembled Ecdysteroid NPs 6_{NP} and 7_{NP}

A 12 mg aliquot of compound **6** or **7** was dissolved in 1.5 ml of acetone (8 mg/ml), and under mild stirring (350 rpm), the prepared solution was added dropwise to a double volume of Milli-Q® (Merck KGaA, Darmstadt, Germany) ultrapure water for 5 min at RT. The spontaneous self-assembly of the bioconjugates occurred immediately, as a consequence of local secondary interactions guided by the hydrophobic squalene chains. Following this, the organic solvent was evaporated at 25°C on a rotary evaporator that afforded the corresponding aq. nanosuspensions $\mathbf{6_{NP}}$ or $\mathbf{7_{NP}}$ in a final concentration of 4 mg/ml.

TABLE 1 | ^{1}H and ^{13}C chemical shifts, multiplicities and characteristic coupling constants (Hz) of the steroid moiety of compounds **6** and **7** in $CDCl_3$.

Atom no.	6[b]			7[a]		
	H	*J* (Hz)	C	H	*J* (Hz)	C
1β	1.20 dd	13.9; 10.7	39.85	1.21 dd	13.9; 10.9	39.88
1α	1.83 dd	13.9; 6.1		1.83 dd	13.9; 6.1	
2	4.42 ddd	10.7; 6.1; 4.5	72.31	4.44 ddd	10.9; 6.1; 4.5	72.26
3	4.31 dd	4.5; 4.5	71.51	4.31 ddd	4.5; 4.5; 1.5	71.48
4β	2.16 m		27.11	2.15 m		27.07
4α	1.80 m			1.78 ddd	17.5; 13.4; 4.5	
5	2.33 m		52.06	2.35 m		52.07
6	–		202.26	–		201.90
7	5.89 d	2.9	122.73	5.89 dd	2.9; 1.0	123.22
8	–		159.52	–		158.22
9	3.13 dd	9.1; 2.9	38.52	3.18 dd	9.1; 2.9	38.59
10	–		38.57	–		38.63
11β	5.31 ddd	10.4; 9.1; 6.5	70.61	5.30 ddd	10.4; 9.1; 6.5	70.21
11α	–			–		
12β	2.01 m		37.18	2.29 m		36.11
12α	2.31 m			2.25 m		
13	–		46.88	–		46.95
14	–		84.42	–		84.20
15β	2.08 m		31.84	2.10 m		32.15
15α	1.55 m			1.65 m		
16β	2.08 m		21.11	2.33 m		21.10
16α	1.87 m			1.93 m		
17	2.24 dd	10.0; 7.9	48.84	3.29 dd	9.7; 7.9	58.18
18	0.85 s		17.66	0.68 s		17.60
19	1.03 s		23.53	1.03 s		23.55
20	–		83.77	–		208.39
21	1.14 s		21.83	2.15 s		31.44
22	3.59 dd	9.2; 2.5	81.58			
23	1.45/1.35 m		26.78			
24	1.48/1.19 m		36.39			
25	1.56 m		28.26			
26	0.90 d	6.6	22.46			
27	0.91 d	6.6	22.58			
			2,3-acetonide:			
Meβ	1.47 s		28.54	1.47 s		28.54
Meα	1.34 s		26.57	1.34 s		26.57
C	–		108.21	–		108.28
			20,22-acetonide:			
Meβ	1.32 s		26.85	–		–
Meα	1.41 s		28.94	–		–
C	–		106.85	–		–

[a] *800/200 MHz;* [b] *500/125 MHz; s=singlet; d=doublet; unresolved multiplet.*

TABLE 2 | ^{1}H and ^{13}C chemical shifts of the R group in compounds **6** and **7** in $CDCl_3$.

Atom no.	7[b]		6[b]	
	H	C	H	C
1′	–	172.83	–	172.82
2′	2.36	34.66	2.33	34.69
3′	1.66	24.64	1.64	24.62
4′	1.34	29.03	1.38-1.29	29.03*
5′	1.36-1.31	29.07*		29.08*
6′		29.08*		29.08*
7′	1.33	29.10		29.10*
8′	1.63	24.96	1.62	24.95
9′	2.30	34.34	2.29	34.33
10′	–	173.92	–	173.91
11′	–	–	–	–
12′	4.04	64.02	4.04	64.01
13′	1.72	26.90	1.73	26.87
14′	2.03	35.79	2.03	35.77
15′	–	133.67	–	133.67
16′	5.13	125.06	5.14	125.03
17′	2.08	26.65	2.07	26.64
18′	1.99	39.66	1.99	39.66
19′	–	135.11	–	135.10
20′	5.15	124.37	5.15	124.35
21′	2.02	28.25*	2.02	28.24*
22′	2.02	28.26*	2.02	28.25*
23′	5.16	124.27	5.15	124.25
24′	–	134.96	–	134.96
25′	1.99	39.74	1.99	39.73
26′	2.08	26.65	2.08	26.64
27′	5.12	124.25	5.12	124.23
28′	–	134.90	–	134.89
29′	1.99	39.72	1.99	39.71
30′	2.07	26.76	2.07	26.74
31′	5.10	124.39	5.10	124.37
32′	–	131.24	–	131.25
33′	1.69	25.68	1.69	25.69
34′	1.60	17.67	1.61	17.66
35′	1.60	15.99	1.61	15.99
36′	1.60	16.04	1.61	16.03
37′	1.60	16.03	1.61	16.02
38′	1.60	15.86	1.61	15.86

[a] *800/200 MHz;* [b] *500/25 MHz; *tentative assignments.*

Characterization of Nanoparticles

Nano assemblies $\mathbf{6_{NP}}$ and $\mathbf{7_{NP}}$ were initially characterized by transmission electron microscopy (TEM) in order to investigate their morphology. The images were taken by a FEI Tecnai G^2 20 X–Twin instrument (FEI Corporate Headquarters, Hillsboro, OR, USA) using 200 kV accelerating voltage. The samples were drop casted on by 200 mesh, copper supported lacey–carbon grids. In order to further investigate the size and colloidal stability of the self–assembled particles in liquid media, dynamic light scattering (DLS) measurements were carried out on a Malvern Zetasizer Nano ZS instrument (Malvern Instruments, Malvern, UK) using disposable folded capillary cells. Particle size distribution (PSD), average hydrodynamic diameter (Z-Average) and polydispersity index (PdI) measurements were performed to assess particle size and dispersity, while zeta potential measurements aimed to determine long-term colloidal stability.

Cell Lines

Two non-adherent cell lines were used, L5178 mouse T-cell lymphoma (ECACC catalog number 87111908, U.S. FDA, Silver Spring, MD, U.S.), and its multidrug resistant counterpart ($L5178_{MDR}$) that swas established by transfection with pHa MDR1/A retrovirus (Pastan et al., 1988). Cells were cultured in McCoy's 5A media supplemented with nystatin, L-glutamine, penicillin, streptomycin, and 10% heat-inactivated horse serum, at 37°C and 5% CO_2. The MDR cell line was selected by culturing the infected cells with 60 ng/L colchicine (Sigma). Media, horse serum, and antibiotics were purchased from Sigma. The human breast cancer cell lines MDA-MB-231 and MCF7 were obtained from ECACC (European Collection of Cell Cultures, Salisbury, UK). Cells were grown in Minimum Essential Medium (MEM) supplemented with 10% fetal calf serum, 1% non-essential amino

acids, and 1% penicillin-streptomycin. All media and supplements for these experiments were obtained from Lonza Group Ltd. (Basel, Switzerland). The cells were maintained at 37°C in humidified atmosphere containing 5% CO_2.

Evaluation of the ABCB1 Inhibitory Activity of Compounds 3 and 4

ABCB1 inhibitory activity of compounds **3** and **4** was evaluated through the intracellular accumulation of rhodamine 123, an ABCB1 substrate fluorescent dye, by flow cytometry as published before (Martins et al., 2012). Briefly, 2 x 10^6 cells/ml were treated with 2 or 20 μM of either compound. After 10 min incubation, rhodamine 123 (Sigma-Aldrich) was added to a final concentration of 5.2 μM and the samples were incubated for 20 min at 37°C in water bath. Samples were centrifuged (Heraeus Labofuge 400, Thermo Fisher Scientific, Waltham, MA, USA) (2000 rpm, 2 min) and washed twice with phosphate buffer saline (PBS, Sigma-Aldrich). The final samples were re-suspended in 0.5 ml PBS and its fluorescence measured with a Partec CyFlow flow cytometer (Partec, Münster, Germany). 100 nM of tariquidar, kindly provided by Milica Pešić (Institute for Biological Research Sinisa Stankovic, Belgrade, Serbia), was used as a positive control.

Evaluation of the Interaction Between Compound 3 or 4 and Doxorubicin or Paclitaxel

The checkerboard microplate method was used to evaluate the combined activity of doxorubicin (Teva, Budapest, Hungary) or paclitaxel (Teva, Budapest, Hungary) and compound **3** and **4** on the cell viability of $L5178_{MDR}$, L5178, MCF-7, and MDA-MB-231 cell lines as described before (Martins et al., 2012).

$L5178_{MDR}$ and L5178cells were incubated at 6,000 cells/well density in presence of doxorubicin and/or compound **3** or **4** in McCoy's 5A medium (Sigma-Aldrich) for 72 h at 37°C, 5% CO_2. Then, 3-(4,5-dimethylthiazol-2-yl)-2,5-diphenyltetrazolium bromide (MTT, Sigma-Aldrich) was added to each well at a final concentration of 0.5 mg/ml, and after 4 h of incubation, 100 ml of 10% sodium dodecyl sulfate (SDS) (Sigma-Aldrich) in 0.01M HCl was added to each well. The plates were further incubated overnight, and the optical densities were read at 540 and 630 nm using an ELISA reader (Multiskan EX, Thermo Labsystem, Milford, MA, USA). Ecdysteroids and doxorubicin were administered at the 3.125–100 μM, and 67.35 nM–8.62 μM concentration ranges respectively.

Regarding MCF-7 and MDA-MB-231, cells were seeded at 5 x 10^3 cells/well and incubated overnight for proper cell adhesion. Afterwards, the cells were treated with the tested compounds for 72 h at 37°C, and 5% CO_2. Ecdysteroids were administered at the same concentration range as indicated above, and the concentration ranges for doxorubicin (Dox) and paclitaxel (PCT) were as follows: Dox: 3.9–500 nM (MCF-7), and 7.8 nM–1.0 μM (MDA-MB-231); PCT: 0.54 pM–7.0 nM (MCF-7), and 0.23–30 nM (MDA-MB-231). Following the incubation, 44 μl/well MTT reagent (5 mg/ml in PBS) was added to the samples, and after 4 h of further incubation, the supernatant was replaced with DMSO (100 μl/well) and the plates were shaken for 45 min at 37°C to dissolve formazan crystals. The optical density was read at 545 nm wavelength using a microplate reader (Stat Fax-2100, Awareness Technology INC, USA).

In all cases, the interaction was evaluated using the CompuSyn software (CompuSyn Inc., Paramus, NJ, USA) at each constant ratio of compound vs. doxorubicin or compound vs. paclitaxel (M/M), and combination index (CI) values were obtained for 50%, 75%, and 90% of growth inhibition.

Evaluation of the Interaction Between Nanoassemblies 6_{NP} or 7_{NP} and Paclitaxel on MCF-7 Cells

MCF-7 cells were cultured as described above, and the effect of PCT on cell viability was tested by MTT assay with or without the presence of $\mathbf{6_{NP}}$ or $\mathbf{7_{NP}}$. Treatment groups were as follows: serial dilutions of PCT (group 1), and serial dilutions of PCT in the presence of a fix concentration of 10 (group 2) or 30 (group 3) μM of $\mathbf{6_{NP}}$ or $\mathbf{7_{NP}}$. Nanoassemblies were added to the wells directly from their aqueous solution so that they were diluted with medium only, and no DMSO was present in any of the wells. Dose-response curves with respect to PCT were calculated by nonlinear regression using the log inhibitor vs. normalized response model of GraphPad Prism 5 software.

Evaluation of the Interaction Between Nanoassemblies 6_{NP} or 7_{NP} and Doxorubicin on $L5178_{MDR}$ Cells

Aqueous nanosuspensions (4 mM) of 6_{NP} or 7_{NP} were incubated in 6-times their volume of horse serum (Sigma-Aldrich) for 24 h at 37°C, 5% CO_2, and the resulting mixture was used as the treatment sample. Treatment groups were as follows: serial dilutions of Dox (group 1), and serial dilutions of Dox in the presence of a fix concentration of 37.5 (group 2), 75 (group 3) or 150 (group 4) μM of $\mathbf{6_{NP}}$ or $\mathbf{7_{NP}}$. Due to the amount of horse serum added to each well in group 3, all wells including cell and solvent controls were substituted with 22.5% of horse serum that did not cause any observable change in the cell growth as compared with the cell control containing 10% of horse serum supplement. In this test, no DMSO was added to any of the wells. Cell viability was evaluated by MTT as described above, and dose-response curves with respect to Dox were calculated by nonlinear regression using the log inhibitor vs. normalized response model of GraphPad Prism 5 software.

RESULTS AND DISCUSSION

Organic Synthesis

We have previously found that sidechain-cleaved ecdysteroid acetonides may act as similarly potent adjuvant antitumor agents as diacetonides of their parent compounds, but without any direct inhibitory activity on the ABCB1 (also referred to as P-glycoprotein or P-gp) efflux transporter (Hunyadi et al., 2017). To further explore this, our work aiming to prepare 11-squalenoylated ecdysteroids

was initiated in two directions: first, we prepared 11α-hydroxypoststerone (**2**) from ajugasterone C (**1**) by oxidative sidechain cleavage using (diacetoxyiodo)benzene (PIDA), a hypervalent iodine(III) reagent that we previously reported to be efficient and selective for this transformation (Issaadi et al., 2019). Compound **2** was obtained in a good yield (74.8%). Both compounds **1** and **2** were then subjected to further transformations as presented in **Scheme 1**.

Previously, we found that dioxolane substitution of ecdysteroids on the vicinal diols, and particularly on the 2,3-diol, is prerequisite of a potent chemo-sensitizing effect (Martins et al., 2013). Therefore, compounds **1** and **2** were converted to their corresponding 2,3;20,22-diacetonide (**3**) or 2,3-acetonide (**4**) analog by phosphomolybdic acid (Martins et al., 2012), which afforded us both derivatives in relatively good yields (**Scheme 1**). These compounds were of particular interest for our study due to their presumed adjuvant antitumor properties, and due to the sterically not hindered 11α-OH group on their structure allowing a convenient coupling of a squalene-derived lipophilic moiety through esterification, and therefore providing a good opportunity for preparing their self-assembling bioconjugate prodrugs.

Since the self-assembly inducer squalene is devoid of a suitable chemical function for the linkage of a drug, its synthetic modification is necessary prior to the coupling (Desmaele et al., 2012). Therefore, we prepared compound **5** following previously published strategies, by first transforming squalene to 1,1′,2-trisnorsqualene alcohol (Maksimenko et al., 2014). Then we conjugated the terminal hydroxyl moiety of this alcohol with sebacic acid, serving as linker, to yield compound **5** whose carboxylic moiety was required for the preparation of esters (Borrelli et al., 2014).

Our preliminary small-scale reactions indicated that the condensation of the inducer (**5**) with ecdysteroid substrates **3** or **4** is chemoselective for the secondary alcohol and allows the synthesis of bioconjugates coupled through the 11α-OH of the ajugasterone C analogs. Following scale-up and chromatographic purification, the conjugates were stored under argon atmosphere at –20°C to ensure their chemical stability until further utilization.

NMR Investigations

Squalenoylated compounds **6** and **7** were subjected to an in-depth study by high-resolution NMR that allowed us to achieve a complete signal assignment. Chemical structures and ^{1}H and ^{13}C NMR data for the steroid core of each compound are shown in **Figure 1** and **Tables 1** and **2**, respectively. NMR spectra and the complete signal assignment including that of the ester sidechain coupled at C-11 are presented in detail as **Supplementary Material, Figures S1–S6**.

Squalenoylation is a rapidly emerging strategy to prepare innovative novel nanoconjugates from various bioactive compounds (Arias et al., 2011; Desmaele et al., 2012; Borrelli et al., 2014; Maksimenko et al., 2014; Fumagalli et al., 2017a; Fumagalli et al., 2017b; Rouquette et al., 2019), therefore our NMR results may be applicable and useful to the description and purity evaluation of a wide range of such compounds. For example, in our case, the signal ratio of ca. 5 between the olefin protons of the sidechain (overlapping signals in the range of 5.10–5.16 ppm) and the H-7 (5.89 ppm) was a diagnostic measure of a complete coupling.

Preparation and Characterization of Self-Assembled NPs

Following structure elucidation, conjugates **6** and **7** were investigated for their ability to self-assemble to NPs in an aqueous medium. Accordingly, 4 mg/ml stock solutions of $\mathbf{6_{NP}}$ and $\mathbf{7_{NP}}$ were prepared through nanoprecipitation in ultrapure water. Characteristics of the NPs obtained are presented in **Figure 2**.

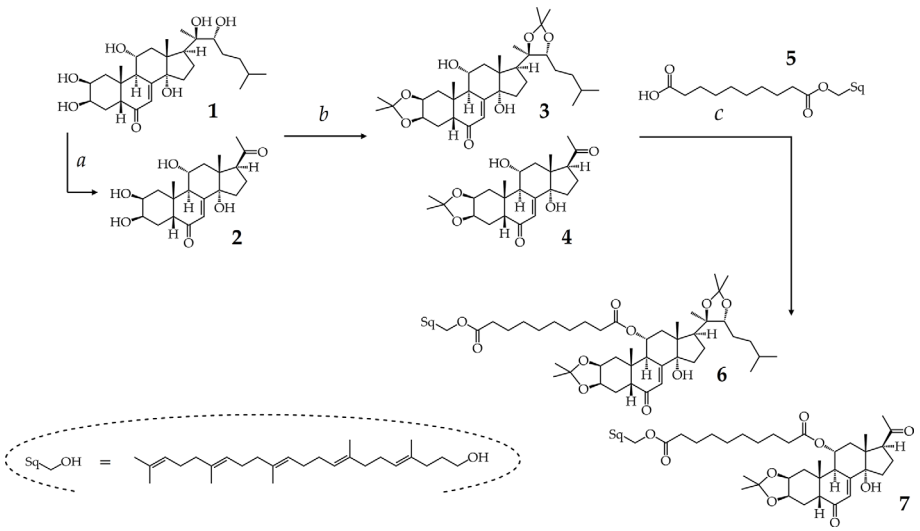

SCHEME 1 | Semi-synthesis of ajugasterone C analogs. Reaction conditions: (a) PIDA (1 equiv.), CH_3OH, RT, 1 h; (b) PMA hydrate, acetone, RT, 25 min; (c) cpd. 5: sebacic acid (1.25 equiv.), DMAP (2 equiv.), EDC·HCl (3 equiv.), RT, Ar, overnight.

The room temperature TEM results indicated that neither samples possessed rigid morphology under such experimental conditions. Both $\mathbf{6_{NP}}$ and $\mathbf{7_{NP}}$ had fluid, droplet-like structures (see **Supplementary Material, Figure S7**). The self-assembled droplets could mostly be located at fiber junctions where they could cover the fibers in a wetting manner. The particles assembled from compound **6** appeared similar in size to those of compound **7**, however, as the observed structure of the particles depended heavily on the carbon lace layout, further investigation was necessary.

Unfortunately, our TEM architecture was not suited for cryo imaging, therefore DLS measurements were performed in their place to get a more accurate picture on the size and dispersity, furthermore the colloidal stability of the nanoparticles. The liquid media allowed the observation of these features in a way that is more representative of *in vitro* characteristics. Aliquots of the nanosuspensions were further diluted with water in order to prepare samples for the evaluation of particle size, represented as PSDs by scattered light intensity (**Figure 2A**) and particle number (**Figure 2B**), furthermore for the investigation of the values of Z-Average, PdI, and zeta potential (**Figure 2C**). The Intensity and Number PSD results were in good agreement with one-another for both samples, with slightly shifted mean values that can be explained by the differences between the two representations (Bhattacharjee, 2016). Based on the number distributions, the mean primer particle diameter of $\mathbf{6_{NP}}$ was around 200 nm, while $\mathbf{7_{NP}}$ comprised from particles of around 145 nm. The average hydrodynamic diameters of the samples were 239.7 and 187.9 nm respectively. These results verified the TEM–based observations, as both samples were in comparable size distributions, although $\mathbf{7_{NP}}$ particles were somewhat smaller. The polydispersity index of the samples was quite low (<0.15) indicating that both samples were highly monodispersed. The zeta absolute value of both $\mathbf{6_{NP}}$ and $\mathbf{7_{NP}}$ were well above the theoretical threshold of ±30 mV, therefore their long-term colloidal stability was verified. Additionally, electric repulsion between $\mathbf{6_{NP}}$ particles appeared to be slightly larger than between $\mathbf{7_{NP}}$ particles, although $\mathbf{6_{NP}}$ particles proved larger than the $\mathbf{7_{NP}}$ ones.

The chemical/biological stability of the nanoprecipitated particles in the presence of horse serum was also investigated by DLS. This was to estimate the rate of compounds **6** and **7** getting dissolved into serum lipoproteins when $\mathbf{6_{NP}}$ and $\mathbf{7_{NP}}$ are placed into a lipoprotein-rich medium, so that we can conduct our *in vitro* bioactivity studies on these nanoassemblies in conditions closer to the situation *in vivo* (see section *Interactions of Nanoassemblies* $\mathbf{6_{NP}}$ *and* $\mathbf{7_{NP}}$ *With Chemotherapeutics*). To this, a 72-h longitudinal study was performed, throughout which the nanoparticle samples were incubated in horse serum (cell culture supplement in the subsequent *in vitro* studies on $L5178_{MDR}$ cells) with 1:6 volume ratios. At the 0-, 24-, 48-, and 72-h marks, small aliquots were collected from the incubating mixtures and DLS measurements were performed on appropriately diluted (150 ppm for nanoparticles) aqueous dispersions.

Both $\mathbf{6_{NP}}$ and $\mathbf{7_{NP}}$ demonstrated similar behavior according to the results provided by the stability measurements. **Figure 3A** shows the average hydrodynamic diameter of the as–prepared samples, and their size decrease as the function of time due to the presence of horse serum. The Z–average of $\mathbf{6_{NP}}$ particles decreased from 240 nm to 166 nm which is roughly a 31% decrease in radius, while $\mathbf{7_{NP}}$ went down from 188 nm to 152 nm, resulting in a 19% radius decrease. The decomposition of the self–assembled particles happened during the first day of the experiments, after which the particle diameters stabilized, most likely due to the depletion of available macromolecules in the system, which could facilitate particle decomposition. The changes in zeta potential values in **Figure 3B** supported the pervious results. The horizontal lines in the graphs represent the zeta potentials of clean horse medium and the original nanoparticles respectively. While the results did not vary substantially throughout the experiments, a change from 0 to 24 h can be observed in both cases here as well. The initial values corresponding to the 0 h experiments were quite close to the zeta potential of the serum, while the later experiments yielded

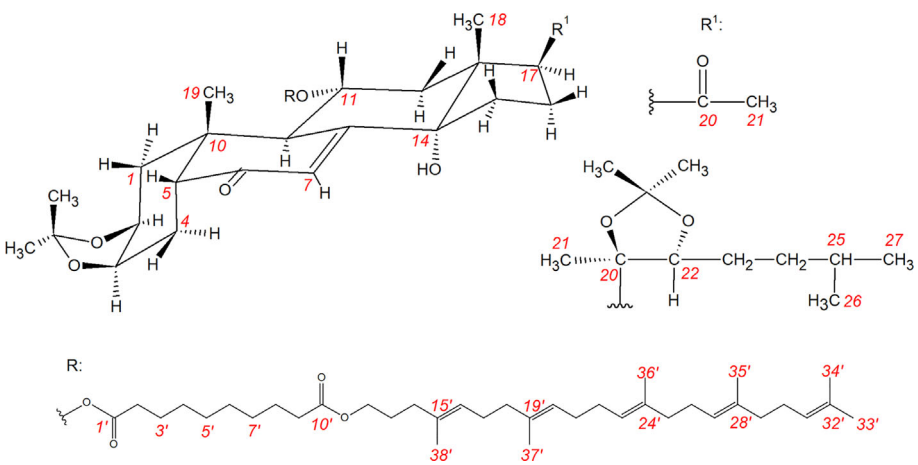

FIGURE 1 | Chemical structures of compounds **6** and **7** and their atomic numbering.

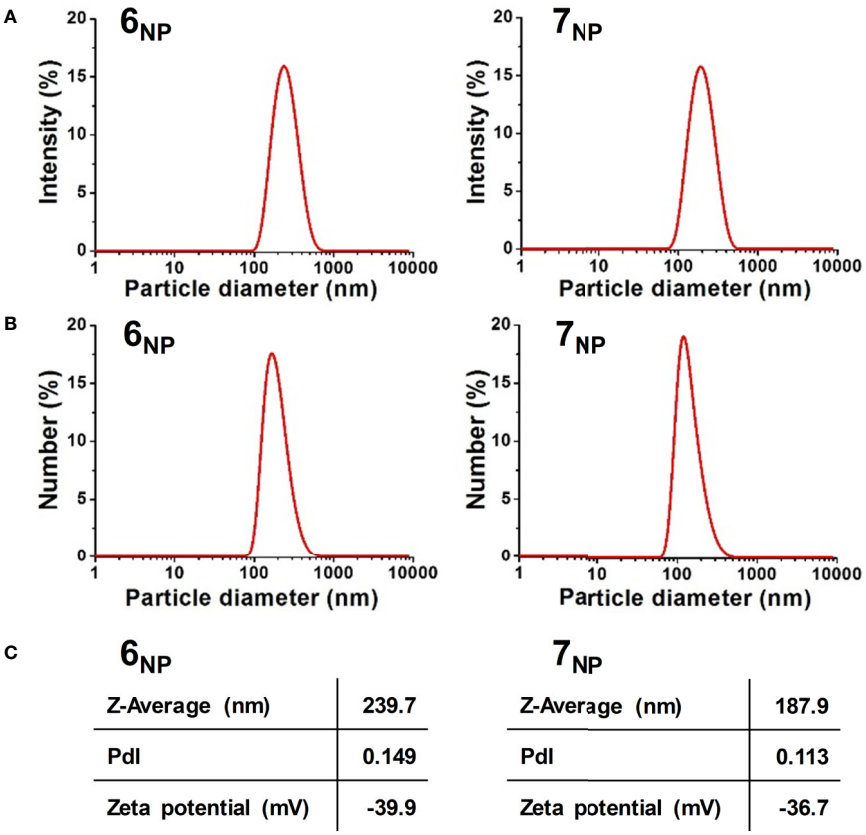

FIGURE 2 | Intensity **(A)** and Number **(B)** particle size distribution graphs, and average hydrodynamic diameter, polydispersity index, and zeta potential values **(C)** of $\mathbf{6_{NP}}$ (left) and $\mathbf{7_{NP}}$ (right).

slightly more negative results, underlining the internal changes within the system.

While hydrodynamic diameter should not be confused with primer article diameter, some assumptions could be made regarding the release of compounds **6** and **7** from their corresponding nanoassemblies. Due to the relatively low standard deviation of the sample sizes, it can be speculated that the decrease in hydrodynamic diameter is proportional to the decrease of primer particle size as well, therefore the radius decreases of 31% and 19% for $\mathbf{6_{NP}}$ and $\mathbf{7_{NP}}$ respectively could be translated into mass, using the expressions of sphere volume (Equation 1) and density (Equation 2). Approximating the self–assembled nanoparticles as ideal spheres with uniform density, and substituting the volume expression into the equation of density (Equation 3), particle radius is directly proportional to the cube root of particle mass (Equation 4):

$$V_{sphere} = \frac{4}{3}\pi r^3 \quad (1) \quad \rho = \frac{m}{V} \quad (2)$$

$$m = \frac{4}{3}\pi r^3 \rho \quad (3) \quad m \propto r^3 \quad (4)$$

$$\mathbf{6}_{NP}: \quad \sqrt[3]{0,31} \approx 68\,\% \quad (5)$$

$$\mathbf{7}_{NP}: \quad \sqrt[3]{0,19} \approx 58\,\% \quad (6)$$

After converting the numbers, $\mathbf{6_{NP}}$ is predicted to release around 68% of its compound **6** contents, while $\mathbf{7_{NP}}$ potentially releases 58% of compound **7** from the self–assembled nanostructures due to the presence of horse serum. Naturally, these numbers are loose estimates at best, however, they could serve as indicators regarding the biological activity of the prepared nanoassemblies.

Interaction of Compounds 3 and 4 With Chemotherapeutics

Compounds **3** and **4**, parent compounds to **6** and **7**, respectively, were tested on the chemoresistance of five cancer cell lines including a susceptible/resistant cell line pair modeling ABCB1 efflux-mediated multi-drug resistance.

First, efflux pump inhibitory activity of the compounds was assessed. To this, multi-drug resistant $L5134_{MDR}$ mouse lymphoma cells were used, that are transfected to express the human ABCB1 transporter (Pastan et al., 1988). The rhodamine 123 accumulation assay indicated a weak efflux inhibition by compound **3** (inactive at 2 μM, 27.4 ± 1.9% inhibition at 20μM), while compound **4** was inactive (<5% inhibition) at up to 20 μM.

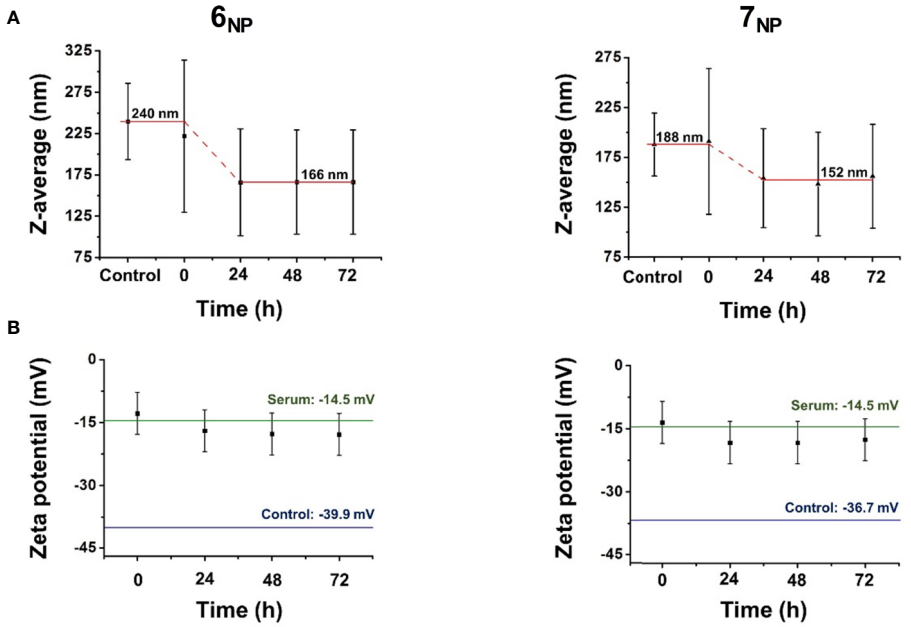

FIGURE 3 | Stability measurements of the self–assembled nanoparticles $\mathbf{6_{NP}}$ and $\mathbf{7_{NP}}$ in horse serum as a function of time according to average hydrodynamic diameter **(A)** and zeta potential **(B)** changes using dynamic light scattering.

This finding was coherent with our previous results on ecdysteroid 2,3;20,22-diacetonides and their sidechain cleaved analogs, namely that removal of the sidechain eliminates efflux pump inhibitory activity (Hunyadi et al., 2017).

Subsequently, the compounds were evaluated on $L5134_{MDR}$ cells for their interaction with doxorubicin, and on MCF-7 and MDA-MB-231 breast cancer cells for their interaction with doxorubicin and paclitaxel. The checkerboard microplate method was used, and the results were evaluated by the Chou-Talalay method (Chou, 2006) as shown in **Table 3**.

As we expected based on our previous results (Martins et al., 2012), compound **3** exerted strong synergism with doxorubicin on the MDR mouse lymphoma cell line. Somewhat surprisingly, however, compound **3** did not show synergism with doxorubicin on MCF-7 or MDA-MB-231 cells, and it even moderately antagonized the effect of paclitaxel on both breast cancer cell lines. Previously we found that 20-hydroxyecdysone 2,3;20,22-diacetonide (20DA) could decrease cytotoxicity of cisplatin on MCF-7 cells but increased the effect of paclitaxel on the same cell line. This suggests that the additional 11α-OH group and/or the missing 25-OH group (compound **4** vs. 20DA) plays a more important and complex role in the structure-activity relationships than previously thought.

As for compound **4** combined with doxorubicin, no synergism was found on the MDR mouse lymphoma or the MCF-7 cells, but a moderate synergism (CI_{avg} 0.7–0.85) was observed on the triple-negative MDA-MB-231 cell line. Several doxorubicin-containing neoadjuvant chemotherapeutic strategies have shown promise in clinical studies on triple-negative breast cancer (TNBC) (Park et al., 2018; Bergin and Loi, 2019). While the activity of compound **4** is rather weak in this regard, mainly when comparing with that of compound **3** on the MDR lymphoma cell line, it may still be of interest to initiate further studies on ecdysteroid derivatives in combination with doxorubicin on various TNBC models.

It was a most unexpected outcome of our study that compound **4** acted in strong antagonism (CI_{avg}>3.3) with paclitaxel, in other words, that it exerted a potent cytoprotective effect against this chemotherapeutic agent on MCF-7 cells. While this makes this compound and, supposedly, its pro-drugs including 7_{NP} completely unsuitable as an adjuvant anticancer agent, it may suggest its possible cytoprotective effect against other stressors.

At this time, it is hard to point out the exact mechanism of action for the above-detailed effects of compounds **3** and **4** on the studied cancer cell lines. The interaction of compound **3** with doxorubicin is clearly connected somehow to the upregulated ABCB1, since it was much weaker on the L5178 cells than on the $L5178_{MDR}$ cells. Further, similarly to our previous results on ecdysteroid 2,3-acetonides, we found that a synergistic interaction does not require that the ecdysteroid acts as a potent efflux inhibitor. It is worth mentioning, however, that the rhodamine123 accumulation is a rapid assay with a 20 min incubation that was designed to assess functional inhibition of the transporter. Therefore, it does not give any information about what happens during the 72 h–long incubation period on the checkerboard plates. To evaluate this, it would be important to conduct further studies on ecdysteroid 2,3-acetonides concerning their potential to interfere with the expression of the pump.

Nevertheless, while the synergistic activity of ecdysteroid acetonides at least with doxorubicin appears to be strongly amplified by upregulated ABCB1, this interaction could also be

TABLE 3 | Interaction of compounds **3** and **4** with chemotherapeutics on cancer cell lines at 50%, 75%, and 90% of growth inhibition (ED_{50}, ED_{75}, and ED_{90}, respectively).

Compounds		Drug	CI at						
combined	Cell line	ratio[a]	ED_{50}	ED_{75}	ED_{90}	Dm	m	r	CI_{avg}
3 + Dox	$L5178_{MDR}$	11.6:1	0.09	0.10	0.12	0.71	1.524	0.962	0.11
		23.2:1	0.10	0.13	0.15	1.31	1.470	0.968	0.14
		46.4:1	0.13	0.17	0.23	2.25	1.360	0.979	0.19
3 + Dox	L5178	75:1	0.40	0.51	0.67	6.97	0.809	0.847	0.57
		150:1	0.88	0.63	0.44	25.27	1.438	0.916	0.58
		300:1	1.22	1.17	1.11	50.82	1.024	0.946	1.15
3 + Dox	MCF-7	100:1	1.26	0.82	0.60	10.5	2.468	0.942	0.78
		200:1	1.12	1.06	1.16	15.6	1.545	0.995	1.12
		400:1	1.21	1.06	1.07	25.3	2.146	0.998	1.09
3 + PCT	MCF-7	7,143:1	1.21	1.34	1.59	16.5	1.545	0.967	1.44
		14,285:1	1.27	1.22	1.25	26.5	2.284	0.999	1.24
		28,571:1	1.10	1.00	0.96	31.3	3.206	0.992	1.00
3 + Dox	MDA-MB-231	100:1	1.43	1.01	1.01	12.8	1.534	0.940	1.08
		200:1	1.09	0.78	0.78	16.9	2.062	0.948	0.83
		400:1	1.10	0.87	0.93	26.5	2.506	0.910	0.94
3 + PCT	MDA-MB-231	1,667:1	1.71	1.15	1.48	17.4	1.265	0.990	1.41
		3,333:1	1.48	1.40	2.28	24.9	1.180	0.988	1.85
		6,667:1	1.31	1.48	2.48	32.9	1.295	0.987	1.95
4 + Dox	$L5178_{MDR}$	11.6:1	1.20	0.93	0.72	6.64	1.727	0.991	0.87
		23.2:1	1.09	0.88	0.72	10.9	1.688	0.995	0.83
		46.4:1	1.17	0.93	0.75	19.74	1.822	0.996	0.88
4 + Dox	L5178	75:1	1.80	1.97	2.17	20.97	2.159	0.964	2.04
		150:1	2.12	2.41	2.80	44.87	1.895	0.977	2.56
		300:1	1.69	2.52	3.84	60.94	1.239	0.923	3.04
4 + Dox	MCF-7	100:1	1.41	1.45	1.51	9.40	1.426	0.976	1.47
		200:1	1.28	1.07	0.89	16.8	1.958	0.966	1.02
		400:1	1.48	1.67	1.91	37.0	1.246	0.995	1.76
4 + PCT	MCF-7	7,143:1	2.78	3.08	3.41	21.2	1.608	0.972	3.19
		14,285:1	2.92	3.25	3.61	43.2	1.591	0.954	3.37
		28,571:1	2.38	3.08	3.98	66.9	1.303	0.998	3.41
4 + Dox	MDA-MB-231	100:1	0.58	0.62	0.78	7.9	1.004	0.996	0.69
		200:1	0.64	0.69	0.92	15.8	1.101	0.992	0.80
		400:1	0.66	0.71	0.94	27.1	1.302	0.976	0.81
4 + PCT	MDA-MB-231	1,667:1	1.74	1.52	1.33	4.730	1.514	0.997	1.46
		3,333:1	1.58	1.10	0.77	8.536	2.165	1.000	1.02
		6,667:1	1.25	1.29	1.34	13.326	1.214	0.973	1.31

CI, combination index; CI_{avg}, weighted average CI value; $CI_{avg} = (CI_{50} + 2CI_{75} + 3CI_{90})/6$. CI < 1, CI = 1, and CI > 1 represent synergism, additivity, and antagonism, respectively. Dm, m, and r represent antilog of the x-intercept, slope, and linear correlation coefficient of the median-effect plot, respectively. Dox, doxorubicin; PCT, paclitaxel. Strongest interactions observed are highlighted as red (synergism) or blue (antagonism).

[a]*Drug ratios represent molar ratios in each case.*

observed at certain drug-drug ratios on the non-MDR mouse lymphoma, suggesting that ABCB1 overexpression is not a prerequisite for this bioactivity. This fits well with our previous results on other ecdysteroid derivatives that very strongly hypersensitized the non-MDR SH-SY5Y neuroblastoma cell line to vincristine (Müller et al., 2017). As in our previous studies, here we also observed the trend that the strength of interaction depends on the ecdysteroid-chemotherapeutic ratio, and it seems to have a "best ratio" where the interaction is the most significant. It may be of interest in this regard that we recently found 20-hydroxyecdysone (20E; structural isomer of compound **1**, differing in the position of one hydroxyl group) and poststerone (11-deoxy analog of compound **2**) to act on protein kinase B (Akt) with a bell-shaped dose-response curve (Issaadi et al., 2019). Ecdysteroids can modulate Akt phosphorylation in a Ca^{2+}-dependent manner (Gorelick-Feldman et al., 2010), and while this was first observed for 20E as an activation, some ecdysteroids may also act as inhibitors (Csábi et al., 2015). Considering the central role of Akt in cell death and survival (Song et al., 2019), one may hypothesize that it should somehow be involved in the chemoresistance altering activity of ecdysteroids. Unfortunately, at this point we have no information about how ecdysteroid acetonides influence this pathway.

Interactions of Nanoassemblies 6_{NP} and 7_{NP} With Chemotherapeutics

To evaluate what relevance the above findings with compounds **3** and **4** may have concerning the bioactivity of their prodrug nanoassemblies ($\mathbf{6_{NP}}$ and $\mathbf{7_{NP}}$, respectively), we focused

subsequent efforts to the two most significant interactions mentioned above. Therefore, we tested $\mathbf{6_{NP}}$ and $\mathbf{7_{NP}}$ in combination with PCT on MCF-7 cells, and in combination with doxorubicin on the $L5178_{MDR}$ cells. First, we tested the chemoresistance modulating activity of $\mathbf{6_{NP}}$ and $\mathbf{7_{NP}}$ by simply adding their aqueous nanosuspensions to the cells. Since neither nanosuspension exerted measurable cytotoxicity on MCF-7 cells, the checkerboard setup could not be used in this case, therefore we selected two fix concentrations (10 and 30 μM) of $\mathbf{6_{NP}}$ and $\mathbf{7_{NP}}$ for testing their effect on the cytotoxicity of paclitaxel; the results are shown in **Figure 4A**. Concerning the MDR mouse lymphoma, cytotoxicity for $\mathbf{6_{NP}}$ was very low but measurable, therefore we first tested it by the checkerboard setup. To our surprise, the interaction with doxorubicin measured this way gave CI_{avg} values in the range of 1.24–1.51 that represents moderate or even stronger antagonism instead of the expected synergism. Considering that this experimental setup might be rather different from the *in vivo* situation where the nanoparticles should get dissolved into serum lipoproteins as individual pro-drug molecules, we then tried to re-evaluate the combination treatment in a possibly more relevant new experiment. To this, horse serum (that is the supplement used for the mouse lymphoma cells) was first added to the nanoparticles in a 6:1 ratio, the mixture was incubated for 24 h (that was the plateau of the decrease in NP size, see section *Preparation and Characterization of Self-Assembled NPs*), and this was then further tested on the doxorubicin resistance of $L5178_{MDR}$ cells. Again, the checkerboard setup was ruled out due to the non-measurable cytotoxicity of the horse serum-pretreated $\mathbf{6_{NP}}$ and $\mathbf{7_{NP}}$, therefore fix concentrations of these were tested; results are shown in **Figure 4B**.

It is clear from our results that both $\mathbf{6_{NP}}$ and $\mathbf{7_{NP}}$, similarly to their corresponding parent compounds **3** and **4**, significantly protected the MCF-7 cells from the cytotoxic effect of paclitaxel. Further, the relative potency of the two nanoassemblies seems to correlate with that of compounds **3** and **4** (i.e. 4 > 3 and $\mathbf{7_{NP}} > \mathbf{6_{NP}}$), which would support the assumption that the nanoparticles indeed worked as prodrugs of the 11α-hydroxylated parent ecdysteroids 3 and 4. On the MDR mouse lymphoma cell line, however, a surprising opposite effect was observed for 3 and $\mathbf{6_{NP}}$: in contrast with the strong synergism between compound **3** and doxorubicin, $\mathbf{6_{NP}}$ significantly decreased the efficacy of the Dox, regardless of the fact that a large fraction of $\mathbf{6_{NP}}$ were pre-dissolved in horse serum to liberate compound **6** in its free form (see **Figure 3** and eq. 5 and 6). Therefore, this nanoassembly cannot deliver compound **3** into $L5178_{MDR}$ cells as a prodrug. A very likely explanation to this is connected to the endocytosis of lipoproteins (Zanoni et al., 2018) in which the squalenoylated prodrug is dissolved. Because of this, the prodrug ends up in the acidic (pH ca. 4.5) environment of lysosomes (Hu et al., 2015). This may already be enough to cleave the acid sensitive 2,3-acetonide group (Martins et al., 2012) that is of major importance to a strong chemosensitizing effect of ecdysteroids (Martins et al., 2013). Therefore, it appears that instead of the adjuvant antitumor ecdysteroid diacetonide **3**, the 20,22-monoacetonide, or, to some extent, even the parent compound ajugasterone C (**1**) gets eventually released from compound **6** after treatment by 6_{NP}. Similarly, this should also be happening with $\mathbf{7_{NP}}$ that, after internalization, likely releases compound **2** instead of 4. It is not without precedence that an ecdysteroid and its diacetonide derivative act in an opposite way on the chemoresistance of tumor cells: we previously found 20-hydroxyecdysone (20E) to act in antagonism with doxorubicin on $L5178_{MDR}$ cells, in contrast with the strong synergism observed for 20E 2,3;20,22-diacetonide (Martins et al., 2012).

The above findings have two major implications. First, the strategy of using squalenoylated ecdysteroid nanoparticles as

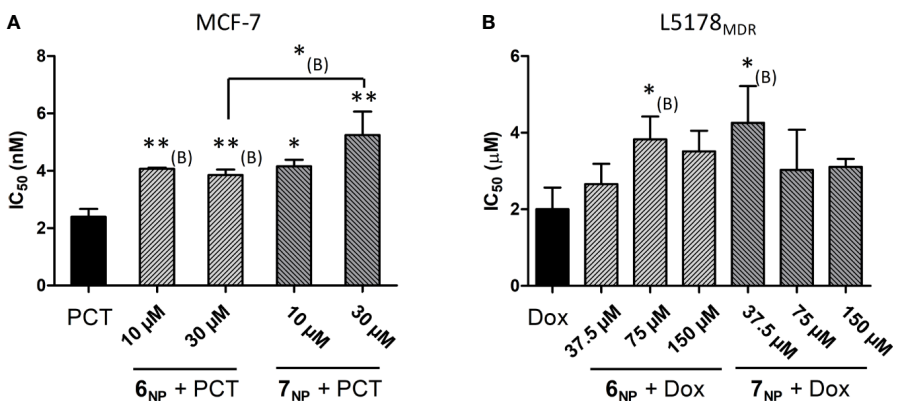

FIGURE 4 | Interaction of $\mathbf{6_{NP}}$ and $\mathbf{7_{NP}}$ with paclitaxel on MCF-7 **(A)** and with doxorubicin on $L5178_{MDR}$ cells **(B)**. The bars show the IC_{50} values of the chemotherapeutic agent with or without the presence of a given fix concentration of $\mathbf{6_{NP}}$ or $\mathbf{7_{NP}}$, error bars show SEM. For the results shown in **(B)**, the nanosuspensions were preincubated with 6x volume of horse serum for 24 h. * and **: $p < 0.05$, and $p < 0.01$, respectively, by one-way ANOVA followed by Dunnett's post-hoc test as compared with the single treatment; $*_{(B)}$ and $**_{(B)}$: $p < 0.05$, and $p < 0.01$, respectively, by one-way ANOVA followed by planned comparisons with the single treatment or with the specified other combination by Bonferroni's post-hoc test.

adjuvant antitumor agents appears to make it a must to replace the 2,3-acetonide moiety with an acid-resistant alternative. Our current results also suggest that our previous success in using this strategy (Fumagalli et al., 2018) may have been connected to the release of 20E 20,22-monoacetonide that is less potent than the diacetonide but still active in decreasing tumor resistance (Martins et al., 2012). If it is indeed the case, that would mean that with an appropriate acid-resistant 2,3-substituent the previously observed antitumor action could be further improved.

Second, while the cytoprotective nature of the herein reported squalenoylated ecdysteroid acetonide nanoparticles makes them certainly not useful against cancer, it points towards a possible new strategy to deliver adaptogen ecdysteroids to target tissues with an aim to increase stress resistance. Above cancer, LDL-R is upregulated in some healthy tissues and organs; a most obvious example for this is the liver (van de Sluis et al., 2017) but LDL-R also plays an important role in the blood-brain barrier (BBB) (Dehouck et al., 1994) and can be exploited for facilitating transport across the BBB (Molino et al., 2017). As such, squalene conjugation offers a means of targeting in many problematic pathologies other than cancer. Therefore, the observed activity of compounds **4**, $\mathbf{6_{NP}}$, and $\mathbf{7_{NP}}$ suggests further studies on relevant, preferably *in vivo* pharmacological models to critically evaluate any possible therapeutic potential of the current findings.

CONCLUSIONS

In this work, two new squalenoylated ecdysteroid pro-drugs were prepared, fully characterized, and formulated to self-assembling nanoparticles. In both cases, the successful submicron assembly of compounds **6** (derived from compound **3**) and **7** (from compound **4**) was achieved into $\mathbf{6_{NP}}$ and $\mathbf{7_{NP}}$ respectively. Both $\mathbf{6_{NP}}$ and $\mathbf{7_{NP}}$ formed monodispersed and stable suspensions consisting of fluid, droplet–like particles in a similar size range. Based on DLS results, $\mathbf{6_{NP}}$ is expected to possess slightly greater colloidal stability, although the *in vivo* behavior of the compounds might vary substantially and requires further investigation. The employed functionalization of the ecdysteroids **3** and **4** allows their targeting to tissues containing high levels of LDL-receptor. Compound **3** strongly potentiated the antitumor action of doxorubicin on an MDR lymphoma cell line, while compound **4** was a potent cytoprotective agent strongly antagonizing the effect of paclitaxel on MCF–7 cells. Surprisingly, however, both nanoassemblies $\mathbf{6_{NP}}$ and $\mathbf{7_{NP}}$ antagonized the chemotherapeutic agents' effect on the studied cancer cell lines. This happens most likely due to the effect of lysosomes resulting in the acid-catalyzed release of the 20,22-monoacetonide and/or the non-substituted form of compound **1** and compound **2** from $\mathbf{6_{NP}}$ and $\mathbf{7_{NP}}$, respectively. We may conclude that i) exploiting the adjuvant antitumor action of squalenoylated ecdysteroid nanoassemblies requires the design and synthesis of appropriate acid-resistant 2,3-substituents instead of the acetonide group, and ii) the herein reported nanoparticles have no antitumor potential but they might be promising cytoprotective agents targeting LDL-R upregulated tissues such as for example the liver or the blood-brain barrier.

DATA AVAILABILITY STATEMENT

The raw data supporting the conclusions of this article will be made available by the authors, without undue reservation, to any qualified researcher.

AUTHOR CONTRIBUTIONS

MV performed chemical synthesis and purification, prepared nano-assemblies, and wrote first draft of the manuscript. MV and PB characterized nanoparticles. DB, TG, and GT performed NMR spectroscopic studies, and analyzed and interpreted all related data. MN, GS, and AL performed studies on the mouse lymphoma cell lines and analyzed related data. AL performed studies on human gynecological cell lines and analyzed related data. IZ supervised studies on human gynecological cell lines. ZK supervised characterization of nanoparticles. AH conceptualized the study, supervised chemical part of the work, calculated combination indices, designed combination studies on the nanoparticles, and finalized the manuscript. All authors contributed to the article and approved the submitted version.

FUNDING

This work was funded by the National Research, Development and Innovation Office, Hungary (NKFIH; K119770), the Ministry of Human Capacities, Hungary grant 20391-3/2018/FEKUSTRAT, and the EU-funded Hungarian grant EFOP-3.6.1-16-2016-00008. MV was supported by the National Talent Program of the Ministry of Human Capacities, Hungary. Publication of the manuscript was supported by the University of Szeged Open Access Fund. The funders had no role in the design of the study; in the collection, analyses, or interpretation of data; in the writing of the manuscript, or in the decision to publish the results.

ACKNOWLEDGMENTS

The authors wish to acknowledge Daniele Passarella (Universitá degli Studi di Milano, Milan, Italy) for training MV to prepare squalenoylated nanoparticles, and Ana Martins (Biological Research Centre, Szeged, Hungary) for scientific discussion on the experimental setup for nanoparticles' bioactivity testing.

SUPPLEMENTARY MATERIAL

The Supplementary Material for this article can be found online at: https://www.frontiersin.org/articles/10.3389/fphar.2020.552088/full#supplementary-material

REFERENCES

Arias, J. L., Reddy, L. H., Othman, M., Gillet, B., Desmaële, D., Zouhiri, F., et al. (2011). Squalene Based Nanocomposites: A New Platform for the Design of Multifunctional Pharmaceutical Theragnostics. *ACS Nano* 5, 1513–1521. doi: 10.1021/nn1034197

Bergin, A. R. T., and Loi, S. (2019). Triple-negative breast cancer: recent treatment advances. *F1000Res* 8. F1000 Faculty Rev-1342. doi: 10.12688/f1000research.18888.1

Bhattacharjee, S. (2016). DLS and zeta potential – What they are and what they are not? *J. Controlled Release* 235, 337–351. doi: 10.1016/j.jconrel.2016.06.017

Bildstein, L., Dubernet, C., and Couvreur, P. (2011). Prodrug-based intracellular delivery of anticancer agents. *Adv. Drug Delivery Rev.* 63, 3–23. doi: 10.1016/j.addr.2010.12.005

Bogdan, D., Haessner, R., Vagvolgyi, M., Passarella, D., Hunyadi, A., Gati, T., et al. (2018). Stereochemistry and complete (1) H and (13) C NMR signal assignment of C-20-oxime derivatives of posterone 2,3-acetonide in solution state. *Magn. Reson. Chem.* 56, 859–866. doi: 10.1002/mrc.4750

Borrelli, S., Christodoulou, M. S., Ficarra, I., Silvani, A., Cappelletti, G., Cartelli, D., et al. (2014). New class of squalene-based releasable nanoassemblies of paclitaxel, podophyllotoxin, camptothecin and epothilone A. *Eur. J. Med. Chem.* 85, 179–190. doi: 10.1016/j.ejmech.2014.07.035

Cheetham, A. G., Chakroun, R. W., Ma, W., and Cui, H. (2017). Self-assembling prodrugs. *Chem. Soc. Rev.* 46, 6638–6663. doi: 10.1039/C7CS00521K

Chou, T. C. (2006). Theoretical basis, experimental design, and computerized simulation of synergism and antagonism in drug combination studies. *Pharmacol. Rev.* 58, 621–681. doi: 10.1124/pr.58.3.10

Csábi, J., Hsieh, T.-J., Hasanpour, F., Martins, A., Kele, Z., Gáti, T., et al. (2015). Oxidized Metabolites of 20-Hydroxyecdysone and Their Activity on Skeletal Muscle Cells: Preparation of a Pair of Desmotropes with Opposite Bioactivities. *J. Natural Prod.* 78, 2339–2345. doi: 10.1021/acs.jnatprod.5b00249

Dehouck, B., Dehouck, M. P., Fruchart, J. C., and Cecchelli, R. (1994). Upregulation of the low density lipoprotein receptor at the blood-brain barrier: intercommunications between brain capillary endothelial cells and astrocytes. *J. Cell Biol.* 126, 465–473. doi: 10.1083/jcb.126.2.465

Delplace, V., Couvreur, P., and Nicolas, J. (2014). Recent trends in the design of anticancer polymer prodrug nanocarriers. *Polym. Chem.* 5, 1529–1544. doi: 10.1039/C3PY01384G

Desmaele, D., Gref, R., and Couvreur, P. (2012). Squalenoylation: a generic platform for nanoparticular drug delivery. *J. Control Release* 161, 609–618. doi: 10.1016/j.jconrel.2011.07.038

Dinan, L., Mamadalieva, N. Z., and Lafont, R. (2020). "Dietary Phytoecdysteroids", in *Handbook of Dietary Phytochemicals*. Eds. J. Xiao, S. D. Sarker and Y. Asakawa (Singapore: Springer), 1–54. doi: 10.1007/978-981-13-1745-3_35-1

Duddeck, H., Dietrich, W., and Tóth, G. (1998). Structure Elucidation by Modern NMR. (Steinkopff, Heidelberg). doi: 10.1007/978-3-642-88310-1

Fumagalli, G., Marucci, C., Christodoulou, M. S., Stella, B., Dosio, F., and Passarella, D. (2016). Self-assembly drug conjugates for anticancer treatment. *Drug Discov. Today* 21, 1321–1329. doi: 10.1016/j.drudis.2016.06.018

Fumagalli, G., Stella, B., Pastushenko, I., Ricci, F., Christodoulou, M. S., Damia, G., et al. (2017a). Heteronanoparticles by self-Assembly of Doxorubicin and Cyclopamine Conjugates. *ACS Med. Chem. Lett.* 8, 953–957. doi: 10.1021/acsmedchemlett.7b00262

Fumagalli, G., Christodoulou, M. S., Riva, B., Revuelta, I., Marucci, C., Collico, V., et al. (2017b). Self-assembled 4-(1,2-diphenylbut-1-en-1-yl)aniline based nanoparticles: podophyllotoxin and aloin as building blocks. *Org. Biomol. Chem.* 15, 1106–1109. doi: 10.1039/C6OB02591A

Fumagalli, G., Giorgi, G., Vagvolgyi, M., Colombo, E., Christodoulou, M. S., Collico, V., et al. (2018). Heteronanoparticles by Self-Assembly of Ecdysteroid and Doxorubicin Conjugates to Overcome Cancer Resistance. *ACS Med. Chem. Lett.* 9, 468–471. doi: 10.1021/acsmedchemlett.8b00078

Gorelick-Feldman, J., Cohick, W., and Raskin, I. (2010). Ecdysteroids elicit a rapid Ca2+ flux leading to Akt activation and increased protein synthesis in skeletal muscle cells. *Steroids* 75, 632–637. doi: 10.1016/j.steroids.2010.03.008

Hu, Y.-B., Dammer, E. B., Ren, R.-J., and Wang, G. (2015). The endosomal-lysosomal system: from acidification and cargo sorting to neurodegeneration. *Transl. Neurodegener.* 4, 18–18. doi: 10.1186/s40035-015-0041-1

Hunyadi, A., Gergely, A., Simon, A., Toth, G., Veress, G., and Bathori, M. (2007). Preparative-scale chromatography of ecdysteroids of Serratula wolffli andrae. *J. Chromatogr. Sci.* 45, 76–86. doi: 10.1093/chromsci/45.2.76

Hunyadi, A., Csabi, J., Martins, A., Molnar, J., Balazs, A., and Toth, G. (2017). Backstabbing P-gp: Side-Chain Cleaved Ecdysteroid 2,3-Dioxolanes Hyper-Sensitize MDR Cancer Cells to Doxorubicin without Efflux Inhibition. *Molecules* 22, 199. doi: 10.3390/molecules22020199

Issaadi, H. M., Csábi, J., Hsieh, T.-J., Gáti, T., Tóth, G., and Hunyadi, A. (2019). Side-chain cleaved phytoecdysteroid metabolites as activators of protein kinase B. *Bioorg. Chem.* 82, 405–413. doi: 10.1016/j.bioorg.2018.10.049

Lafont, R., and Dinan, L. (2003). Practical uses for ecdysteroids in mammals including humans: an update. *J. Insect Sci.* 3, 7. doi: 10.1673/031.003.0701

Li, Z., Tan, S., Li, S., Shen, Q., and Wang, K. (2017). Cancer drug delivery in the nano era: An overview and perspectives (Review). *Oncol. Rep.* 38, 611–624. doi: 10.3892/or.2017.5718

Maksimenko, A., Dosio, F., Mougin, J., Ferrero, A., Wack, S., Reddy, L. H., et al. (2014). A unique squalenoylated and nonpegylated doxorubicin nanomedicine with systemic long-circulating properties and anticancer activity. *Proc. Natl. Acad. Sci. U. S. A.* 111, E217–E226. doi: 10.1073/pnas.1313459110

Martins, A., Toth, N., Vanyolos, A., Beni, Z., Zupko, I., Molnar, J., et al. (2012). Significant activity of ecdysteroids on the resistance to doxorubicin in mammalian cancer cells expressing the human ABCB1 transporter. *J. Med. Chem.* 55, 5034–5043. doi: 10.1021/jm300424n

Martins, A., Csabi, J., Balazs, A., Kitka, D., Amaral, L., Molnar, J., et al. (2013). Synthesis and structure-activity relationships of novel ecdysteroid dioxolanes as MDR modulators in cancer. *Molecules* 18, 15255–15275. doi: 10.3390/molecules181215255

Martins, A., Sipos, P., Der, K., Csabi, J., Miklos, W., Berger, W., et al. (2015). Ecdysteroids sensitize MDR and non-MDR cancer cell lines to doxorubicin, paclitaxel, and vincristine but tend to protect them from cisplatin. *BioMed. Res. Int.* 2015, 895360. doi: 10.1155/2015/895360

Molino, Y., David, M., Varini, K., Jabes, F., Gaudin, N., Fortoul, A., et al. (2017). Use of LDL receptor-targeting peptide vectors for in vitro and in vivo cargo transport across the blood-brain barrier. *FASEB J.* 31, 1807–1827. doi: 10.1096/fj.201600827R

Müller, J., Martins, A., Csábi, J., Fenyvesi, F., Könczöl, Á., Hunyadi, A., et al. (2017). BBB penetration-targeting physicochemical lead selection: Ecdysteroids as chemo-sensitizers against CNS tumors. *Eur. J. Pharm. Sci.* 96, 571–577. doi: 10.1016/j.ejps.2016.10.034

Park, J. H., Ahn, J.-H., and Kim, S.-B. (2018). How shall we treat early triple-negative breast cancer (TNBC): from the current standard to upcoming immuno-molecular strategies. *ESMO Open* 3, e000357. doi: 10.1136/esmoopen-2018-000357

Pastan, I., Gottesman, M. M., Ueda, K., Lovelace, E., Rutherford, A. V., and Willingham, M. C. (1988). A retrovirus carrying an MDR1 cDNA confers multidrug resistance and polarized expression of P-glycoprotein in MDCK cells. *Proc. Natl. Acad. Sci.* 85, 4486. doi: 10.1073/pnas.85.12.4486

Pretsch, E., Tóth, G., Munk, E. M., and Badertscher, M. (2002). *Computer-Aided Structure Elucidation* (Weinheim, Germany: Wiley-VCH).

Rouquette, M., Lepetre-Mouelhi, S., Dufrancais, O., Yang, X., Mougin, J., Pieters, G., et al. (2019). Squalene-Adenosine Nanoparticles: Ligands of Adenosine Receptors or Adenosine Prodrug? *J. Pharmacol. Exp. Ther.* 369, 144–151. doi: 10.1124/jpet.118.254961

Shi, J., Kantoff, P. W., Wooster, R., and Farokhzad, O. C. (2017). Cancer nanomedicine: progress, challenges and opportunities. *Nat. Rev. Cancer* 17, 20–37. doi: 10.1038/nrc.2016.108

Sobot, D., Mura, S., Yesylevskyy, S. O., Dalbin, L., Cayre, F., Bort, G., et al. (2017). Conjugation of squalene to gemcitabine as unique approach exploiting endogenous lipoproteins for drug delivery. *Nat. Commun.* 8, 15678. doi: 10.1038/ncomms15678

Song, M., Bode, A. M., Dong, Z., and Lee, M.-H. (2019). AKT as a Therapeutic Target for Cancer. *Cancer Res.* 79 (6), 1019–1031. doi: 10.1158/0008-5472.CAN-18-2738

van de Sluis, B., Wijers, M., and Herz, J. (2017). News on the molecular regulation and function of hepatic low-density lipoprotein receptor and LDLR-related protein 1. *Curr. Opin. Lipidol.* 28, 241–247. doi: 10.1097/MOL.0000000000000411

Xu, X., Ho, W., Zhang, X., Bertrand, N., and Farokhzad, O. (2015). Cancer nanomedicine: from targeted delivery to combination therapy. *Trends Mol. Med.* 21, 223–232. doi: 10.1016/j.molmed.2015.01.001

Zanoni, P., Velagapudi, S., Yalcinkaya, M., Rohrer, L., and von Eckardstein, A. (2018). Endocytosis of lipoproteins. *Atherosclerosis* 275, 273–295. doi: 10.1016/j.atherosclerosis.2018.06.881

Conflict of Interest: The authors declare that the research was conducted in the absence of any commercial or financial relationships that could be construed as a potential conflict of interest.

frontiers in Pharmacology

ORIGINAL RESEARCH
published: 15 September 2020
doi: 10.3389/fphar.2020.546439

Effects of Selected Nigerian Medicinal Plants on the Viability, Mobility, and Multidrug-Resistant Mechanisms in Liver, Colon, and Skin Cancer Cell Lines

Aljawharah AlQathama[1,2], Udoamaka F. Ezuruike[1], Andre L. D. A. Mazzari[1], Ahmed Yonbawi[1,3], Elisabetta Chieli[4] and Jose M. Prieto[1]*

[1] School of Pharmacy, University College London, London, United Kingdom, [2] Department of Pharmacognosy, Faculty of Pharmacy, Umm Al-Qura University, Makkah, Saudi Arabia, [3] Department of Natural Products and Alternative Medicine, Faculty of Pharmacy, King Abdulaziz University, Jeddah, Saudi Arabia, [4] Department of Translational Research and New Technologies in Medicine and Surgery, University of Pisa, Pisa, Italy

OPEN ACCESS

Edited by:
Patrícia Mendonça Rijo, CBIOS, Universidade Lusófona Research Center for Biosciences & Health Technologies, Portugal

Reviewed by:
Sayeed Ahmad, Jamia Hamdard University, India
Francis-Alfred Unuagbe Attah, University of Ilorin, Nigeria

***Correspondence:**
Aljawharah AlQathama
aaqathama@uqu.edu.sa

Specialty section:
This article was submitted to Ethnopharmacology, a section of the journal Frontiers in Pharmacology

Received: *28 March 2020*
Accepted: *26 August 2020*
Published: *15 September 2020*

Citation:
AlQathama A, Ezuruike UF, Mazzari ALDA, Yonbawi A, Chieli E and Prieto JM (2020) Effects of Selected Nigerian Medicinal Plants on the Viability, Mobility, and Multidrug-Resistant Mechanisms in Liver, Colon, and Skin Cancer Cell Lines. Front. Pharmacol. 11:546439. doi: 10.3389/fphar.2020.546439

Medicinal plants indicated for chronic diseases usually have good safety margins as they are intended for lifelong treatments. We hypothesized that they may provide patients with baseline protection to cancers and multidrug resistance-reversing phytochemicals resulting in successful prevention and/or adjuvant treatment of chemotherapy-resistant cancers. We selected 27 popular herbal infusions widely used in Nigeria for diabetes and studied their effects on a panel of liver (HepG2), colon (Caco2), and skin (B16-F10) cancer cells. Cytotoxicity was measured using the SRB staining assay. The 2D antimigratory effect was evaluated using an Oris™ platform. The P-glycoprotein (P-gp) efflux activity was evaluated using Rh-123 as a fluorescent probe. The inhibition of tyrosinase-mediated melanogenesis was evaluated by colorimetric enzymatic assays. Our results show that melanoma cell proliferation was strongly inhibited by *Anogeissus leiocarpus* (Combretaceae), *Bridelia ferruginea* (Phyllanthaceae), *D. ogea* (Leguminosae), and *Syzygium guineense* (Myrtaceae) extracts (GI_{50} = 50 µg/ml). *Alstonia boonei* (Apocynaceae), *Gongronema latifolium* (Asclepiadaceae), and *Strophanthus hispidus* (Apocynaceae) were preferentially toxic against Caco2 (GI_{50} = 50, 5 and 35 µg/ml, respectively). The most active extracts against different drug resistance mechanisms were *B. ferruginea* (inhibition of P-gp efflux, and impairing tyrosinase activity) and *X. americana* (inhibition of P-gp efflux). *A. leiocarpus, Kaya senegalensis* (Meliaceae), *S. guineense*, and *Terminalia avicennioides* (Combretaceae) significantly inhibited B16-F10 cell migration. Lupeol, ursolic acid, quercitrin, epicatechin, gallic acid, and ellagic acid were dereplicated by HPLC and HPTLC as their bioactive phytochemicals. In conclusion, the above in-vitro activities of herbal infusions regularly consumed by Nigerian diabetic patients may either act as a baseline chemoprotection or as sensitizing agents.

Keywords: cell viability, cell migration, multi drug resistance, tyrosinase, medicinal plants

INTRODUCTION

Natural products are both the base of traditional medicine and important sources of lead molecules in drug discovery (Thomford et al., 2018). One of the main global challenges to current cancer treatment is the emergence of multidrug resistance (MDR) to chemotherapeutic drugs, defined as acquired resistance to structurally and/or functionally unrelated drugs (Viale and Draetta, 2016). It is known that many herbal extracts (traditional medicines) act as chemosensitizers or resistance modulators (Tinoush et al., 2020). A key aspect of their activity is their ability to modulate multiple survival pathways with very low toxicity (Aung et al., 2017). Despite intense research, the choice of synthetic drugs against MDR is very limited (Dallavalle et al., 2020). The search for new natural product addressing this gap offers potential new avenues. Hence, our research groups is actively screening and testing for candidates from natural sources that can modulate the function, or expression, of disease-linked ABC transporters (Syed and Coumar, 2016).

The selected 27 plants in this work are widely used for diabetes and metabolic disorders in Nigeria, the most populated African country. Most of them are easily found in herbal markets all over the country for other primary indications including both common infective and non-communicable diseases Some of them have anecdotical records of use for the treatment of cancer without in-depth studies (Ezuruike and Prieto, 2014). These traditional medicines are consumed for years with apparently little toxicity and therefore may provide with a baseline defense against cancer, by killing or preventing tumor cells to acquire new hallmarks (Pan and Ho, 2008; Hodek et al., 2009). The real impact of cancer in Nigeria was largely unknown due to either a lack of statistics or under-reporting until the creation of the Nigerian National System of Cancer Registries in 2009 (The African Cancer Registry Network; Jedy-Agba et al., 2012). Emerging figures point out that more than 100,000 patients diagnosed with cancer and 70,000 deaths occur every year. These figures mean that about 1 in 10 Nigerians develop cancer before age 75 (International Agency for Research on Cancer).

In line with the topic of this special issue, we studied the cytotoxicity of the aqueous plant extracts (infusions) toward a panel of liver (HepG2), colon (Caco2) and skin (B16-F10) cancer cells as well as their effects upon selected mechanisms of drug resistance in cancer cells, namely, the efflux of xenobiotics by P-gp (Ozben, 2006), and the ability to inhibit tyrosinase-mediated melanogenesis and melanoma migration capacity (Pinon et al., 2011). Finally, we have proceeded to the identification of potential bioactive metabolites contributing to the effects of these plant extracts.

MATERIALS AND METHODS

Plant Material

Plant materials were either bought in markets or collected from different regions in Nigeria in November 2012 by one of the authors (U.F. Ezuruike). **Table 1** summarizes their botanical details and precedence. Identification of collected plant samples collected in the north was done by Mr. Ibrahim Muazzam, an ethnobotanist and staff of the Department of Medicinal Plant Research & Traditional Medicine, National Institute for Pharmaceutical Research & Development (NIPRD). Plant samples collected in the south were verified by staff of the Forestry Research Institute of Nigeria (FRIN) in Ibadan. Vouchers were deposited in the Department of Pharmaceutical and Biological Chemistry, University College London School of Pharmacy, United Kingdom. Voucher numbers are provided in **Supplementary materials**.

Plant Sample Preparation and Extraction

All plant samples were air-dried for about two weeks (average temperature 30°C) to remove as much moisture as possible to prevent deterioration. Samples were then packed in freezer bags and shipped to the School of Pharmacy, University College London. Upon arrival, they were further dried in a Samas Vickers® laboratory drying chamber electrically heated to 30°C with continuous ventilation. Samples were powdered using a laboratory scale mill (MF 10 Basic IKA WERKE blender) or an industrial size mill (Fritsch, Germany), depending on the part of the plant collected and the quantity of plant material.

The procedure for extraction of the plant samples (infusion or decoction) was based on the traditional use of the plants as described by the respondents (**Table 1**). For infusion, 300 ml of boiled distilled water was added to 10 g of plant material with continuous stirring for 15 min on a laboratory hot plate magnetic stirrer (IKA WERKE labortechnik electric stirrer). For decoction, 20 g of plant material was heated continuously under reflux in a round bottom flask containing 400 ml of distilled water for 1 h using an Electrothermal® 3-in-1 laboratory heating mantle. All extracted plant samples were then allowed to stand until cold before filtering with a Buchner flask. All the filtered extracts were frozen in round bottom flasks and then freeze dried (Edwards Pirani 50 L Savant super modulo freeze drier) to obtain the dried extract. All dried plant extracts were then stored in 10 ml sample bottles at −20°C until needed.

For analyses and cell assays, plant stock concentrations (50 mg/ml) were prepared by dissolving crude extracts in bidistilled, microfiltered, aseptic water (MiliQ). The solutions were cold sterilized by microfiltration (Millipore disk filters, 0.22 microns) in a laminar flow cabinet into sterile microcentrifuge tubes. These aliquots were at −80°C until further testing.

HPTLC Analyses

Plant extracts and phytochemical standards were diluted in methanol to a concentration of 50 and 1 mg/ml, respectively. A Linomat 5 (CAMAG, Switzerland) was used to apply 5 µl of the samples to HPTLC silica gel (Merck, Germany). The plates were developed using a CAMAG ADC2 automatic developing chamber. The method included 30-s pre-drying, 10 min humidity control using magnesium chloride to 48.3% relative humidity and 20 min saturation time, using saturation pads all done at 25.2°C. The mobile phase used was Chloroform-Methanol (8:2). During development, the solvent front was

TABLE 1 | Summary of the botanical origin and extraction methods of the plant extracts.

Sample ID	Plant name	Family	Plant Part	Place of collection/purchase	Extraction method	Yield (%w/w)
AB	*Alstonia boonei* De Wild.	Apocynaceae	Stembark	Herbal market, Mushin	Decoction	5.03
AS	*Annona senegalensis* Pers.	Annonaceae	Stembark	Forest, Agbede	Decoction	7.10
AL	*Anogeissus leiocarpa* (DC.) Guill. & Perr.	Combretaceae	Stembark	Herbal shop, Abuja	Decoction	6.21
AD	*Anthocliesta djalonensis* A.Chev.	Gentianaceae	Stembark	Forest, Agbede	Decoction	3.05
AR	*Aristolochia repens* Mill.	Aristolochiaceae	Stem	Herbal market, Mushin	Infusion	18.11
BF	*Bridelia ferruginea* Benth.	Phyllanthaceae	Stembark	Herbal market, Ibadan	Decoction	75.86
CS	*Cassia sieberiana* DC.	Leguminosae	Root	Forest, Agbede	Decoction	10.27
CF	*Cassytha filiformis* L.	Lauraceae	Whole plant	NIPRD, Abuja	Decoction	12.66
DO	*Daniellia ogea* (Harms) Holland	Leguminosae	Stembark	Forest, Agbede	Decoction	6.05
GL	*Gongronema latifolium* Benth.	Apocynaceae	Leaves	Herbal market, Mushin	Infusion	8.37
ID	*Isoberlinia doka* Craib & Stapf	Leguminosae	Stem	Herbal market, Zaria	Decoction	4.69
KI	*Khaya ivorensis* A.Chev.	Meliaceae	Stembark	Herbal market, Mushin	Decoction	7.83
KS	*Khaya senegalensis* (Desv.) A.Juss.	Meliaceae	Stembark	Forest, Agbede	Decoction	5.02
MO	*Moringa oleifera* Lam.	Moringaceae	Leaves	Home garden, Imo	Infusion	35.54
MW	*Mondia whitei* (Hook.f.) Skeels	Apocynaceae	Stem	Herbal market, Mushin	Infusion	20.24
OG	*Ocimum gratissimum* L.	Lamiaceae	Leaves	Herbal market, Mushin	Infusion	17.04
PN	*Picralima nitida* (Stapf) T.Durand & H.Durand	Apocynaceae	Seeds	Herbal market, Ibadan	Infusion	23.71
RV	*Rauvolfia vomitoria* Afzel.	Apocynaceae	Stembark	Herbal market, Ibadan	Decoction	3.9
SD	*Scoparia dulcis* L.	Plantaginaceae	Whole plant	NIPRD, Abuja	Decoction	16.35
SL	*Securidaca longipedunculata* Fresen.	Polygalaceae	Root	Herbal market, Mushin	Decoction	7.49
SH	*Strophanthus hispidus* DC.	Apocynaceae	Stem	Herbal market, Ibadan	Decoction	12.2
SG	*Syzygium guineense* (Willd.) DC.	Myrtaceae	Stem	Herbal market, Zaria	Decoction	8.01
TA	*Terminalia avicennioides* Guill. & Perr.	Combretaceae	Stem	Herbal market, Zaria	Decoction	13.25
TB	*Tapinanthus bangwensis* (Engl. & K.Krause)	Loranthaceae	Leaves	Herbal shop, Imo	Infusion	32.2
TI	*Tamarindus indica* L.	Leguminosae	Stem	Herbal market, Zaria	Decoction	6.05
VA	*Vernonia amygdalina* Delile	Compositae	Leaves	Home garden, Lagos	Infusion	15.54
XA	*Ximenia americana* L.	Olacaceae	Stem	Herbal market, Zaria	Decoction	11.5

allowed to migrate 80 mm before a drying time of 5 min. For derivatization, we used Anisaldehyde/H_2SO_4. All visualization and analysis were done using CAMAG TLC visualizer both before and after derivatization. Phytochemical standards and solvents were from Sigma-Aldrich (UK).

HPLC-DAD Analyses

Active plant samples were fingerprinted by HPLC-UV. Chromatograms were obtained in an Agilent 1100 Series (Gradient Quaternary Pump, Online degasser, Photodiode array detector) Software ChemStation. Elution conditions for phytomarkers were as previously described (Giner et al., 1993) on a Phenomenex® C18 column (250 × 4.6 mm id, 5 µm). Solvent A (H2O + Acetic Acid 0.2%) and B (methanol + Acetic Acid 0.2% were mixed in gradient mode as follows: 0 min 90% A, 0 to 5 min 80% A, 5 to 45 min 50% A, 45 to 55 min 20% A; flow rate 0.8 ml/min. The injection volume, column temperature, and UV wavelength were set at 80 µl, 30°C and 254 nm, respectively. Phytochemical standards and solvents were from Sigma-Aldrich (UK).

Cell Lines and Cell Culture

Caco-2 wild type cells (Sigma-Aldrich) were cultured in DMEM medium (GIBCO) supplemented with 10% FBS, penicillin (100 U/ml), streptomycin (100 µg/ml), and 1% non-essential amino acid (NEEA). The HepG2 and Caco2 cells were purchased from Sigma (UK). B16-F10 murine melanoma cell lines were from Professor Kostas Kostarelos (Centre for Drug Delivery Research, School of Pharmacy, UCL, UK). HepG2 cells (Sigma-Aldrich) were cultured in MEM medium (GIBCO) supplemented with 10% FBS, penicillin (100 U/ml), streptomycin (100 µg/ml). B16-F10 cells were cultured in DMEM medium (GIBCO) supplemented with 10% FBS, penicillin (100 U/ml), streptomycin (100 µg/ml). B16-F10 Cells were grown at 37°C and maintained in DMEM Glutamex (Dulbecco's Modified Eagle Media) containing 4,500 mg/L D-glucose, L-glutamine (3.97 mM) and sodium pyruvate. The media was supplemented with 10% of heat-inactivated fetal bovine serum (FBS) (Gibco) and 1% penicillin-streptomycin antibiotic which consists of 10,000 units of penicillin and 10,000 µl of streptomycin per ml to inhibit bacterial growth. All cells were kept at 37°C in an incubator with a humidified atmosphere of 5% CO_2.

Antiproliferation Assays

The NCI protocol for SRB staining was followed as previously described (Skehan et al., 1990; National Cancer Institute, 2020). Briefly, HepG2, Caco-2, and B16-F10 cells were cultured in 96-well tissue culture plates by adding 200 µl/well of a suspension of 2×10^4, 1×10^4, and 2×10^4 cells/well respectively. After cells reached 80% confluence the culture medium was replaced with fresh medium containing 100 µg/ml of plant extracts. After 24-h incubation with the plant extracts, media containing the samples was removed, and cells were fixed with 100 µl of cold 40% *w/v* trichloroacetic acid (TCA) solution in deionized water. The plates were incubated at 4°C for 1 h and then rinsed five times with slow running-tap water. The TCA-fixed cells were stained by adding 100 µl of SRB solution (0.4% SRB in 0.1% acetic acid) and left at room temperature for 1 h. Afterward, the plates were quickly rinsed four times with 1% acetic acid and flicked to remove unbound dye and then left to air-dry overnight. After drying completely, the protein bound SRB was solubilized by adding 100

µl of 10 mM Tris base buffer solution to each well. The plates were agitated in an orbital shaker for 30 min. The optical density was measured at 492 nm by using a microtiter plate reader (Tecan, Switzerland). Both Growth Inhibition 50% (GI_{50}) and Maximum Non-Toxic Concentrations (MNTC) were calculated for each cell line.

Rhodamine 123 Uptake Assay

Rhodamine uptake/efflux assays were conducted as previously described (Chieli et al., 2009) with minor modifications. Cells were seeded into 96-well plates for 24 h to allow for attachment. Then, the growth media was changed to serum free media. Rhodamine (5 µg/ml) was added to the wells containing 100 µg/ml of all the extracts to be tested. 20 µM verapamil was used as positive control. After 2 h incubation, cells were washed with 20 µM verapamil in PBS. Cells were lysed with 100 µl of 0.1% Triton X-100 in PBS and the plates were placed in the incubator for 15 min. 80 µl of each of the cell lysates in each well was transferred to a 96-well black plate and the fluorescence intensity of each well was measured in a Tecan® plate reader (Exc-485 nm, Em-525 nm). The cellular accumulation of Rh-123 for each of the extracts was expressed as the percentage of the accumulation measured for rhodamine only, that is under control conditions.

Tyrosinase Activity Assay

Tyrosinase inhibitory activity was assessed as previously described (Masuda et al., 2007). Briefly, L-tyrosine 2.5 mM -in PBS- and the sample- in DMSO- are mixed in a total volume of 160 µl to which 40 µl of Mushroom tyrosinase (46 units/ml) is added. After 20 min, the absorbance was measured for each well at 475 nm, then the % of Tyrosinase inhibition calculated against the control and corrected with matched blanks. All reagents were from Sigma-Aldrich (UK).

2D Migration Assay

The cell migration was measured using Oris™ Universal Cell Migration Assembly Kit. In this assay, inserts were used to create an exclusion zone in a cell monolayer. For the migration assay, the sterile stoppers were introduced in a flat-bottom 96-well plate before starting cell seeding. B16-F10 cells were plated at a density of 7.5×10^4 cells per well. After 24 h of incubation, a monolayer had been formed with an exclusion zone in the center. Afterward, the stoppers were removed manually and then the cells were incubated with the MNTC of each extract, vehicle control and hydroxyurea at (75 µM), which used as a positive control in this assay. At the end of the incubation period, the cells were fixed with 100 µl of cold 40% TCA. The plates were kept at 4°C for 1 h and rinsed with water. The cells were stained by the addition of 50 µl of trypan blue and incubated at room temperature for 1 h. Another washing step was performed, and the plate was then left to air-dry completely overnight. Measurement of zone closure was performed by digital images obtained by optical scanning (transmittance mode) by a Snapscan e50 (Agfa-Gevaert, Germany). Image J (National Health Institute, USA) was used to measure an average gap distance value and compare to the vehicle control in order to monitor the migratory capacity of the treated cells. The migration rate was calculated as follows: % Migration rate = [gap distance (day 0) − gap distance of the extract (24 h)]/[gap distance (day 0) − gap distance of vehicle control (24 h)].

Statistics

Curve fittings, GI_{50}s and IC_{50}s were performed with Excel® (Microsoft, Redmon) and GraphPad® Instat version 3 (GraphPad Software, La Jolla, US). Significance of the results was assessed with Instat® (GraphPad Software, La Jolla, US).

RESULTS AND DISCUSSION

Cytotoxicity of the Extracts

Rather than calculating exact values, we classified the GI_{50} between standard doses and applied the threshold proposed by Suffness and Pezzuto (1999), which establishes that crude extracts showing an $GI_{50} \leq 100$ µg/ml can be considered to be cytotoxic and selected for further studies, whereas the most promising ones are those with an GI_{50} lower than 30 µg/ml. None of the plants shown cytotoxicity toward all the cells in the panel, thus providing certain degree of specificity. The most promising cytotoxic activity was shown by *G. latifolium* against Caco2 colorectal cancer cells ($GI_{50} < 10$ µg/ml). Three species (*D. ogea, S. hispidus*, and *A. senegalensis*) were able to exert toxic effects on two different cell lines. Rat melanoma B16-F10 cells proliferation was strongly inhibited by *A. leiocarpus, B. ferruginea*, and *S. guineense* extracts, while *A. boonei G. latifolium, S. dulcis*, and *S. hispidus* were preferentially toxic against the human colon carcinoma Caco2 cell line. Finally, extracts from *K. ivorensis* and *S. hispidus* affected HepG2 human liver carcinoma cells only (**Table 2**).

Effect on Putative Drug Resistance Mechanisms

The MDR-1 gene and its product, P-glycoprotein, are considered to be among the most important drug-resistance mechanisms in cancer cells (Ozben, 2006). Nine extracts obtained from *A. senegalensis*, *B. ferruginea*, *C. filiformis*, *D. ogea*, *K. ivorensis*, *S. guineense*, *T. avicennioides*, and *X. americana* produced a change in intracellular accumulation of Rh-123 which was significantly different from the control cells in Caco-2 cells (**Figure 1**) which

TABLE 2 | Effects of active plant extracts on cancer cell using the SRB assay.

Plant extract	Proliferation (GI_{50} µg/ml)		
	HepG2	CACO2	B16-F10
A. boonei	–	≈50	–
A. leiocarpus	–	–	≈ 50
A. senegalensis.	–	≈75	≈ 100
B. ferruginea	–	–	≈ 50
C. filiformis	–	–	–
D. ogea	≈50	–	≈ 50
G. latifolium.	–	≈5	–
K. ivorensis	≈100	–	–
K. senegalensis	–	–	–
S. guineense	–	–	≈50
S. hispidus	≈75	≈35	–
T. avicennioides	–	–	≈ 100
T. bangwensis	–	–	≈100
Paclitaxel	≈0.03	≈0.01	≈0.09

suggests that they are acting as P-gp inhibitors.

In Caco-2 cells, the highest observed inhibitory effect was produced by *B. ferruginea* with more than 500% increase in Rh-123 accumulation compared to control cells followed by XA1 with more than 400% increase. The inhibitory effects of *B. ferruginea* and *X. americana* were thrice and twice higher than the effect of the positive control verapamil, respectively. Such high changes in intracellular Rh-123 accumulation by plant extracts are not uncommon. A similar study carried out with the stem bark extract of *Mangifera indica* produced a 1,000% increase in intracellular Rh-123 accumulation (Chieli et al., 2009).

Another emerging multidrug resistance mechanism in melanoma is melanin synthesis. Chen et al. demonstrated that melanosomes contribute to the refractory properties of melanoma cells by sequestering cytotoxic drugs and increasing melanosome-mediated drug export. Thus, preventing melanosomal sequestration of cytotoxic drugs by inhibiting the functions of melanosomes may have great potential as an approach to improving the chemosensitivity of melanoma cells (Chen et al., 2006). Furthermore, the same authors later established that the intrinsic MDR of melanoma cells is related to the ABC transporter systems -which includes P-gp- that may also play a critical role in reducing toxic melanin intermediates and metabolites (Chieli et al., 2009). The extracts that inhibited DOPA production under 100 μg/ml were *A. senegalensis* (22% ± 12), *B. ferruginea* (48% ± 10), *D. ogea* (32%± 14) and *S. guineense* (11%± 1) with Kojic acid showing an IC_{50} of 12.65 ± 3 μM in our conditions.

Antimigratory Activity

Figure 2 shows the effect of the active extracts on the cellular migration of the B16-F10. In vitro antimigratory activity against the highly metastatic B16-F10 cell line at 200 μg/ml was shown by *A. boonei*, *A. leiocarpus*, *K. senegalensis*, and *T. avicennioides*, while pro-migratory activity was detected for *C. filiformis*. The decoction of *S. guineense* was the most active at inhibiting migration but the cell population shown signs of toxicity. Of note, *D. ogea, A. senegalensis, B. ferruginea, M. whiteii*, and *T. bangwensis* did not exhibit a significant inhibitory effect of the 2D cell migration assay even when assayed at cytotoxic concentrations. When tested at MNTC only *A. boonei*, *K. senegalensis*, and *T. avicennioides* kept their activity.

A sequential liquid/liquid extraction of the extracts was performed to obtain chloroform (C), butanol (B) and water (W) fractions with significant antimigratory effects at 100 μg/ml as shown in **Figure 3**: AB-C, AL-B, KS-B, KS-W, SG-B, SG-W, and TA-W. When tested at MNTC only AB-C, KS-B, and KS-W kept their activity intact.

Dereplication of Known Bioactive Compounds

Screening of natural products for potential anticancer activities must always be accompanied by dereplication strategies so to avoid needless isolation of known bioactive compounds (Corley and Durley, 1994).

All extracts were chromatographed and dereplicated for Gallic acid, caffeic acid, epicatechin, epigallocatechin, catechin, vitexin rhamnoside, vitexin, rutin, ellagic acid, quercitrin, hesperidin, quercetin, luteolin, kaempferol, ursolic acid, betulinic acid, and lupeol. The resulting chromatograms are provided as supplementary materials. **Supplementary Table 1** summarizes the phenolic compounds detected in our plant samples *versus* those already reported in literature for the plant species.

The activities of *A. boonei* may be explained by the presence of lupeol [**1**], ursolic acid [**2**] (TLC) and quercitrin [**6**] (HPLC); *A. leiocarpus* contains Epicatechin [**5**], Gallic acid [**3**], and ellagic acid [**4**] (HPLC) and *S. guineense* Gallic acid [**3**] (HPLC). Their chemical structures are presented in **Figure 4**.

Lupeol [**1**] and ursolic acid [**2**] are regarded as powerful inducers of apoptosis in cancer cells with added modulatory effects upon drug resistance mechanisms in cancer cells including P-gp activity (Yan et al., 2014). Gallic acid [**3**] besides its well- known antioxidant activity can decrease P-gp expression in HK-2 cells (Chieli et al., 2010) and directly modify

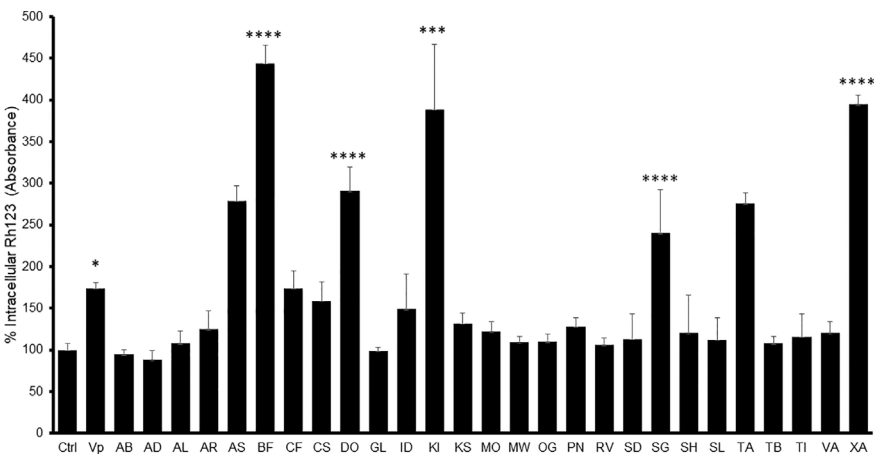

FIGURE 1 | Intracellular Rh-123 concentration in Caco-2 cells after treatment with either extract (final concentration 100 μg/ml) or reference drug (Verapamil, VP). One-way ANOVA followed by Bonferroni's post-test; Data are presented as the mean ± SD (n = 3), (****) p <0.0001 (***) p < 0.001; (*) p < 0.05, respectively.

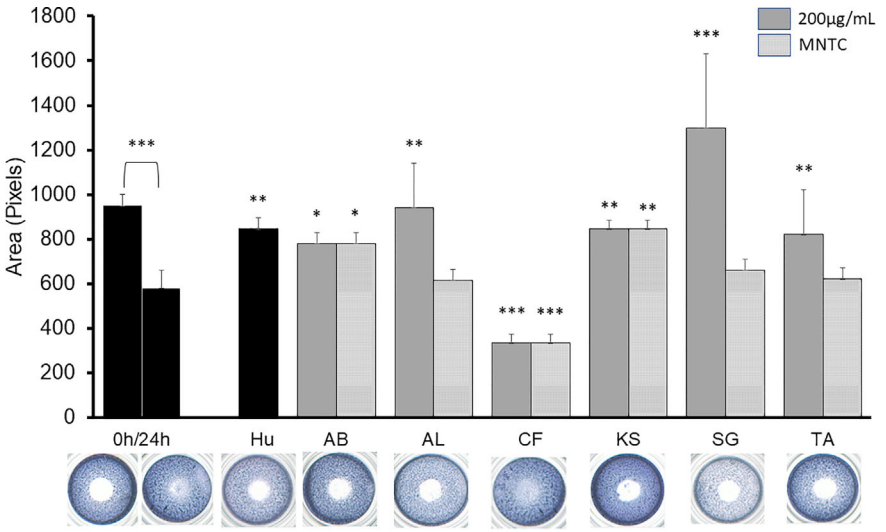

FIGURE 2 | 2D anti-migratory effects of the selected extracts at both GI_{50}, MNTC and reference compound (HU 75 µM) on B16-F10 murine melanoma cells for 24 h. Area of the gap (measured in pixels) in a confluent cell monolayer immediately after gap generation (0 h) and at 24 h post-wounding (n = 3) with representative microscopy images for the treated gaps. The significance of inhibitory effect was determined by one-way ANOVA followed by Bonferroni's post-test with respect to t24 control; Data are presented as the mean ± SD (n = 3), (***) $p < 0.001$; (**) $p < 0.01$; (*) $p < 0.05$, respectively.

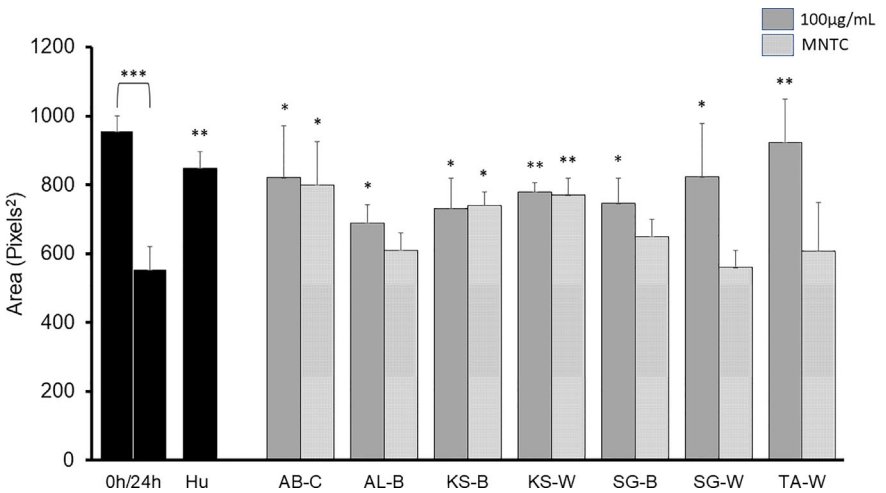

FIGURE 3 | 2D anti-migratory effects of fractions of active plant extracts with inhibitory effect at both GI_{50} and MNTC on B16-F10 murine melanoma cells after 24 h. Area of the gap (measured in pixels) in a confluent cell monolayer immediately after gap generation (0 h) and at 24 h post-wounding. HU: Hydroxyurea (reference compound, 75 µM); C: chloroform fraction; B: butanol fraction; W: water fraction. Data are presented as the mean ± SD (n = 3), (***) $p < 0.001$; (**) $p < 0.01$; (*) $p < 0.05$, respectively.

its function on KB-C2 cells (Kitagawa et al., 2004). Ellagic acid [**4**], Epicatechin [**5**], and quercitrin [**6**] are also endowed with anticarcinogenic effects by inhibiting tumor cell proliferation, inducing apoptosis and inhibiting drug-resistance processes—specially efflux pumps and transporters—required for tumor growth (Tan et al., 2013; Zhang et al., 2014). Moreover, all these chemicals are inhibitors of migration of melanoma cell lines (Alqathama and Prieto, 2015).

CONCLUSIONS

This study results demonstrated that some of these herbal medicines are endowed with significant *in vitro* cytotoxicity and inhibit MDR mechanisms. More refined studies would be necessary to ascertain the *in vivo* and/or clinical significance of such properties. In terms of direct cytotoxic effects, the aqueous extracts of G. *latifolium* and *S. hispidus* emerge as promising

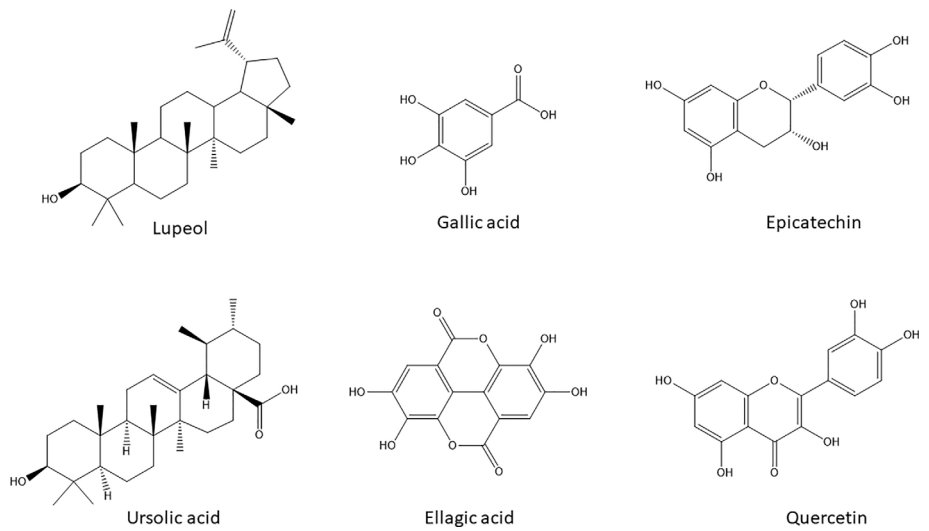

FIGURE 4 | Chemical structures of the natural products with potential anticancer and antimigratory activities dereplicated by HPLC-DAD and HPTLC in the selected active extracts.

leads according the strictest standards (GI_{50} < 30 μg/ml, Caco2 cells). It is conceivable that traditional infusions can reach pharmacologically active levels in the gastrointestinal system. Therefore, their chronic intake by diabetic patients may provide a baseline protection against colon cancer. This warrants further *in vivo* studies to confirm if their active principles are not degraded in the stomach and can reach the colon.

On the other hand, *B. ferruginea* and *X. americana* shown the largest effects on P-gp efflux, a clinically relevant target. These herbs have additional inhibitory effects on other putative MDR mechanisms namely depletion of glutathione as per our previous work (Ezuruike et al., 2019) and impairing tyrosinase activity (as per this work), respectively. Thus, they are clear candidates for adjuvant or combination cancer therapy.

Our study also shows for first time that the following herbal extracts exert *in vitro* antimigratory activity against the highly metastatic B16-F10 cell line: *A. leiocarpus, K. senegalensis*, *S. guineense*, and *T. avicennioides*. Some of their bioactive phytochemicals (lupeol, ursolic acid gallic acid, ellagic acid, epicatechin, and quercitrin) were dereplicated by HPLC and HPTLC.

Although further studies are needed to attest the clinical relevance of our findings, we hope that this work will stimulate similar research toward establishing the clinical relevance of these herbal medicines in Nigeria.

DATA AVAILABILITY STATEMENT

The raw data supporting the conclusions of this article will be made available by the authors, without undue reservation, to any qualified researcher.

AUTHOR CONTRIBUTIONS

AA performed cytotoxicity assays and 2D migratory assays (B16-F10 cells). UE collected plant materials in the field, performed cytotoxicity assays (Caco2, HepG2) and P-gp assay. AY performed tyrosinase activity assays. AM and EC designed, supervised, and advised on P-gp assay. JP designed the overall work, supervised all assays, performed HPLC analyses, and wrote the manuscript.

FUNDING

This research project was conducted with support from the Saudi Arabian Ministry of Education, Umm Al-Qura University (SACB Ref. UMU397) and The Commonwealth (Scholarship NGCS-2010-306).

ACKNOWLEDGMENTS

AA was a holder of a full-PhD scholarship from the Saudi Arabian Ministry of Education. AM was a holder of a full-PhD scholarship from the CNPq—Grant number: 201327/2012-0Ms. AE was a holder of a full-PhD scholarship from The Commonwealth. AY was a holder of a full-MSc scholarship from the Saudi Arabian Ministry of Education.

SUPPLEMENTARY MATERIAL

The Supplementary Material for this article can be found online at: https://www.frontiersin.org/articles/10.3389/fphar.2020.546439/full#supplementary-material

REFERENCES

Alqathama, A., and Prieto, J. M. (2015). Natural products with therapeutic potential in melanoma metastasis. *Nat. Prod. Rep.* 32, 1170–1182. doi: 10.1039/C4NP00130C

Aung, T. N., Qu, Z., Kortschak, R. D., and Adelson, D. L. (2017). Understanding the Effectiveness of Natural Compound Mixtures in Cancer through Their Molecular Mode of Action. *Int. J. Mol. Sci.* 18, 656. doi: 10.3390/ijms18030656

Chen, K. G., Valencia, J. C., Lai, B., Zhang, G., Paterson, J. K., Rouzaud, F., et al. (2006). Melanosomal sequestration of cytotoxic drugs contributes to the intractability of malignant melanomas. *Proc. Natl. Acad. Sci. U. States America* 103, 9903–9907. doi: 10.1073/pnas.0600213103

Chieli, E., Romiti, N., Rodeiro, I., and Garrido, G. (2009). In vitro effects of Mangifera indica and polyphenols derived on ABCB1/P-glycoprotein activity. *Food Chem. Toxicol.* 47, 2703–2710. doi: 10.1016/j.fct.2009.07.017

Chieli, E., Romiti, N., Rodeiro, I., and Garrido, G. (2010). In vitro modulation of ABCB1/P-glycoprotein expression by polyphenols from Mangifera indica. *Chem. Biol. Interact.* 186, 287–294. doi: 10.1016/j.cbi.2010.05.012

Corley, D. G., and Durley, R. C. (1994). Strategies for database dereplication of natural products. *J. Natural Prod.* 57, 1484–1490. doi: 10.1021/np50113a002

Dallavalle, S., Dobričić, V., Lazzarato, L., Gazzano, E., Machuqueiro, M., Pajeva, I., et al. (2020). Improvement of conventional anti-cancer drugs as new tools against multidrug resistant tumors. *Drug Resist. Update* 50, 100682. doi: 10.1016/j.drup.2020.100682

Ezuruike, U. F., and Prieto, J. M. (2014). The use of plants in the traditional management of diabetes in Nigeria: pharmacological and toxicological considerations. *J. Ethnopharmacol.* 155, 857–924. doi: 10.1016/j.jep.2014.05.055

Ezuruike, U. F., Chieli, E., and Prieto, J. M. (2019). In Vitro Modulation of Glibenclamide Transport by P-glycoprotein Inhibitory Antidiabetic African Plant Extracts. *Planta Med.* 85, 987–996. doi: 10.1055/a-0948-9072

Giner, R. M., Recio, M. C., Cuellar, M. J., Máñez, S., Peris, J. B., Stübing, G., et al. (1993). A Taxonomical Study of the Subtribe Leontodontinae Based on the Distribution of Phenolic Compounds. *Biochem. Syst. Ecol.* 21, 613–616. doi: 10.1016/0305-1978(93)90061-U

Hodek, P., Krízková, J., Burdová, K., Sulc, M., Kizek, R., Hudecek, J., et al. (2009). Chemopreventive compounds–view from the other side. *Chem. Biol. Interact.* 180, 1–9. doi: 10.1016/j.cbi.2009.01.003

International Agency for Research on Cancer *I. Global Cancer Observatory [Online]*. Available at: https://gco.iarc.fr/ (Accessed 2020 2020).

Jedy-Agba, E., Curado, M. P., Ogunbiyi, O., Oga, E., Fabowale, T., Igbinoba, F., et al. (2012). Cancer incidence in Nigeria: A report from population-based cancer registries. *Cancer Epidemiol.* 36, e271–e278. doi: 10.1016/j.canep.2012.04.007

Kitagawa, S., Nabekura, T., Kamiyama, S., and Kitagawa, S. (2004). Inhibition of P-glycoprotein function by tea catechins in KB-C2 cells. *JPP* 56, 1001–1005. doi: 10.1211/0022357044003

Masuda, T., Fujita, N., Odaka, Y., Takeda, Y., Yonemori, S., Nakamoto, K., et al. (2007). Tyrosinase inhibitory activity of ethanol extracts from medicinal and edible plants cultivated in okinawa and identification of a water-soluble inhibitor from the leaves of Nandina domestica. *Biosci. Biotechnol. Biochem.* 71, 2316–2320. doi: 10.1271/bbb.70249

National Cancer Institute (2020). *NCI-60 Screening Methodology. [Online]*. Available at: https://dtp.cancer.gov/discovery_development/nci-60/methodology.htm (Accessed 2018 2018).

Ozben, T. (2006). Mechanisms and strategies to overcome multiple drug resistance in cancer. *FEBS Lett.* 580, 2903–2909. doi: 10.1016/j.febslet.2006.02.020

Pan, M. H., and Ho, C. T. (2008). Chemopreventive effects of natural dietary compounds on cancer development. *Chem. Soc. Rev.* 37, 2558–2574. doi: 10.1039/b801558a

Pinon, A., Limami, Y., Micallef, L., Cook-Moreau, J., Liagre, B., Delage, C., et al. (2011). A novel form of melanoma apoptosis resistance: melanogenesis up-regulation in apoptotic B16-F0 cells delays ursolic acid-triggered cell death. *Exp. Cell Res.* 317, 1669–1676. doi: 10.1016/j.yexcr.2011.04.014

Skehan, P., Storeng, R., Scudiero, D., Monks, A., Mcmahon, J., Vistica, D., et al. (1990). New colorimetric cytotoxicity assay for anticancer-drug screening. *J. Natl. Cancer Inst.* 82, 1107–1112. doi: 10.1093/jnci/82.13.1107

Suffness, M., and Pezzuto, J. (1999). *Assays related to cancer drug discovery* (London: Academic Press).

Syed, S. B., and Coumar, M. S. (2016). P-Glycoprotein Mediated Multidrug Resistance Reversal by Phytochemicals: A Review of SAR & Future Perspective for Drug Design. *Curr. Top. Med. Chem.* 16, 2484–2508. doi: 10.2174/1568026616666160212123814

Tan, K. W., Li, Y., Paxton, J. W., Birch, N. P., and Scheepens, A. (2013). Identification of novel dietary phytochemicals inhibiting the efflux transporter breast cancer resistance protein (BCRP/ABCG2). *Food Chem.* 138, 2267–2274. doi: 10.1016/j.foodchem.2012.12.021

The African Cancer Registry Network Nigerian National System of Cancer Registries.

Thomford, N. E., Senthebane, D. A., Rowe, A., Munro, D., Seele, P., Maroyi, A., et al. (2018). Natural Products for Drug Discovery in the 21st Century: Innovations for Novel Drug Discovery. *Int. J. Mol. Sci.* 19, 1578. doi: 10.3390/ijms19061578

Tinoush, B., Shirdel, I., and Wink, M. (2020). Phytochemicals: Potential Lead Molecules for MDR Reversal. *Front. Pharmacol.* 11, 832. doi: 10.3389/fphar.2020.00832

Viale, A., and Draetta, G. F. (2016). Metabolic Features of Cancer Treatment Resistance. *Recent Results Cancer Res.* 207, 135–156. doi: 10.1007/978-3-319-42118-6_6

Yan, X. -J., Gong, L. -H., Zheng, F. -Y., Cheng, K. -J., Chen, Z. -S., Shi, Z., et al. (2014). Triterpenoids as reversal agents for anticancer drug resistance treatment. *Drug Discov. Today* 19, 482–488. doi: 10.1016/J.DRUDIS.2013.07.018

Zhang, H.-M., Zhao, L., Li, H., Xu, H., Chen, W.-W., and Tao, L. (2014). Research progress on the anticarcinogenic actions and mechanisms of ellagic acid. *Cancer Biol. Med.* 11, 92–100. doi: 10.7497/j.issn.2095-3941.2014.02.004

Conflict of Interest: The authors declare that the research was conducted in the absence of any commercial or financial relationships that could be construed as a potential conflict of interest.

frontiers in Pharmacology

ORIGINAL RESEARCH
published: 17 November 2020
doi: 10.3389/fphar.2020.557789

Royleanone Derivatives From *Plectranthus* spp. as a Novel Class of P-Glycoprotein Inhibitors

Catarina Garcia[1,2†], *Vera M. S. Isca*[1,3†], *Filipe Pereira*[1], *Carlos M. Monteiro*[3], *Epole Ntungwe*[1,2], *Francisco Sousa*[1], *Jelena Dinic*[4], *Suvi Holmstedt*[5], *Amílcar Roberto*[1], *Ana Díaz-Lanza*[2], *Catarina P. Reis*[3], *Milica Pesic*[4], *Nuno R. Candeias*[5,6], *Ricardo J. Ferreira*[7], *Noélia Duarte*[3], *Carlos A. M. Afonso*[3] *and Patrícia Rijo*[1,3]*

[1] Center for Research in Biosciences & Health Technologies (CBIOS), Universidade Lusófona de Humanidades e Tecnologias, Lisboa, Portugal, [2] Department of Biomedical Sciences, Faculty of Pharmacy, University of Alcalá, Alcalá de Henares, Spain, [3] Instituto de Investigação do Medicamento (iMed.ULisboa), Faculty of Pharmacy, Universidade de Lisboa, Lisboa, Portugal, [4] Institute for Biological Research "Siniša Stanković"- National Institute of Republic of Serbia, University of Belgrade, Belgrade, Serbia, [5] Faculty of Engineering and Natural Sciences, Tampere University, Tampere, Finland, [6] LAQV-REQUIMTE, Department of Chemistry, University of Aveiro, Aveiro, Portugal, [7] Science for Life Laboratory, Department of Cell and Molecular Biology, Uppsala University, Uppsala, Sweden

OPEN ACCESS

Edited by:
Jose Maria Prieto, Liverpool John Moores University, United Kingdom

Reviewed by:
Marialessandra Contino, University of Bari Aldo Moro, Italy
Guillermo Raul Schinella, National University of La Plata, Argentina

***Correspondence:**
Patrícia Rijo
patricia.rijo@ulusofona.pt

[†]*These authors share first authorship.*

Specialty section:
This article was submitted to Ethnopharmacology, a section of the journal Frontiers in Pharmacology

Received: *30 April 2020*
Accepted: *30 September 2020*
Published: *17 November 2020*

Citation:
Garcia C, Isca VMS, Pereira F, Monteiro CM, Ntungwe E, Sousa F, Dinic J, Holmstedt S, Roberto A, Díaz-Lanza A, Reis CP, Pesic M, Candeias NR, Ferreira RJ, Duarte N, Afonso CAM and Rijo P (2020) Royleanone Derivatives From Plectranthus *spp. as a Novel Class of P-Glycoprotein Inhibitors. Front. Pharmacol. 11:557789. doi: 10.3389/fphar.2020.557789*

Cancer is among the leading causes of death worldwide. One of the most challenging obstacles in cancer treatment is multidrug resistance (MDR). Overexpression of P-glycoprotein (P-gp) is associated with MDR. The growing incidence of cancer and the development of MDR drive the search for novel and more effective anticancer drugs to overcome the MDR problem. Royleanones are natural bioactive compounds frequently found in *Plectranthus* spp. The cytotoxic diterpene 6,7-dehydroroyleanone (**1**) is the main component of the *P. madagascariensis* (Pers.) Benth. essential oil, while 7α-acetoxy-6β-hydroxyroyleanone (**2**) can be isolated from acetonic extracts of *P. grandidentatus* Gürke. The reactivity of the natural royleanones **1** and **2** was explored to obtain a small library of new P-gp inhibitors. Four new derivatives (6,7-dehydro-12-*O*-*tert*-butyl-carbonate-royleanone (**20**), 6,7-dehydro-12-*O*-methylroyleanone (**21**), 6,7-dehydro-12-*O*-benzoylroyleanone (**22**), and 7α-acetoxy-6β-hydroxy-12-*O*-benzoylroyleanone (**23**) were obtained as pure with overall modest to excellent yields (21–97%). P-gp inhibition potential of the derivatives **20**–**23** was evaluated in human non-small cell lung carcinoma NCI-H460 and its MDR counterpart NCI-H460/R with the P-gp overexpression, through MTT assay. Previously prepared diterpene 7α-acetoxy-6β-benzoyloxy-12-*O*-(4-chloro)benzoylroyleanone (**4**), has also been tested. The P-gp inhibiting effects of compounds **1**–**4** were also assessed through a Rhodamine 123 accumulation assay. Derivatives **4** and **23** have significant P-gp inhibitory potential. Regarding stability and P-gp inhibition potential, results suggest that the formation of benzoyl esters is a more convenient approach for future derivatives with enhanced effect on the cell viability decrease. Compound **4** presented higher anti-P-gp potential than the natural diterpenes **1**, **2,** and **3**, with comparable inhibitory potential to Dexverapamil. Moreover, derivative **4** showed the ability to sensitize the resistant NCI-H460/R cells to doxorubicin.

Keywords: *Plectranthus*, Diterpenes, Royleanones, stability, *Artemia salina*, P-pg activity

INTRODUCTION

Cancer is among the leading causes of death worldwide with an estimated 18.1 million new cancer cases and 9.6 million cancer deaths in 2018 (Bray et al., 2018). One of the most challenging obstacles in cancer treatment is multidrug resistance (MDR). MDR is responsible for over 90% of deaths in cancer patients receiving traditional chemotherapeutics or novel targeted drugs. MDR can be caused by numerous mechanisms in cancer cells, such as activation of DNA repair mechanisms, elevated metabolism of xenobiotics, genetic factors, and increased activity of drug efflux pumps. (Bukowski et al., 2020). Nonetheless, the most common mechanism of MDR is the overexpression of drug efflux transporters of the ATP binding cassette (ABC) family. Three major proteins of the ABC family, namely P-glycoprotein (P-gp, also referred to as MDR1), MDR-associated protein 1 (MRP1), and breast cancer resistance protein (BCRP), were shown to play a critical role in MDR (Mohammad et al., 2018). These efflux pumps are present in the cell membrane of a variety of normal tissues and have a protecting role against xenobiotic substances and toxic compounds. Therefore, they can interfere with drug administration, by reducing the intracellular accumulation of many anticancer drugs to sub-therapeutic levels, thus decreasing or abolishing chemotherapy efficacy (Nanayakkara et al., 2018). P-gp is the best-studied drug efflux pump of the family of ABC transporters. Cancer cells upregulate P-gp expression as an adaptive response to evade chemotherapy mediated cell death. This process leads to resistance against the currently available anti-cancer drugs in many different types of cancers (Sharom, 2007; Nanayakkara et al., 2018; Robinson and Tiriveedhi, 2020) Consequently, the development of P-gp inhibitors is gaining much importance in numerous research works. Several P-gp inhibitors have been discovered by *in silico* and pre-clinical studies. Although P-gp inhibitors showed high efficacy *in vitro* and *in vivo* studies, very few have successfully passed all phases of the clinical trials and none of them have been approved by the U.S. Food and Drug Administration (FDA) for clinical use in cancer treatment (Nanayakkara et al., 2018; Robinson and Tiriveedhi, 2020). After three generations of P-gp inhibitors, a fourth generation comprised of nature-originated compounds has emerged (Dinić et al., 2020). Therefore, identification of natural compounds that can exert anticancer effects and at the same time revert the MDR contributes to the efforts of the cancer research community to combat this multifactorial disease.

The genus *Plectranthus* (Lamiaceae) is used in traditional medicine in southern Africa and it is known as a source of bioactive natural products (Lukhoba et al., 2006; Rice et al., 2011). The major classes of secondary metabolites present in these plants are diterpene quinones, coleones, and royleanones, with pharmacological activities (Bernardes et al., 2018; Rijo et al., 2013), including antiproliferative properties (Burmistrova et al., 2013; Ladeiras et al., 2016). One of those diterpenes, 6,7-dehydroroyleanone (**1**) (**Figure 1**), which has been reported with antioxidant, antimicrobial, and cytotoxic activities (Gazim et al., 2014; Garcia et al., 2018), is the main component of *P. madagascariensis* (Pers.) Benth essential oil (Kubínová et al., 2014). Other example is the 7α-acetoxy-6β-hydroxyroyleanone (**2**) (**Figure 1**), that can be isolated from extracts of *P. grandidentatus* Gürke and identified as an antimicrobial agent (Rijo et al., 2014a; Bernardes et al., 2018) with a strong inhibitory effect against five human cancer cell lines MCF-7 (breast adenocarcinoma), NCI-H460 (non-small cell lung cancer), SF-268 (CNScancer), TK-10 (renal cancer) and UACC-62 (melanoma) (Marques et al., 2002). Although the derivatization of aromatic abietane diterpenoids has been described (González, 2014), the two non-aromatic *p*-quinone abietanes, **1** and **2**, are suitable for derivatization. The analysis of the royleanone **one** chemical structure pointed to the particular acidity of the 12-hydroxyl group, due to the presence of the *p*-quinone in ring C. Alongside with the presence of this group, compound **2** possesses another free hydroxyl group at C-6, suitable for coupling different moieties.

In a previous hemi-synthetic study, the derivatives 6,7-dihydroxyroyleanone (**3**) and 7α-acetoxy-6β-benzoyloxy-12-*O*-(4-chloro)benzoylroyleanone (**4**) (**Figure 1**) were successfully prepared from the lead molecule **2** (Rijo, 2013). Compound **3** is a natural product isolated from *P. grandidentatus* Gürke, which can also be obtained by basic hydrolysis of compound **2** (Rijo, 2013). Furthermore, the patented

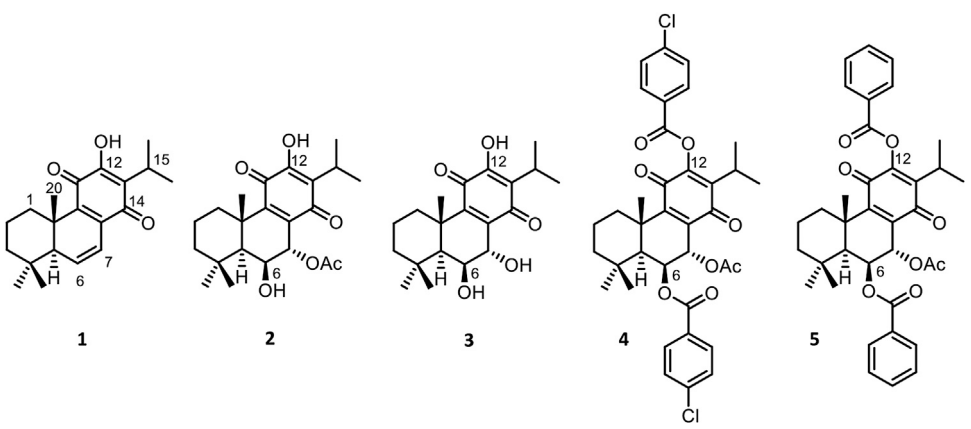

FIGURE 1 | Natural and semisynthetic royleanones: 6,7-dehydroroyleanone (1) and 7α-acetoxy-6β-hydroxyroyleanone (2), 6,7-dihydroxyroyleanone (**3**), 7α-acetoxy-6β-benzoyloxy-12-*O*-(4-chloro)benzoylroyleanone (**4**) and 7α-acetoxy-6β-benzoyloxy-12-*O*-benzoylroyleanone (**5**).

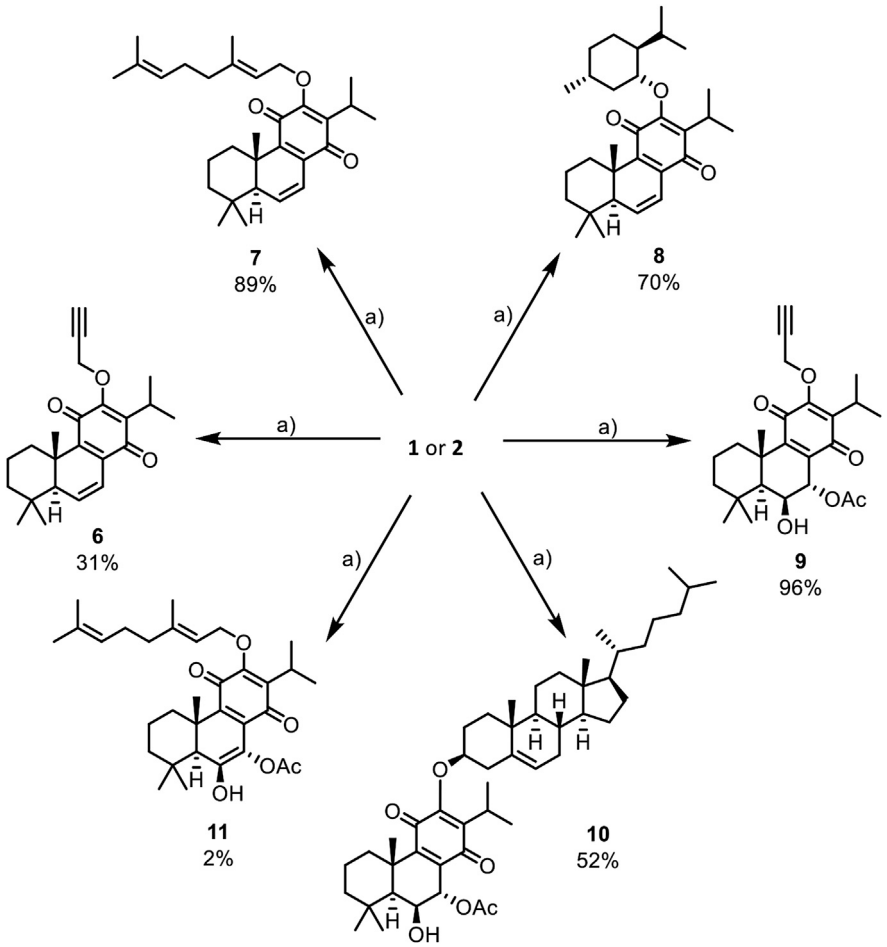

SCHEME 1 | Mitsunobu reactions of natural products **1** and **2** that afford unstable derivatives: a) Triphenylphosphine (5 eq.), DIAD (5 eq.), corresponding alcohol (5 eq.), and dry THF, under argon atmosphere, derivatives **6** to **11**. *Reactional conditions described in Material and Methods (section *Reaction Procedures*) and NMR characterization available on **Supplementary Material**.

diterpene 7α-acetoxy-6β-benzoyloxy-12-*O*-benzoylroyleanone (**5**) (**Figure 1**) was also obtained by semi-synthesis from compound **2**. The derivate **5** has shown selective modulation on Protein kinase delta isoform (PKC-δ). A key study reports that **5** strongly inhibited the proliferation of colon cancer cells by inducing a PKC-δ-dependent mitochondrial apoptotic pathway involving caspase-3 activation (Bessa et al., 2018). Besides, another study reported an important Structure-Activity Relationship (SAR) for substituted royleanone abietanes, where an electron-donating group at positions 6 and/or 7 in the abietane skeleton is required for improving cytotoxic effect. Additionally, higher cytotoxic effects were observed for substituents with log *p* values between 2 and 5 (Matias et al., 2019). Herein in this study, we report some royleanone reactivity features, which will allow us to obtain insights on the SAR and identify hit cytotoxic molecules.

RESULTS AND DISCUSSION

Semisynthesis and Stability of Royleanones

In this work, the reactivity of two royleanones was explored to prepare a small library of compounds of enhanced effect on the cell viability decrease potential and anti-P-gp activity. Several hemisynthetic reactions were performed on natural compounds **1** and **2** (**Figure 1**). Compounds **1** and **2** were subjected to short time microwave-assisted Mitsunobu and benzoylation reactions. Additionally, molecule **1** was subjected to carbamoylation, tosylation, and introduction of TBDPS (*tert*-butyldiphenylsilyl) group. Royleanone **2** was also subjected to methylation reaction and introduction of Boc (*tert*-butyloxycarbonyl) group. The predicted structures and the isolated derivatives (**6**–**23**) are shown in **Schemes 1**–**3**.

Unfortunately, the obtained products have encountered stability issues: the derivatives **6** to **19** (**Scheme 1** and **2**) tend to degrade after isolation. On the other hand, the introduction of Boc group (**20**), methylation (**21**), and benzoylation (**22** and **23**) reactions (**Scheme 3**) were accomplished with success, affording pure products with overall good yields (97% for derivative **20**, 28% for methylated derivative **21** and 50% and 69% for benzoylated derivatives **22** and **23**, respectively).

The Mitsunobu products (**6** to **11**, **Scheme 1**) have displayed a high rate of decomposition, thus hampering their isolation as

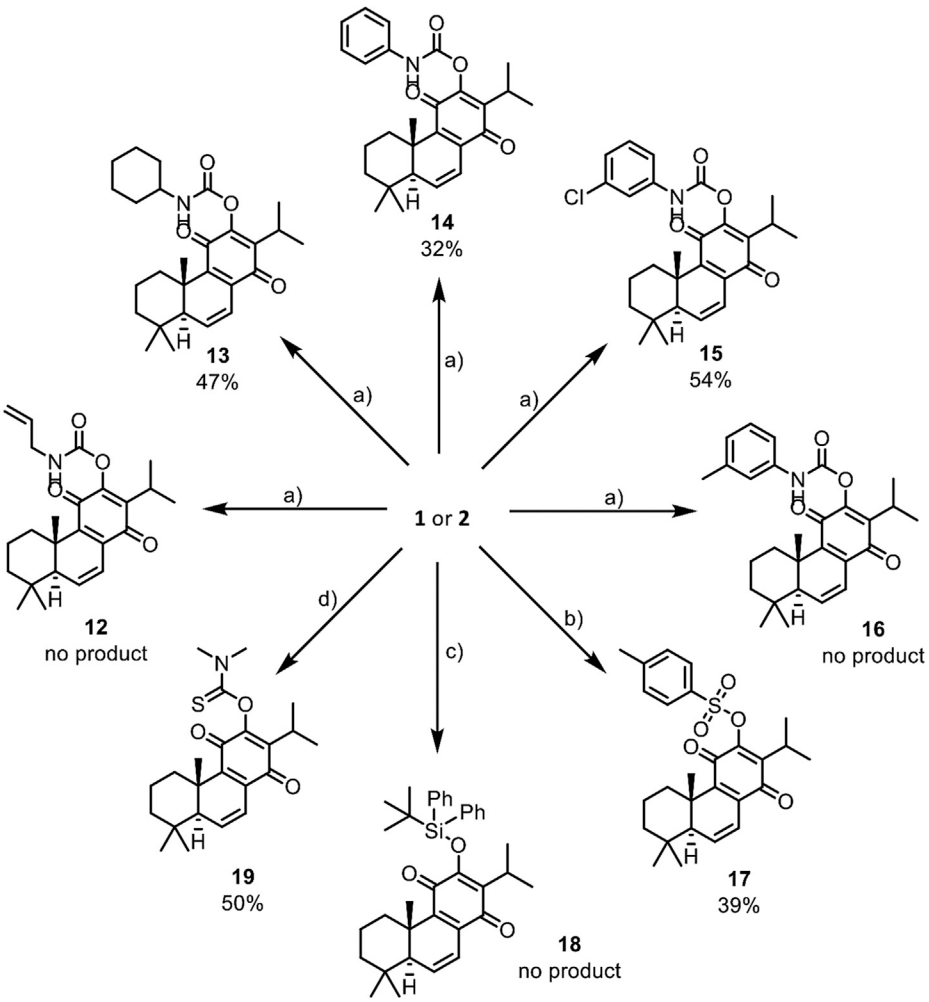

SCHEME 2 | Reactions of natural products **1** and **2** that afford unstable derivatives: a) DMAP (5 eq.), corresponding isocyanate (large excess), and dry CH_2Cl_2, under inert conditions, expected derivatives **12** to **16**; b) triethylamine (4.5 eq.), DMAP (0.3 eq.), *p*-toluenosulfonyl chloride (3 eq.) and dry CH_2Cl_2, derivative **17**; d) imidazole (2 eq.), TBDPSCl (large excess) and dry CH_2Cl_2, expected derivative **18**; e) dimethylthiocarbamoyl chloride (1.2 eq.), NaH (1 eq), NaI (0.5 eq.) and THF, derivative **19**. *Reactional conditions described in Material and Methods (section *Reaction Procedures*) and NMR characterization available on **Supplementary Material**.

pure products. Several chromatographic techniques have been used, namely silica preparative TLC, silica and alumina columns as well as preparative HPLC. Despite the several purification techniques tested for the isolation of derivatives **6** to **11,** they invariably decomposed during such steps. This degradation was also observed in the carbamoylation reactions (derivatives **13** to **15**, **Scheme 2**), tosylation (**17**), and thiocarbamoylation (**19**). Despite the presence of allyl (**12**) and *m*-tolyl (**16**) carbamates and silyl ether (**18**) in the TLC analysis of the reaction mixtures, the compounds decomposed before purification and no characterization could be done.

The mechanism of decomposition was deduced to be the same, regardless the *O*-substituents, and we used the derivative 6,7-dehydro-12-(prop-2′-yn-1′-yloxy)-royleanone (**6**, **Scheme 1**), as a substrate model in further studies. The hemisynthesis of derivative **6** was repeated several times, and the isolation of the compound of interest was attempted through numerous methods. An alumina column was used for its isolation, as well as preparative TLC and semi-preparative HPLC. Nonetheless, regardless of the technique, the compound isolated was never obtained in its pure form.

In the analytical HPLC analysis of compound **6** three peaks stand out, one of which was identified as the parent compound **1** (23.31 min), using its characteristic UV spectrum as a fingerprint. This fact may indicate that compound **6** tends to decompose to a much more stable scaffold–the starting material (**1**).

In an attempt to better understand the lack of stability of the compounds, derivative **6** was subjected to LC-MS analysis. The ESI positive mass spectra indicated a mass of m/z 355 $[M + Na]^+$. Although it was not possible to identify the moiety or cleavage pattern responsible for the result, some decomposition mechanisms based on the presence of the mentioned fragment were considered (**Figure 2**).

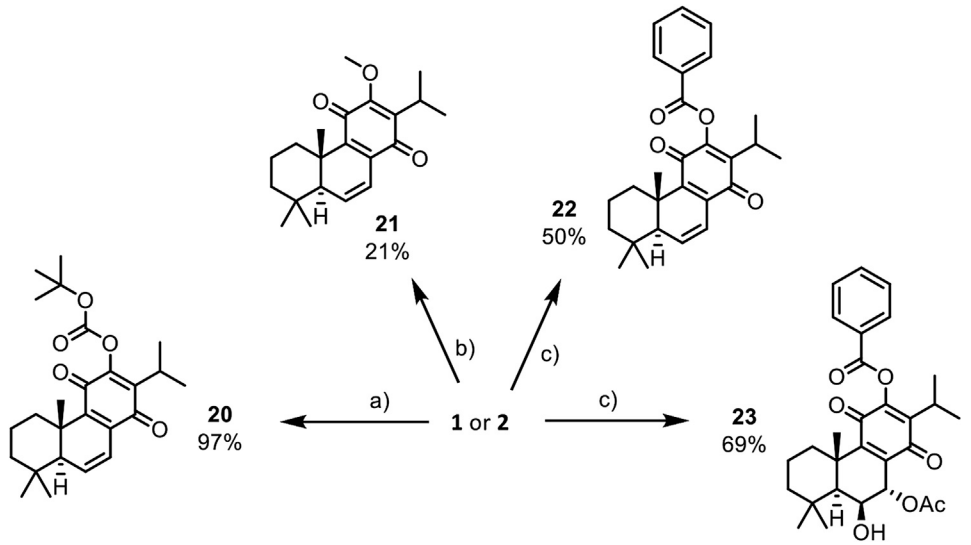

SCHEME 3 | Reactions of **1** and **2** that afford stable derivatives: a) DMAP (0.5 eq.), Boc_2O (2.2 eq.) and dry CH_2Cl_2, derivative **20**; b) CH_3I (8.4 eq.), Ag_2O (8.4 eq.) and dry CH_2Cl_2, derivative **21**; c) Pyridine (12 eq.), benzoyl chloride (12 eq.) and dry CH_2Cl_2, derivatives **22** and **23**. *Reactional conditions described in Material and Methods (section *Reaction Procedures*) and NMR characterization available on **Supplementary Material**.

Decomposition Mechanism of Unstable Derivatives

The decomposition of derivative **6** was studied by Density Functional Theory (Parr and Yang, 1989) to elaborate a mechanism and facilitate the future preparation of more stable derivatives (**Figure 2**). Different mechanisms for decomposition have been suggested based on computational calculations. Nucleophilic substitution at a more reactive side chain seems the preferential route, while an acid-catalyzed conjugate addition should operate in the case of less electrophilic side chains. The decomposition is likely to start with a nucleophilic attack by water on position 6 to provide $\mathbf{6_A}$, being followed by a bimolecular nucleophilic substitution by water on the propargylic position, through calculated $\mathbf{6_{AB}}$, as shown in **Figure 2A**). This second step was determined to have an energy barrier ($\Delta G^{\ddagger}$) of 42.0 kcal/mol and, upon the establishment of hydrogen bonds network with water molecules. Notwithstanding the high energy barrier, the process is energetically favorable with the intermediate $\mathbf{6_B}$ being 9.3 kcal/mol more stable than $\mathbf{6_A}$. The 1,2-hydride migration in $\mathbf{6_B}$ delivers the aromatized molecule identified in HRMS.

The attack of water at position 12 of $\mathbf{6_A}$ in a conjugate addition fashion, was considered but determined highly unlikely due to an energy barrier of 55.6 kcal/mol. However, this energy barrier lowers significantly when in the presence of acid catalysis (**Figure 2B**). In that case, tetrahedral intermediate $\mathbf{6_{C+}}$ was identified in the computational calculations, with the overall energy barrier of the release of propargyl alcohol being 41.6 kcal/mol. This alternative mechanism, in which a proton source is required, is likely to be more relevant in decomposing derivatives that miss the electrophilic position prone for an SN2 reaction. This being the case for most of the unstable products.

Effects of Royleanones in Multidrug Resistance Mechanisms of Cancer Cells

The P-gp inhibition potential of all stable derivatives obtained, derivatives **20** to **23**, was investigated. Moreover, derivative **4**, previously prepared (Rijo, 2013), was also assessed. Non-small cell lung carcinoma is particularly hard to treat due to its highly resistant and metastatic profile. Therefore, NCI-H460 and its corresponding MDR cell line NCI-H460/R with the overexpression of P-gp was a suitable model for testing the anticancer effect and P-gp inhibitory effect of our compounds. MRC-5 was selected as a normal cell line due to its bronchial epithelial origin. The effect of derivatives **20** to **23** was illustrated according to the fluorescence activity ratio (FAR) and sensitivity index (SI) (**Table 1**). Based on the FAR (values above 1.50 indicate P-gp inhibition) and SI (values above 20 account for P-gp inhibition), we could see that only derivatives **4** and **23** have the ability to inhibit P-gp activity, with FAR values of 1.71 and 2.10, respectively, and SI of 21.60 and 26.50, respectively. Additionally, derivative **23** has shown a comparable inhibitory potential to the well-known P-gp inhibitor, Dexverapamil (FAR 2.13 and SI 26.90) (Isca et al., 2020). A recent study used molecular docking and molecular dynamics to explore the interaction of derivatives **4** and **23** with P-gp and suggested that the presence of aromatic moieties increases the binding affinity of royleanone derivatives toward P-gp (Isca et al., 2020). On the other hand, derivative **22** is also a benzoylated derivative, nonetheless, it does not show the ability to inhibit P-gp activity. The difference between derivatives **4**, **23**, and **22** is that they are obtained from different natural products. Namely, derivative **4** and **23** are prepared from royleanone **2,** and derivative **22** is obtained from royleanone **1**. It means that derivatives **4** and **23** displayed a hydroxyl group in position 6

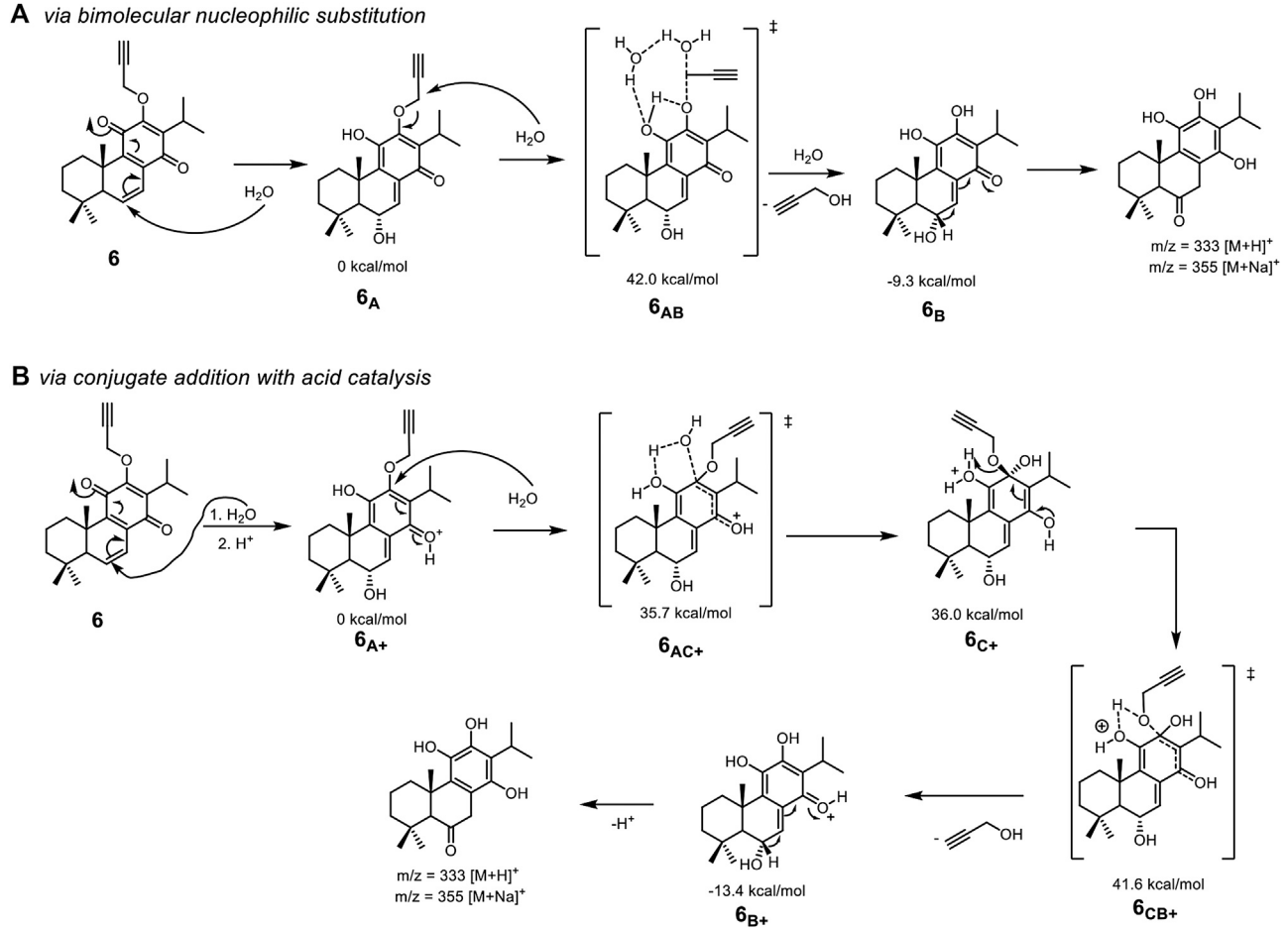

FIGURE 2 | Decomposition mechanism proposal for the unstable derivatives, using derivative **6** as a working model.

and an acetoxy group in position 7, while derivative **22,** displayed a double-bound (C=C) in these 6 and 7 positions. This suggests that the substituents in position 6 (-OH) and 7 (-OAc) can also contribute to P-gp interaction. Further studies should be conducted to assess this hypothesis.

Derivatives **4** and **23** showed to be promising candidates for P-gp inhibition, nonetheless, due to the small amount of compound **23** available, we choose the royleanone **4** for further studies. Accordingly, the effect of compound **4** was investigated in NCI-H460, NCI-H460/R cell lines, and normal embryonal bronchial epithelial cells MRC-5. Royleanone **4** showed high toxicity in all cell lines tested, with IC_{50} of 1.9 ± 0.4 μM for NCI-H460, 2.2 ± 0.4 μM for NCI-H460/R, and 2.0 ± 0.3 μM for MRC-5 cell lines. In previous studies, Garcia et al. (2018) and Matias et al. (2019) established the toxicity of the natural diterpenes **1**, **2**, and **3** in the same cell lines. Royleanone **2** is more efficient than **1** and **3**, with IC_{50} of 2.7 μM for NCI-H460, 3.1 μM for NCI-H460/R, and 8.6 μM for MRC-5 cell lines (Garcia et al., 2018; Matias et al., 2019). According to these results, the derivatization of royleanone **2** into derivative **4** lead to a decrease in cell viability in all cell lines tested. However, compounds **1**, **2,** and **three** were selective toward cancer cells (Garcia et al., 2018; Matias et al., 2019), while derivative **4** was equally active against normal cells.

In general, P-gp inhibitors can block drug binding sites either competitively, non-competitively, or allosterically. Many inhibitors, namely, verapamil, cyclosporin A, *trans*-flupenthixol, among others, are themselves transported by P-gp (Amin, 2013). On the contrary, royleanones **1–4** showed the same efficacy in sensitive and MDR cancer cells implying that they could not be P-gp substrates. Moreover, Isca et al. (2020) based on docking simulations also suggest that derivatives **4** and **23** act as non-competitive efflux inhibitors.

The P-gp inhibiting effects of compounds **1** to **4** were additionally assessed through a Rhodamine 123 (Rho123) accumulation assay (**Figure 3**). The obtained results indicate that derivative **4** has comparable inhibitory potential to Dexverapamil (**Figure 3**). Dexverapamil belongs to the second generation of P-gp inhibitors, known as a competitive inhibitor (Robey et al., 2018). In our experiments with Rho123, Dexverapamil competes with Rho123 for binding P-gp and thus increases the Rho123 accumulation. Recent publications imply that verapamil (first-generation inhibitor) can increase the ATPase activity of P-gp and thus by exhausting the ATP

TABLE 1 | P-gp inhibition by derivatives 4, 20, 21, 22, and 23 in the human NSCLC MDR cancer cell line.

Treatments	MFI[a]	FAR[b]	SI[c]
NCI-H460 control	134.10		
NCI-H460/R control	16.96		12.65
DexVER	36.07	2.13	26.90
4[d]	28.97	1.71	21.60
20	23.71	1.40	17.68
21	19.48	1.15	14.53
22	18.25	1.08	13.61
23[d]	35.54	2.10	26.50

[a]*The measured mean fluorescence intensity (MFI) was used for the calculation of the fluorescence activity ratio (FAR).*
[b]*via the following equation: FAR = $MFI_{MDR\ treated}/MFI_{MDR\ control}$. FAR values above 1.50 indicate P-gp inhibition.*
[c]*The sensitivity index (SI) was calculated on the basis of the measured mean fluorescence intensity (MFI) expressed via the following equation: SI = ($MFI_{MDR\ treated}$ * 100)/$MFI_{sensitive\ control}$. SI values above 20 account for P-gp inhibition.*
[d]*Results published in Isca et al. (2020).*
Sensitive cancer cell line and its MDR counterpart used in the study: non-small cell lung carcinoma-NSCLC (NCI-H460 and NCI-H460/R).
DexVER was applied at the same concentration (20 μM) as tested derivatives.

suppress P-gp function (Lee et al., 2019). It is well known that some substrates of P-gp can exert an inhibitory effect on P-gp if they are applied in higher concentrations (Durmus et al., 2015). On the other side, there are substrates of P-gp such as doxorubicin which cannot inhibit P-gp. Quite opposite, doxorubicin induces the expression of P-gp (Wu et al., 2016). Accordingly, we also evaluated the ability of **4** to sensitize resistant NCI-H460/R cells to doxorubicin (**Table 2**). Results showed that derivative **4** was able to sensitize MDR cells to doxorubicin. All three concentrations of compound **4** used to reverse the doxorubicin resistance achieved similar efficacy.

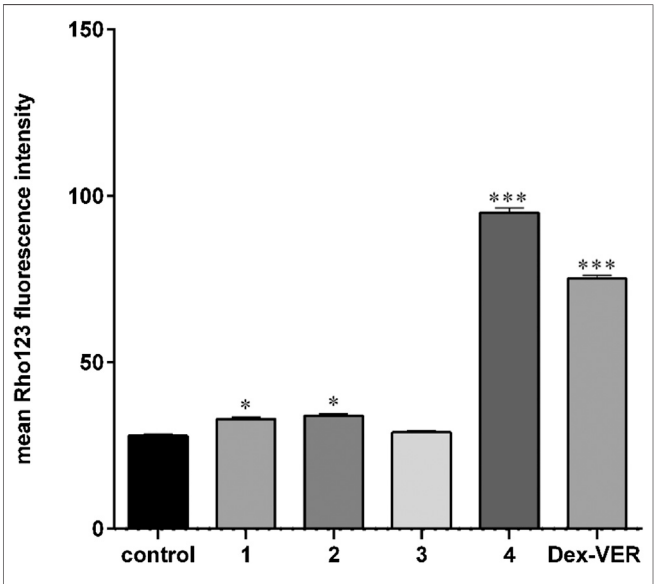

FIGURE 3 | Royleanone derivatives increase the Rhodamine 123 accumulation implying anti-P-gp activity. Experiments were performed in triplicates (n = 3). Significant difference compared to control: * $p < 0.05$, *** $p < 0.001$.

TABLE 2 | Derivative 4 sensitizes the NCI-H460/R cell line to doxorubicin.

Combined treatments	IC_{50} for DOX (μM)	Relative reversal factor
DOX	2.774 ± 0.025	—
4 (0.5 μM) + DOX	0.823 ± 0.016	3.37
4 (1.0 μM) + DOX	0.594 ± 0.017	4.67
4 (2.0 μM) + DOX	0.608 ± 0.020	4.56

DOX concentrations used in the experiments: 0.1, 0.25, 0.5, 1 and 2.5 μM.

Importantly, sub-IC_{50} concentrations (0.5 and 1 μM) can reverse doxorubicin resistance. Therefore, derivative **4** can be considered as a new P-gp inhibitor useful in combination with classic chemotherapeutics.

CONCLUSIONS

In this work, the reactivity of two natural royleanones was explored to obtain a small library of new P-gp modulators. Several hemisynthetic reactions were performed and successful results were obtained when performing methylation and benzoylation, and introduction of Boc group, affording compounds **20** to **23** as pure with overall good yields.

P-gp inhibition potential of the stable derivatives (**20**–**23**) was evaluated. Previously prepared diterpene **4**, has also been tested. From the tested derivatives, compounds **4** and **23** have significant P-gp inhibitory potential.

Regarding stability and P-gp inhibition potential, results suggest that the formation of benzoyl esters is a more convenient approach for future derivatives with enhanced cytotoxicity. Furthermore, this study suggests that the moieties in positions 6 and 7 of royleanones are also important for interaction with the P-pg. Further studies are needed to disclosure this hypothesis.

Additional studies with royleanone **4**, indicate an increase of anti-P-gp potential in comparison to the natural diterpenes **1**, **2**, and **3**, similar to Dexverapamil inhibitory potential. Moreover, derivative **4**, showed the ability to sensitize the resistant NCI-H460/R cells to doxorubicin. This diterpene could be considered as a novel P-gp inhibitor useful in combination with classic chemotherapeutics.

MATERIALS AND METHODS

Plant Material

The plant material, *P. madagascariensis* (Pers.) Benth. and *P. grandidentatus* Gürke were cultivated in Parque Botânico da Tapada da Ajuda (Instituto Superior Agrário, Lisbon, Portugal) from cuttings obtained from the Kirstenbosch National Botanical Garden (Cape Town, South Africa). Voucher specimens were deposited in Herbarium João de Carvalho e Vasconcellos (ISA). The plant name has been checked with http://www.theplantlist.org (The Plant List. Version 1.1, 2013). The extraction and isolation process of **1** and **2** were performed according to Garcia et al. (2018) and Bernardes et al. (2018), respectively.

Reaction Procedures

The Mitsunobu reactions were carried out with microwave irradiation, according to a previous report (Buonomo and Aldrich, 2015): **1** (10 mg, 0.032 mmol) or **2** (10 mg, 0.026 mmol), corresponding alcohol (5 eq.), triphenylphosphine (5 eq.) and DIAD (5 eq.) in 4.5 ml dry THF, were irradiated with microwaves at 300 W and 60 °C for 45 min under argon atmosphere. Conditions for Carbamoylation: A mixture of **1** (20 mg, 0.064 mmol), DMAP (5 eq.) and excess of the corresponding isocyanate, in 0.5 ml dry CH_2Cl_2, were stirred at room temperature under inert conditions until consumption of the starting material as judged from TLC. Tosylation Conditions: A mixture of **1** (15 mg, 0.048 mmol), triethylamine (4.5 eq.), DMAP (0.3 eq.) and *p*-toluenosulfonyl chloride (3 eq.), in 0.5 ml dry CH_2Cl_2 were stirred until consumption of the starting material as judged from TLC. Introduction of the TBDPS group: A mixture of **1** (15 mg, 0.048 mmol), imidazole (2 eq.) and excess of *tert*-butyldiphenylchlorosilane in 1 ml dry CH_2Cl_2 was stirred at room temperature Thiocarbamoyl: **1** (15 mg, 0.048 mmol) was added to a suspension of sodium hydride (1 eq.) in 0.4 ml THF, followed by sodium iodide (0.5 eq.) and dimethylthiocarbamoyl chloride (1.2 eq.). The mixture was left stirring at room temperature until consumption of the starting material. Introduction of Boc group: A mixture of **1** (15 mg, 0.048 mmol), DMAP (0.5 eq.) and Boc_2O (2.2 eq.) in 0.5 ml of dry CH_2Cl_2 was left stirring at room temperature. Methylation: A mixture of **1** (15 mg, 0.048 mmol) (1 eq.), methyl iodide (8.4 eq.) and silver oxide (8.4 eq.), in 0.5 ml of dry CH_2Cl_2 was left stirring at room temperature. Benzoylation: A mixture of **1** (15 mg, 0.048 mmol) or **2** (10 mg, 0.026 mmol), pyridine (12 eq.) and benzoyl chloride (12 eq.), in 2 ml dry CH_2Cl_2 was left stirring at room temperature until complete consumption of the starting material as judged by TLC.

Semi-preparative HPLC-Diode Array Detector Analysis

The analytical method was carried out in an Agilent Technologies 1200 Infinity Series system with a diode array detector (DAD), equipped with a Zorbax® XDB-C18 (250 × 4.0 mm i.d., 5 μm) column, from Merck and ChemStation Software. The sample was injected in acetone, 10 mg/ml. Each injection was analyzed with a gradient elution mixture composed of solution A (methanol), solution B (acetonitrile), and solution C (0.3% trichloroacetic acid in water) was used as follows: 0 min, 15% A, 5% B, and 80% C; 20 min, 70% A, 30% B and 0% C; 25 min, 70% A, 30% B and 0% C; and 28 min, 15% A, 5% B and 80% C. The flow rate was set at 1 ml/min and 20 μL of the sample were injected.

Chemical Stability Evaluation by LC-MS

LC-MS/MS analysis was performed using a Zorbax Eclipse XBD-C18, 4.6 × 250 mm (5 μm) and the mobile phase consisted of 0.5% formic acid in Milli-Q water (eluent A) and acetonitrile + 0.5% formic acid (eluent B). A flow rate of 0.3 ml/min was used, with the following gradient program: 0–30 min from 70 to 5% A, 30–45 min at 5% A, 45–65 min 70% A.

Cells and Cell Culture

Non-small cell lung carcinoma cell line NCI-H460 was purchased from the American Type Culture Collection, Rockville, MD. NCI-H460/R cells were selected originally from NCI-H460 cells and cultured in a medium containing 100 nM doxorubicin (Pesic et al., 2006). Cell lines were subcultured at 72 h intervals using 0.25% trypsin/EDTA and seeded into a fresh medium at the following densities: 8,000 cells/cm^2 for NCI-H460 and 16,000 cells/cm^2 for NCI-H460/R.

MTT Test

MTT assay is based on the reduction of 3-(4, 5-dimethyl-2-thizolyl)-2,5-diphenyl-2H-tetrazolium bromide into formazan dye by active mitochondria of living cells. Cells grown in 25 cm^2 tissue flasks were trypsinized, seeded into flatbottomed 96-well tissue culture plates (2,000 cells/well), and incubated overnight in 100 μL of appropriate medium. After 24 h, the cells were treated with compounds **1** to **4** (1–25 μM) and incubated for 72 h in complete medium. The combined effects of **4** simultaneously applied with doxorubicin were also studied. In simultaneous treatments, three concentrations of **4** (0.5, 1, and 2 μM) were combined with five concentrations of doxorubicin (0.1, 0.25, 0.5, 1, and 2.5 μM). After 72 h, 100 μL of MTT solution (1 mg/ml) was added to each well, and plates were incubated at 37°C for 4 h. Formazan product was dissolved in 200 ml dimethyl sulfoxide. The absorbance of the obtained dye was measured at 540 nm using an automatic microplate reader (LKB 5060–006 Micro Plate Reader, LKB, Vienna, Austria). Half maximal inhibitory concentration (IC_{50} value) was defined as the concentration of the drug that inhibited cell growth by 50% and calculated by non-linear regression analysis using GraphPad Prism6 software.

Rhodamine 123 Flow Cytometry Assay

Rhodamine 123 accumulation was analyzed by flow cytometry utilizing the ability of Rhodamine 123 to emit fluorescence. The intensity of the fluorescence is proportional to Rhodamine 123 accumulation. Studies were carried out with Dexverapamil and compounds **1** to **4**. NCI-H460 and NCIH460/R cells were grown to 80% confluence in 75 cm^2 flasks, trypsinized, and resuspended in 10 ml centrifuge tubes in a Rhodamine 123-containing medium. The cells were treated with diterpenes and Dexverapamil (5 and 20 μM) and incubated at 37°C in 5% CO_2 for 30 min. At the end of the incubation period, the cells were pelleted by centrifugation, washed with PBS, and placed in cold PBS. The samples were kept on ice in dark until the analysis of the CyFlow Space Partec flow-cytometer (Sysmex Partec GmbH, Germany). The fluorescence of Rhodamine 123 was assessed on the FL1 channel. A minimum of 20,000 events was assayed for each sample and the obtained results were analyzed using Summit Dako Software.

Density Functional Theory

All calculations were performed using the Gaussian 16 software package (Frisch et al., 2016), without symmetry constraints. The PBE1PBE functional was employed in the geometry optimizations. That functional uses a hybrid generalized gradient approximation (GGA), including a 25% mixture of Hartree-Fock (Hehre et al., 1986)

exchange with DFT (Parr and Yang, 1989) exchange-correlation, given by Perdew, Burke, and Ernzerhof functional (PBE) (Perdew, 1986; Perdew et al., 1997). The optimized geometries were obtained with a standard 6–31G(d,p) (Ditchfield et al., 1971; Hehre et al., 1972; Hariharan and Pople, 1974; Gordon, 1980) basis set.

Transition state optimizations were performed with the Synchronous Transit-Guided Quasi-Newton Method (STQN) developed by Peng and Bernhard Schlegel (1993) and Peng et al. (1996). Frequency calculations were performed to confirm the nature of the stationary points, yielding one imaginary frequency for the transition states and none for the minima. Each transition state was further confirmed by following its vibrational mode downhill on both sides and obtaining the minima presented on the energy profile.

DATA AVAILABILITY STATEMENT

The raw data supporting the conclusions of this article will be made available by the authors, without undue reservation, to any qualified researcher.

AUTHOR CONTRIBUTIONS

The manuscript was written through the contributions of all authors.

FUNDING

Support for this work was provided by FCT through UIDP/04567/2020, UIDB/04567/2020, and Ph.D. grant SFRH/BD/137671/2018. CSC-IT center for Science Ltd., Finland is acknowledged for the computational resources' allocation. The Academy of Finland is acknowledged for the financial support to N.R.C (Decisions No. 326487 and 326486).

SUPPLEMENTARY MATERIAL

The Supplementary Material for this article can be found online at: https://www.frontiersin.org/articles/10.3389/fphar.2020.557789/full#supplementary-material

REFERENCES

Amin, M. L. (2013). P-glycoprotein inhibition for optimal drug delivery. *Drug Target Insights* 7, 27–34. doi:10.4137/DTI.S12519.

Bernardes, C. E. S., Garcia, C., Pereira, F., Mota, J., Pereira, P., Cebola, M. J., et al. (2018). Extraction optimization, structural and thermal characterization of the antimicrobial abietane 7α-acetoxy-6β-hydroxyroyleanone. *Mol. Pharm.* 5, 1412–1419. doi:10.1021/acs.molpharmaceut.7b00892.

Bessa, C., Soares, J., Raimundo, L., Loureiro, J. B., Gomes, C., Reis, F., et al. (2018). Discovery of a small-molecule protein kinase Cδ-selective activator with promising application in colon cancer therapy article. *Cell Death Dis.* 9. doi:10.1038/s41419-017-0154-9.

Bray, F., Ferlay, J., Soerjomataram, I., Siegel, R. L., Torre, L. A., and Jemal, A. (2018). Global cancer statistics 2018: GLOBOCAN estimates of incidence and mortality worldwide for 36 cancers in 185 countries. *CA Cancer J. Clin.* 68, 394–424. doi:10.3322/caac.21492.

Bukowski, K., Kciuk, M., and Kontek, R. (2020). Mechanisms of multidrug resistance in cancer chemotherapy. *Int. J. Mol. Sci.* 21, 3233. doi:10.3390/ijms21093233.

Buonomo, J. A., and Aldrich, C. C. (2015). Mitsunobu reactions catalytic in phosphine and a fully catalytic system. *Angew. Chemie - Int. Ed.* 54, 13041–13044. doi:10.1002/anie.201506263.

Burmistrova, O., Simões, M. F., Rijo, P., Quintana, J., Bermejo, J., and Estévez, F. (2013). Antiproliferative activity of abietane diterpenoids against human tumor cells. *J. Nat. Prod.* 76, 1413–1423. doi:10.1021/np400172k.

Dinić, J., Efferth, T., García-Sosa, A. T., Grahovac, J., Padrón, J. M., Pajeva, I., et al. (2020). Repurposing old drugs to fight multidrug resistant cancers. *Drug Resist. Updates* 52, 100713. doi:10.1016/j.drup.2020.100713.

Ditchfield, R., Hehre, W. J., and Pople, J. A. (1971). Self consistent molecular-orbital methods. IX. An extended Gaussian-type basis for molecular-orbital studies of organic molecules. *J. Chem. Phys.* 54, 724–728. doi:10.1063/1.1674902.

Durmus, S., Hendrikx, J. J., and Schinkel, A. H. (2015). Apical ABC transporters and cancer chemotherapeutic drug disposition. *Adv. Cancer Res.* 125, 1–41. doi:10.1016/bs.acr.2014.10.001.

Frisch, M. J., Trucks, G. W., Schlegel, H. B., Scuseria, G. E., Robb, M. A., Cheeseman, J. R., et al. (2016). *Gaussian 16, revision C.01*. Available at: https://gaussian.com/gaussian16/.

Garcia, C., Silva, C. O., Monteiro, C. M., Nicolai, M., Viana, A., Andrade, J. M., et al. (2018). Anticancer properties of the abietane diterpene 6,7-dehydroroyleanone obtained by optimized extraction. *Future Med. Chem.* 1, 1177–1189. doi:10.4155/fmc-2017-0239.

Gazim, Z. C., Rodrigues, F., Amorin, A. C. L., De Rezende, C. M., Sokovic, M., Teševic, V., et al. (2014). New natural diterpene-type abietane from tetradenia riparia essential oil with cytotoxic and antioxidant activities. *Molecules* 19, 514–524. doi:10.3390/molecules19010514.

González, M. A. (2014). Synthetic derivatives of aromatic abietane diterpenoids and their biological activities. *Eur. J. Med. Chem.* 87, 834–842. doi:10.1016/j.ejmech.2014.10.023.

Gordon, M. S. (1980). The isomers of silacyclopropane. *Chem. Phys. Lett.* 76, 163–168. doi:10.1016/0009-2614(80)80628-2.

Hariharan, P. C., and Pople, J. A. (1974). Accuracy of AH n equilibrium geometries by single determinant molecular orbital theory. *Mol. Phys.* 27, 209–214. doi:10.1080/00268977400100171.

Hehre, W. J., Ditchfield, R., and Pople, J. A. (1972). Self-consistent molecular orbital methods. XII. Further extensions of Gaussian-type basis sets for use in molecular orbital studies of organic molecules. *J. Chem. Phys.* 56, 2257–2261. doi:10.1063/1.1677527.

Hehre, W. J., Radom, L., Schleyer, P. v. R., and Pople, J. (1986). *Ab initio molecular orbital theory*. New York: John Wiley & Sons.

Isca, V. M. S., Ferreira, R. J., Garcia, C., Monteiro, C. M., Dinic, J., Holmstedt, S., et al. (2020). Molecular docking studies of royleanone diterpenoids from *Plectranthus* spp. as P-glycoprotein inhibitors. *ACS Med. Chem. Lett.* 11 (5), 839–845. doi:10.1021/acsmedchemlett.9b00642.

Kubínová, R., Pořízková, R., Navrátilová, A., Farsa, O., Hanáková, Z., Bačinská, A., et al. (2014). Antimicrobial and enzyme inhibitory activities of the constituents of Plectranthus madagascariensis (Pers.) Benth. *J. Enzyme Inhib. Med. Chem.* 29, 749–752. doi:10.3109/14756366.2013.848204.

Ladeiras, D., Monteiro, C. M., Pereira, F., Reis, P., Afonso, C. A. M., and Rijo, P. (2016). Reactivity of diterpenoid quinones: royleanones. *Curr. Pharmaceut. Des.* 22, 1682–1714. doi:10.2174/1381612822666151211094521.

Lee, T. D., Lee, O. W., Brimacombe, K. R., Chen, L., Guha, R., Lusvarghi, S., et al. (2019). A high-throughput screen of a library of therapeutics identifies cytotoxic substrates of P-glycoprotein. *Mol. Pharmacol.* 119, 115964. doi:10.1124/mol.119.115964.

Lukhoba, C. W., Simmonds, M. S. J., and Paton, A. J. (2006). Plectranthus: a review of ethnobotanical uses. *J. Ethnopharmacol.* 103, 1–24. doi:10.1016/j.jep.2005.09.011.

Marques, C. G., Pedro, M., Simões, M. F., Nascimento, M. S., Pinto, M. M., and Rodríguez, B. (2002). Effect of abietane diterpenes from *Plectranthus grandidentatus* on the growth of human cancer cell lines. *Planta Med.* 68, 839–840. doi:10.1055/s-2002-34407.

Matias, D., Nicolai, M., Saraiva, L., Pinheiro, R., Faustino, C., Diaz Lanza, A., et al. (2019). Cytotoxic activity of royleanone diterpenes from *Plectranthus madagascariensis* Benth. *ACS Omega* 4, 8094–8103. doi:10.1021/acsomega.9b00512.

Mohammad, I. S., He, W., and Yin, L. (2018). Understanding of human ATP binding cassette superfamily and novel multidrug resistance modulators to overcome MDR. *Biomed. Pharmacother.* 100, 335–348. doi:10.1016/j.biopha.2018.02.038.

Nanayakkara, A. K., Follit, C. A., Chen, G., Williams, N. S., Vogel, P. D., and Wise, J. G. (2018). Targeted inhibitors of P-glycoprotein increase chemotherapeutic-induced mortality of multidrug resistant tumor cells. *Sci. Rep.* 8, 967. doi:10.1038/s41598-018-19325-x.

Parr, R. G., and Yang, W. (1989). Density functional theory of atoms and molecules. New York: Oxford University Press. doi:10.1002/qua.560470107.

Peng, C., Ayala, P. Y., Schlegel, H. B., and Frisch, M. J. (1996). Using redundant internal coordinates to optimize equilibrium geometries and transition states. *J. Comput. Chem.* 17, 49–56. doi:10.1002/(SICI)1096-987X(19960115)17:1<49::AID-JCC5>3.0.CO;2-0.

Peng, C., and Bernhard Schlegel, H. (1993). Combining synchronous transit and quasi-Newton methods to find transition states. *Isr. J. Chem.* 33, 449–454. doi:10.1002/ijch.199300051.

Perdew, J. P., Burke, K., and Ernzerhof, M. (1997). Generalized gradient approximation made simple [Phys. Rev. Lett. 77, 3865 (1996)]. *Phys. Rev. Lett.* 78, 1396. doi:10.1103/PhysRevLett.78.1396.

Perdew, J. P. (1986). Density-functional approximation for the correlation energy of the inhomogeneous electron gas. *Phys. Rev. B* 33, 8822–8824. doi:10.1103/PhysRevB.33.8822.

Pesic, M., Markovic, J. Z., Jankovic, D., Kanazir, S., Markovic, I. D., Rakic, L., et al. (2006). Induced resistance in the human non small cell lung carcinoma (NCI-H460) cell line *in vitro* by anticancer drugs. *J. Chemother.* 18, 66–73. doi:10.1179/joc.2006.18.1.66.

XXX. The plant list. Version 1.1 (2013). Available at: http://www.theplantlist.org/. (Accessed May 15, 2019).

Rice, L. J., Brits, G. J., Potgieter, C. J., and Van Staden, J. (2011). Plectranthus: a plant for the future? *South Afr. J. Bot.* 77, 947–959. doi:10.1016/j.sajb.2011.07.001.

Rijo, P., Duarte, A., Francisco, A. P., Semedo-Lemsaddek, T., and Simões, M. F. (2014a). *In vitro* antimicrobial activity of royleanone derivatives against gram-positive bacterial pathogens. *Phyther. Res.* 28, 76–81. doi:10.1002/ptr.4961.

Rijo, P., Faustino, C., and Simões, M. F. (2013). Antimicrobial natural products from Plectranthus plants. *Formatex Res. Cent.* 2, 922–931.

Rijo, P., Matias, D., Fernandes, A. S., Simões, M. F., Nicolai, M., and Reis, C. P. (2014b). Antimicrobial plant extracts encapsulated into polymeric beads for potential application on the skin. *Polymers.* 6, 479–490. doi:10.3390/polym6020479.

Rijo, P., Faustino, C., and Simões, M. F. (2014). "Antimicrobial natural products from Plectranthus plants; Formatex Research Center," in Microbial pathogens and strategies for combating them: science, technology and education, Editor A. Méndez-Vilas, 922–931, ISBN (13) Vol. 2: 978-84-942134-0-3.

Robey, R. W., Pluchino, K. M., Hall, M. D., Fojo, A. T., Bates, S. E., and Gottesman, M. M. (2018). Revisiting the role of ABC transporters in multidrug-resistant cancer. *Nat. Rev. Canc.* 18, 452–464. doi:10.1038/s41568-018-0005-8.

Robinson, K., and Tiriveedhi, V. (2020). Perplexing role of P-glycoprotein in tumor microenvironment. *Front. Oncol.* 10, 265. doi:10.3389/fonc.2020.00265.

Sharom, F. J. (2007). ABC multidrug transporters: structure, function and role in chemoresistance. *Pharmacogenomics* 9, 105–127. doi:10.2217/14622416.9.1.105.

Wu, J., Lin, N., Li, F., Zhang, G., He, S., Zhu, Y., et al. (2016). Induction of P-glycoprotein expression and activity by aconitum alkaloids: implication for clinical drug–drug interactions. *Sci. Rep.* 6, 25343. doi:10.1038/srep25343.

Conflict of Interest: The authors declare that the research was conducted in the absence of any commercial or financial relationships that could be construed as a potential conflict of interest.

frontiers in Oncology

ORIGINAL RESEARCH
published: 02 December 2020
doi: 10.3389/fonc.2020.597672

Magnolol Suppresses Pancreatic Cancer Development *In Vivo* and *In Vitro via* Negatively Regulating TGF-β/Smad Signaling

Shuo Chen[1], Jiaqi Shen[2], Jing Zhao[3], Jiazhong Wang[1], Tao Shan[1], Junhui Li[1], Meng Xu[1], Xi Chen[1], Yang Liu[1] and Gang Cao[1]**

[1] Department of General Surgery, The Second Affiliated Hospital of Xi'an Jiaotong University, Xi'an Jiaotong University, Xi'an, China, [2] School of Life Science, Xiamen University, Xiamen, China, [3] School of Science, Xi'an Jiaotong University, Xi'an, China

OPEN ACCESS

Edited by:
Patrícia Mendonça Rijo, Universidade Lusófona Research Center for Biosciences & Health Technologies, Portugal

Reviewed by:
Ana Fernandes, Universidade Lusófona Research Center for Biosciences & Health Technologies, Portugal
Qiyang Shou, Zhejiang Chinese Medical University, China
Qinhong Xu, First Affiliated Hospital of Xi'an Jiaotong University, China

***Correspondence:**
Yang Liu
Liu-yang@xjtu.edu.cn
Gang Cao
chenxijiaoda@163.com

Specialty section:
This article was submitted to Pharmacology of Anti-Cancer Drugs, a section of the journal Frontiers in Oncology

Received: 21 August 2020
Accepted: 21 October 2020
Published: 02 December 2020

Citation:
Chen S, Shen J, Zhao J, Wang J, Shan T, Li J, Xu M, Chen X, Liu Y and Cao G (2020) Magnolol Suppresses Pancreatic Cancer Development In Vivo and In Vitro via Negatively Regulating TGF-β/Smad Signaling. Front. Oncol. 10:597672. doi: 10.3389/fonc.2020.597672

Magnolol, a hydroxylated biphenyl extracted from *Magnolia officinalis*, has recently drawn attention due to its anticancer potential. The present study was aimed to explore the effects of Magnolol on restraining the proliferation, migration and invasion of pancreatic cancer *in vivo* and *in vitro*. Magnolol showed significant anti-growth effect in an orthotopic xenograft nude mouse model, and immunohistochemical staining of the xenografts revealed that Magnolol suppressed vimentin expression and facilitated E-cadherin expression. The cytoactive detection using CCK-8 assay showed Magnolol inhibited PANC-1 and AsPC-1 concentration-dependently. Scratch healing assay and the Transwell invasion assay proved the inhibiting effects of Magnolol on cellular migration and invasion at a non-cytotoxic concentration. Western blot and rt-PCR showed that Magnolol suppressed epithelial-mesenchymal-transition by increasing the expression level of E-cadherin and decreasing those of N-cadherin and vimentin. Magnolol suppressed the TGF-β/Smad pathway by negatively regulating phosphorylation of Smad2/3. Moreover, TGF-β1 impaired the antitumor effects of Magnolol *in vivo*. These results demonstrated that Magnolol can inhibit proliferation, migration and invasion *in vivo* and *in vitro* by suppressing the TGF-β signal pathway and EMT. Magnolol could be a hopeful therapeutic drug for pancreatic malignancy.

Keywords: magnolol, pancreatic cancer, TGF-β, epithelial-mesenchymal-transition, Smad

INTRODUCTION

Pancreatic cancer is a common malignancy and ranks as the 7th leading cancer-associated mortality in developed nations (1). Although great improvement has been reached in surgery, chemotherapeutics and radiotherapeutics, the prognosis is still poor due to the local invasion and metastasis upon diagnosis (2, 3). Furthermore, no definite cure strategy can be provided to treat the patients with advanced stages or metastasis (2). Therefore, it is urgent to develop new and effective drugs to treat pancreatic cancer.

Epithelial-mesenchymal-transition (EMT) is an important segment in cancer invasion, metastasis, proliferation and maintenance of stem cell characteristics (4). When EMT occurs,

tumor cells lose epithelial integrity and cell polarity and gain an invasive and motile phenotype (5). Accumulated evidence demonstrates that transforming growth factor-β (TGFβ) signaling is a prime inducer of EMT in the tumor microenvironment (6). The increased pretreatment of soluble TGF-β1 in serum of unresectable pancreatic cancer patients indicates a poor prognosis for chemotherapy (7).

Magnolol (MAG, $C_{18}H_{18}O_2$, CAS Number 528-43-8, PubChem CID 72300) is a natural hydroxylated biphenyl extracted from the root and stem bark of *Magnolia officinalis*, *Magnolia obovata* and *Magnolia grandiflora* (8). Magnolol is reported to have a good safety profile and anti-tumor effects in accumulated studies. Magnolol mediates cell death *via* PI3K/Akt-mediated epigenetic modifications and benefits the management of melanoma (9). Magnolol inhibits the growth and invasion of cholangiocarcinoma cells *via* the NF-kappaB pathway (10). However, whether Magnolol inhibits the EMT and invasion and migration *in vivo*, how it restrains growth of the tumor *in vitro* remains unclear.

In the present study, a pancreatic orthotopic xenograft in a model nude mouse was applied to access the effect of Magnolol on the tumor growth, and pancreatic cancer cell lines (Panc-1 and AsPC-1) were employed to evaluate the impacts of Magnolol on cell biological behavior. TGF-β1-induced EMT was also investigated as a potential mechanism of action of Magnolol.

MATERIALS AND METHODS

Chemicals

Magnolol ($C_{18}H_{18}O_2$, 5'-Diallyl-2,2'-dihydroxybiphenyl, molecular weight: 266.33, purity ≥98%) was purchased from Aladdin Company (Cat. M111378, Aladdin, Shanghai, China). Dimethyl sulfoxide (DMSO, Aladdin, Shanghai, China) was used as solvent. A stock solution of magnolol (125 mM, 332.9 mg magnolol in 10 ml DMSO) was stored at −15°C. Magnolol stock was diluted in PBS (1.5mM for magnolol, 1.2% v/v for DMSO) and PBS-DMSO (1.2%) was served as a negative control. Recombinant Human Transforming Growth Factor β1 (TGF-β1) was obtained from R&D systems (Cat. 240-B-002, Shanghai, China) and dissolved with sterile ddH_2O when need.

Cell Culture

The human pancreatic cancer cell lines PANC-1 and AsPC-1 were obtained from American Type Culture Collection (ATCC, Manassas, VA, USA) and were cultured with DMEM medium with 10% fetal bovine serum (Gibco), 100 U/ml penicillin, and 100 μg/ml streptomycin in incubators under 5% CO_2 at 37°C.

CCK-8 Assay

Approximately 2,000 cells were inoculated in each well of 96-well plates and incubated with a concentration range of Magnolol. A Cell Counting Kit-8 (ab228554, abcam, shanghai China) was applied to test the cellular viability. The experiments were performed five times independently.

Colony Formation Assay

Approximately 200 cells were seeded in each well of 6-well culture plates, and the plates were incubated for 10 h. Then, fresh media containing 0, 15, 30 μM Magnolol were applied to replace the old media, and the samples were then cultured for 14 days. The colonies were fixed in 4% paraformaldehyde (Aladdin, Shanghai, China) and then stained with crystal violet (Aladdin, Shanghai, China). Formatted colonies were gently washed and air seasoned before photos of them were taken. The experiments were performed three times independently.

Transwell Assay for Invasion

Transwell chambers with 24 wells and 8.0-μm pore membranes (Corning USA) were applied following the manufacturer's protocol. Approximately 100,000 cells were seeded in each well in the upper chamber. The upper chamber was filled with serum-free medium which was covered by thin layers of matrigel basement membrane matrix while the lower chamber was filled with complete medium. The invaded cells were fixed with 4% paraformaldehyde and stained with 0.1% crystal violet solution after being incubated for 24 h at 37°C. Photos were taken using light microscopy and the invaded cells in five random fields were counted.

Scratch-Wound Migration Assay

Cells were seeded and confluently cultured in 6-well plates. The scratches were made by scraping with a sterile 1-ml pipette tip in confluently cultured cells. The medium was changed to medium containing 0, 15, or 30 μM Magnolol, and the samples were incubated for 48 h. Photos were captured using a phase-contrast microscope at 0, 24, and 48 h. The rate of cell migration equals the ratio of the coalesced area of the scratch in 48 h to total the area of the scratch at 0 h. The experiments were performed three times independently.

Evaluation of Cell Morphology

To measure changes in cell shape during EMT, we applied the published methods (11). Photos taken by an inverted phase contrast microscope during cell culture were analyzed by Image Plus software. Cell area, major axis, minor axis of random 50 cells per condition were collected and used to calculate the hybrid morphology parameters. Roundness ($4 \times \text{area}/(\pi \times \text{major axis})^2$), for which a high value indicates a high degree of roundness in cell shape (11). Aspect ratio (major axis/minor axis), for which a high value indicates an elongated cell shape (11).

Western Blot

RIPA buffer (Beyotime, China) was applied to obtain total protein from cells. Same amounts of protein were isolated by SDS-PAGE and then passed on to a polyvinylidene difluoride membrane (Millipore). The membrane was incubated with primary antibodies against E-cadherin (wl01482, WanleiBio, Shenyang, China), vimentin (WL01960, WanleiBio), pSMAD2/3 (WL02305, WanleiBio), SMAD2/3 (WL01520, WanleiBio), and β-actin (WL10372, WanleiBio) and were then incubated with HPR-conjugated secondary antibody. Chemiluminescence

reagents (WanleiBio) were applied to visualize Protein bands. The experiments were performed three times independently.

Orthotopic Xenograft Study

Five to six-week-old BALB/C nude mice were purchased from Shanghai SLAC Animal Center (Shanghai, China). An orthotopic xenograft nude mouse model was established by Orthotopic Injection Technique as described previously (12). Briefly, luciferase-tagged AsPC-1 cells (1×10^6/50 μl) were injected into the pancreas of immunocompromised mice. Pinholes were sutured with Prolene 7-0. Once orthotopic xenograft became palpable (approximately 7 days after injection), the mice were divided into two groups randomly (four mice per group). The MAG group received i.p. injection of Magnolol (50 mg/kg, once daily), and the Control group received vehicle (equal amount of DMSO) only. Tumor growth was assessed per week by bioluminescence imaging following intravenous d-luciferin injection (150 mg/kg). Final imaging was obtained at 28 days, and then mice were sacrificed. The primary orthotopic xenografts were harvested, weighed, and fixed in Bouin's solution.

Immunohistochemical Staining

Paraffin specimens of harvested xenografts were cut into 4-μm-thick sections and mounted on silanized slides. The immunohistochemical staining was performed as published (13). The antibodies used were anti-Ki67 (Abcam, ab15580), anti-E-cadherin (Abcam, ab231303), anti-vimentin (Abcam, ab92547) and goat anti-rabbit secondary antibody (Abcam, ab205719). Finally, 3,3-diaminobenzidine was applied to visualize the results, and photographs were taken under a microscope (×100 and ×400).

Statistical Analysis

All data are expressed as the mean ± SD and were analyzed using Student's t test or one-way ANOVA where necessary. GraphPad Prism V6 was applied to analyze and visualize the data. All experiments were performed independently at least 3 times. A P value more than 0.05 was defined as statistically significant.

RESULTS

MAG Inhibits Pancreatic Orthotopic Xenograft Growth in a Mouse Model

We assessed the antitumor effect of MAG with a pancreatic orthotopic xenograft in a mouse model. We chose AsPC-1 for its high tumorigenicity in mice. The experimental design is shown in **Figure 1A**. The living imaging analysis revealed that xenograft progression with MAG treatment was significantly slower compared with that in the control group (**Figures 1B, C**). Additionally, the final harvested xenografts had an average weight of 0.46 g in MAG group compared with 0.28 g in the control group (**Figures 1D, E**). There were no differences among groups besides tumor size, while no signs of toxicity.

EMT and Proliferation Is Restrained in Pancreatic Xenografts of MAG-Treated Mice

EMT plays a critical role in cancer proliferation and maintenance of stem cell characteristics, which is reported to be significant from experimental and clinical points of view (4). We further assessed the effect of MAG on the EMT and proliferation in harvested xenografts. The proliferation and EMT was assessed using immunohistochemical staining for Ki67, E-cadherin and vimentin which are widely accepted markers (14–16). The results showed intense staining of Ki67 and vimentin in xenograft sections from the control group, whereas weak staining was detected in the MAG group (**Figures 2A, B, D**). Furthermore, strong staining of E-cadherin was detected in xenograft sections from the MAG group, while weak staining was detected in the control group (**Figures 2A, C**). These results indicate that MAG restrains EMT and proliferation in pancreatic xenografts in mice.

MAG Suppressed the Viability of Pancreatic Cancer Cells

The impact of Magnolol on the viability of PANC-1 and AsPC-1 cells was determined using an MTT assay. PANC-1 and AsPC-1 cells were incubated with a concentration range of Magnolol for 24, 48, and 72 h. The data revealed that Magnolol suppressed the viability of these cells both time- and concentration-dependently (**Figures 3A, D**). Respectively, the half inhibition concentrations (IC50) on Panc-1 cells were 140.5, 117.3, and 96.4 μM for 24, 48, and 72 h, while the IC50 values on the AsPC-1 cells were 160.0, 104.2, and 75.4 μM. The IC20 and IC10 of Magnolol of Panc-1 cell were 30.7 and 14.0 μM for 48 h, while those of the AsPC-1 cells were 24.6 and 10.6 μM. Panc-1 and AsPC-1 cells incubated with Magnolol at 15 and 30 μM for 14 days showed compromised capability in colony formation assay (**Figures 3B, C, E, F**).

Magnolol Suppressed Cellular Migration and Invasion *In Vitro*

The scratch-wound assay showed that Magnolol treatment weakened the migration of cancer cells (**Figures 4A–D**). MAG-treated cells displayed epithelial-like phenotype while untreated cells showed mesenchymal-like phenotype in morphology (**Figure 4E**). The treatment of Magnolol (30 μM) in PANC-1 and (15μM & 30 μM) in AsPC-1 caused significant increase in Roundness and decrease in Aspect ratio (**Figures 4G, H**). Magnolol treatment reduced the invasive rate of PANC-1 and AsPC-1 cells in transwell invasion assay (**Figures 4F, I**). These findings indicated that the inhibiting effects of Magnolol on migration and invasion may be related to EMT.

Magnolol Inhibited EMT *via* the Suppression of TGF-β1/Smad Signaling

TGF-β1 is the main inducer of EMT in the tumor microenvironment (17). To further explore the mechanism of action, the expression levels of EMT-associated genes and TGF-β signaling were detected in Magnolol-treated cells. Western blot showed elevated expression of E-cadherin and reduced expression of Vimentin in Magnolol-treated cells at the protein level (**Figures 5A–C**). Considering that

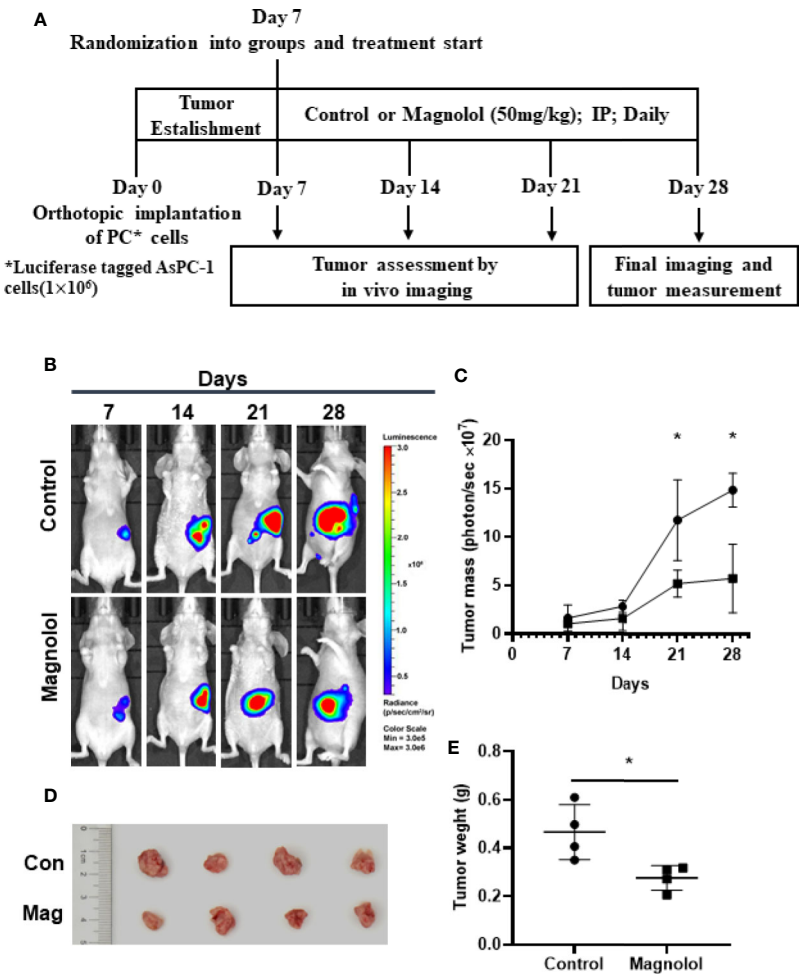

FIGURE 1 | Magnolol (MAG) inhibits pancreatic orthotopic xenograft growth in a mouse model. **(A)** Schematic representation of *in vivo* treatment strategy. **(B)** Images by the living imaging analysis of mice from both the groups at different time points. **(C)** Tumor growth curve (total photons per second) showing tumor growth at different time points. **(D)** The image and **(E)** weight of the tumors harvested at the end point. *$P < 0.05$.

the phosphorylation of Smads is a critical event in the TGF-β signaling, we determined the phosphorylation level of Smad2/3 in Magnolol-treated cells using western blot. The results showed that Magnolol reduced the phosphorylation of Smad2/3 in PANC-1 and AsPC-1 cells (**Figures 5A–C**).

Magnolol Abolished TGF-β1-Induced Migration and Invasion *In Vitro*

Because Magnolol restrained the migration, invasion and altered the cell morphology, we further explored whether these effects of Magnolol relied on TGF-β1-induced EMT. Cancer cells were incubated with 10 ng/ml TGF-β1 cytokine alone or with 15 μM of Magnolol for 48 h. TGF-β1 significantly promoted the migration and invasion and Magnolol markedly impaired these effects of TGF-β1 in the PANC-1 and AsPC-1 cells (**Figure 6**). The morphological characteristics these cells were more mesenchymal after being induced by 10 ng/ml TGF-β1 alone than when incubated with 10 ng/ml TGF-β1 cytokine and 15 μM Magnolol (**Figure 7A**). The Roundness was significantly decreased while the Aspect ratio was significantly increased after being induced by 10 ng/ml TGF-β1 (**Figure 7B**). These effects were abolished by 15 μM Magnolol treatment (**Figure 7B**). Western blot showed that incubation of cancer cells with Magnolol and TGF-β1 simultaneously markedly decreased the levels of E-cadherin and phosphorylation of Smad2/3 compared with incubation with TGF-β1 alone (**Figures 7C–F**). These results demonstrated that Magnolol suppressed the aggressive behavior of these cells by inhibiting TGF-β1-induced EMT.

DISCUSSION

Current study was aimed to explore the therapeutic effect of Magnolol on pancreatic cancer *in vivo* and *in vitro*. Magnolol inhibited pancreatic tumor development in mouse model and suppressed the aggressive behavior of pancreatic cancer cells in a

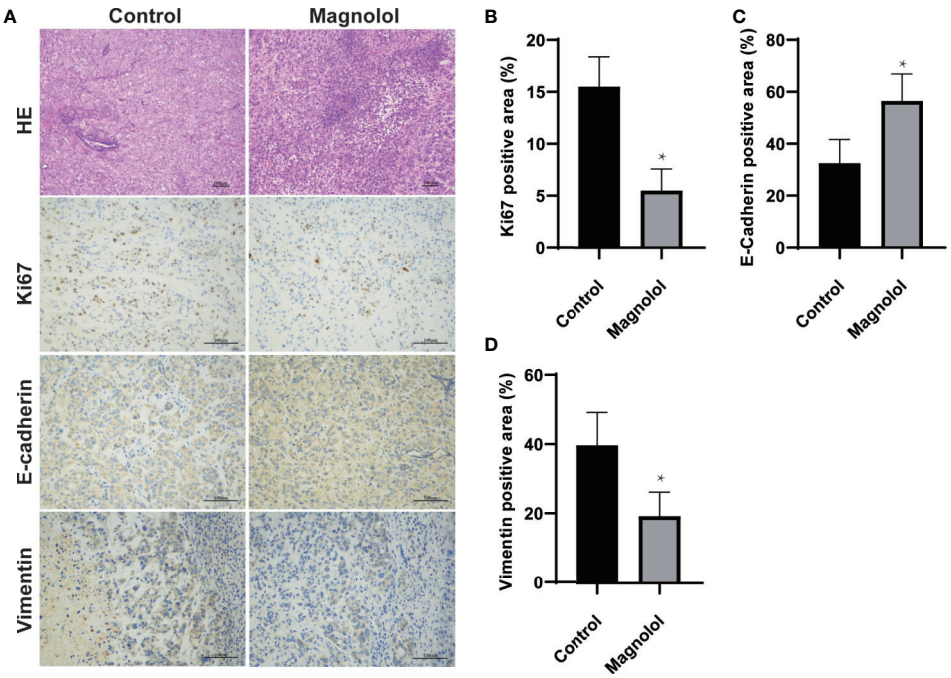

FIGURE 2 | Epithelial-mesenchymal-transition (EMT) and proliferation is restrained in pancreatic xenografts of Magnolol (MAG)-treated mice. **(A)** HE staining was applied to confirm the xenografts formation while Immunohistochemical staining was used to access the expression of Ki67, E-cadherin and vimentin. **(B–D)** The expression of Ki67, E-cadherin and vimentin were analyzed. *$P < 0.05$.

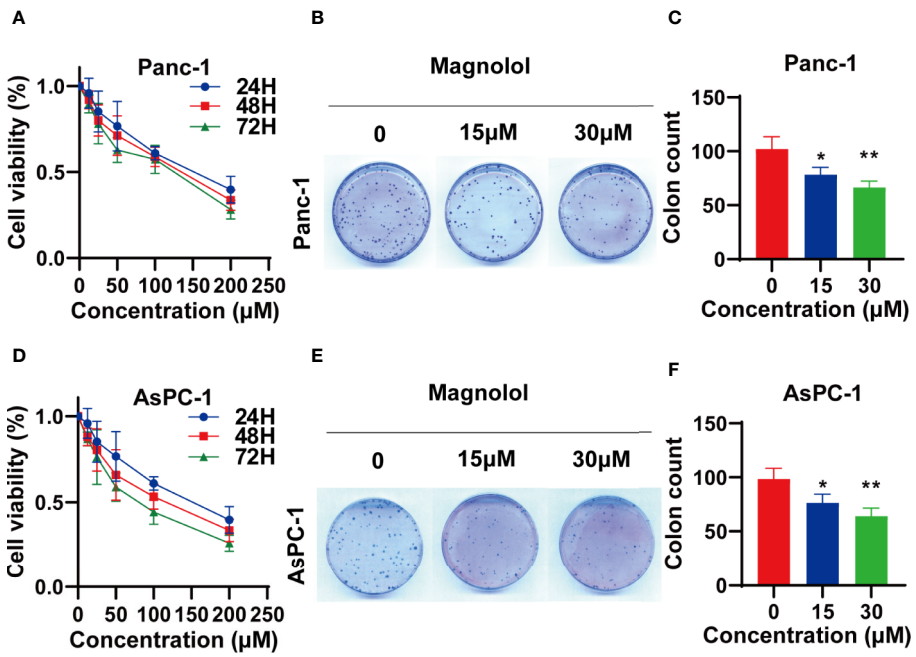

FIGURE 3 | Magnolol (MAG) suppressed the viability of pancreatic cancer cells **(A, D)** MAG suppressed the viability of Panc-1 and AsPC-1 in time- and concentration-dependent manner. **(B, C, E, F)** MAG (15 or 30 μM) reduced colony formation of Panc-1 and AsPC-1. *P < 0.05; **P < 0.01.

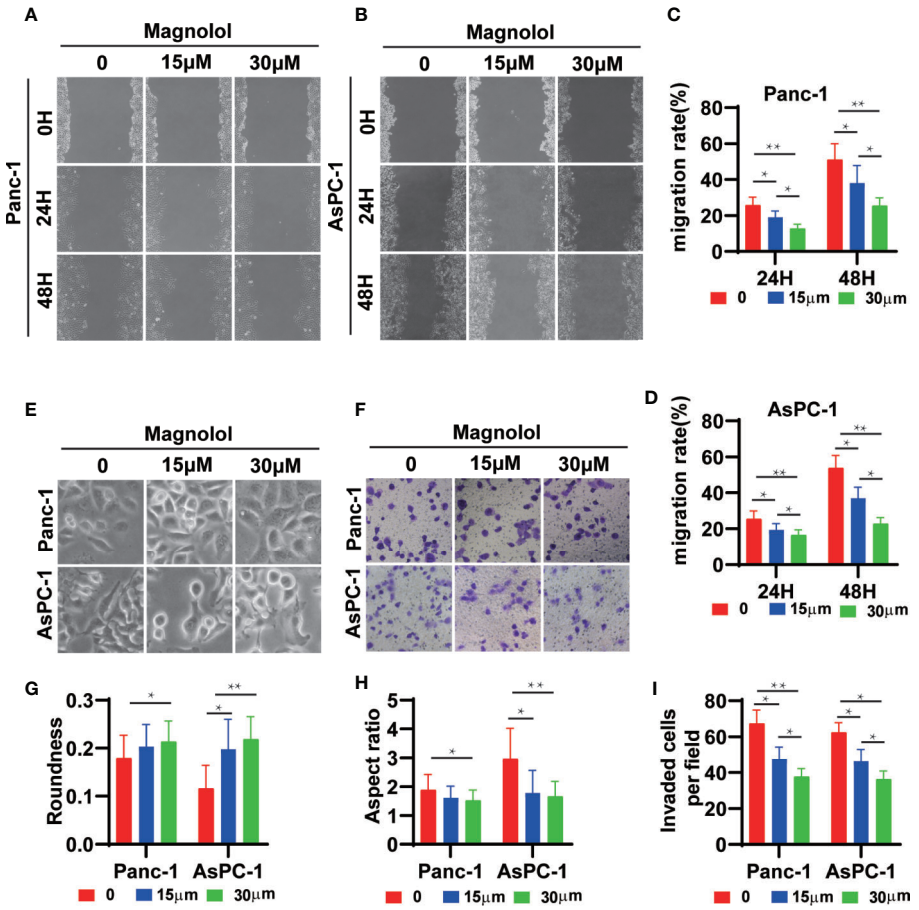

FIGURE 4 | Magnolol Suppressed Cellular Migration and Invasion *in vitro* **(A, B)** The wound-healing of cells treated with Magnolol(0, 15, 30 μM) was shown at 0, 24 and 48 h after scratching. **(C, D)** The results of the scratch-wound assay were analyzed. **(E)** Morphological changes in Panc-1 and AsPC-1 cells after culture with Magnolol(0, 15, 30 μM). **(G, H)** Evaluation of cell morphology for Panc-1 and AsPC-1 cells after culture with Magnolol(0, 15, 30 μM). **(F, I)** Transwell invasion assay showed Magnolol treatment reduced the invasive rate of PANC-1 and AsPC-1 cells. *P < 0.05; **P < 0.01.

time- and concentration-dependent manner. As far as we know, the current study is the first to demonstrate these effects of Magnolol on pancreatic cancer. These data suggested that Magnolol inhibited TGF-β1-induced EMT *via* negatively regulating the phosphorylation of Smad2/3. Thus, we recommend Magnolol as a potential therapeutic for the treatment of pancreatic cancer. Further study will be needed to confirm molecular targets and loci.

Metastasis is a hallmark of tumors that contributes to cancer-associated death (18). The majority of patients are found with metastasis when diagnosed with pancreatic cancer (19). Tumor metastasis refers to a multi-step process of tumor cell migration from the primary site to distant sites (4). Epithelial-to-mesenchymal transition (EMT) features the evanishment of adhesion between cells accompanied by elevated levels of epithelial markers and reduced levels of mesenchymal markers (4). A series of pathways including Wnt, β-catenin, Notch, and tyrosine kinases is related to the induction of EMT. Among them, TGF-β1 is known as not only an inflammatory cytokine but also a pivotal inducer and sustainer of EMT (20). EMT is closely involved in not only invasion and metastasis but also proliferation and chemotherapy resistance. TGF-β-induced EMT plays an important role in PDAC progression, especially in metastases (20). Once bonded to its receptor on the cytomembrane, TGF-β induces phosphorylation of its downstream factors, including but not limited to SMAD proteins. The phosphorylated SMAD2/3 and SMAD4 subsequently form a regulatory complex that promotes the transcription of target genes (21).

Magnolol is a natural neolignan from magnolia plants and is reported to present antitumor, anti-oxidative, anti-inflammatory, and antibacterial effects (8). The antitumor properties of magnolol were reported to be related but not limited to the PI3K-AKT, p53, NF-κB, and p53-mediated mitochondrial pathways (9, 10, 22, 23). Unlike well-reported anti-proliferative effects, the anti-metastasis effects of magnolol are not as well studied. Magnolol has been reported to inhibit the ERK-modulated metastatic potential of hepatocellular carcinoma cells (24) and the HER2-modulated metastatic potential of ovarian cancer cells (25). Moreover, magnolol suppresses

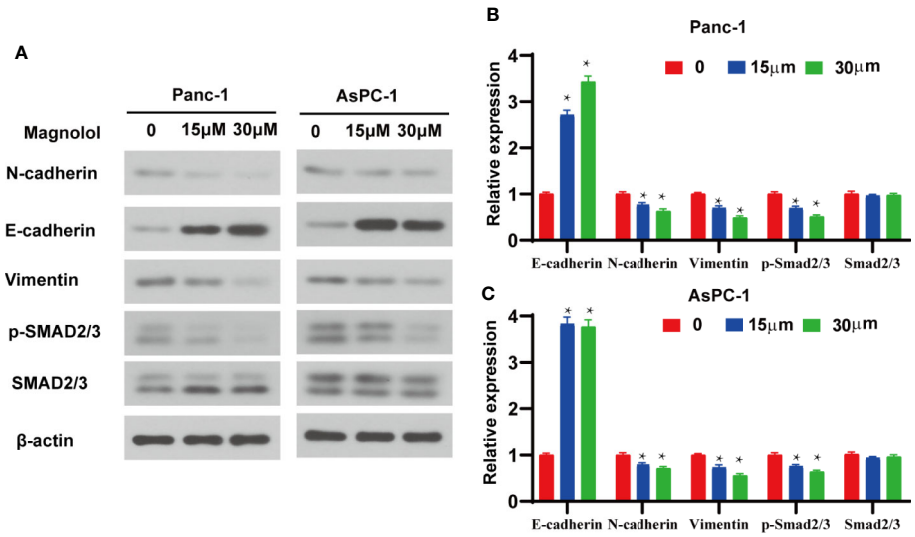

FIGURE 5 | Magnolol inhibited epithelial-mesenchymal-transition (EMT) *via* the suppression of transforming growth factor-β1 (TGF-β1)/Smad Signalling. **(A)** Western blot analysis of protein levels of E-cadherin, N-cadherin, Vimentin, p-Smad2/3, Smad2/3 in Panc-1 and AsPC-1 cells treated with Magnolol(0, 15, 30 μM) for 48 h. **(B, C)** Histograms show the change of relative protein expression of E-cadherin, N-cadherin, Vimentin, p-Smad2/3, Smad2/3 in Panc-1 and AsPC-1 cells treated with Magnolol(0, 15, 30 μM) for 48 h. *P < 0.05.

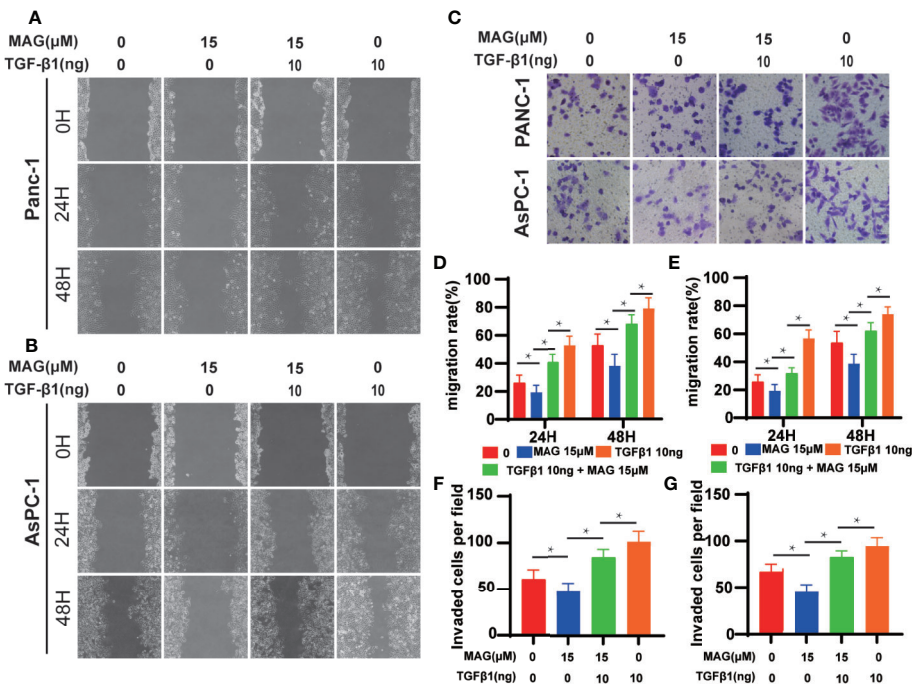

FIGURE 6 | Magnolol abolished transforming growth factor-β1 (TGF-β1)-Induced Migration and Invasion *in vitro*. **(A, B)** The wound-healing of cells treated with with Magnolol or TGF-β1 was shown at 0, 24, and 48 h after scratching. **(D, E)** The migration rate of the scratch-wound assay was analyzed. **(E)** Morphological changes in Panc-1 and AsPC-1 cells after culture with Magnolol or TGF-β1. **(C, F, G)** Transwell invasion assay showed Magnolol treatment abolished TGF-β1 induced invasion of PANC-1 and AsPC-1 cells. *P < 0.05.

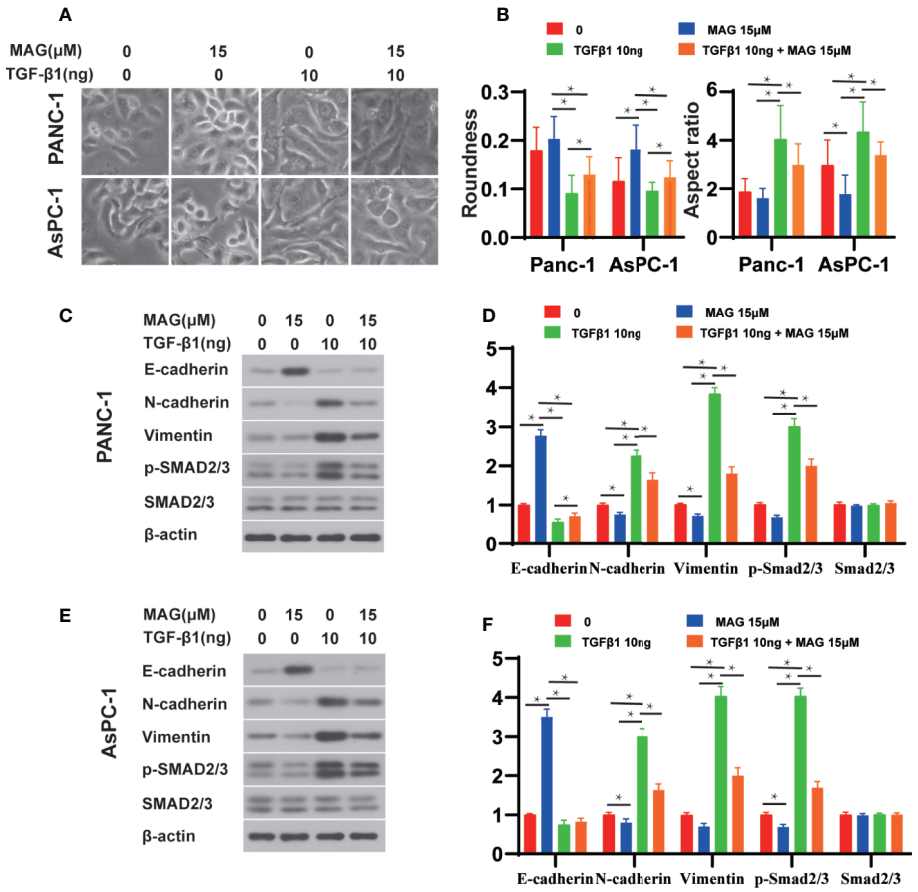

FIGURE 7 | Magnolol abolished transforming growth factor-β1 (TGF-β1)-Induced epithelial-mesenchymal-transition (EMT) amd phosphorylation of Smad2/3 *in vitro*. **(A)** Morphological changes in Panc-1 and AsPC-1 cells after culture with Magnolol or TGF-β1. **(B)** Evaluation of cell morphology for Panc-1and AsPC-1 treated with Magnolol or TGF-β1. **(C, E)** Western blot results of E-cadherin, N-cadherin, Vimentin, p-Smad2/3, Smad2/3 in Panc-1or AsPC-1 treated with Magnolol or TGF-β1. **(D, F)** Histograms show the changes of relative expression of E-cadherin, N-cadherin, Vimentin, p-Smad2/3, Smad2/3 in Panc-1or AsPC-1 treated with Magnolol or TGF-β1. *P < 0.05.

metastasis *via* matrix metalloproteinase-2/-9 activities in prostate carcinoma cells (26). However, the anti-metastatic function of magnolol remains unclear, especially in pancreatic cancer. In default of known research on this issue, we conducted this research.

The TGF-β/Smad signaling pathway is related to the occurrence of neurological disorders, fibrosis and malignancies (6). The TGF-β pathway presents a growth-repressive effect in the early stage of tumorigenesis in the pancreas by facilitating cell cycle arrest and apoptosis. Conversely, TGF-β signaling accelerates tumor progression in advanced-stage pancreatic cancer by inducing EMT, metastasis, invasion, migration, and immune evasion (27). In fact, the contribution of TGFβ to metastases has been well proven in pancreatic cancer (28, 29). Zhang et al. showed that Magnolol reduces bleomycin-induced rodent lung fibrosis by reducing TGF-β1 expression (30). Chei et al. reported that Magnolol does not influence apoptosis, but restrains cell migration, invasion and EMT in human colorectal tumor cells *via* suppressing the TGF-β pathway (31).

In the current study, we explored the effects of magnolol on pancreatic cancer *in vivo* and *in vitro*. First, the anti-tumor effect of magnolol was verified using orthotopic xenograft, and the changes in the expression of EMT markers were detected using immunohistochemical staining. Second, we studied the role of magnolol in impairing TGF-β1-mediated migration, invasion, proliferation and EMT in pancreatic cancer cells. Cancer cells were cultured with different concentrations of magnolol for 24, 48, and 72 h to explore the concentration-effect relationship. We chose concentrations of magnolol that suppress migration and invasion without inducing apparent cell proliferation arrest to perform our experiments. As published, 10 ng/ml of TGF-β1 induced EMT and facilitated pancreatic cancer cell migration and invasion (32, 33). We confirmed the EMT-inductive effects of that concentration in pancreatic cancer cells and then used it in our experiments. Our study verified that EMT played an important role in the aggressive actions of pancreatic cancer, while magnolol suppressed the migration, invasion, and proliferation of pancreatic cancer *via* EMT *in vivo* and *in vitro*.

There are also some limitations in our research. First, we studied the anti-tumor effects of magnolol on EMT by the Smad-dependent TGF-β pathway; however, the Smad-independent TGF-β pathway or other signaling pathways related to EMT and cancer were not detected. Second, while we found that magnolol suppressed phosphorylation of SMAD2/3, we did not verify the responsible molecular site of action. Third, we observed the tumor-suppressing effect of magnolol *in vitro*, and we focused on cancer cells to explore the antitumor effects of magnolol, but the effect of magnolol on the tumor environment also needs investigation. It will be necessary to perform in-depth research on the effects and mechanism of magnolol to determine whether magnolol could be used in the treatment of pancreatic cancer.

DATA AVAILABILITY STATEMENT

The raw data supporting the conclusions of this article will be made available by the authors, without undue reservation.

ETHICS STATEMENT

The animal study was reviewed and approved by animal ethics committee of Xi'an Jiaotong University.

AUTHOR CONTRIBUTIONS

All authors listed have made a substantial, direct, and intellectual contribution to the work and approved it for publication.

FUNDING

The project was supported by National Natural Science Foundation of China, NSFC (No:82003998, 81602401); Natural Science Foundation of Shaanxi Province (No: 2019JQ-969); and the Xi'an Jiaotong University Education Foundation, XJTUEF (No: xjj2018141).

REFERENCES

1. Siegel RL, Miller KD, Jemal A. Cancer statistics, 2019. *CA Cancer J Clin* (2019) 69:7–34. doi: 10.3322/caac.21551
2. Peixoto RD, Speers C, McGahan CE, Renouf DJ, Schaeffer DF, Kennecke HF. Prognostic factors and sites of metastasis in unresectable locally advanced pancreatic cancer. *Cancer Med* (2015) 4:1171–7. doi: 10.1002/cam4.459
3. Von Hoff DD, Ervin T, Arena FP, Chiorean EG, Infante J, Moore M, et al. Increased survival in pancreatic cancer with nab-paclitaxel plus gemcitabine. *N Engl J Med* (2013) 369:1691–703. doi: 10.1056/NEJMoa1304369
4. Tanabe S, Quader S, Cabral H, Ono R. Interplay of EMT and CSC in Cancer and the Potential Therapeutic Strategies. *Front Pharmacol* (2020) 11:904. doi: 10.3389/fphar.2020.00904
5. Faheem MM, Seligson ND, Ahmad SM, Rasool RU, Gandhi SG, Bhagat M, et al. Convergence of therapy-induced senescence (TIS) and EMT in multistep carcinogenesis: current opinions and emerging perspectives. *Cell Death Discov* (2020) 6:51. doi: 10.1038/s41420-020-0286-z
6. Batlle E, Massague J. Transforming Growth Factor-beta Signaling in Immunity and Cancer. *Immunity* (2019) 50:924–40. doi: 10.1016/j.immuni.2019.03.024
7. Park H, Bang JH, Nam AR, Park JE, Jin MH, Bang YJ, et al. The prognostic role of soluble TGF-beta and its dynamics in unresectable pancreatic cancer treated with chemotherapy. *Cancer Med* (2020) 9:43–51. doi: 10.1002/cam4.2677
8. Ranaware AM, Banik K, Deshpande V, Padmavathi G, Roy NK, Sethi G, et al. Magnolol: A Neolignan from the Magnolia Family for the Prevention and Treatment of Cancer. *Int J Mol Sci* (2018) 19:2362. doi: 10.3390/ijms19082362
9. Emran AA, Chinna Chowdary BR, Ahmed F, Hammerlindl H, Huefner A, Haass NK, et al. Magnolol induces cell death through PI3K/Akt-mediated epigenetic modifications boosting treatment of BRAF- and NRAS-mutant melanoma. *Cancer Med* (2019) 8:1186–96. doi: 10.1002/cam4.1978
10. Zhang FH, Ren HY, Shen JX, Zhang XY, Ye HM, Shen DY. Magnolol suppresses the proliferation and invasion of cholangiocarcinoma cells via inhibiting the NF-kappaB signaling pathway. *Biomed Pharmacother Biomed Pharmacother* (2017) 94:474–80. doi: 10.1016/j.biopha.2017.07.085
11. Uynuk-Ool T, Rothdiener M, Walters B, Hegemann M, Palm J, Nguyen P, et al. The geometrical shape of mesenchymal stromal cells measured by quantitative shape descriptors is determined by the stiffness of the biomaterial and by cyclic tensile forces. *J Tissue Eng Regener Med* (2017) 11:3508–22. doi: 10.1002/term.2263
12. Hotz HG, Reber HA, Hotz B, Yu T, Foitzik T, Buhr HJ, et al. An orthotopic nude mouse model for evaluating pathophysiology and therapy of pancreatic cancer. *Pancreas* (2003) 26:e89–98. doi: 10.1097/00006676-200305000-00020
13. Shan T, Chen S, Chen X, Lin W, Li W, Ma J, et al. Association of family history of tumors with clinicopathological characteristics and prognosis of colorectal cancer. *Eur J Cancer Prev* (2019) 28:258–67. doi: 10.1097/CEJ.0000000000000482
14. Menon SS, Guruvayoorappan C, Sakthivel KM, Rasmi RR. Ki-67 protein as a tumour proliferation marker. *Clin Chim Acta* (2019) 491:39–45. doi: 10.1016/j.cca.2019.01.011
15. Sommariva M, Gagliano N. E-Cadherin in Pancreatic Ductal Adenocarcinoma: A Multifaceted Actor during EMT. *Cells* (2020) 9:1040. doi: 10.3390/cells9041040
16. Strouhalova K, Prechova M, Gandalovicova A, Brabek J, Gregor M, Rosel D. Vimentin Intermediate Filaments as Potential Target for Cancer Treatment. *Cancers (Basel)* (2020) 12:181. doi: 10.3390/cancers12010184
17. Dudas J, Ladanyi A, Ingruber J, Steinbichler TB, Riechelmann H. Epithelial to Mesenchymal Transition: A Mechanism that Fuels Cancer Radio/Chemoresistance. *Cells* (2020) 9:428. doi: 10.3390/cells9020428
18. Ksiazkiewicz M, Markiewicz A, Zaczek AJ. Epithelial-mesenchymal transition: a hallmark in metastasis formation linking circulating tumor cells and cancer stem cells. *Pathobiology* (2012) 79:195–208. doi: 10.1159/000337106
19. Zhao C, Gao F, Li Q, Liu Q, Lin X. The Distributional Characteristic and Growing Trend of Pancreatic Cancer in China. *Pancreas* (2019) 48:309–14. doi: 10.1097/MPA.0000000000001222
20. Dardare J, Witz A, Merlin JL, Gilson P, Harle A. SMAD4 and the TGFbeta Pathway in Patients with Pancreatic Ductal Adenocarcinoma. *Int J Mol Sci* (2020) 21:3534. doi: 10.3390/ijms21103534
21. Chen Y, Di C, Zhang X, Wang J, Wang F, Yan JF, et al. Transforming growth factor beta signaling pathway: A promising therapeutic target for cancer. *J Cell Physiol* (2020) 235:1903–14. doi: 10.1002/jcp.29108
22. Li M, Zhang F, Wang X, Wu X, Zhang B, Zhang N, et al. Magnolol inhibits growth of gallbladder cancer cells through the p53 pathway. *Cancer Sci* (2015) 106:1341–50. doi: 10.1111/cas.12762
23. Zhou S, Wen H, Li H. Magnolol induces apoptosis in osteosarcoma cells via G0/G1 phase arrest and p53-mediated mitochondrial pathway. *J Cell Biochem* (2019) 120:17067–79. doi: 10.1002/jcb.28968
24. Kuan LY, Chen WL, Chen JH, Hsu FT, Liu TT, Chen WT, et al. Magnolol Induces Apoptosis and Inhibits ERK-modulated Metastatic Potential in

Hepatocellular Carcinoma Cells. *Vivo (Athens Greece)* (2018) 32:1361–8. doi: 10.21873/invivo.11387

25. Chuang TC, Hsu SC, Cheng YT, Shao WS, Wu K, Fang GS, et al. Magnolol down-regulates HER2 gene expression, leading to inhibition of HER2-mediated metastatic potential in ovarian cancer cells. *Cancer Lett* (2011) 311:11–9. doi: 10.1016/j.canlet.2011.06.007
26. Hwang ES, Park KK. Magnolol suppresses metastasis via inhibition of invasion, migration, and matrix metalloproteinase-2/-9 activities in PC-3 human prostate carcinoma cells. *Biosci Biotechnol Biochem* (2010) 74:961–7. doi: 10.1271/bbb.90785
27. Zhang Y, Li JH, Yuan QG, Cao G, Yang WB. Upregulation of LASP2 inhibits pancreatic cancer cell migration and invasion through suppressing TGF-beta-induced EMT. *J Cell Biochem* (2019) 120:13651–7. doi: 10.1002/jcb.28638
28. Hong E, Park S, Ooshima A, Hong CP, Park J, Heo JS, et al. Inhibition of TGF-beta signalling in combination with nal-IRI plus 5-Fluorouracil/Leucovorin suppresses invasion and prolongs survival in pancreatic tumour mouse models. *Sci Rep* (2020) 10:2935. doi: 10.1038/s41598-020-59893-5
29. Ottaviani S, Stebbing J, Frampton AE, Zagorac S, Krell J, de Giorgio A, et al. TGF-beta induces miR-100 and miR-125b but blocks let-7a through LIN28B controlling PDAC progression. *Nat Commun* (2018) 9:1845. doi: 10.1038/s41467-018-03962-x
30. Zhang H, Ju B, Zhang X, Zhu Y, Nie Y, Xu Y, et al. Magnolol Attenuates Concanavalin A-induced Hepatic Fibrosis, Inhibits CD4(+) T Helper 17 (Th17) Cell Differentiation and Suppresses Hepatic Stellate Cell Activation: Blockade of Smad3/Smad4 Signalling. *Basic Clin Pharmacol Toxicol* (2017) 120:560–70. doi: 10.1111/bcpt.12749
31. Chei S, Oh HJ, Song JH, Seo YJ, Lee K, Lee BY. Magnolol Suppresses TGF-beta-Induced Epithelial-to-Mesenchymal Transition in Human Colorectal Cancer Cells. *Front Oncol* (2019) 9:752. doi: 10.3389/fonc.2019.00752
32. Ellenrieder V, Hendler SF, Boeck W, Seufferlein T, Menke A, Ruhland C, et al. Transforming growth factor beta1 treatment leads to an epithelial-mesenchymal transdifferentiation of pancreatic cancer cells requiring extracellular signal-regulated kinase 2 activation. *Cancer Res* (2001) 61:4222–8.
33. Wang H, Wu J, Zhang Y, Xue X, Tang D, Yuan Z, et al. Transforming growth factor β-induced epithelial-mesenchymal transition increases cancer stem-like cells in the PANC-1 cell line. *Oncol Lett* (2012) 3:229–33. doi: 10.3892/ol.2011.448

Conflict of Interest: The authors declare that the research was conducted in the absence of any commercial or financial relationships that could be construed as a potential conflict of interest.

frontiers in Pharmacology

ORIGINAL RESEARCH
published: 29 April 2021
doi: 10.3389/fphar.2021.518406

A Combined Phytochemistry and Network Pharmacology Approach to Reveal Potential Anti-NSCLC Effective Substances and Mechanisms in *Marsdenia tenacissima* (Roxb.) Moon (Stem)

Pei Liu[1,2], *Dong-Wei Xu*[1,2], *Run-Tian Li*[1,2], *Shao-Hui Wang*[3], *Yan-Lan Hu*[1,2], *Shao-Yu Shi*[1,2], *Jia-Yao Li*[1,2], *Yu-He Huang*[1,2], *Li-Wei Kang*[1,2] *and Tong-Xiang Liu*[1,2]*

[1]*School of Pharmacy, Minzu University of China, Beijing, China,* [2]*Key Laboratory of Ethnomedicine (Minzu University of China), Minority of Education, Beijing, China,* [3]*Medical College of Qingdao Binhai University, Affiliated Hospital of Qingdao Binhai University, Qingdao, China*

Marsdeniae tenacissimae Caulis is a traditional Chinese medicine, named Tongguanteng (TGT), that is often used for the adjuvant treatment of cancer. In our previous study, we reported that an ethyl acetate extract of TGT had inhibitory effects against adenocarcinoma A549 cells growth. To identify the components of TGT with anti-tumor activity and to elucidate their underlying mechanisms of action, we developed a technique for isolating compounds, which was then followed by cytotoxicity screening, network pharmacology analysis, and cellular and molecular experiments. We isolated a total of 19 compounds from a TGT ethyl acetate extract. Two novel steroidal saponins were assessed using an ultra-performance liquid chromatography-photodiode array coupled with quadrupole time-of-flight mass (UPLC-ESI-Q/TOF-MS). Then, we screened these constituents for anti-cancer activity against non-small cell lung cancer (NSCLC) *in vitro* and obtained six target compounds. Furthermore, a compound-target-pathway network of these six bioactive ingredients was constructed to elucidate the potential pathways that controlled anticancer effects. Approximately 205 putative targets that were associated with TGT, as well as 270 putative targets that were related to NSCLC, were obtained from online databases and target prediction software. Protein–protein interaction networks for drugs as well as disease putative targets were generated, and 18 candidate targets were detected based on topological features. In addition, pathway enrichment analysis was performed to identify related pathways, including PI3K/AKT, VEGF, and EGFR tyrosine kinase inhibitor resistance, which are all related to metabolic processes and intrinsic apoptotic pathways involving reactive oxygen species (ROS). Then, various cellular experiments were conducted to validate drug-target mechanisms that had been predicted using network pharmacology analysis. The experimental results showed the four C21 steroidal saponins could upregulate Bax and downregulate Bcl-2 expression, thereby changing the mitochondrial membrane potential, producing ROS, and

OPEN ACCESS

Edited by:
Francisco Estévez, University of Las Palmas de Gran Canaria, Spain

Reviewed by:
Chee Wun How, Monash University Malaysia, Malaysia
Juan Francisco Leon, University of South Carolina, United States

***Correspondence:**
Tong-Xiang Liu
tongxliu123@hotmail.com

Specialty section:
This article was submitted to Ethnopharmacology, a section of the journal Frontiers in Pharmacology

Received: *27 March 2020*
Accepted: *12 February 2021*
Published: *29 April 2021*

Citation:
Liu P, Xu D-W, Li R-T, Wang S-H, Hu Y-L, Shi S-Y, Li J-Y, Huang Y-H, Kang L-W and Liu T-X (2021) . Front. Pharmacol. 12:518406. doi: 10.3389/fphar.2021.518406

releasing cytochrome C, which finally activated caspase-3, caspase-9, and caspase-8, all of which induced apoptosis in A549 cells. In addition, these components also downregulated the expression of MMP-2 and MMP-9 proteins, further weakening their degradation of extracellular matrix components and type IV collagen, and inhibiting the migration and invasion of A549 cells. Our study elucidated the chemical composition and underlying anti-tumor mechanism of TGT, which may be utilized in the treatment of lung cancer.

Keywords: *Marsdeniae tenacissimae*, C21 steroidal saponins, network pharmacology, migration, invasion, apoptosis, A549 cells, NSCLC

INTRODUCTION

Lung cancer severely affects human health and survival and has become the main cause of cancer-related deaths over the past several years (Gu et al., 2018). An estimated 1.6 million individuals have received a diagnosis of lung cancer, resulting in more than 1.3 million deaths worldwide in the past decade (Torre et al., 2015). In 2017, the US pointed out that approximately 85–90% of lung cancer cases were non-small cell lung cancer (NSCLC) (DeSantis et al., 2016; Paci et al., 2017). Over the past 10 years, various major advances in cancer research have uncovered the genetics and pathologies of NSCLC, facilitating the development of novel anticancer drugs (Hare et al., 2017). Interestingly, multiple bioactive ingredients obtained from Chinese herbal medicine have been considered potential candidates for the treatment of cancer (Tang et al., 2009; Gao et al., 2020).

Marsdeniae tenacissimae Caulis is the dried lianoid stem of *Marsdenia tenacissima* (Roxb.) Moon (Fam. Asclepiadaceae), known as "Tong-guang-teng" or "Tong-guang-san", recorded in the 2009 edition of "Standards of Traditional Chinese Medicines in Hunan Province" and the 2020 edition of "Pharmacopeia of the People's Republic of China", and it can suppress cough, relieve wheezing, dispel phlegm, unblock lac feminium, clear heat, and remove toxins (Commission, C. P., 2020). The medicinal use of this plant can be traced back to the Ming Dynasty and was primarily recorded in "Dian Nan Ben Cao" by Mao Lan (1397–1470) (Wang et al., 2018). Extensive evidence indicates that C21 steroid glycosides, extracted by ethyl acetate from TGT, have a significant inhibitory effect against different cancer cell lines, such as A549, Caco-2, SACC83, PC-3, K562, and HepG2 (Ye et al., 2014; Wang et al., 2015). We found that the four C21 steroidal glycosides isolated from TGT had a higher rate of inhibition of A549 cells proliferation than other cell lines (Xu, 2018; Hu et al., 2020). To elucidate the relationship between the chemical structure and cytotoxic activities of steroidal glycosides and to investigate the anti-cancer mechanism of TGT, we isolated and characterized novel compounds from this medicinal plant.

Over the past decade, network-based pharmacological analyses have been employed to assess the mechanisms of herbs and formulae as well as their potential bioactive components at both the molecular and systemic levels (Fang et al., 2017). In particular, network pharmacology has been utilized by Chinese medicine researchers in order to predict the interactions between various components and targets (Mao et al., 2017; Zhang et al., 2019). Furthermore, network pharmacology is also a useful *in silico* prediction tool for identifying active components and elucidating the mechanisms of herbal medicines that, in turn, allows more investigations of these bioactive compounds.

This study developed an approach that integrated cytotoxicity screening, phytochemical analysis, cellular and molecular biology, and network pharmacology construction to identify effective antitumor substances and the underlying mechanisms of TGT. To our knowledge, this is the first integral study that employed several methods to identify efficacious antitumor substances and elucidated their mechanisms of action.

MATERIALS AND METHODS

Chemicals and Materials

The dry cane of TGT was procured from Huayu Pharmaceutical Co., Ltd. (Guangzhou, Guangdong, China). Reference standards of TGT and marsdenoside H (purity >98%) (purity were obtained from the National Institutes for Food and Drug Control (Beijing, China). Four C21 steroidal glycosides, 11α-*O*-benzoyl-12β-*O*-tigloyltenacigenin B (TGT-**15**), marsdenoside C (TGT-**7**), 11α-*O*-tigloyl-12β-*O*-benzoyltenacigenin B (TGT-**9**), and 11α-*O*-2-methylbutyryl-l2β-*O*-benzoyltenacigenin B (TGT-**13**), were isolated from an ethyl acetate extract of TGT in our laboratory, and their purities were all >98% based on HPLC normalization and silica gel TLC analysis (Xu, 2018). Dulbecco's modified Eagle's medium (DMEM) was obtained from Gibco Invitrogen (Carlsbad, CA, United States). Fetal bovine serum (FBS) was obtained from Hyclone, Co. (Fremont, CA, United States). A549 cells were obtained from the National Infrastructure of Cell Line Resource (Beijing, China). Annexin-FITC cell apoptosis assay and cell cycle assay kits were obtained from Sanjian Biotechnology Co. (Tianjin, China). Reactive oxygen species and mitochondrial membrane potential assay kits were obtained from Boster Biological Technology (Wuhan, Hubei, China). Primary antibodies against MMP-2, cleaved caspase-3, Bcl-2, Bax, cytochrome C, and GAPDH were obtained from Abcam (Cambridge, United Kingdom). MMP-9, cleaved caspase-9, and cleaved caspase-8 were obtained from Shanghai Rebiosci Biotechnology Co.

(Shanghai, China), and β-actin was obtained from Sigma–Aldrich (St. Louis, MO, United States). A CX-21 Ordinary Optical Microscope was obtained from Olympus (Shanghai, China). A DR-200Bs ELISA instrument was obtained from Wuxi Hiwell Diatek Instruments Co., Ltd (Wuxi, Jiangsu, China). A FACSCalibur flow cytometer was obtained from Becton, Dickinson and Company (BD, United States).

Marsdeniae tenacissimae Extract Preparation

The dry cane of *Marsdeniae tenacissimae* (5.0 kg) was soaked overnight in 85% ethanol-H_2O until fully saturated and was extracted with 90 l 85% ethanol-H_2O three times for two hours each time. The ethanol solvent was then concentrated under reduced pressure to yield a crude lysate, of which 940.3 g was obtained using an extractor at room temperature (25°C). The total ethanol extract was dissolved in water with a total volume of 5 l and then partitioned with petroleum ether (4 L × 4) for depigmentation, yielding 35.1 g of extract. The aqueous layer was sequentially partitioned with ethyl acetate (4 L × 8) and n-butanol (4 L × 8) to yield ethyl acetate-soluble (370.1 g) and n-butanol-soluble (340.0 g) fractions, respectively. The remaining part was the aqueous layer (154.7 g).

Marsdeniae tenacissimae Separation and Purification

The ethyl acetate layer extract was dissolved in organic solvent, and thin-layer chromatography was used to screen a solvent elution system. This ethyl acetate-soluble fraction was then subjected to silica gel column chromatography (using 10 times the amount of extract) and was eluted with petroleum ether–acetone (v/v, 50:1, 30:1, 10:1, 5:1, 3:1, 2:1, or 1:1) to obtain fractions Fr.1 to Fr.9 based on their TLC profiles. Fr.3 was mixed with a portion of Fr.4, and Fr.7 was mixed with a portion of Fr.8.

Fraction 1 was fractionated by silica gel column chromatography and was eluted with $CHCl_3$–MeOH to obtain six fractions, namely, Fr.1.1–Fr.1.6 based on TLC analysis. Fr.1.3 and Fr.1.5 were fractionated on an ODS column with a 40–80% methanol–water gradient elution to obtain 4 (17.0 mg), 12 (9.6 mg), and 20 (10.5 mg), respectively.

Fraction 2 was fractionated using silica gel column chromatography and was eluted with $CHCl_3$–MeOH to obtain six fractions, namely, Fr.2.1–Fr.2.6, based on TLC analysis. Fr.2.1 and Fr.2.4 on the ODS column with a methanol–water gradient were eluted to obtain 3 (17.5 mg), 9 (10.5 mg), and 10 (18.1 mg).

Fraction 3 was separated by silica gel column chromatography and preparative PHPLC (detection at a wavelength of 210 nm, 55% MeOH, 2.2 ml/min) to obtain 1 (10.6 mg), 2 (15.6 mg), 7 (10.8 mg), and 8 (15.6 mg). Fr.3.2 was resolved by ODS column chromatography and was eluted with $CHCl_3$–MeOH to obtain 5 (13.3 mg). Fr.3.4 was resolved using ODS column chromatography, eluted with $CHCl_3$–MeOH, and assessed using PHPLC (detection wavelength: 210 nm, 30% acetonitrile, and 2.2 ml/min) to obtain 11 (15.6 mg) and 19 (4.2 mg).

Fraction 5 was resolved by silica gel column chromatography and was eluted with $CHCl_3$–MeOH to obtain three fractions, Fr.5.1–Fr.5.3, based on TLC analysis. Fr.5.2 was resolved by ODS column chromatography and was eluted with MeOH–water to obtain 6 (4.8 mg).

Fraction 6 was resolved by silica gel column chromatography and was eluted with $CHCl_3$–MeOH to obtain four fractions, Fr.6.1–Fr.6.4, based on TLC analysis. Fr.6.1 was resolved by ODS column chromatography and was eluted with MeOH–water to obtain 13 (6.4 mg). Fr.6.4 was also resolved by ODS column chromatography and was eluted with MeOH–water. Subsequently, the distillates were further resolved by Sephadex LH-20 column chromatography and were eluted with MeOH–water to obtain 17 (4.0 mg).

Fraction 7 was resolved by silica gel column chromatography and was eluted with $CHCl_3$–MeOH to obtain six fractions, Fr.7.1–Fr.7.6, using TLC analysis. Fr.7.2 was resolved by Sephadex LH-20 column chromatography and was eluted with MeOH–water to obtain 14 (6.4 mg). Fr.7.4 was separated by preparative PHPLC (detection at 210 nm, 30% acetonitrile, 2.2 ml/min) to obtain 15 (4.0 mg).

Fraction 9 was resolved using Sephadex LH-20 column chromatography and was eluted with MeOH–water and was further separated by silica gel column chromatography to obtain 18 (6.0 mg). **Figure 1** shows the specific extraction and separation process.

Spectral Data

Compound 15, white powder, $[\alpha]_D^{20}$ −43.224 (c 0.0188, CH_3OH); UV λ_{max} (CH_3OH)/nm: 202 nm. IR (KBr) λ_{max} 3,384 cm^{-1}, 12,963 cm^{-1}, 2,930 cm^{-1}, 2,868 cm^{-1}, 1,736 cm^{-1}, 1,456 cm^{-1}, 1,364 cm^{-1}, 1,170 cm^{-1}, 1,070 cm^{-1}, 1,022 cm^{-1}, 972 cm^{-1}, 835 cm^{-1}; HR-ESI-MS: m/z 573.4 $[M+Na]^+$, 551.6 $[M+H]^+$, 585.4 $[M+Cl]^-$, 549.1 $[M-H]^-$, $C_{33}H_{42}O_7$;^{1}H NMR ($CDCl_3$, 500 MHz), δ_H: 1.25 (1H, m, H-1a), 1.25 (1H, m, H-1b), 132 (1H, m, H-2), 3.56 (3H, m, H-3), 1.40 (2H, m, H-3), 1.42 (2H, m, H-4), 2.05 (1H, m, H-6), 1.90 (2H, m, H-7), 2.18 (1H, d, J = 10.2 Hz, H-9), 5.66 (1H, t, J = 10.2 Hz, H-11, 5.66 (1H, t, J = 10.2 Hz, H-125.66 (1H, tH, m, H-15), 2.40 (2H, m, H-16), 2.96 (1H, d, J = 7.2 Hz, H-1725.66 (1H, tH, m, H-15)$_3$), 1.10 (3H, s, 19-CH_3), 2.23 (3H, s, 21-CH_3), 7.88 (2H, d, J = 7.8 Hz, H-3′, 7′), 7.36 (2H, t, J = 7.8 Hz, H-4′, 6′), 7.50 (1H, t, J = 7.2 Hz, H-5′), 7.36 (2H, t, J = 7.8 Hz, H-4′, 6′), 7.88 (2H, d, J = 7.8 Hz, H-3′,7′), 6.57 (1H, q, J = 6.0 Hz, H-3″), 1.49 (3H, d, J = 6.6 Hz, 4″-CH3), 1.45 (3H, s, 5″-CH_3).^{13}C NMR ($CDCl_3$,125 MHz) δ_C: 37.3 (C-1), 31.3 (C-2), 70.5 (C-3), 38.3 (C-4), 44.0 (C-5), 26.7 (C-6), 31.8 (C-7), 66.9 (C-8), 51.2 (C-9), 38.9 (C-10), 69.7 (C-11), 74.7 (C-12), 46.1 (C-13), 71.5 (C-14), 26.7 (C-15), 25.0 (C-16), 59.8 (C-17), 16.6 (C-18), 12.8 (C-19), 211.0 (C-20), 30.3 (C-21), 166.1 (C-1′), 130.3 (C-2′), 129.6 (C-3′), 128.2 (C-4′), 132.9 (C-5′), 128.2 (C-6′), 129.6 (C-7′), 167.4 (C-1″), 127.6 (C-2″), 138.3 (C-3″), 14.2 (C-4″), 11.5 (C-5″).

Compound **18**, white powder, $[\alpha]_D^{20}$16.118 (c 0.0225, CH_3OH); UV λ_{max} (CH_3OH)/nm: 216 nm; IR λ_{max}: 3,390 cm^{-1}, 2,927 cm^{-1}, 2,860 cm^{-1}, 1,687 cm^{-1}, 1,441 cm^{-1}, 1,382 cm^{-1}, 1,272 cm^{-1}, 1,245 cm^{-1}, 1.129 cm^{-1}, 1.023 cm^{-1}, 897 cm^{-1}, 873 cm^{-1}; HR-ESI-MS: m/z 695.6 $[M+H]^+$, 671.7 $[M-Na]^-$, $C_{29}H_{51}NaO_{17}$; ^{1}H NMR (CD_3OD, 500 MHz), δ_H: 2.66 (each 1H, dd, J = 4.8, 9.6 Hz,

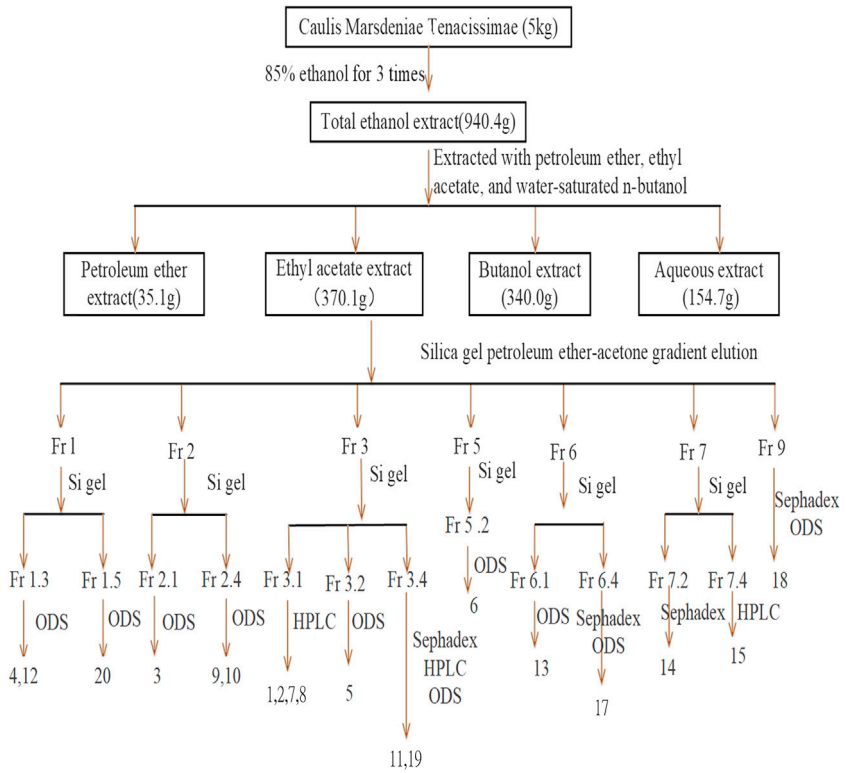

FIGURE 1 | Separation and purification processes.

H-2), 2.86 (each 1H, dd, J = 4.8, 9.6 Hz, H-2), 3.98 (1H, m, H-3), 3.55 (1H, dd, J = 3.6, 8.4 Hz, H-4), 3.63 (1H, m, H-5), 1.19 (3H, d, J = 7.2 Hz, H-6), 2.61 (each 1H, dd, J = 4.8, 9.6 Hz, H-2′), 2.81 (each 1H, dd, J = 4.8, 9.6 Hz, H-2′), 4.05 (1H, m, H-3′), 3.61 (1H, m, H-4′), 3.71 (1H, m, H-5′), 1.23 (3H, d, J = 7.8 Hz, H-6′), 3.39 (3H, s, H-OCH_3), 3.68 (3H, s, H-1′-OCH_3), 3.41 (3H, s, H-3′-OCH_3), 4.60 (1H, d, J = 9.6 Hz, H-Allo-1), 3.18 (1H, m, H-Allo-2), 3.62 (1H, m, H-Allo-3), 3.35 (1H, m, H-Allo-4), 3.92 (1H, m, H-Allo-5), 1.30 (3H, d, J = 7.8 Hz, H-Allo-6), 3.59 (3H, s, H-3-OCH_3), 4.70 (1H, d, J = 10.2 Hz, H-Allo-1′), 3.18 (1H, m, H-Allo-2′), 3.62 (1H, m, H-Allo-3′), 3.35 (1H, m, H-Allo-4′), 4.32 (1H, m, H-Allo-5′), 1.47 (3H, d, J = 7.8 Hz, H-Allo-6′), 3.61 (3H, s, H-3′-OCH_3); ^{13}C NMR (CD_3OD, 125 MHz) δ_C: 173.4 (C-1), 33.8 (C-2), 79.7 (C-3), 84.0 (C-4), 71.1 (C-1), 18.1 (C-5), 174.2 (C-1′), 36.3 (C-2′), 79.0 (C-3′), 82.6 (C-4′), 71.1 (C-5′), 18.1 (C-6′), 57.5 (C-3-OCH_3), 52.1 (C-1′-OCH_3), 58.9 (C-3′-OCH_3), 102.7 (C-Allo-1), 75 (C-Allo-2), 83.7 (C--Allo-4), 73.6 (C-Allo-4), 68.3 (C-Allo-5), 20.0 (C-Allo-6), 62.5 (C-3-OCH_3), 103.9 (C-Allo-1′), 74.9 (C-Allo-2′), 83.7 (C-Allo-3′), 74.0 (C-Allo-4′), 78.0 (C-Allo-5′), 19.3 (C-Allo-6′), 62.5 (C-3′-OCH_3).

Constituent Identification

All LC-MS and MS/MS results were processed using MassLynx™ (V4.1). Molecular formula estimations of the compounds were performed using Elemental Composition software (Waters Technologies, Milford, MA, United States). Structure determination of the main compounds, such as the chemical structure, precise molecular mass, as well as potential molecular fragmentation pathways, was performed using Mass Fragment software. Previously published compounds were collected by comprehensively searching various databases such as PubMed[1], Chemspider[2], HMDB[3], and Metlin[4] (Guijas and Siuzdak, 2018). Validation of compounds with standard materials was performed using reference standards.

Cell Culture

A549 cells were propagated in Dulbecco's modified Eagle medium (DMEM) supplemented with 10% fetal bovine serum (FBS) and 1% penicillin-streptomycin at 37°C in a humid atmosphere with 5% CO_2.

Cytotoxicity Experiment

The cytotoxic effects of *M. tenacissimae* extracts were assessed using the CCK-8 calorimetric procedure. Briefly, cells (density: 5×10^3 cells/well) were seeded into 96-well plates and cultured for 24 h. The supernatant was then discarded, and the cells were treated with extracts at various concentrations using a volume of 100 ul in 96-well plates to which DMEM was added with serum.

[1]https://www.ncbi.nlm.nih.gov/pubmed
[2]http://www.chemspider.com/
[3]http://www.hmdb.ca/
[4]https://metlin.scripps.edu/landing_page.php?pgcontent=mainPage

Five wells were used for each concentration. Five blank controls with only the medium (no addition of cells) were used as the negative control group. After incubation for 24 h, the original medium in each well was replaced with 100 µl of medium containing 10% CCK-8. Thereafter, the 96-well plates were placed in an incubator for 3 h. The absorbance of each well at a wavelength of 450 nm was then determined with a microplate reader (TECAN, Switzerland). The experiment was performed three times in parallel.

Network Pharmacology Construction and Analysis

ChemSketch was used to draw the structure of the above six C21 steroidal saponins and to obtain their SMILES number. Then, we used SciFinder[5] to confirm their molecular structure and obtained their CAS numbers. The Swiss Target Prediction[6] (Gfeller et al., 2014) and STITCH[7] (Kuhn et al., 2010) databases were used to screen potential targets of six C21 steroidal glycosides. The DigSee (Kim et al., 2017). DisGeNET[8] (Pinero et al., 2015) and OMIM[9] databases (Amberger et al., 2015) were employed to screen potential targets of NSCLC. Furthermore, the targets of disease were matched with the targets of the compound, and a compound-target-NSCLC network was constructed with Cytoscape 3.7.2 (Settle et al., 2018). The KEGG[10] database (Amberger et al., 2015) was used to enrich the target signal pathway. Then, the compound-target and target-pathway networks were merged to obtain a compound-target-pathway network. String APP in Cytoscape 3.7.2 was employed, and the Network analysis and Generatestyle functions were used to generate the protein-target-interaction network. DAVID[11] was used to conduct Gene Ontology (GO) and KEGG pathway analyses. Finally, we used the KEGG Mapper tool to obtain and integrate the pathway related to the anti-NSCLC effect of the six C21 steroidal saponins.

Migration Assay

The IC_{50} values of compounds TGT-7, TGT-9, TGT-13, and TGT-15 were determined to be 28.36, 44.01, 29.03, and 47.33 µm, respectively, in a previous study (Xu, 2018; Hu et al., 2020). Based on the IC_{50} values of compounds, we determined the concentration necessary for tests with A549 cells. A549 cells (density: 1×10^6 cells per well) were first seeded into six-well plates. Upon reaching a confluency of 90%, the A549 monolayer was scraped in the middle of each well using a 20 µl pipette tip, and then the plates were washed three times with PBS, and media with TGT-**7**, TGT-**9**, TGT-**13**, and TGT-**15** were added separately at concentrations of 28 µM, 44 µM, 29 µM, and 47 µM, respectively, for 36 h. The control group was supplemented with DMEM. Then, three fields of every wound were selected, and the rate of wound closure was calculated using ImageJ (Wayne Rasband, National Institutes of Health, United States).

INVASION ASSAY

Matrigel® was left to stand at 4°C overnight and was then thawed. The Matrigel® gel was prepared with serum-free medium at a final concentration of 1 mg/ml. Approximately 100 µl of the prepared Matrigel® gel was vertically added to the bottom of the upper chamber, and 600 ul of each well consisting of 10% FBS was placed in the lower chamber. Then, 1×10^5 A549 cells were resuspended in 100 µl in the bottom of the well, supplemented with 0.1% BSA and TGT-**7** (28 µM), TGT-**9** (44 µM), TGT-**13** (29 µM), or TGT-**15** (47 µM) and cultured for 48 h to allow cell migration across the filter membrane. Cell fixation was performed with methanol for 30 min, followed by 1% crystal violet staining for 25 min and the washing away of excess crystal violet stain. A total of five images were randomly captured with an inverted microscope, which were then used to count the number of transmembrane cells.

Cell Cycle Analysis

Cell cycle analysis was conducted using flow cytometry. A549 cells were treated with TGT-**7** (28 µM), TGT-**9** (44 µM), TGT-**13** (29 µM), and TGT-**15** (47 µm) for 24 h, and then the cell pellet was washed three times in ice-cold PBS. The cells were shaken using 70% ethanol and resuspended in a −20°C refrigerator for at least 24 h. After the cells were fixed, they were centrifuged at 1,000 rpm for 5 min. The ethanol was discarded, and the cells were washed three times in ice-cold PBS. The cells were then centrifuged, the supernatant was decanted, and the cell pellet was resuspended in annexin-binding buffer. Then, 0.5 ml of PI/rnase was added to the cells and left to stand in the dark for approximately 15 min. Cell cycle analysis was immediately conducted using flow cytometry.

Cell Apoptosis Analysis

Cell apoptosis was analyzed using flow cytometry. A549 cells were treated with TGT-**7** (28 µM, 56 µM), TGT-**9** (44 µM, 88 µM), TGT-**13** (29 µM, 58 µM), and TGT-**15** (47 µM, 94 µM) for 24 h. Then, the supernatants were collected in a 15 ml centrifuge tube, and the adherent cells were trypsinized, detached, and collected in a corresponding centrifuge tube and centrifuged at 1,000 rpm for 5 min. Then, the supernatant was discarded, and the cells were washed twice using 1× binding buffer and were sequentially stained with Annexin V and PI following the manufacturer's instructions. Finally, the A549 cells were observed by fluorescence microscopy and then analyzed by flow cytometry.

Mitochondrial Membrane Potential Assay

JC-1, a cationic fluorescent dye when added to living cells, is known to be localized exclusively in mitochondria, particularly in good physiological conditions characterized by sufficient mitochondrial membrane potential ($\Delta\Psi$). The current paper is

[5]https://sso.cas.org/as/kNab3/resume/as/authorization.ping
[6]http://www.swisstargetprediction.ch/
[7]http://stitch.embl.de/
[8]http://www.disgenet.org/
[9]https://omim.org/
[10]https://www.genome.jp/kegg/ligand.html
[11]https://david.ncifcrf.gov/relatedGenes.jsp

dealing with the study of differences in the effects of four compounds (TGT-7, TGT-9, TGT-13, and TGT-15) on the JC-1 loading and fluorescence in A549 cells. A549 cells were treated with TGT-7 (28 μM), TGT-**9** (44 μM), TGT-**13** (29 μM), and TGT-**15** (47 μM), respectively, for 24 h. Then, the A549 cells were stained using JC-1 at 37°C for 20 min, and images were captured using a fluorescence microscope. A decrease in the mitochondrial membrane potential was indicated by a change in the wavelength, i.e., from red to green. ImageJ was used to assess the intensity of red and green fluorescent emissions, which represented potential alterations in the mitochondrial membrane.

Intracellular ROS Detection

The amount of intracellular ROS produced was determined using an ROS assay. After the A549 cells were treated with TGT-**7** (28 μM), TGT-**9** (44 μM), TGT-**13** (29 μM), and TGT-**15** (47 μM) for 24 h, the A549 cells were incubated in the presence of 10 μM DCFH-DA at 37°C for 30 min, followed by washing twice using PBS. Finally, the A549 cells were assessed under a fluorescence microscope and were processed by flow cytometry to measure DCFH-DA fluorescence.

Western Blotting

A549 cells that were treated with various concentrations of TGT-**7** (28 and 56 μM), TGT-**9** (44 and 88 μM), TGT-**13** (29 and 58 μM), and TGT-**18** (47 and 94 μM), were lyzed using RIPA buffer containing protease inhibitors. Then, the BCA assay was performed to determine protein concentrations. Proteins were resolved by SDS-PAGE and then immunoblotted onto PVDF membranes. MMP-2, MMP-9, caspase-9, caspase-3, and caspase-8, Bax, Bcl-2, and cytochrome C primary antibodies were used to detect the corresponding proteins, followed by incubation with the corresponding secondary antibodies. Finally, ImageJ (developed by the National Institute of Health) was used to quantify the immunoblots, and the images presented are representative of three separate experiments.

Statistical Analysis

The experimental data were analyzed using SPSS 20.0. Unless otherwise stated, the data were presented as the arithmetic means of three independent experiments. The results were shown as the mean ± SD. We employed one-way ANOVA to assess variance when homogeneous variance was observed, with the least significant difference (LSD). In addition, the Dunnett T3 test was utilized when the variance was determined to be not uniform. Statistical significance was considered at $^{*}p < 0.05$, $^{**}p < 0.01$, and $^{***}p < 0.001$ in the analyses of TGT-**7**-, TGT-**9**-, TGT-**13**-, and TGT-**15**-treated *vs.* untreated control cells.

RESULTS

Characterization of *Marsdeniae tenacissimae* Caulis Chemical Constituents

In this study, we reported the isolation of 19 compounds from the dry cane of *Marsdeniae tenacissimae* Caulis. We elucidated their structures, which included two novel compounds, namely, 11α-*O*-benzoyl-12β-*O*-tigloyltenac-igenin B (15, 4.0 mg) (**Figure 2**, **Table 1**) and sodium 5-hydroxy-4-(((2*S*,3*R*,4*S*,5*R*,6*R*)-5-hydroxy-3-(((2*R*,3*R*,4*R*,5R,6*S*)-5-hydroxy-6-((2-hydroxy-4,6-dimethoxy-6-oxohexan-3-yl)oxy)-4-methoxy-2-methyltetrahydro-2H-pyran-3-yl)oxy)-4-methoxy-6-methyltetrahydro-2H-pyran-2-yl)oxy)-3-methoxyhexanoate (18, 6.0 mg) (**Figure 3**, **Table 1**), as well as 17 other known compounds (1–14, 17, 19, 20) (**Figure 4**, **Supplementary Tables S1, S2**).

Compound **15** was obtained as a white powder. It was identified qualitatively by TLC and colored with anisaldehyde and concentrated sulfuric acid, displaying a yellow–green color, and dark spots were observed under a UV lamp at a wavelength of 254 nm. The ion peaks at m/z 573.4 $[M+Na]^+$, 551.6 $[M+H]^+$, 585.4 $[M+Cl]^-$, and 549.1 $[M-H]^-$ for positive and negative ions were obtained using ESI-MS and were assumed to have a molecular weight of 550.3 $[\alpha]_D^{20}$–43.224 (c 0.0188, CH_3OH). Elemental analysis indicated that the molecular formula was $C_{33}H_{42}O_7$, and its unsaturation number was 13. The ^{1}H-NMR and ^{13}C-NMR spectra (**Table 1**, **Supplementary Figure S1**) were similar to compound **9** and showed a phenyl ring signal. The ^{1}H-NMR spectrum had a monophenyl ring-substituted matrix signal at δ_H 7.36 (2H, t, J = 7.8 Hz), 7.50 (1H, t, J = 7.8 Hz), and 7.88 (2H, d, J = 7.8 Hz), corresponding to the C (128.2, 129.6, 132.9, 138.3, 166.1) signal on the phenyl ring in our ^{13}C-NMR spectrum, and thus was assumed to be a benzoyl moiety. In addition, the ^{1}H-NMR spectrum showed a methylbutyryl signal at δ_H 1.49 (3H, d, J = 6.6 Hz, -CH_3), 1.45 (3H, s, -CH_3), δ_H 2.23 (3H, s, 21-CH_3), and 6.57 (1H, q, J = 7.2 Hz), and combined with the ^{13}C-NMR spectra at δ_C 127.6, 130.3 had two olefinic carbon signals, with δ_C 167.4 being the carbonyl signal of the methacryloyl group. In addition, δ_C 211.0 was a 20-position

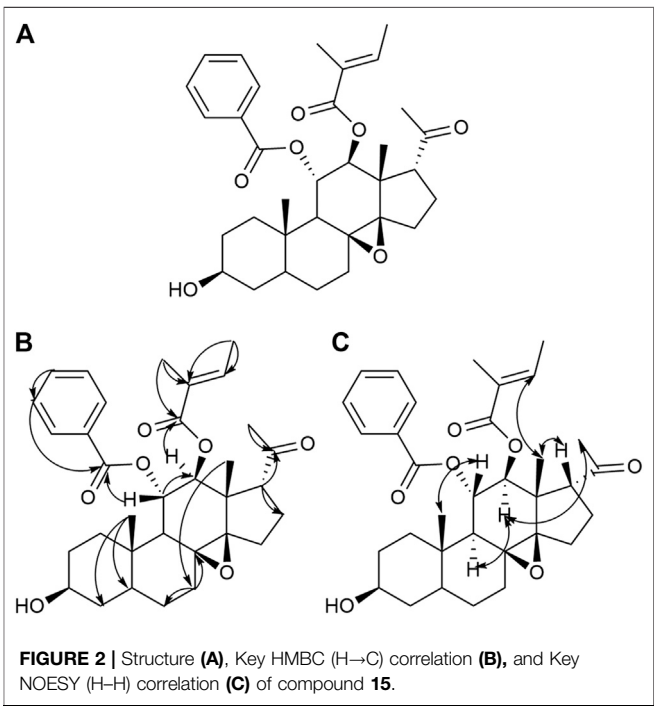

FIGURE 2 | Structure **(A)**, Key HMBC (H→C) correlation **(B),** and Key NOESY (H–H) correlation **(C)** of compound **15**.

TABLE 1 | ^{1}H (500 MHz) and ^{13}C (150 MHz) NMR date of compounds 15 (in $CDCl^{3}$) and 18 (in MeOD).

Position	Compound 15		Compound 18	
	δ_C (ppm)	δ_H (ppm)	δ_C (ppm)	δ_H (ppm)
1	37.3	1.25, 1.61, each 1H, m	173.4	
2	31.3	1.32, m	33.8	2.66, 2.86, each 1H, dd, *J* = 4.8, 9.6 Hz
3	70.5	3.56 (1H, m, H-3)	79.7	3.98, 1H, m
4	38.3	1.40, m	84.0	3.55, 1H, dd, *J* = 3.6, 8.4 Hz
5	44.0	1.42, m	71.1	3.63, 1H, m
6	26.7	2.05, m	18.1	1.19, 3H, d, *J* = 7.2 Hz
7	31.8	1.90, m		
8	66.9			
9	51.2	2.18 (1H, d, *J* = 10.2Hz, H-9)		
10	38.9			
11	69.7	5.66(1H, t, *J* = 10.2Hz, H-11β)		
12	74.7	5.17 (1H, d, *J* = 10.2 Hz, H-12α)		
13	46.1			
14	71.5			
15	26.7	2.14, m		
16	25.0	2.40, m		
17	59.8	2.96 (1H, d, *J* = 7.2Hz, H-17β)		
18	16.6	1.13 (3H, s, 18-CH_3)		
19	12.8	1.10 (3H, s, 19-CH_3)		
20	211.0			
21	30.3	2.23 (3H, s, 21-CH_3)		
Bz				
1′	166.1		174.2	
2′	130.3		36.3	2.61, 2.81, each 1H, dd, *J* = 4.8, 9.6 Hz
3′	129.6	7.88 (2H, d, *J* = 7.8Hz, H-3′,7′)	79.0	4.05, 1H, m
4′	128.2	7.36 (2H, t, *J* = 7.8 Hz, H-4′, 6′)	82.6	3.61, 1H, m
5′	132.9	7.50 (1H, t, *J* = 7.2Hz, H-5′)	71.1	3.71, 1H, m
6′	128.2	7.36 (2H, t, *J* = 7.8 Hz, H-4′, 6′)	18.1	1.23, 3H, d, *J* = 7.8 Hz
7′	129.6	7.88 (2H, d, *J* = 7.8Hz, H-3′,7′)		
Tig				
1″	167.4			
2″	127.6			
3″	138.3	6.57 (1H, q, *J*=6.0Hz, H-3″)		
4″	14.2	1.49 (3H, d, *J*=6.6Hz, 4″-CH_3)		
5″	11.5	1.45 (3H, s, 5″-CH_3)		
4-CH3				
10 (=CH_2)				
3-O-Me			57.5	3.39, 3H, s
1′-O-Me			52.1	3.68, 3H, s
3′-O-Me			58.9	3.41, 3H, s
Allo-1			102.7	4.60, 1H, d, *J* = 9.6 Hz
2			75	3.18, 1H
3			83.7	3.62, 1H, m
4			73.6	3.35, 1H, m
5			68.3	3.92, 1H, m
6			20.0	1.30, 3H, d, *J* = 7.8 Hz
3-O-Me			62.5	3.59, 3H, s
Allo-1′			103.9	4.70, 1H, d, *J* =10.2 Hz
2′			74.9	3.18, 1H
3′			83.7	3.62, 1H, m
4′			74.0	3.35, 1H, m
5′			78.0	4.32, 1H, m
6′			19.3	1.47, 3H, d, *J* = 7.8 Hz
3′-O-Me			62.5	3.61(3H, s)

carbonyl signal. In the HMBC spectrum (**Figure 2B**) and **Supplementary Figure S1**), the 11β hydrogen δ_H 5.66 (1H, t, *J* = 10.2 Hz, H-11β) was related to δ_C 166.1 in benzoyl, showing the benzoyl at the C_{11} position of the aglycone. The 12α-hydrogen δ_H 5.17 (1H, d, *J* = 10.2 Hz, H-12e was related to the carbonyl carbon δ_C167.4 in the methacryloyl group, which indicated that the methacryloyl group was attached to the carbon atom at the 12-position. The 17-site conformation was further confirmed by NOESY spectroscopy (**Figure 2C** and **Supplementary Figure S1**). There was an NOE effect between δ_H 1.13 (H-18) and 2.96 (H-17) in the NOESY spectrum, indicating that the 17-position hydrogen of compound 15 was in the β-configuration. A NOE

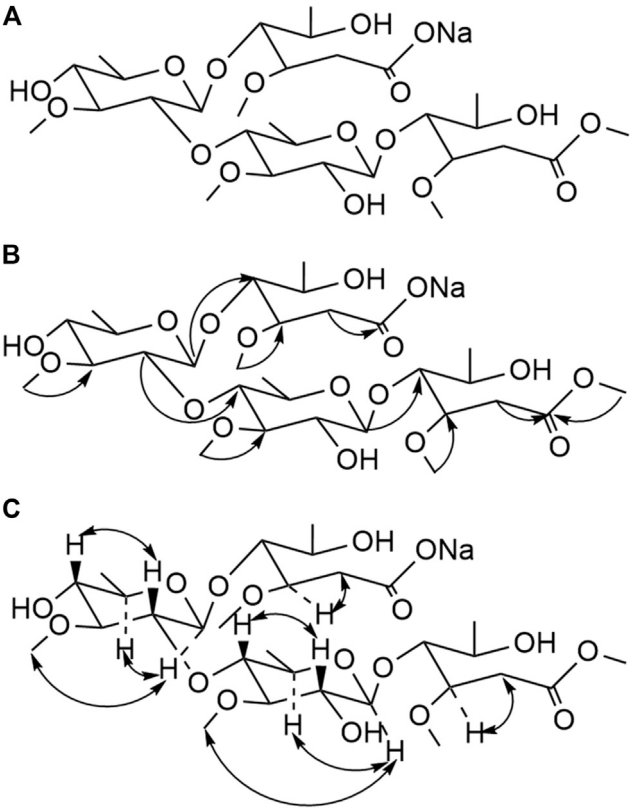

FIGURE 3 | Structure **(A)**, Key HMBC (H→C) correlation **(B),** and Key NOESY (H–H) correlation **(C)** of compound **18**.

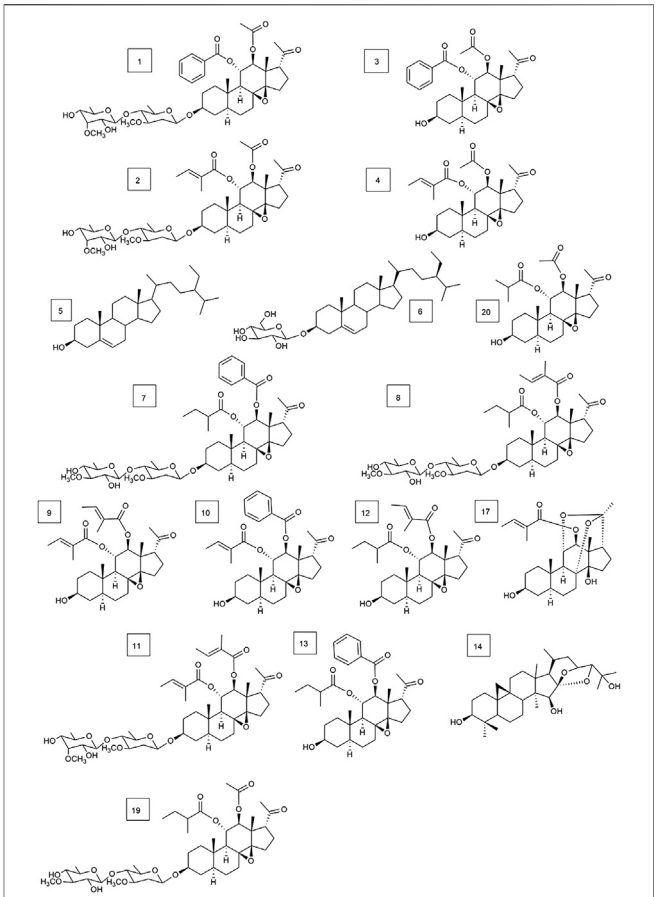

FIGURE 4 | Structures of 17 types of known compounds isolated from *Marsdenia tenacissima* (compounds **1–14**, **17**, **19**, and **20.**).

effect was present between δ_H 1.10 (H-19) and 5.66 (H-11), and the 11-position hydrogen of compound 15 was in the β-configuration. Based on the above analysis, compound **15** was determined to be 11α-*O*-benzoyl-12β-*O*-tigloyltenacigenin B (**Figure 2A**).

Compound **18** was obtained as a white powder. The ion peaks, m/z 695.6 $[M+H]^+$, 671.7 $[M-Na]^-$, for the positive and negative ions, respectively, were obtained using ESI-MS and were assumed to have a molecular weight of 694.3 $[\alpha]_D^{20}$ 16.118 (c 0.0225, CH_3OH). Elemental analysis indicated that the molecular formula was $C_{29}H_{51}NaO_{17}$, and the unsaturation number was 4. According to the ^{13}C-NMR spectrum (**Table 1**, **Supplementary Figure S2**), there were two carbonyl signals, δ_C 174.2 and 173.4, and there was no olefin carbon signal. According to the degree of unsaturation, we presumed that the compound had two rings. According to the number of oxygens, we presumed that the oligosaccharide chain broke the linked compound, and the compound had four methyl signals in the high field, δ_H1.19 (3H, d, J = 7.2 Hz), 1.23 (3H, d, J = 7.8 Hz), 1.30 (3H, d, J = 7.8 Hz), and 1.47 (3H, d, J = 7.8 Hz), based on ^{1}H-NMR spectroscopy (**Table 1**, **Supplementary Figure S2**), corresponding to the four methyl carbon signals of the carbon spectrum δ_C18.1, 18.1, 19.3, and 20.0 according to the HSQC spectrum; ^{1}H-NMR spectral analysis also revealed that there were five -OCH_3 signals at δ_H 3.39 (3H, s), 3.41 (3H, s), 3.59 (3H, s), 3.61 (3H, s), and 3.68 (3H, s). The ^{1}H-NMR spectrum indicated sugar end group signals at δ_H 4.70 (1H, d, J = 10.2 Hz) and 4.60 (1H, d, J = 9.6 Hz), corresponding to the anomeric carbon signals of the carbon spectrum at δ_C 103.9 and 102.7. A previous study on *Marsdeniae tenacissimae* Caulis showed that an extracted component contained *Marsdenia sinensis* disaccharide (Shi et al., 2007). We presumed from the source route that the compound was likely to be a cleavage product after polymerization of two *Marsdenia sinensis* disaccharides. In combination with HMBC (**Figure 3B**) and **Supplementary Figure S2**), δ_H 4.6 (allo-H-1) was related to δ_C 84 (C-4), δ_H 3.18 (allo-H-2) was related to δ_C74 (allo-C-4′), and δ_H 4.7 (allo-H-1′) was related to δ_C 82.6 (C-4′). This showed the position of each sugar unit structure of compound **18** in the connection position. A combination of the HSQC, NOESY (**Figure 3C**), and ^{1}H-^{1}H-COSY profiles (**Supplementary Figure S2**) indicated that compound **18** was identified as 2-*Marsdenia sinensis* dimethyl ester-*Marsdenia sinensis* sodium bicarbonate (**Figure 3A**).

In addition, 17 known compounds (**1–14, 17, 19, 20**) were isolated from the ethyl acetate extract of *Marsdeniae tenacissima* Caulis (**Figure 4**) and were identified as tenacissoside I (1, 10.6 mg), tenacissoside G (2, 15.6 mg) (Zhang et al., 2010), 11α-*O*-benzoyl-12β-*O*-acetyltenacigenin B (3, 17.5 mg) (Yao et al., 2014), 11α-*O*-

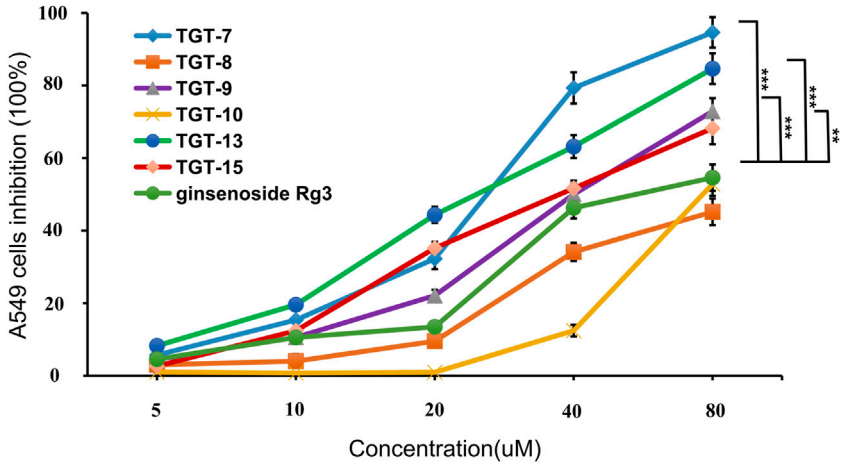

FIGURE 5 | Cytotoxic activity of compounds 7, 8, 9, 10, 13, 15 and ginsenoside Rg3 against the growth of A549 cells. Values are expressed as the mean ± SD, ***$p < 0.001$, **$p < 0.01$ vs. Ginsenoside Rg3 IC50 ($n = 3$).

tigloyl-12β-*O*-acetyltenacigenin B (4, 17.0 mg), β-sitosterol (5, 13.3 mg), daucosterol (6, 4.8 mg) (Dong and Cui, 2013), marsdenoside C (7, 10.8 mg), marsdenoside A (8, 15.6 mg) (Deng et al., 2005), 11α-*O*-tigloyl-12β-*O*-benzoyltenacigenin B (9, 10.5 mg) (Liu and Kong, 2018), 11α-*O*-2-methylbutyryl-12β-*O*-tiglo-yltenacigenin B (10, 18.1 mg), marsdenoside B (11, 15.6 mg), 11α, 12β-*O*, *O*-ditigloyl-17β-tenacigenin B (**12**, 9.6 mg) 11α-*O*-2-methylbutyryl-l2β-*O*-benzoyltenacigenin B (13, 6.4 mg), cimigenol (14, 6.4 mg), 12β-*O*-tigloyltenacigenin A (17, 4.0 mg) (Li and Sun, 2008), tenacissoside H (19, 4.2 mg), and 11α-*O*-2-methylbutyryl-12β-*O*-acetyltenacigenin B (20, 10.5 mg). Cimigenol 14 was the first compound isolated from these extractions. The 1H NMR spectrum and 13C NMR spectrum spectrum data of these compounds are detailed in the supplementary file (**Supplementary File S1**, **Supplementary Tables S1–S3**).

Cell Cytotoxicity Assay of *Marsdeniae tenacissimae* Extracts

The inhibitory activity of all of the isolated compounds against A549 cells was assessed using an *in vitro* assay. The effect of *Marsdeniae tenacissimae* Caulis monomer compounds on the activity of A549 cells showed that six steroidal saponins effectively had inhibitory effects on A549 cells *in vitro*. The IC_{50} values of these six compounds and ginsenoside Rg3 were compared and were arranged in decreasing order as follows: compound **7** < compound **13** < compound **9** < compound **15** < ginsenoside Rg3 < compound **10** < compound **8** (**Figure 5**, **Table 2**).

Prediction of Putative Targets of *Marsdeniae tenacissimae*

Chemical Information and Construction of the Compound-Target-NSCLC Network

SMILES numbers of the compounds were downloaded from the Swiss Target Prediction (Daina et al., 2019) and STITCH databases (Kuhn et al., 2010) used in screening potential targets of the six effective C21 steroidal glycosides. A total of 247 potential targets of the six steroidal saponins were predicted (37 for TGT-**7**, 58 for TGT-**8**, 1 for TGT-**9**, 149 for TGT-**10**, 1 for TGT-**13**, and 1 for TGT-**15**) using the Swiss Target Prediction and STITCH databases, and 205 targets remained after deleting duplicates and false positives.

Searching for NSCLC targets was performed using DigSee (275, Evidence Sentence Score ≥0.6), DisGeNET (225, Score ≥0.1), Malacards (62), and OMIM (142). After the removal of overlapping genes, 270 NSCLC-related targets remained.

Finally, 18 distinct potentially therapeutic genes were identified as targets of the six C21 steroidal glycosides components. This network showed that in terms of anti-NSCLC activity, multiple components acting on multiple targets acted synergistically. Basic information on the six C21 steroidal saponins of *Marsdeniae tenacissimae* Caulis is shown in **Table 3** and **Figure 6**.

Construction of the Compound-Target-Pathway Network

The KEGG and DAVID databases were then employed to enrich the target signal pathways. The network of the compound-target-pathway was constructed by Cytoscape 3.7.2, consisting of 44 nodes and 175 edges. The edges indicated the interactions between active ingredients and targets and pathways.

TABLE 2 | The inhibitory effect of 19 compounds from *Marsdeniae tenacissimae* and Ginsenoside Rg3 on A549 cells.

Compound	IC_{50}, μm	Compound	IC_{50}, μm
TGT 1-6	/	TGT-12	/
TGT-7	28.36 ± 1.96***	TGT-13	29.03 ± 2.05***
TGT -8	78.14 ± 1.85	TGT-14	/
TGT -9	44.01 ± 1.74***	TGT-15	47.33 ± 2.23**
TGT -10	77.47 ± 2.38	TGT-17-20	/
TGT -11	99.80 ± 2.13	Ginsenoside Rg3	57.32 ± 2.03

*Tip: "/" represents the compound $IC_{50} > 100$ μm,***$P < 0.001$, **$P < 0.01$ vs.Ginsenoside Rg3 IC_{50} (n = 3).*

TABLE 3 | 1 Basic information on the six C21 steroidal saponins.

Number	Compound	Molecular formula	Molecular mass (g/moL)	CAS	Degree	Bioavailability	Betweenness centrality
TGT-7	Marsdenoside C	$C_{47}H_{68}O_{14}$	857.03	858360-58-4	37	0.17	0.202702
TGT-8	Marsdenoside A	$C_{45}H_{70}O_{14}$	835.03	858360-56-2	58	0.17	0.321595
TGT-9	11α-O-Tigloyl-12β-O-benzoyltenacigenin B	$C_{33}H_{42}O_7$	550.68	1854092-75-3	1	0.55	0
TGT-10	11α-O-2-Methylbutyryl-12β-O-tigloyltenacigenin B	$C_{31}H_{46}O_7$	530.69	154022-54-5	149	0.55	0.857652
TGT-13	11-α-O-2-Methylbutyryl-l2β-O-benzoyltenacigenin B	$C_{33}H_{44}O_7$	552.7	154022-55-6	1	0.55	0
TGT-15	11α-O-Benzoyl-12β-O-tigloyltenacigenin B	$C_{33}H_{42}O_7$	550.68	2288756-09-0	1	0.55	0

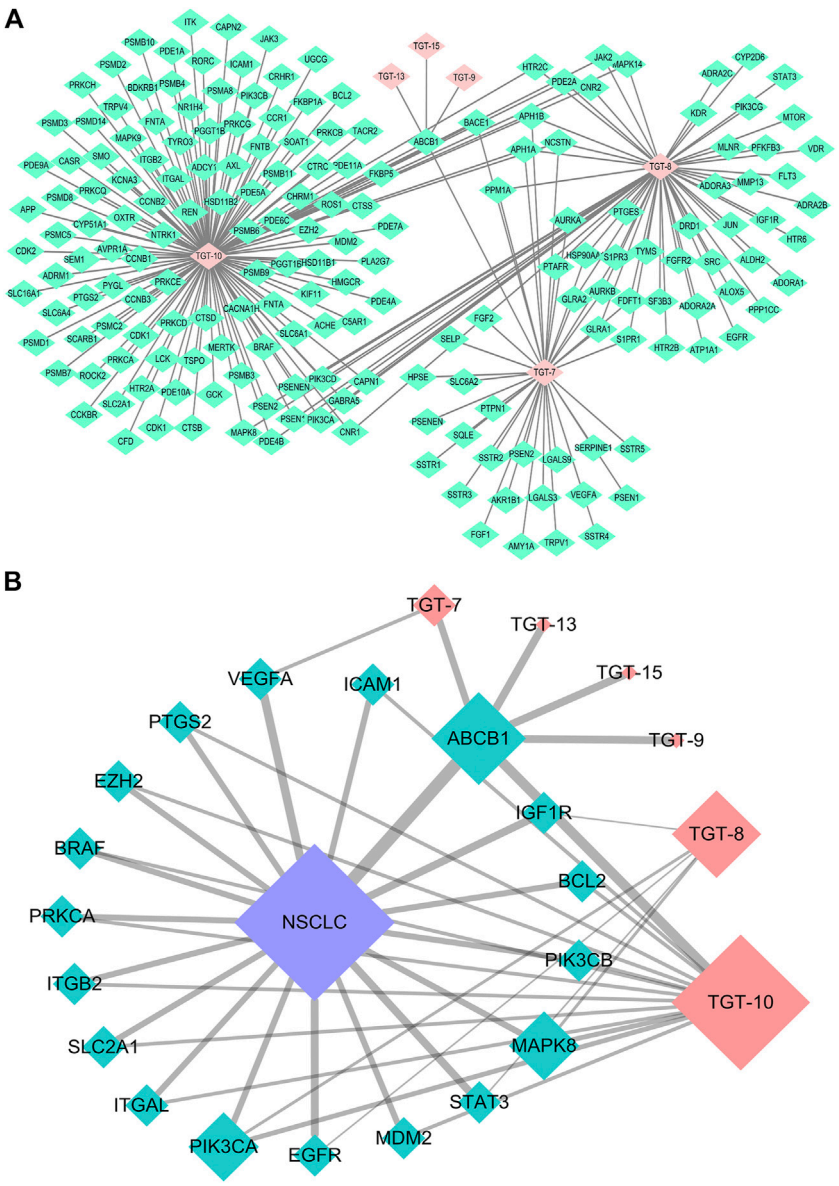

FIGURE 6 | Network pharmacology approach of compounds 7, 8, 9, 10, 13, and 15 **(A)** Compound-target network. Pink represents C21 steroidal saponins (TGT-7, TGT-8, TGT-9, TGT-10, TGT-13, and TGT-15), and green represents their respective targets **(B)** Component-target-NSCLC network. Pink represents C21 steroidal saponins, blue represents NSCLC disease, and green represents their common targets.

TABLE 4 | Basic information on potential anti-NSCLC targets of C21 steroidal saponins.

Gene	UniProt	Degree	Betweenness centrality	Compound
ABCB1	P08183	6	0.14573713	TGT-7, 9, 10, 13, 15
BCL-2	P10415	8	0.02058895	TGT-10
BRAF	P15056	14	0.04937426	TGT-10
EGFR	P00533	17	0.07256819	TGT-8
EZH2	Q15910	2	0.00068448	TGT-10
IGF1R	P08069	12	0.02322063	TGT-8
ITGAL	P20701	6	0.01079787	TGT-10
ICAM1	P05362	4	0.00486475	TGT-10
ITGB2	P05107	5	0.00718665	TGT-10
MAPK8	P45983	9	0.02437828	TGT-8, 10
MDM2	Q00987	10	0.03250911	TGT-10
PIK3CA	P42336	21	0.12547087	TGT-8, 10
PIK3CB	P42338	20	0.10824658	TGT-10
PRKCA	P17252	15	0.07196801	TGT-10
PTGS2	P35354	4	0.00565462	TGT-10
SLC2A1	P11166	3	0.00236935	TGT-10
STAT3	P40763	8	0.01133759	TGT-8
VEGFA	P15692	11	0.06155873	TGT-7

This network showed that the six C21 steroidal saponins participated in the regulation of different pathways that were related to tumor pathogenesis *via* multi-target synergistic activity. These pathways included cancer-related pathways, PI3K/AKT, HIF-1 pathogenesis *via* multi-target synergistic activity-regulated changes in the tumor cell cycle, and angiogenesis, thus inhibiting cancer cell invasion and migration and inducing tumor apoptosis (**Tables 4**, **5 Figures 7A**, **8A**).

Construction and Analysis of the Protein-Interaction Network

STRING was used to assess target protein interactions. **Figure 7B** shows that the network graph consisted of 18 nodes and 127 edges. The definitions and equations for these parameters revealed the topological significance of the nodes in these networks, and the more important nodes showed higher quantitative values. DisGeNET was used to obtain the corresponding types of targets (**Table 6**). The results showed that signaling molecules, enzymes, and proteins were involved in the anti-lung cancer effect of *Marsdeniae tenacissima*.

Gene Function and Pathway Analysis

DAVID was used to conduct Gene Ontology (GO) and KEGG pathway analyses. A threshold of $p < 0.05$ was used in screening the biological process or pathway, and GraphPad Prism 7.0 was employed for drawing enriched terms in the CC, BP, and MF categories (**Figure 8A**).

BP analysis indicated that these targets were mainly related to biological processes, including negative regulation of apoptotic

TABLE 5 | Key targets and topological properties of C21 steroidal saponins anti-NSCLC.

Gene	Full name	Protein class	Degree	Betweenness centrality	Closeness centrality
EGFR	Epidermal growth factor receptor	None	15	0.15757761	0.89473684
STAT3	Signal transducer and activator of transcription 3	Nucleic acid-binding; transcription factor	13	0.10224673	0.80952381
VEGFA	Vascular endothelial growth factor A	Signaling molecule	13	0.08755544	0.80952381
MAPK8	Mitogen-activated protein kinase 8	kinase; transferase	11	0.0569707	0.73913043
PIK3CA	Phosphatidylinositol-4,5-bisphosphate 3-kinase catalytic subunit alpha	Kinase; transferase	10	0.04892624	0.70833333
PTGS2	Prostaglandin-endoperoxide synthase 2	Oxidoreductase	10	0.0194707	0.70833333
IGF1R	Insulin-like growth factor 1 receptor	None	9	0.02212885	0.65384615
MDM2	MDM2 proto-oncogene	Nucleic acid-binding	8	0.0035014	0.62962963
ITGB2	Integrin subunit beta 2	Cell adhesion molecule; extracellular matrix	7	0.06950572	0.62962963
ICAM1	Intercellular adhesion molecule 1	None	7	0.06517565	0.62962963
SLC2A1	Solute carrier family 2 member 1	None	7	0.00122549	0.60714286
ABCB1	ATP binding cassette subfamily B member 1	Hydrolase; protease	6	0	0.5862069
EZH2	Enhancer of zeste 2 polycomb repressive complex 2 subunit	None	6	0.00105042	0.5862069
PRKCA	Protein kinase C alpha	Calcium-binding protein; kinase; transfer/carrier protein; transferase	5	0.025	0.5862069
BRAF	B-Raf proto-oncogene, serine/threonine kinase	None	4	0.00183824	0.5483871
PIK3CB	Phosphatidylinositol-4,5-bisphosphate 3-kinase catalytic subunit beta	Kinase; transferase	4	0.5483871	0.53846154
BCL-2	BCL-2, apoptosis regulator	Signaling molecule	3	0.00428922	0.51515152

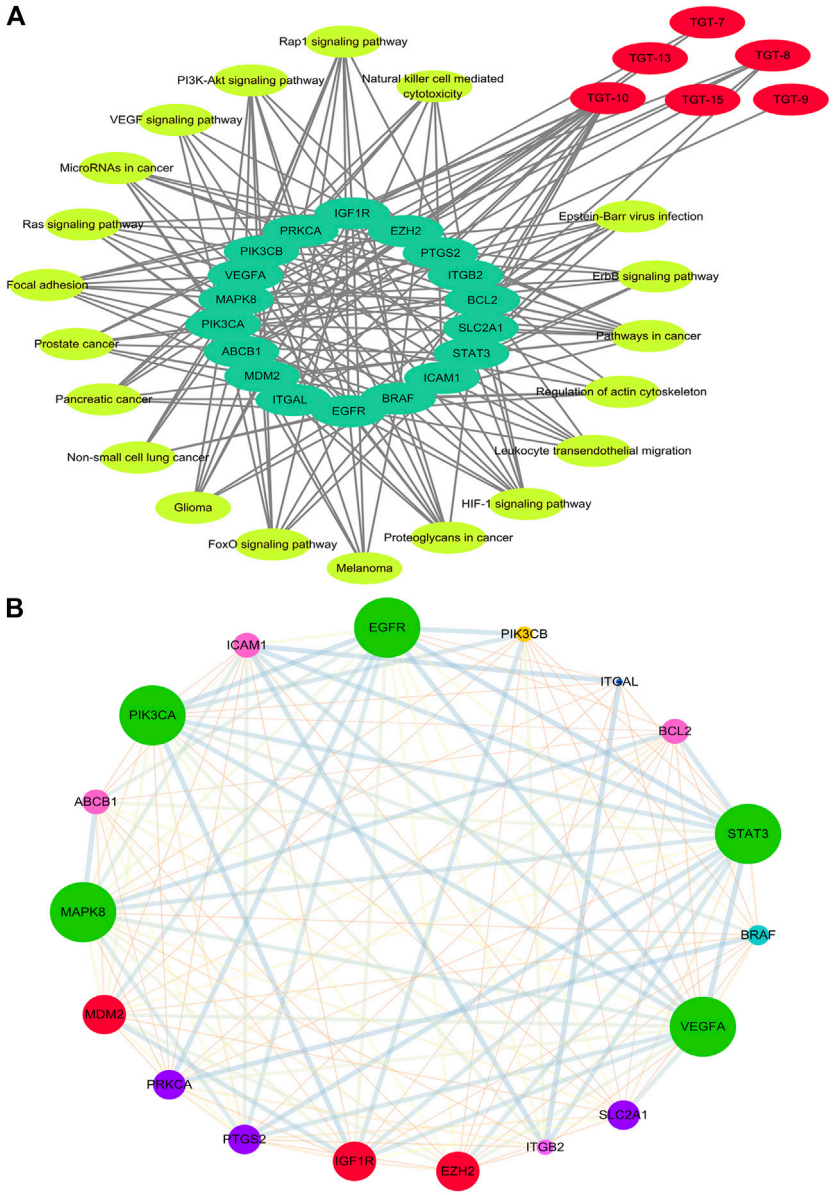

FIGURE 7 | Network of Compound-target-pathway and Protein–protein interaction **(A)** Compound-target-pathway network. Red represents C21 steroidal saponins, bright yellow represents pathways, and green represents their targets **(B)** Protein–protein interaction network (PPI). The larger the node, the greater position occupied in the whole network. The lines between nodes represent the interactions between two proteins that are interconnected. Different-colored lines represent various types of interactions. The thicker the line, the closer the interaction.

processes, positive control of cell proliferation, positive control of cell migration, angiogenesis, regulation of phosphatidylinositol 3-kinase signaling, and the vascular endothelial growth factor receptor signaling pathway (**Figure 8A**).

CC analysis revealed that markedly enriched terms were mainly concentrated in the formation of the phosphatidylinositol 3-kinase complex, plasma membrane, and receptor complex (**Figure 8A**).

MF analysis showed enriched terms including protein binding, ATP binding, protein serine/threonine kinase activity, phosphatidylinositol-4,5-bisphosphate3-kinase activity, ubiquitin protein ligase binding, phosphatidylinositol3-kinase activity, and 1-phosphatidylinositol-4-phosphate 3-kinase activity (**Figure 8A**).

Target Pathway Analysis

KEGG Mapper was used to obtain the pathway map of *Marsdenia tenacissima* resistance to NSCLC, and the major pathways were integrated to construct a pathway map (**Figure 8B**). The arrows in the figure indicated promoting effects, T-arrows represented inhibitory effects, the pathway targets were in blue, the network pharmacological prediction

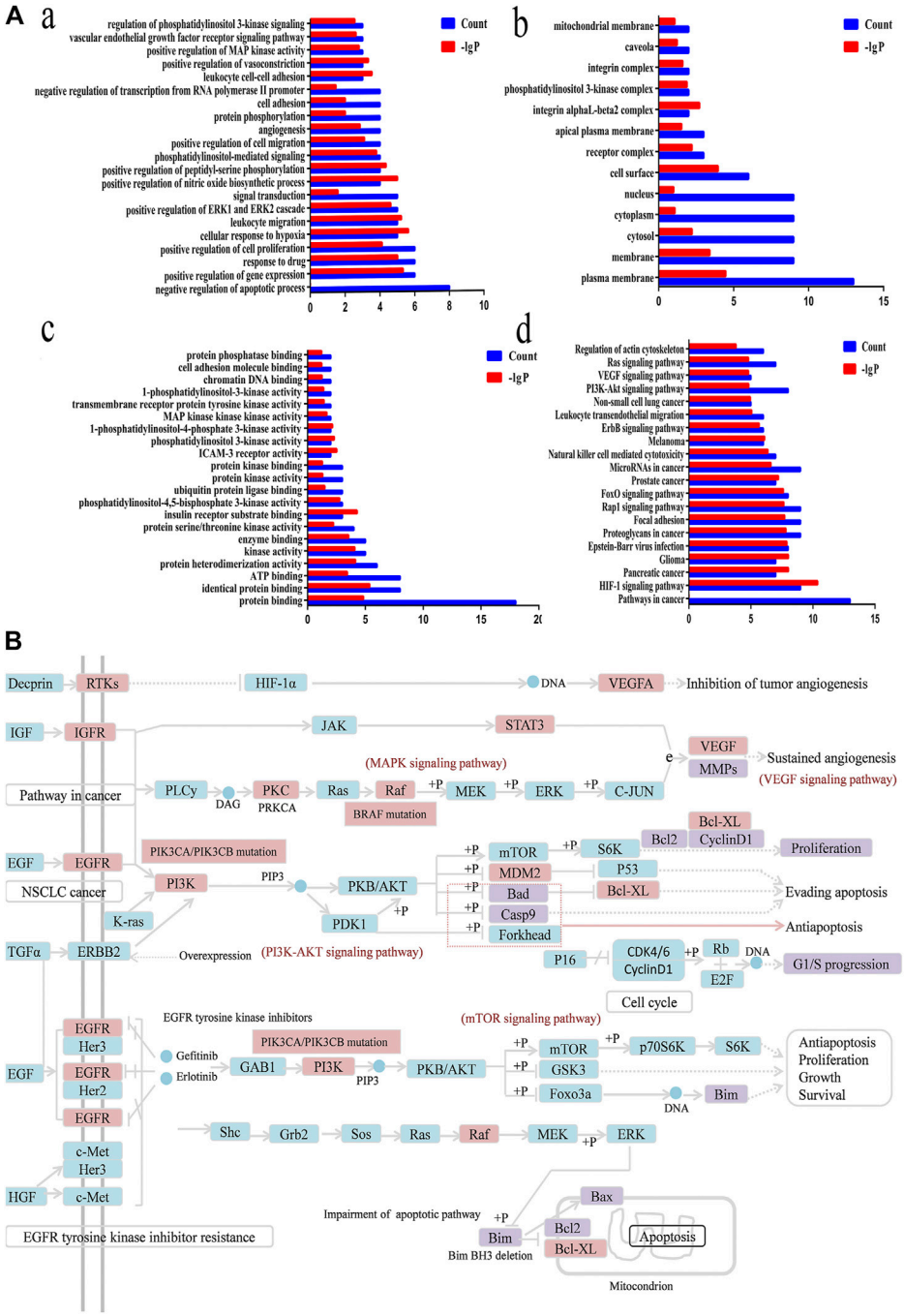

FIGURE 8 | Functional annotation, pathway analysis and Anti-NSCLC pathway of C21 steroidal saponins. **(A)** Functional annotation and pathway analysis of key target genes of C21 steroidal saponins against NSCLC. (a) Enriched Gene Ontology terms for the BP of potential anti-NSCLC targets. (b) MF enrichment analysis of potential anti-NSCLC targets. (c) CC enrichment analysis of potential anti-NSCLC targets. (d) KEGG pathway of anti-NSCLC targets. **(B)** Anti-NSCLC pathway of C21 steroidal saponins. Blue squares represent targets in the pathway, pink squares represent anti-NSCLC targets, and purple squares represent targets that were verified in subsequent experiments in this study.

targets of resistance to NSCLC were in pink, and the experimentally verified targets were in purple. The figure showed that the anti-NSCLC effects of the six C21 steroidal saponins mainly involved pathways in cancer, including HIF-1 signaling, PI3K-Akt signaling, VEGF signaling, EGFR tyrosine kinase inhibitor resistance, and Ras signaling. The integrated pathway diagram was shown in (**Figure 8B**). To further explore the specific role and mechanism of its anti-NSCLC, we conducted preliminary experimental verification on the predicted potentially key targets in the pathway.

TABLE 6 | KEEG pathway enrichment of C21 steroidal saponins anti-NSCLC.

Pathway	Count	*P* Value	Protein
Pathways in cancer	13	0.000000	BRAF,BCL2,MDM2,EGFR,IGF1R,MAPK8,PIK3CA,PIK3CB,PTGS2,PRKCA,STAT3,SLC2A1,VEGFA
HIF-1 signaling pathway	9	0.000000	BCL2,EGFR,IGF1R,PIK3CA,PIK3CB,PRKCA,STAT3,SLC2A1,VEGFA
Pancreatic cancer	7	0.000000	BRAF,EGFR,MAPK8,PIK3CA,PIK3CB,STAT3,VEGFA
Glioma	7	0.000000	BRAF,MDM2,EGFR,IGF1R,PIK3CA,PIK3CB,PRKCA
Epstein-Barr virus infection	8	0.000000	BCL2,MDM2,ITGAL,ICAM1,MAPK8,PIK3CA,PIK3CB,STAT3
Proteoglycans in cancer	9	0.000000	BRAF,MDM2,EGFR,IGF1R,PIK3CA,PIK3CB,PRKCA,STAT3,VEGFA
Focal adhesion	9	0.000000	BRAF,BCL2,EGFR,IGF1R,MAPK8,PIK3CA,PIK3CB,PRKCA,VEGFA
Rap1 signaling pathway	9	0.000000	BRAF,EGFR,IGF1R,ITGAL,ITGB2,PIK3CA,PIK3CB,PRKCA,VEGFA
FoxO signaling pathway	8	0.000000	BRAF,MDM2,EGFR,IGF1R,MAPK8,PIK3CA,PIK3CB,STAT3
Prostate cancer	7	0.000000	BRAF,BCL2,MDM2,EGFR,IGF1R,PIK3CA,PIK3CB
MicroRNAs in cancer	9	0.000000	ABCB1,BCL2,MDM2,EZH2,EGFR,PTGS2,PRKCA,STAT3,VEGFA
Natural killer cell mediated cytotoxicity	7	0.000000	BRAF,ITGAL,ITGB2,ICAM1,PIK3CA,PIK3CB,PRKCA
Melanoma	6	0.000001	BRAF,MDM2,EGFR,IGF1R,PIK3CA,PIK3CB
ErbB signaling pathway	6	0.000002	BRAF,EGFR,MAPK8,PIK3CA,PIK3CB,PRKCA
Leukocyte transendothelial migration	6	0.000009	ITGAL,ITGB2,ICAM1,PIK3CA,PIK3CB,PRKCA
Non-small cell lung cancer	5	0.000011	BRAF,EGFR,PIK3CA,PIK3CB,PRKCA
PI3K-Akt signaling pathway	8	0.000015	BCL2,MDM2,EGFR,IGF1R,PIK3CA,PIK3CB,PRKCA,VEGFA
VEGF signaling pathway	5	0.000016	PIK3CA,PIK3CB,PTGS2,PRKCA,VEGFA
Ras signaling pathway	7	0.000016	EGFR,IGF1R,MAPK8,PIK3CA,PIK3CB,PRKCA,VEGFA
Regulation of actin cytoskeleton	6	0.000157	BRAF,EGFR,ITGAL,ITGB2,PIK3CA,PIK3CB

Effects of TGT-7, TGT-9, TGT-13, and TGT-15 on the Migration and Invasion of A549 Cells

To investigate whether TGT-**7**, TGT-**9**, TGT-**13**, and TGT-**15** (**Figure 9A**) affected the migration and invasion of A549 cells, we first tested the four compounds (TGT-**7**, TGT-**9**, TGT-**13**, and TGT-**15**) in migration and invasion assays. A549 cells were exposed to TGT-**7** (28 μm), TGT-**9** (44 μm), TGT-**13** (29 μm), and TGT-**15** (47 μm) for 36 h. Migration experiments indicated that control cells significantly migrated after treatment with TGT-**7** (28 μm), TGT-**9** (44 μm), TGT-**13** (29 μm), and TGT-**15** (47 μm), with relative widths of the cell scratches of 0.852 ± 0.087, 0.549 ± 0.033, 0.909 ± 0.045, and 0.538 ± 0.056, respectively. Compared with the control group (0.443 ± 0.075), the results were statistically significant (**Figure 9B**). The invasion assays showed that many A549 cells in the control group were filtered from the upper region of transwell chambers and moved to the lower part after treatment with TGT-**7** (28 μm), TGT-**9** (44 μm), as well as TGT-**13** (29 μm). The number of A549 cells that moved across the filtration membrane significantly decreased. However, after treatment with TGT-**15** (47 μm), the number of A549 cells that moved across the filtration membrane significantly decreased. However, *t*-test results indicated the change was not significant. The number of A549-invading cells after treatment with TGT-7 (28 μm), TGT-9 (44 μm), TGT-13 (29 μm), and TGT-15 (47 μm) were 29.87 ± 0.70, 26.33 ± 0.50, 58.8 ± 0.92, and 66.00 ± 3.74, respectively. Compared with the control group (68.40 ± 2.09), the TGT-**7** (28 μm), TGT-**9** (44 μm), and TGT-**13** (29 μm) groups were statistically significant (**Figure 9C**). These results showed that TGT-**7**, TGT-**9,** TGT-**13**, and TGT-**15** could inhibit A549 cells migration and invasion.

TGT-7, TGT-9, TGT-13, and TGT-15 Induced A549 Cells Cycle Arrest at the G0/G1 Phase

A549 cells were exposed to TGT-**7** (28 μm), TGT-**9** (44 μm), TGT-**13** (29 μm), as well as TGT-**15** (47 μm) for 24 h and were fixed and stained using propidium iodide, and alterations in the cell cycle were evaluated by flow cytometry. The results showed that the proportion of G0/G1 cells after treatment with TGT-7 (28 μm), TGT-9 (44 μm), TGT-13 (29 μm), as well as TGT-15 (47 μm) increased from 65.31 ± 3.79% to 75.58 ± 0.44%, 71.63 ± 2.02%, 80.27 ± 2.13%, and 69.17 ± 1.05%, respectively. Compared with the control group, the number of G0/G1 cells increased to different degrees (**Figures 10A,B**). These results demonstrated that TGT-**7**, TGT-**9**, TGT-**13,** and TGT-**15** could arrest A549 cells at the G0/G1 phase.

TGT-7, TGT-9, TGT-13, and TGT-15 Induce A549 CellS Apoptosis

Annexin V-FITC/PI double-staining was employed to detect apoptotic cells. The A549 cells were treated with TGT-**7** (28 μm, 56 μm), TGT-**9** (44 μm, 88 μm), TGT-**13** (29 μm, 58 μm), and TGT-**15** (47 μm, 94 μm) for 24 h, and the results revealed higher green fluorescence staining relative

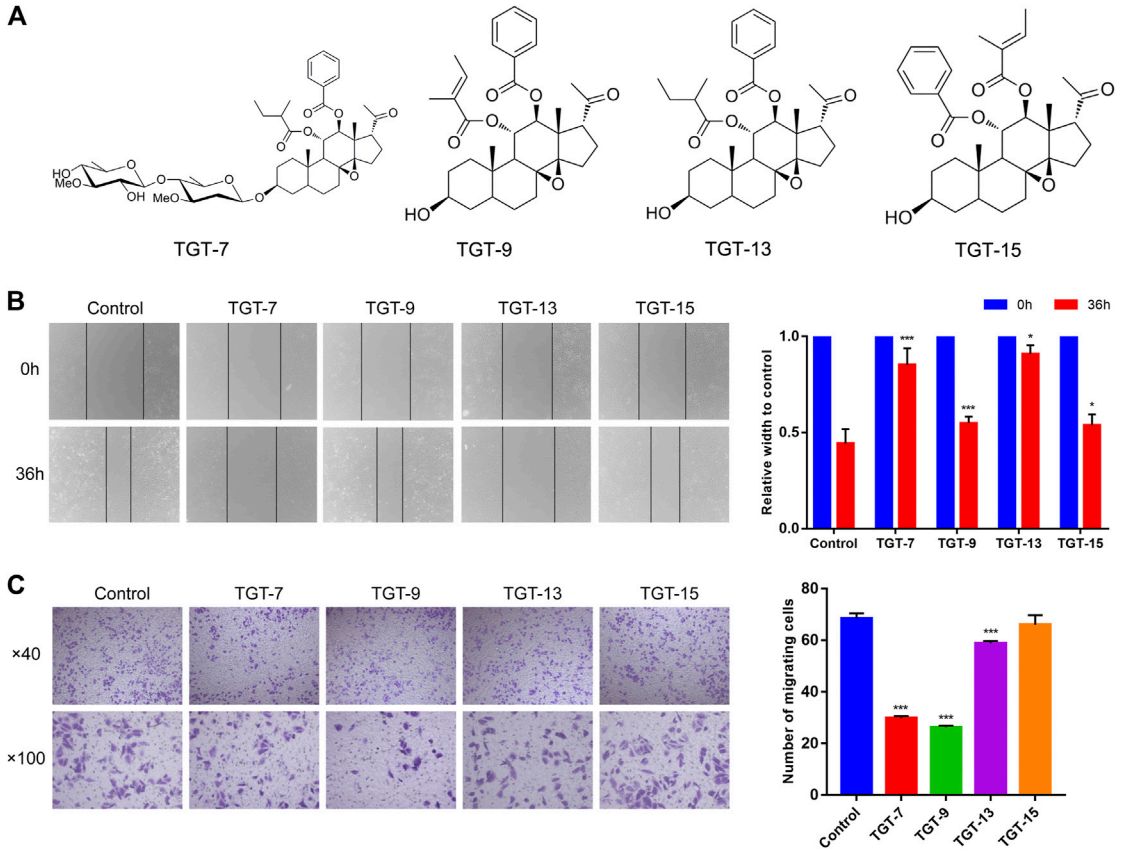

FIGURE 9 | Effects of TGT-7 (28 μm), TGT-9 (44 μm), TGT-13 (29 μm), and TGT-15 (47 μm) on migration and invasion of A549 cells **(A)** Structure of marsdenoside C (TGT-**7**), 11α-*O*-tigloyl-12of*O*-benzoyltenacigenin B (TGT-**9**), and 11-α-*O*-2-methylbutyryl-l2 BO-benzoyltenacigenin B (TGT-**13**), 11α-*O*-benzoyl-12ac*O*-tigloyltenacigenin B (TGT-**15**) **(B)** Wound-healing assays were performed to measure the effect of the four C21 steroidal glycosides on the migration ability of A549 cells (original magnification ×40) **(C)** Transwell–Matrigel invasion assay was performed to evaluate the effect of the change in the four C21 steroidal glycosides on the migration ability of A549 cells (original magnification ×100). These results were obtained from three independent experiments, and all of the data are expressed as the mean ± SD, $^{*}p < 0.05$, $^{***}p < 0.001$ *vs.* the control group ($n = 3$).

to the control group (**Figure 11A**). In addition, the number of apoptotic cells was determined using flow cytometry, and compared with the control group, the apoptotic cells (the sum of early and late apoptotic cells) in the drug-treated group significantly increased, and an increase in concentration was correlated with a higher number of apoptotic cells (**Figure 11B**). These data suggested that TGT-**7**, TGT-**9**, TGT-**13**, and TGT-**15** induced apoptosis in A549 cells in a concentration-dependent fashion.

TGT-7, TGT-9, TGT-13, and TGT-15 Reduce the Mitochondrial Membrane Potential of A549 Cells

Next, we assessed the effects of TGT-**7**, TGT-**9**, TGT-**13**, and TGT-**15** on A549 cells mitochondrial membrane potential by evaluating changes in the red–green fluorescence ratio after JC-1 staining. The results showed that in A549 cells treated with TGT-**7**, TGT-**9**, TGT-**13**, and TGT-**15**, green fluorescence increased, red fluorescence decreased, and the ratio of red–green fluorescence decreased from 14.24 ± 1.14 to 3.10 ± 0.43, 2.74 ± 0.55, 9.54 ± 0.58, and 9.64 ± 1.10, respectively. Compared to the control group, we observed statistically significant differences (**Figure 12A**). Then, we verified the findings through flow cytometry experiments, and the results were consistent with the above results (**Figure 12B**). These results demonstrated that TGT-**7**, TGT-**9**, TGT-**13**, and TGT-**15** treatment resulted in depolarization of the mitochondrial membrane potential.

TGT-7, TGT-9, TGT-13, and TGT-15 Increase Intracellular ROS Levels in A549 Cells

We also examined the effects of TGT-**7**, TGT-**9**, TGT-**13**, and TGT-**15** on ROS production in A549 cells by measuring changes in ROS in A549 cells after DCFH-DA staining. The experimental results showed that after treatment with TGT-**7**, TGT-**9**, TGT-**13**, and TGT-**15**, compared to the control group, green fluorescence in the A549 cells significantly increased. This indicated that these four compounds all caused an increase in intracellular ROS

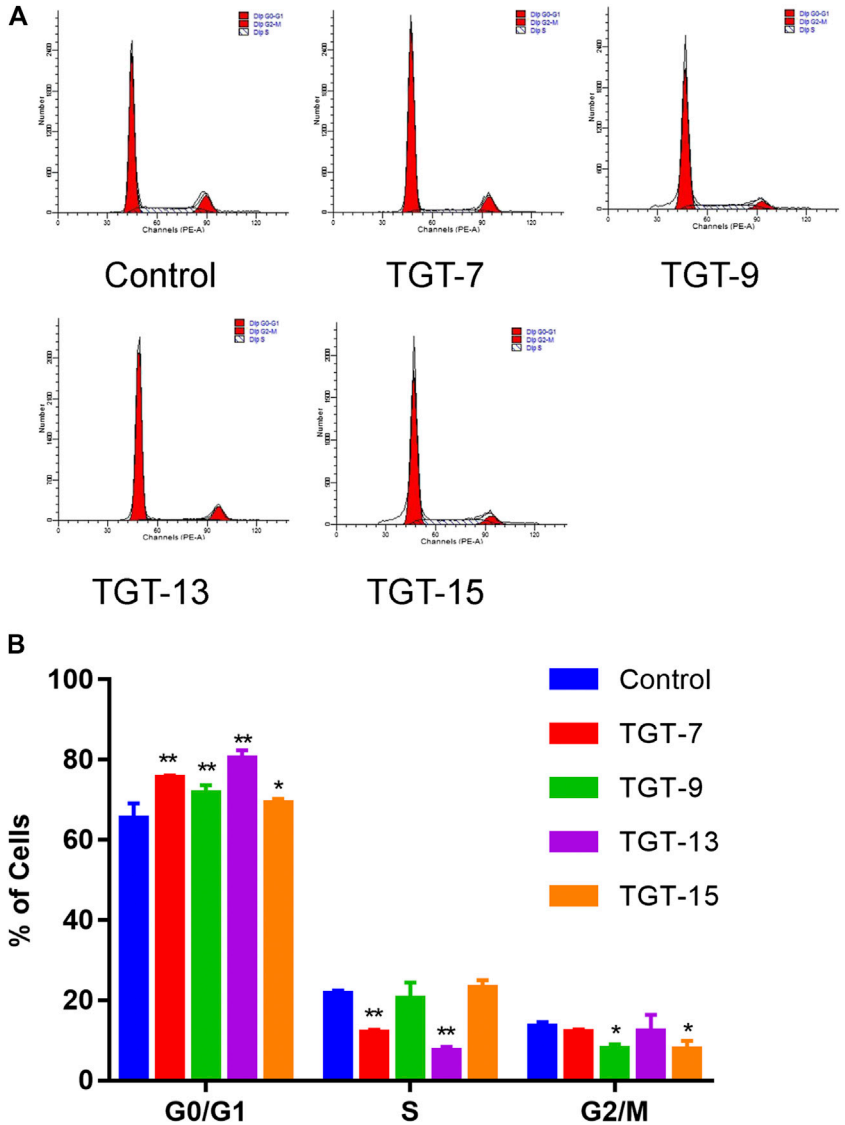

FIGURE 10 | TGT-7 (28 μm), TGT-9 (44 μm), TGT-13 (29 μm) and TGT-15 (47 μm) induce A549 cells cycle arrest in the G0/G1 phase **(A)** Changes in cell cycle phases of A549 cells were detected by flow cytometry **(B)** The number of A549 cells in the G0/G1 phase were significantly increased. These results were obtained from three independent experiments, and all of the data are expressed as the mean ± SD, $^{*}p < 0.05$, $^{**}p < 0.01$ *vs.* the control group ($n = 3$).

levels (**Figures 13A–C**). These results demonstrated that TGT-**7**, TGT-**9**, TGT-**13**, and TGT-**15** all induced ROS production in A549 cells, which led to an increase in the concentration of ROS.

TGT-7, TGT-9, TGT-13, and TGT-15 Modulate Migration and Apoptosis-Related Key Proteins

To further clarify the potential molecular mechanisms of TGT-**7**, TGT-**9**, TGT-**13**, and TGT-**15** inhibiting the growth of A549 cells, we next examined key proteins that were closely related to migration and apoptosis. The results showed that TGT-**7**, TGT-**9**, TGT-**13**, and TGT-**15** decreased MMP-2 and MMP-9 expression in A549 cells. However, this gradually decreased with increasing concentrations and showed a dose-dependent manner. In addition, we examined the expression patterns of cytochrome C, Bax, Bcl-2, cleaved caspase-3, and cleaved caspase-9 (**Figures 14A–C**). The results showed that the high and low concentrations of TG-T-7, TGT-**9**, TGT-**13**, and TGT-**15** increased the expression of cytochrome C, and the high and low concentrations of TGT-**7**, TGT-**9**, and TGT-**13** and the high concentrations of TGT-**15** increased the expression of caspase-9 and caspase-3, indicating that all four compounds could promote the release of mitochondrial cytochrome C and TGT-7, TGT-9, and TGT-13 could activate caspase-9 and

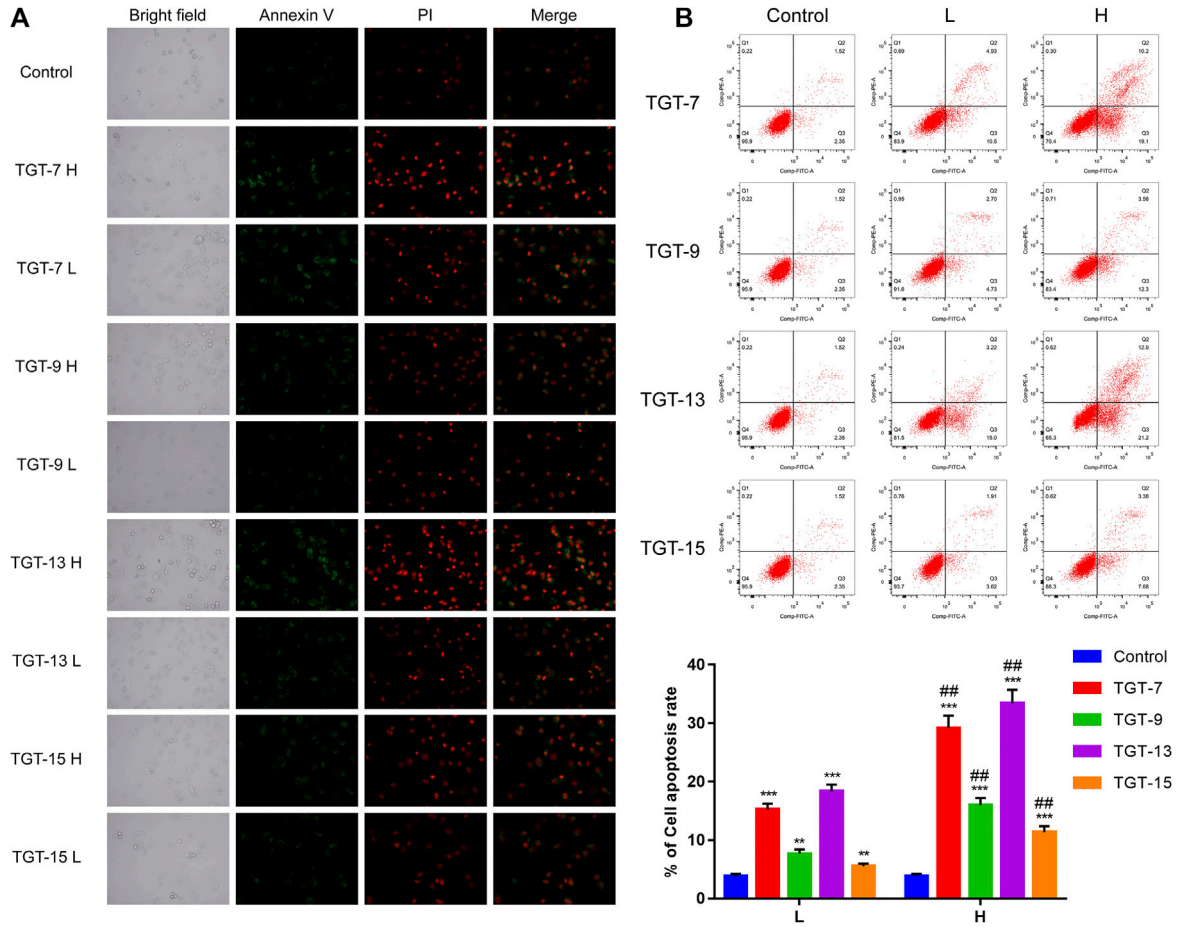

FIGURE 11 | Effects of TGT-7 (28 μm, 56 μm), TGT-9 (44 μm, 88 μm), TGT-13 (29 μM, 58 μm), and TGT-15 (47 μm, 94 μm) on the apoptosis of A549 cells **(A)** Fluoroscope micrographs of apoptotic cells after Annexin V-FITC/PI double staining. Apoptotic cells are indicated in green, whereas necrotic cells are indicated in red (original magnification: ×100) **(B)** Cell apoptosis profiles were assessed using Annexin V-FITC/PI staining and flow cytometry. The biparametric histogram reveals cells in the early (bottom right quadrant) and late apoptotic states (upper right quadrant); viable cells are shown as double-negatives (bottom left quadrant). The numbers show the percentages of each fraction. These results were obtained from three independent experiments, and all data are expressed as the mean ± SD, $^{**}p < 0.01$, $^{***}p < 0.001$ *vs*. the control group, $^{\#\#}p < 0.01$, *vs*. the low-dose group ($n = 3$).

then activate caspase-3 to induce apoptosis. TGT-**7**, TGT-**9**, TGT-**13**, and TGT-**15** could increase the expression of cleaved caspase-8 at high concentrations, which suggested that TGT-**7**, TGT-**9**, TGT-**13**, and TGT-**15** could induce apoptosis in the mitochondrial pathway and possibly through the death receptor pathway.

DISCUSSION

Marsdeniae tenacissimae Caulis extract (Xiao-Ai-Ping) has been clinically used in the treatment of malignant tumors, such as liver cancer, leukemia, lung cancer, etc. Some scholars have specifically used the MTT method to detect the effect of extracts of TGT on the proliferation of normal human lymphocyte cells induced by concanavalin A (ConA) and lipopolysaccharide (LPS). Results have shown that TGT extracts have no obvious cytotoxic effects on normal immune cells and hematopoietic stem cells *in vitro*, but can promote the proliferation of T and B cells, which were closely related to tumor patients' immunity capacity against the aforementioned diseases (Chen et al., 2010; Wang et al., 2017; Zheng et al., 2017; Zhan et al., 2019). Studies have found that C21 steroidal glycosides in *Marsdeniae tenacissimae* Caulis were the main active components. Intriguingly, extensive research demonstrated that C21 steroidal glycosides harbor anti-tussive, anti-asthma, and antitumor activities (Pang et al., 2018; Wang et al., 2018).

Our preliminary research showed the ethyl acetate extracted from a TGT extract had the strongest growth inhibition against A549 cells *in vitro*. We also demonstrated the anti-tumor activity of this extract *in vivo*. Results from others showed that LLC tumor-bearing male C57BL/6 mice in a cisplatin group lost more weight than others, indicating *M. tenacissima* extracts did not cause severe side effects while reducing tumor size (Xu, 2018; Hu et al., 2020). Therefore, this study was aimed at separating the

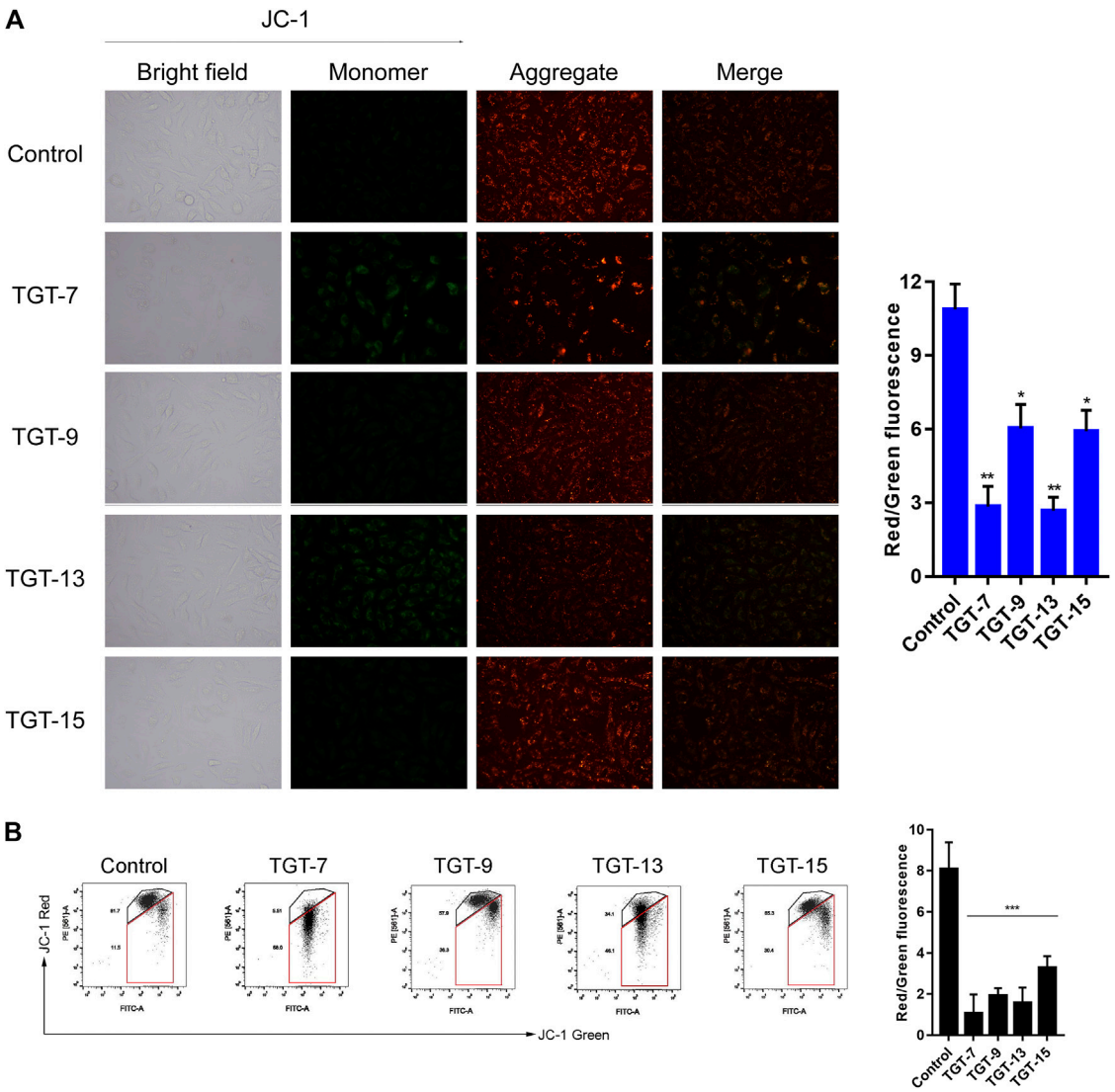

FIGURE 12 | TGT-7, TGT-9, TGT-13, and TGT-15 cause mitochondrial membrane potential dysfunction of A549 cells **(A)** Mitochondrial membrane potential observed using fluorescence miscopy (original magnification ×200) **(B)** Mitochondrial membrane potential observed using flow cytometry. These results were obtained from three independent experiments, and all of the data are expressed as the mean ± SD, *$p < 0.05$, **$p < 0.01$, ***$p < 0.001$ *vs*. the control group ($n = 3$).

components of an ethyl acetate fraction in order to identify compounds with strong anti-NSCLC activity.

First, we isolated and purified the ethyl acetate part of *Marsdeniae tenacissimae* Caulis. A total of 19 compounds were isolated from an ethyl acetate fraction, 15 of which were C21 steroidal glycosides (**Figure 1**). At the same time, we elucidated their structures, which included 2 novel compounds, namely, 11*α*-*O*-benzoyl-12*β*-*O*-tigloyltenacigenin B **15**) (**Figure 2**, **Table 1**) and sodium 5-hydroxy-4-(((2*S*,3*R*,4*S*,5*R*,6*R*)-5-hydroxy-3-(((2*R*,3*R*,4*R*,5*R*,6*S*)-5-hydroxy-6-((2-hydroxy-4,6-dimethoxy-6-oxohexan-3-yl)oxy)-4-methoxy-2-methyltetrahydro-2H-pyran-3-yl)oxy)-4-methoxy-6-methyltetrahydro-2H-pyran-2-yl)oxy)-3-methoxyhexanoate **18**) (**Figure 3**, **Table 1**), and 17 known compounds (**1–14, 17, 19, 20**) (**Figure 4**, **Supplementary Tables S1,S2**). Among all the isolated monomeric compounds, most were C21 steroids. These findings indicated that C21 steroidal saponins might be the effective anti-tumor components of *Marsdeniae tenacissimae* Caulis.

Second, we evaluated all of the isolated compounds against A549 cells using an *in vitro* assay (**Table 2**). The results indicated that the six types of steroidal saponins had inhibitory effects against A549 cells *in vitro*, as their IC50 values were less than 100 μm. At the same time, we observed that A549 cells were sensitive to these four C21 steroidal glycosides in a dose-dependent manner after 24 h of drug stimulation (Xu, 2018). Moreover, we assessed the cytotoxic effect of the four C21 steroidal glycosides against BEAS-2B normal human pulmonary epithelial cells using trypan blue dye exclusion assay, and the results showed that they had no obvious cytotoxicity against BEAS-2B cells.

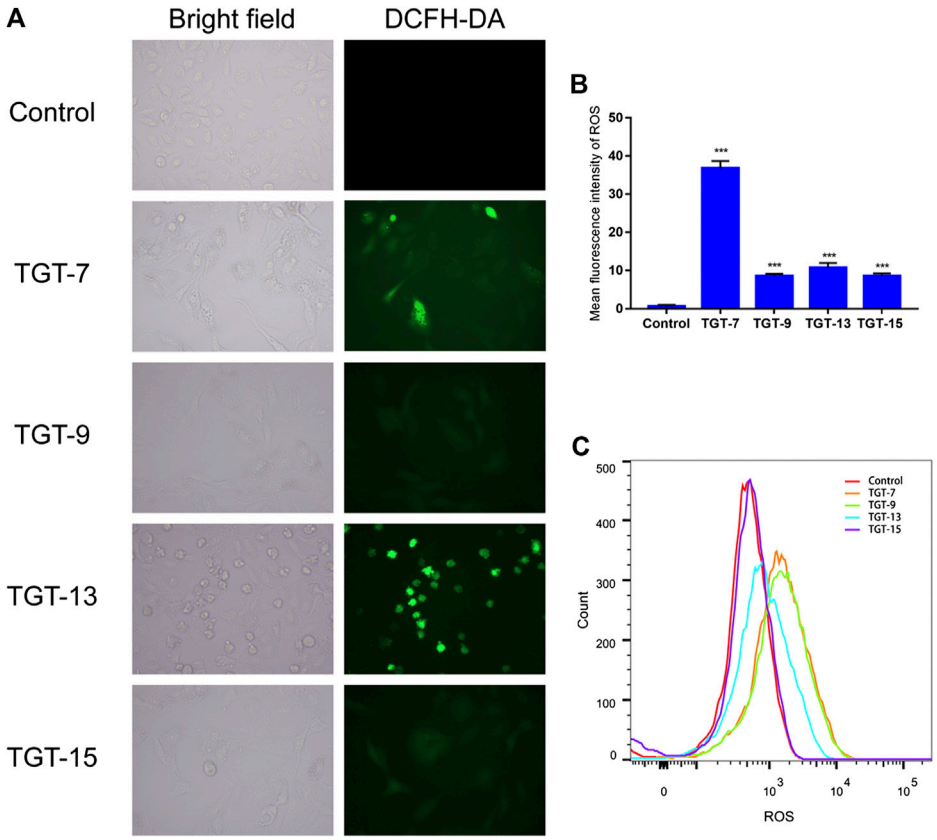

FIGURE 13 | TGT-7, TGT-9, TGT-13, and TGT-15 increase intracellular ROS levels in A549 cells **(A)** and **(B)** Intracellular ROS levels of A549 cells observed using fluorescence microscopy (original magnification ×200) **(C)** Intracellular ROS levels of A549 cells determined by flow cytometry. Results were obtained from three separate experiments, and data are presented as the mean ± SD, ***$p < 0.001$ *vs*. the control group (n = 3).

Next, we analyzed the structure–activity relationships of these isolated compounds. Their structures were very similar, but their activities varied widely in A549 cells *in vitro* (**Table 2**). The main differences in their structure were due to 11-position and 12-position substituents. When the 12-position was acetyl-substituted, these compounds were essentially inactive in A549 cells *in vitro,* such as compounds **1, 2, 3, 4,** and **19**. When the 12-position was substituted by benzoyl, they had the best activity, such as compounds **7**, **9**, and **13**, followed by methylcrotonyl substitution (compounds **8**, **10**, and **15**). Therefore, we postulated that the steroidal compounds that acted on the activity of A549 cells *in vitro* were mainly C-12 substituents, and when benzoyl was substituted, the inhibitory effect against A549 cells was the strongest, whereas the effect of the sugar chain was minimal. Differences in activity were attributable to variations in substituents at the C-12 position. This finding might be further utilized as a reference for structural modifications to identify active compounds.

Traditional Chinese medicine (TCM) network pharmacology is a novel research approach that predicts target profiles as well as the pharmacological actions of various herbal compounds and identifies drug–gene–disease comodule correlations to determine the integrated rules and network regulatory effects of different herbal formulae (Wu et al., 2016). This provides a new paradigm for elucidating the pharmacodynamic substance basis and unraveling the mechanisms of action of TCM (Lee et al., 2019; Zhang et al., 2019).

In order to better determine the best anti-NSCLC substances and potential mechanisms of *M. tenacissimae*, we preliminarily used network pharmacology to screen six active compounds. Network pharmacological analysis showed that steroidal saponins imparted anti-cancer effects mainly *via* 18 targets that were closely related to the PI3K/AKT, RAS/RAF/MEK/ERK, VEGF, and MAPK signaling pathways. These pathways were associated with angiogenesis, cell cycle change, migration, invasion, and cancer cell apoptosis (**Figures 6B**, **7A**). According to the size of the node and degree in the network of the NSCLC-compound-target and PPI (**Figure 7B**), we determined the anti-NSCLC effect of a compound and the importance of a protein in the development of NSCLC so as to provide references for follow-up research focused on deepening our understanding of this mechanism.

One of the major goals of cancer treatment is to disrupt tumor cell proliferation *via* cell cycle progression blockage (Evan and Vousden, 2001; Wang et al., 2020). Currently, a number of chemotherapeutic drugs can block tumor cells in the G0/G1, S, or G2/M phases and thus can achieve the aim of inhibiting tumor cell

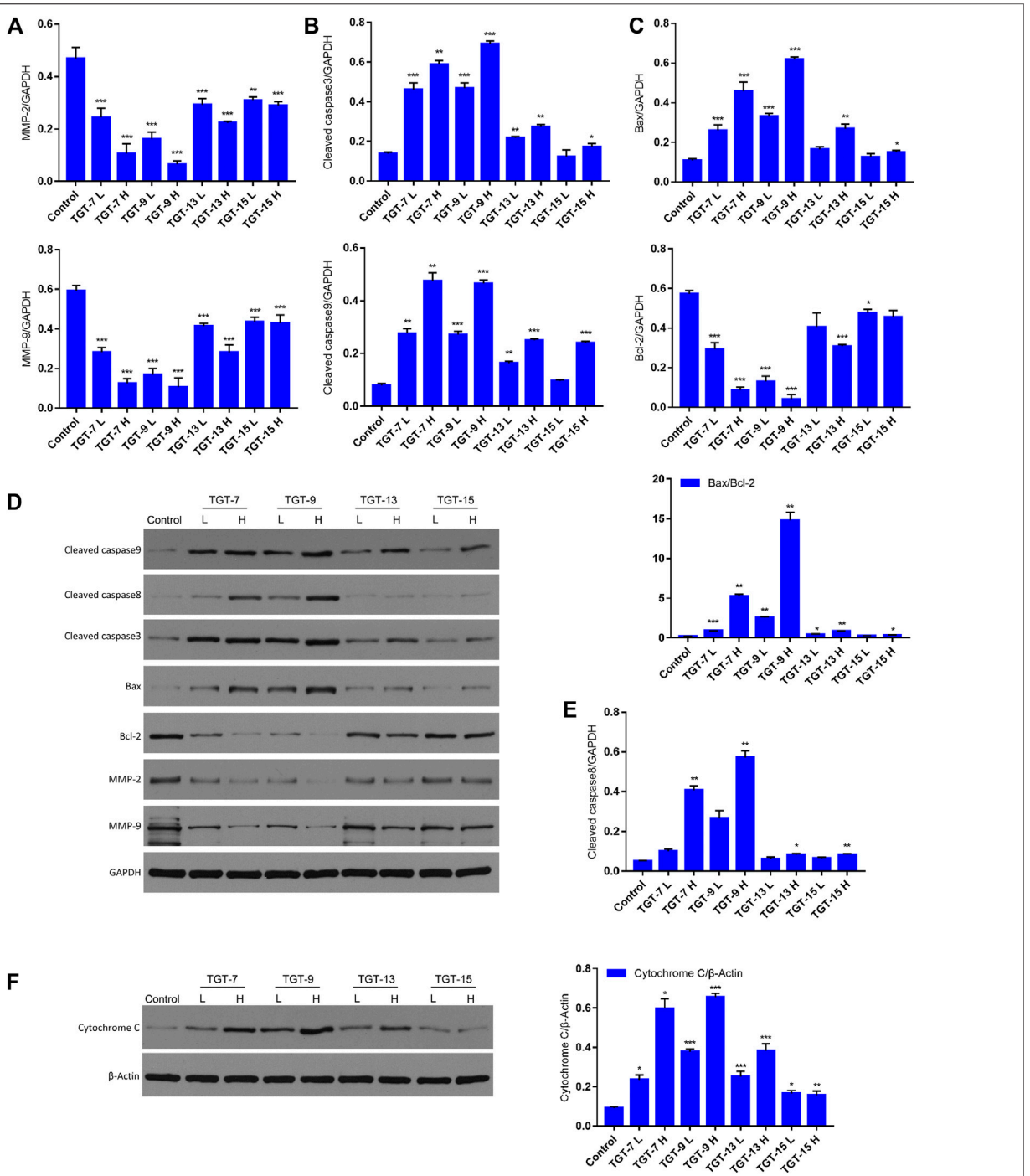

FIGURE 14 | TGT-7, TGT-9, TGT-13, and TGT-15 modulate migration and expression of apoptosis-related key proteins **(A)** The histograms show MMP2 and MMP9 expression **(B)** Histograms showing cleaved caspase-3 and cleaved caspase-9 expression **(C)** Histograms showing Bax and Bcl-2 expression **(D)** Migration and apoptosis-related key proteins were analyzed by Western blotting using *GAPDH* for data normalization **(E)** Histograms showing cleaved caspase-8 expression **(F)** Expression of cytochrome C analyzed by Western blotting and using *β-Actin* for data normalization. These results were obtained from three independent experiments, and all of the data are expressed as the mean ± SD, $^{*}p < 0.05$, $^{**}p < 0.01$, $^{***}p < 0.001$ *vs*. the control group ($n = 3$).

proliferation (Schwartz and Shah, 2005; Chen et al., 2016). Based on the results of literature research and our above network pharmacological analysis, our experiment demonstrated that the four C21 steroidal glycosides (TGT-**7**, TGT-**9**, TGT-**13**, and TGT-**15**) also blocked A549 cells at the G0/G1 phase and prevented cells from progressing toward the S (DNA replication) and M (cell division) phases, as well as

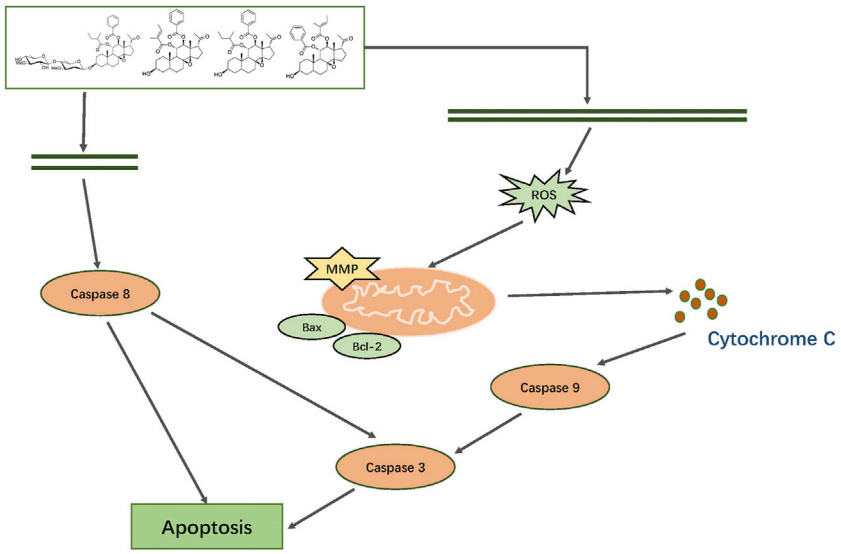

FIGURE 15 | Mechanism by which TGT-7, TGT-9, TGT-13, and TGT-15 isolated from *Marsdeniae tenacissimae* disrupt A549 cells growth and induce apoptosis *via* mitochondrial and death receptor pathways.

decreased the rates of cell growth and proliferation (**Figure 10**). Cell proliferation was closely linked to the cell cycle, which normally operates in an orderly manner under the supervision of cell cycle-related genes, and thus cancer occurs when cell cycle errors cause cells to proliferate (Yang et al., 2008).

MMP-2 and MMP-9 have been strongly linked to angiogenesis, invasion, and metastasis in tumor cells (Webb et al., 2017). Our study illustrated that four C21 steroidal glycosides could decrease the expression of MMP-2 and MMP-9 in A549 cells. Moreover, with increasing concentration, their expression slowly decreased in a dose-dependent manner (**Figures 14A,D**).

Apoptosis induction is considered an essential mechanism of antitumor therapeutics (Stepczynska et al., 2001). Previous studies have revealed that anticancer agents impart anti-proliferative effects using two distinct apoptosis pathways that involve mitochondria or death receptors (Kuo et al., 2018; Han et al., 2019). Specifically, the mitochondria-associated pathway is a classic intrinsic pathway that is caused by ROS overproduction, which in turn results in the depletion of $\triangle\varphi$in (Shi et al., 2014; Wang et al., 2019). Generally, various protein molecules participate in regulating the mitochondrial apoptotic pathway such as pro-apoptotic members (Bax and Bad) and anti-apoptotic members (Bcl-2 and Bcl-xl) (Dong et al., 2019). Moreover, the pathway activated specific pivotal proteinases such as initiator caspase-9 and effector caspase-3 and subsequently resulted in DNA fragmentation as well as nuclear PARP degradation during apoptosis (Duangprompo et al., 2016; Chao et al., 2018). Therefore, Annexin V-FITC/PI staining was conducted to detect apoptotic alterations that may be related to A549 cells cytotoxicity. We detected changes in fluorescence intensities after A549 cells were stained by Annexin V-FITC/PI and observed that the four C21 steroidal glycosides influenced A549 cells apoptosis. In this experiment, we discovered that the rate of cell apoptosis increased in the drug treatment group as measured by flow cytometry and was positively correlated with the drug concentration. Therefore, the results indicated that the four C21 steroidal glycosides could effectively promote A549 cells apoptosis (**Figure 11**).

Mitochondria serve as the regulatory center of endogenous pathways of apoptosis. Mitochondrial status can be interrogated by measuring the mitochondrial membrane potential (Green and Reed, 1998). Based on this point, our experimental results showed that the four C21 steroidal glycosides could reduce the mitochondrial membrane potential, indicating that this might induce A549 apoptosis *via* endogenous pathways of the mitochondria (**Figure 12**). ROS are mainly produced in the mitochondria, and ROS overproduction could lead to lipid overoxidation of the mitochondrial membrane, further influencing the mitochondrial membrane potential and triggering the release of cytochrome C, which, in turn, induces endogenous apoptosis (Zhao and Xu, 2001). Some studies have shown that ROS can also cause exogenous apoptosis mainly by increasing the sensitivity of tumor cells to Fasl, then activating caspase-8 to mediate exogenous apoptosis through the death receptor Fas/Fasl pathway (Shang et al., 2016). In our experiment, the effect of the four C21 steroidal glycosides on the ROS level was assessed in A549 cells. The experimental results indicated that the green fluorescence of every drug group was significantly more intense relative to the control group after TGT-**7**, TGT-**9**, TGT-**13**, and TGT-**15** treatment. Thus, this experiment clearly showed that TGT-**7**, **9**, **13**, and **15** could raise the level of ROS in A549 cells and then induce cell apoptosis (**Figure 13**).

The cytochrome C-mediated mitochondrial apoptosis pathway is controlled by the Bcl-2 protein family, and in terms of apoptosis, the Bcl-2 family consists of two members, anti-apoptotic protein (Bcl-2) and pro-apoptotic protein (Bax). The ratio of these two is usually an indicator of apoptosis (Adams and Cory, 1998; Li et al., 2017). In our studies, the

expression level of Bax increased with increasing concentrations of TGT-**7**, TGT-**9**, TGT-**13**, and TGT-**15**, whereas the Bcl-2 expression level showed the opposite pattern, i.e., it was negatively correlated with dose: an increase in the Bax/Bcl-2 ratio induced the release of cytochrome C that in turn induced cell apoptosis (**Figures 14B–D,F**). Caspase-8 is a major apoptosis factor in the death receptor pathway (Munoz-Pinedo and Lopez-Rivas, 2018). The four C21 steroidal glycosides at high concentrations could increase cleaved caspase-8 protein expression, suggesting that the four C21 steroidal glycosides could induce apoptosis *via* the death receptor pathway in addition to the mitochondrial pathway (**Figures 14D,E**).

CONCLUSION

In summary, we first isolated and characterized 19 major constituents of *Marsdeniae tenacissimae* Caulis by ^{1}H-NMR, ^{13}C-NMR and DEPT, 2D NMR (^{1}H-^{1}HCOSY NOESY, HSQC and HMBC) spectra. Then, we demonstrated that the six main active components of ethyl acetate dramatically suppressed A549 cancer cell proliferation. Furthermore, network pharmacology analysis of the six compounds of *Marsdeniae tenacissimae* Caulis revealed that possible targets were mainly related to the positive regulation of ROS-associated metabolic processes, as well as intrinsic apoptotic pathways. Next, a series of cellular tests verified the results of the network pharmacology prediction. The four C21 steroidal glycosides (TGT-**7**, TGT-**9**, TGT-**13**, and TGT-**15**) disrupted A549 cells migration and invasion *via* downregulation of MMP-2 and MMP-9 expression. We also found that C21 steroidal glycosides of *Marsdeniae tenacissimae* Caulis triggered apoptosis of A549 cells through a mitochondrial-mediated pathway *via* upregulation of Bax and downregulation of Bcl-2 expression, thus releasing cytochrome C and finally activating caspase-3 and caspase-9. At the same time, the four C21 steroidal glycosides also activated caspase-8, which activated the death receptor pathway to promote apoptosis. The four C21 steroidal glycosides disrupted A549 growth and triggered apoptosis *via* mitochondrial and death receptor pathways (**Figure 15**).

At present, there are many studies on the treatment of cancer by *Marsdeniae tenacissimae* Caulis and its clinical preparation Xiao-Ai-Ping injection, but these studies have not excavated its pharmacodynamic material basis. In our research, we have defined the antitumor compounds as well as their mechanisms, which can be potentially employed as a therapeutic option for the treatment alone of NSCLC or in combination with anticancer chemical drugs to reduce their toxicity and side effects. In addition, we also analyzed the structure-activity relationship of these isolated compounds, which provides experimental basis for the development of clinical anticancer drugs or to improve the clinical efficacy of existing anticancer chemical drugs by structural modification in the future. Due to the approaching completion time, the relevant targets and pathways predicted by the network pharmacology in this study on the anti-NSCLC caused by *M. tenacissima* have not been fully verified, which will be studied in our later research.

DATA AVAILABILITY STATEMENT

All datasets generated for this study are included in the article/**Supplementary Material**.

ETHICS STATEMENT

The animal experiment research related to this subject has obtained ethical certification, but this research does not involve animal experiments.

AUTHOR CONTRIBUTIONS

PL performed the experiment and wrote the essay. D-WX and R-TL processed the data. S-HW and Y-LH modified the paper. J-YL, L-WK, S-YS, and Y-HH assisted the completion of the experiment. T-XL designed the experiment and provided financial support.

FUNDING

The National Natural Science Foundation of China (No. 81973977) and the Creative Item of Innovative Team of Ministry of Education (No. IRT-13R63) supported this study.

ACKNOWLEDGMENTS

We thank LetPub (www.letpub.com) for its linguistic assistance during the preparation of this manuscript.

SUPPLEMENTARY MATERIAL

The Supplementary Material for this article can be found online at: https://www.frontiersin.org/articles/10.3389/fphar.2021.518406/full#supplementary-material.

REFERENCES

Adams, J. M., and Cory, S. (1998). The Bcl-2 protein family: arbiters of cell survival. *Science* 281 (5381), 1322–1326. doi:10.1126/science.281.5381.1322

Amberger, J. S., Bocchini, C. A., Schiettecatte, F., Scott, A. F., and Hamosh, A. (2015). OMIM.org: online Mendelian Inheritance in Man (OMIM), an online catalog of human genes and genetic disorders. *Nucleic Acids Res.* 43 (Database issue), D789–D798. doi:10.1093/nar/gku1205

Chao, T.-L., Wang, T.-Y., Lee, C.-H., Yiin, S.-J., Ho, C.-T., Wu, S.-H., et al. (2018). Anti-cancerous effect of inonotus taiwanensis polysaccharide extract on human acute monocytic leukemia cells through ROS-independent intrinsic mitochondrial pathway. *Int. J. Mol. Sci.* 19 (2), 393. doi:10.3390/ijms19020393

Chen, B., Chen, L., J, O., and X, S. (2010). Effect of extractive of marsdenia tenacissima on human normal immunocytes and hemopoietic stem cells in vitro. *Chin. Clin. Oncol.* 15 (10), 887–890.

Chen, F., Zheng, S. L., Hu, J. N., Sun, Y., He, Y. M., Peng, H., et al. (2016). Octyl ester of ginsenoside Rh2 induces apoptosis and G1 cell cycle arrest in human HepG2 cells by activating the extrinsic apoptotic pathway and modulating the akt/p38 MAPK signaling pathway. *J. Agric. Food Chem.* 64 (40), 7520–7529. doi:10.1021/acs.jafc.6b03519

Commission, C. P. (2020). "Pharmacopoeia of the People's Republic of China (Part I)", in: *Marsdeniae Tenacissimae Caulis*. (Beijing: The Medicine Science and Technology Press of China).

Daina, A., Michielin, O., and Zoete, V. (2019). SwissTargetPrediction: updated data and new features for efficient prediction of protein targets of small molecules. *Nucleic Acids Res.* 47 (W1), W357–w364. doi:10.1093/nar/gkz382

Deng, J., Liao, Z., and Chen, D. (2005). Marsdenosides A-H, polyoxypregnane glycosides from *Marsdenia* tenacissima. *Phytochemistry* 66 (9), 1040–1051. doi:10.1016/j.phytochem.2005.03.018

DeSantis, C. E., Siegel, R. L., Sauer, A. G., Miller, K. D., Fedewa, S. A., Alcaraz, K. I., et al. (2016). *Cancer* statistics for African Americans, 2016: progress and opportunities in reducing racial disparities. *CA: A Cancer J. Clinicians* 66 (4), 290–308. doi:10.3322/caac.21340

Dong, Y., and Cui, M. (2013). Current situation and development trend of Chinese medicine information research. *Zhongguo Zhong Xi Yi Jie He Za Zhi* 33 (4), 559–564.

Dong, Y., Qiu, P., Zhu, R., Zhao, L., Zhang, P., Wang, Y., et al. (2019). A combined phytochemistry and network pharmacology approach to reveal the potential antitumor effective substances and mechanism of phellinus igniarius. *Front. Pharmacol.* 10, 266. doi:10.3389/fphar.2019.00266

Duangprompo, W., Aree, K., Itharat, A., and Hansakul, P. (2016). Effects of 5,6-dihydroxy-2,4-dimethoxy-9,10-dihydrophenanthrene on G2/M cell cycle arrest and apoptosis in human lung carcinoma cells. *Am. J. Chin. Med.* 44 (7), 1473–1490. doi:10.1142/S0192415X16500828

Evan, G. I., and Vousden, K. H. (2001). Proliferation, cell cycle and apoptosis in cancer. *Nature* 411 (6835), 342–348. doi:10.1038/35077213

Fang, J., Wang, L., Wu, T., Yang, C., Gao, L., Cai, H., et al. (2017). Network pharmacology-based study on the mechanism of action for herbal medicines in Alzheimer treatment. *J. Ethnopharmacol.* 196, 281–292. doi:10.1016/j.jep.2016.11.034

Gao, Y., Chen, S., Sun, J., Su, S., Yang, D., Xiang, L., et al. (2020). Traditional Chinese medicine may be further explored as candidate drugs for pancreatic cancer: a review. *Phytotherapy Res.* 35 (2), 603–628. doi:10.1002/ptr.6847

Gfeller, D., Grosdidier, A., Wirth, M., Daina, A., Michielin, O., and Zoete, V. (2014). SwissTargetPrediction: a web server for target prediction of bioactive small molecules. *Nucleic Acids Res.* 42 (W1), W32–W38. doi:10.1093/nar/gku293

Green, D. R., and Reed, J. C. (1998). Mitochondria and apoptosis. *Science* 281 (5381), 1309–1312. doi:10.1126/science.281.5381.1309

Gu, X., Zheng, R., Xia, C., Zeng, H., Zhang, S., Zou, X., et al. (2018). Interactions between life expectancy and the incidence and mortality rates of cancer in China: a population-based cluster analysis. *Cancer Commun.* 38 (1), 44. doi:10.1186/s40880-018-0308-x

Guijas, C., and Siuzdak, G. (2018). Reply to comment on metlin: a technology platform for identifying knowns and unknowns. *Anal. Chem.* 90 (21), 13128–13129. doi:10.1021/acs.analchem.8b04081

Han, K. W. W., Po, W. W., Sohn, U. D., and Kim, H.-J. (2019). Benzyl isothiocyanate induces apoptosis via reactive oxygen species-initiated mitochondrial dysfunction and DR4 and DR5 death receptor activation in gastric adenocarcinoma cells. *Biomolecules* 9 (12), 839. doi:10.3390/biom9120839

Hare, J. I., Lammers, T., Ashford, M. B., Puri, S., Storm, G., and Barry, S. T. (2017). Challenges and strategies in anti-cancer nanomedicine development: an industry perspective. *Adv. Drug Deliv. Rev.* 108, 25–38. doi:10.1016/j.addr.2016.04.025

Hu, Y., Liu, P., Kang, L., Li, J., Li, R., and Liu, T. (2020). Mechanism of *Marsdenia* tenacissima extract promoting apoptosis of lung cancer by regulating Ca2+/CaM/CaMK signaling. *J. Ethnopharmacol.* 251, 112535. doi:10.1016/j.jep.2019.112535

Kim, J., Kim, J.-j., and Lee, H. (2017). An analysis of disease-gene relationship from Medline abstracts by DigSee. *Sci. Rep.* 7 (1), 40154. doi:10.1038/srep40154

Kuhn, M., Szklarczyk, D., Franceschini, A., Campillos, M., von Mering, C., Jensen, L. J., et al. (2010). Stitch 2: an interaction network database for small molecules and proteins. *Nucleic Acids Res.* 38 (suppl_1), D552–D556. doi:10.1093/nar/gkp937

Kuo, H.-M., Tseng, C.-C., Chen, N.-F., Tai, M.-H., Hung, H.-C., Feng, C.-W., et al. (2018). MSP-4, an antimicrobial peptide, induces apoptosis via activation of extrinsic fas/FasL- and intrinsic mitochondria-mediated pathways in one osteosarcoma cell line. *Mar. Drugs* 16 (1), 8. doi:10.3390/md16010008

Lee, W.-Y., Lee, C.-Y., Kim, Y.-S., and Kim, C.-E. (2019). The methodological trends of traditional herbal medicine employing network pharmacology. *Biomolecules* 9 (8), 362. doi:10.3390/biom9080362

Li, H., Lv, B., Kong, L., Xia, J., Zhu, M., Hu, L., et al. (2017). Nova1 mediates resistance of rat pheochromocytoma cells to hypoxia-induced apoptosis via the Bax/Bcl-2/caspase-3 pathway. *Int. J. Mol. Med.* 40 (4), 1125–1133. doi:10.3892/ijmm.2017.3089

Li, R., and Sun, H. (2008). Studies on the chemical constituents and bioactivities of five Schisandra medicina lspecies and Elsholtzia bodinier. *J. Graduate Sch. Chin. Acad. Sci.* (04), 569–575.

Liu, M., and Kong, J.-Q. (2018). The enzymatic biosynthesis of acylated steroidal glycosides and their cytotoxic activity. *Acta Pharmaceutica Sinica B* 8 (6), 981–994. doi:10.1016/j.apsb.2018.04.006

Mao, Y., Hao, J., Jin, Z.-Q., Niu, Y.-Y., Yang, X., Liu, D., et al. (2017). Network pharmacology-based and clinically relevant prediction of the active ingredients and potential targets of Chinese herbs in metastatic breast cancer patients. *Oncotarget* 8 (16), 27007–27021. doi:10.18632/oncotarget.15351

Muñoz-Pinedo, C., and López-Rivas, A. (2018). A role for caspase-8 and TRAIL-R2/DR5 in ER-stress-induced apoptosis. *Cell Death Differ* 25 (1), 226. doi:10.1038/cdd.2017.155

Paci, E., Puliti, D., Lopes Pegna, A., Carrozzi, L., Picozzi, G., Falaschi, F., et al. (2017). Mortality, survival and incidence rates in the ITALUNG randomised lung cancer screening trial. *Thorax* 72 (9), 825–831. doi:10.1136/thoraxjnl-2016-209825

Pang, X., Kang, L.-P., Fang, X.-M., Yu, H.-S., Han, L.-F., Zhao, Y., et al. (2018). C21 steroid derivatives from the Dai herbal medicine Dai-Bai-Jie, the dried roots of *Marsdenia* tenacissima, and their screening for anti-HIV activity. *J. Nat. Med.* 72 (1), 166–180. doi:10.1007/s11418-017-1126-1

Pinero, J., Queralt-Rosinach, N., Bravo, A., Deu-Pons, J., Bauer-Mehren, A., Baron, M., et al. (2015). DisGeNET: a discovery platform for the dynamical exploration of human diseases and their genes. *Database (Oxford)* 2015 (0), bav028. doi:10.1093/database/bav028

Schwartz, G. K., and Shah, M. A. (2005). Targeting the cell cycle: a new approach to cancer therapy. *J. Clin. Oncol.* 23 (36), 9408–9421. doi:10.1200/jco.2005.01.5594

Settle, B., Otasek, D., Morris, J. H., and Demchak, B. (2018). Copycat layout: network layout alignment via Cytoscape automation. *F1000Res* 7, 822. doi:10.12688/f1000research.15144.2

Shang, H.-S., Shih, Y.-L., Lu, T.-J., Lee, C.-H., Hsueh, S.-C., Chou, Y.-C., et al. (2016). Benzyl isothiocyanate (BITC) induces apoptosis of GBM 8401 human brain glioblastoma multiforms cells via activation of caspase-8/Bid and the reactive oxygen species-dependent mitochondrial pathway. *Environ. Toxicol.* 31 (12), 1751–1760. doi:10.1002/tox.22177

Shi, H., Cui, J., Guan, A., and Zhao, Y. (2008). Chemical constituents of Marsdenia tenacissima. *Chin. Traditional Herbal Drugs* 39 (07), 970–972.

Shi, Y.-L., Feng, S., Chen, W., Hua, Z.-C., Bian, J.-J., and Yin, W. (2014). Mitochondrial inhibitor sensitizes non-small-cell lung carcinoma cells to TRAIL-induced apoptosis by reactive oxygen species and Bcl-XL/p53-mediated amplification mechanisms. *Cell Death Dis* 5 (12), e1579. doi:10.1038/cddis.2014.547

Stepczynska, A., Lauber, K., Engels, I. H., Janssen, O., Kabelitz, D., Wesselborg, S., et al. (2001). Staurosporine and conventional anticancer drugs induce overlapping, yet distinct pathways of apoptosis and caspase activation. *Oncogene* 20 (10), 1193–1202. doi:10.1038/sj.onc.1204221

Tang, J., Feng, Y., Tsao, S., Wang, N., Curtain, R., and Wang, Y. (2009). Berberine and Coptidis rhizoma as novel antineoplastic agents: a review of traditional use and biomedical investigations. *J. Ethnopharmacol.* 126 (1), 5–17. doi:10.1016/j.jep.2009.08.009

Torre, L. A., Bray, F., Siegel, R. L., Ferlay, J., Lortet-Tieulent, J., and Jemal, A. (2015). Global cancer statistics, 2012. *CA: A Cancer J. Clinicians* 65 (2), 87–108. doi:10.3322/caac.21262

Wang, F., Fan, Q. X., Wang, H. H., Han, D. M., Song, N. S., and Lu, H. (2017). Efficacy and safety of Xiaoaiping combined with chemotherapy in the treatment of advanced esophageal cancer. *Zhonghua Zhong Liu Za Zhi* 39 (6), 453–457. doi:10.3760/cma.j.issn.0253-3766.2017.06.010

Wang, K., Gong, Q., Zhan, Y., Chen, B., Yin, T., Lu, Y., et al. (2019). Blockage of autophagic flux and induction of mitochondria fragmentation by paroxetine hydrochloride in lung cancer cells promotes apoptosis via the ROS-MAPK pathway. *Front. Cel Dev. Biol.* 7, 397. doi:10.3389/fcell.2019.00397

Wang, Q., Cao, J., Wang, P., and Ge, M. (2015). Antitumor effect of C21 steroidal glycosides on adenoid cystic carcinoma cell line SACC83. *Clin. Lab.* 61 (10), 1553–1560. doi:10.7754/clin.lab.2015.141218

Wang, X., Chang, H., Gao, G., Su, B., Deng, Q., Zhou, H., et al. (2020). Silencing of PRDM5 increases cell proliferation and inhibits cell apoptosis in glioma. *Int. J. Neurosci.* 131 (2), 144–153. doi:10.1080/00207454.2020.1733563

Wang, X., Yan, Y., Chen, X., Zeng, S., Qian, L., Ren, X., et al. (2018). The antitumor activities of *Marsdenia* tenacissima. *Front. Oncol.* 8, 473. doi:10.3389/fonc.2018.00473

Webb, A. H., Gao, B. T., Goldsmith, Z. K., Irvine, A. S., Saleh, N., Lee, R. P., et al. (2017). Inhibition of MMP-2 and MMP-9 decreases cellular migration, and angiogenesis in *in vitro* models of retinoblastoma. *BMC Cancer* 17 (1), 434. doi:10.1186/s12885-017-3418-y

Wu, C. W., Lu, L., Liang, S. W., Chen, C., and Wang, S. M. (2016). Application of drug-target prediction technology in network pharmacology of traditional Chinese medicine. *Zhongguo Zhong Yao Za Zhi* 41 (3), 377–382. doi:10.4268/cjcmm20160303

Xu, D. W. (2018). Study on the substance basis and mechanism of *Marsdenia* tenacissima regulating apoptosis and inhibiting the growth and metastasis of A549 cells. *PhD Thesis*. Beijing: Minzu University of China

Yang, C., Przyborski, S., Cooke, M. J., Zhang, X., Stewart, R., Anyfantis, G., et al. (2008). A key role for telomerase reverse transcriptase unit in modulating human embryonic stem cell proliferation, cell cycle dynamics, and *in vitro* differentiation. *Stem Cells* 26 (4), 850–863. doi:10.1634/stemcells.2007-0677

Yao, S., To, K. K.-W., Wang, Y.-Z., Yin, C., Tang, C., Chai, S., et al. (2014). Polyoxypregnane steroids from the stems of *Marsdenia* tenacissima. *J. Nat. Prod.* 77 (9), 2044–2053. doi:10.1021/np500385b

Ye, B., Yang, J., Li, J., Niu, T., and Wang, S. (2014). *In vitro* and *in vivo* antitumor activities of tenacissoside C from *Marsdenia* tenacissima. *Planta Med.* 80 (1), 29–38. doi:10.1055/s-0033-1360128

Zhan, J., Shi, L.-l., Wang, Y., Wei, B., and Yang, S.-l. (2019). *In Vivo* study on the effects of xiaoaiping on the stemness of hepatocellular carcinoma cells. *Evidence-Based Complement. Altern. Med.* 2019, 1–10. doi:10.1155/2019/4738243

Zhang, H., Tan, A.-M., Zhang, A.-Y., Chen, R., Yang, S.-B., and Huang, X. (2010). Five new C21 steroidal glycosides from the stems of *Marsdenia* tenacissima. *Steroids* 75 (2), 176–183. doi:10.1016/j.steroids.2009.11.003

Zhang, R., Zhu, X., Bai, H., and Ning, K. (2019). Network pharmacology databases for traditional Chinese medicine: review and assessment. *Front. Pharmacol.* 10, 123. doi:10.3389/fphar.2019.00123

Zhao, Y. G., and Xu, J. X. (2001). Mitochondria, reactive oxygen species and apoptosis. *Prog. Biochem. Biophys.* 28 (2).

Zheng, A.-W., Chen, Y.-Q., Fang, J., Zhang, Y.-L., and Jia, D.-D. (2017). Xiaoaiping combined with cisplatin can inhibit proliferation and invasion and induce cell cycle arrest and apoptosis in human ovarian cancer cell lines. *Biomed. Pharmacother.* 89, 1172–1177. doi:10.1016/j.biopha.2017.03.012

Conflict of Interest: The authors declare that the research was conducted in the absence of any commercial or financial relationships that could be construed as a potential conflict of interest.

Advantages of publishing in Frontiers

OPEN ACCESS
Articles are free to read for greatest visibility and readership

FAST PUBLICATION
Around 90 days from submission to decision

HIGH QUALITY PEER-REVIEW
Rigorous, collaborative, and constructive peer-review

TRANSPARENT PEER-REVIEW
Editors and reviewers acknowledged by name on published articles

Frontiers
Avenue du Tribunal-Fédéral 34
1005 Lausanne | Switzerland

Visit us: www.frontiersin.org
Contact us: frontiersin.org/about/contact

REPRODUCIBILITY OF RESEARCH
Support open data and methods to enhance research reproducibility

DIGITAL PUBLISHING
Articles designed for optimal readership across devices

FOLLOW US
@frontiersin

IMPACT METRICS
Advanced article metrics track visibility across digital media

EXTENSIVE PROMOTION
Marketing and promotion of impactful research

LOOP RESEARCH NETWORK
Our network increases your article's readership